# *SYNTHESIS AND CHARACTERISATION OF NOVEL BIOPOLYMERS VIA CLICK CHEMISTRY*

AHMED MOHAMED EISSA-MOHAMED

# SYNTHESIS AND CHARACTERISATION OF NOVEL BIOPOLYMERS VIA CLICK CHEMISTRY

**Ahmed Mohamed Eissa Mohamed**

A thesis submitted for the degree of Doctor of Philosophy


Department of Chemistry
University of Durham
England

2010

*“I would like to dedicate my thesis to my beloved parents,*

*Mr Mohamed Eissa and Mrs Fatimah Sayyid”*

# Abstract

The work throughout is the exploitation of copper catalysed Huisgen 1,3-dipolar azide–alkyne cycloaddition, as an efficient Click reaction, for the synthesis of novel biopolymers with a broad range of potential medical/industrial applications. The strategy is to develop a powerful tool for the synthesis of libraries of materials, which will be discussed in separate chapters.

Chapter one is a general introduction on biopolymers and Click chemistry with emphasis on the related literature to the present work.

Chapter two involves the application of Click chemistry on model compounds; 3-methyl benzyl alcohol and phenol. The resulting products were successfully prepared *via* Click chemistry. NMR spectroscopy was found to be a good choice for characterisation of the resulting products.

Chapter three describes the application of Click chemistry on a disaccharide compound, α,α-D-trehalose. The di-azide functionalised trehalose was synthesised by tosylation followed by acetylation and subsequent reaction with sodium azide. Different functionalities such as ester, acrylate and epoxide groups were successfully introduced *via* Click chemistry. NMR and FT-IR spectroscopies were found to be efficient characterisation tools to follow up the Click modification reactions. The di-acrylate functionalised trehalose showed a great potential as a cross-linker in the free radical polymerisation of HEMA to generate hydrogels.

Chapter four presents the utilisation of Click chemistry to produce trehalose-based glycopolymers which have a wide range of potential applications. Biodegradable glycopolymers containing PCL or PLA were synthesised *via* combination of ring opening polymerisation (ROP) and Click chemistry. The ROP of lactide and ε-caprolactone, using stannous octoate and propargyl alcohol, was carried out to synthesise alkyne end capped PLA and PCL which were then coupled with di-azide functionalised trehalose by Click reaction. NMR and IR were used to prove the structure of the materials. A new class of temperature responsive glycopolymers was also synthesised *via* copper wire catalysed Click-polymerisation of di-azide functionalised trehalose with di-alkyne terminated PEG. The cloud point of the aqueous solution of glycopolymer was evaluated and showed an LCST at ~39 $^{o}$C, known as fever temperature. In addition, the phase transition was shown to be reversible.

Chapter five involves the modification of 2-hydroxyethyl cellulose (HEC) *via* Click chemistry. For the first time, the azide functionalisation reaction of HEC was disclosed using a one pot reaction procedure. Neutral and ionic compositions of HEC were successfully synthesised by introducing different functionalities on HEC. The compositions containing carboxylic acid or $1^{ry}$ amine functionalities can be treated in basic or acidic media to give polyelectrolytes based on HEC. The compositions containing both functionalities, carboxylic acid and $1^{ry}$ amine, could produce polyampholytes. Sequential Click reactions were implemented to synthesise polydimethylsiloxane (PDMS) grafted HEC as well as potentially charged functionalities. These compositions are expected to receive a great interest in personal care and cosmetics applications. Mainly, solid state $^{13}$C-NMR and FT-IR spectroscopies were used to characterise these materials. Hydrophobically and hydrophilically modified HEC were also prepared by grafting PLA, PCL or PEG onto HEC using Click coupling reaction. AFM analysis showed that some exhibit a brushlike architecture.

Chapter six describes the combination of Click chemistry and ROMP to synthesise various graft polymers. Two different grafting techniques; "grafting through" (the macromonomer approach) and "grafting onto" were involved in the synthesis. The "grafting through" method involved the synthesis of oxanorbornenyl di-PEG macromonomer by Click coupling of azide terminated PEG with di-alkyne functionalised oxanorbornene. The macromonomer was then subjected to ROMP to produce PEG grafted polyoxanorbornene. Polynorbornene-g-PCL and polynorbornene-g-PEG were prepared by "grafting onto" process. This was achieved by ROMP of bromide functionalised norbornene followed by reaction with sodium azide and then Click reaction with alkyne terminated PCL and PEG. The surface analysis of these graft polymers were studied using AFM. Random graft copolymer containing PEG and PCL side chains was also prepared by ROMP of a mixture of oxanorbornenyl di-PEG and bromide functionalised norbornene followed by reaction with sodium azide and then Click reaction with alkyne end capped PCL.

Chapter seven entails general conclusions and suggestions for future work.

## Acknowledgements

Firstly, I am indebted to my supervisor, Dr Ezat Khosravi. It is the pleasant task of me to acknowledge his gratitude for guidance, great care, continuous help in all ways, valuable discussion and following this work step by step to be done successfully. I would like to express my sincere thanks to Dr Alan Kenwright for advice and valuable conversations in many things, especially NMR characterisation. I must acknowledge Catherine Heffernan and Ian Mckeag for their work in obtaining high field NMR spectra. I should also acknowledge Dr David Apperley and Mr Fraser Markwell for their work and advice in obtaining high field solid-state NMR spectra, which have contributed significantly to this work. Many thanks go to Dr Lian Hutchings for assistance and advice in GPC measurements and Doug Carswell for help in TGA and DSC analysis. The patience and willingness of Dr Richard Thomson to produce AFM images is much appreciated. I am also grateful to all of the technical staff in the department for their assistance and advice.

I would like to extend my thanks to all members of the IRC, especially members of the Khosravi research group, past and present, for their support and friendship during my time in Durham. In particular, I would like to mention Dr Zhanru Yu, Dr Mariusz Majchrzak, Dr Solomon Kimani, Dr Yulia Rogan, Barry Dean, Lynn Donlon, Jessica Breen, Ladan Bayati and Ian Johnson, have been invaluable friends and were always ready to give a hand in the lab.

My sincere appreciation and great thanks go to industrial collaborators, in particular, Dr Osama Musa who has extensively contributed in the early stages of the work related to modification of HEC for the personal care applications, for his valuable advice and guidance. I would like to extend my appreciation to Dr Levent Cimecioglu for his interest in the work and constructive conversations.

Last but not least, there are no words to express my thanks and feelings to my parents for their great care and continuous support (emotionally and financially) from day one. I pray to God to reward them for all what they have done/been doing for me. I am truly grateful for the help offered by my sisters (Amal, Eman and Omima) and their husbands (Tarek, Ahmed and Atef) who are always just a phone call away, God bless them all. Abd-Allah and Mariam, for just being my beloved son and daughter. And finally, I must express my deepest thanks to the greatest wife, Manar, whose support and devotion means everything for me.

## Memorandum

The work reported in this thesis has been carried out at the Interdisciplinary Research Centre in Polymer Science and Technology, Department of Chemistry, Durham University between October 2006 and December 2009. This work has not been submitted for any other degree in either Durham or elsewhere and is the original work of the auther except where acknowledged by means of appropriate reference.

## Statement of Copyright



## Financial Support

None of this would have been possible without the generous financial support of the Egyptian government presented by the Egyptian Cultural Centre and Educational Bureau in London. I gratefully acknowledge the Ministry of Higher Education and National Research Centre (NRC) in Cairo, Egypt for fully funded PhD scholarship. My thanks also go to Akzo Nobel Surface Chemistry, LLC, US (formerly known as ICI National Starch) for chemical and travel grants.

## Contents

## Chapter 2

## Click Chemistry on Model Compounds



## Chapter 3

## Click Chemistry on α,α-D-Trehalose

**Chapter 5**

**Modification of 2-Hydroxyethyl Cellulose (HEC)**

**Chapter 7**

**General Conclusions and Future Work**

# Chapter 1
# Introduction

## 1.1. Biopolymers

Biopolymers are defined as biologically derived polymers and their attractiveness is due to their availability, biocompatibility, and biodegradability. Biopolymers may originate from natural sources such as proteins and carbohydrates or can be synthetically prepared such as poly(lactic acid).

Most natural biopolymers degrade or denature soon after processing, which creates a significant barrier to industrial use. There are two main successful synthetic options to create durable bio-based materials. One is to form composites by incorporating biopolymers into synthetic materials. The other option is to modify biopolymers with the addition of functional groups.

## 1.2. Natural Biopolymers

### 1.2.1. Proteins and polypeptides

Amino acids in proteins are linked by an amide linkage which is often called the peptide bond. There are simple proteins composed only of amino acids, such as albumin, gelatin, casein, collagen, or keratin. Other proteins contain not only amino acid residues, but also other groups such as carbohydrates in glycoproteins, or lipids in lipoproteins. Proteins that possess catalytic activity are known as enzymes.

### 1.2.2. Carbohydrates and Polysaccharides

Carbohydrates are organic compounds with the empirical formula $C_m(H_2O)_n$, which are also known as saccharides or sugars. A carbohydrate could be in a di-, oligo-, or polysaccharide form, determined by the number of single carbohydrate molecules that are bound together. Sugars have D- & L- stereoisomers as a result of the presence of chiral centres in the structure.

The study of carbohydrates began in the late nineteenth century with the work of Emil Fischer. Carbohydrate ring structure was elucidated in the 1930s by Haworth and colleagues. Polysaccharides were discovered soon after and appeared to be present in every living organism; vegetable and animal. Polysaccharides display a very wide range of biological functions from acting as nature's energy source (starch **1**), to providing structural materials (chitin **2** and cellulose **3**), Fig. 1.1.[1]

Carbohydrates are now known to assume an even wider variety of biological roles. For example, the sulfated polysaccharide, heparin **4** (Fig. 1.1) plays an essential role in blood coagulation,[2] while hyaluronan **5** (Fig. 1.1), which acts as a lubricant in joints, has also been used in the implantation of plastic intra-ocular lenses.[3] Moreover, hyaluronan, as well as another sulfated polysaccharide, chondroitin sulfate **6** (Fig. 1.1), exhibit anti-inflammatory activity and were investigated for the treatment of ostheoarthritis and rheumatoid arthritis.[4]

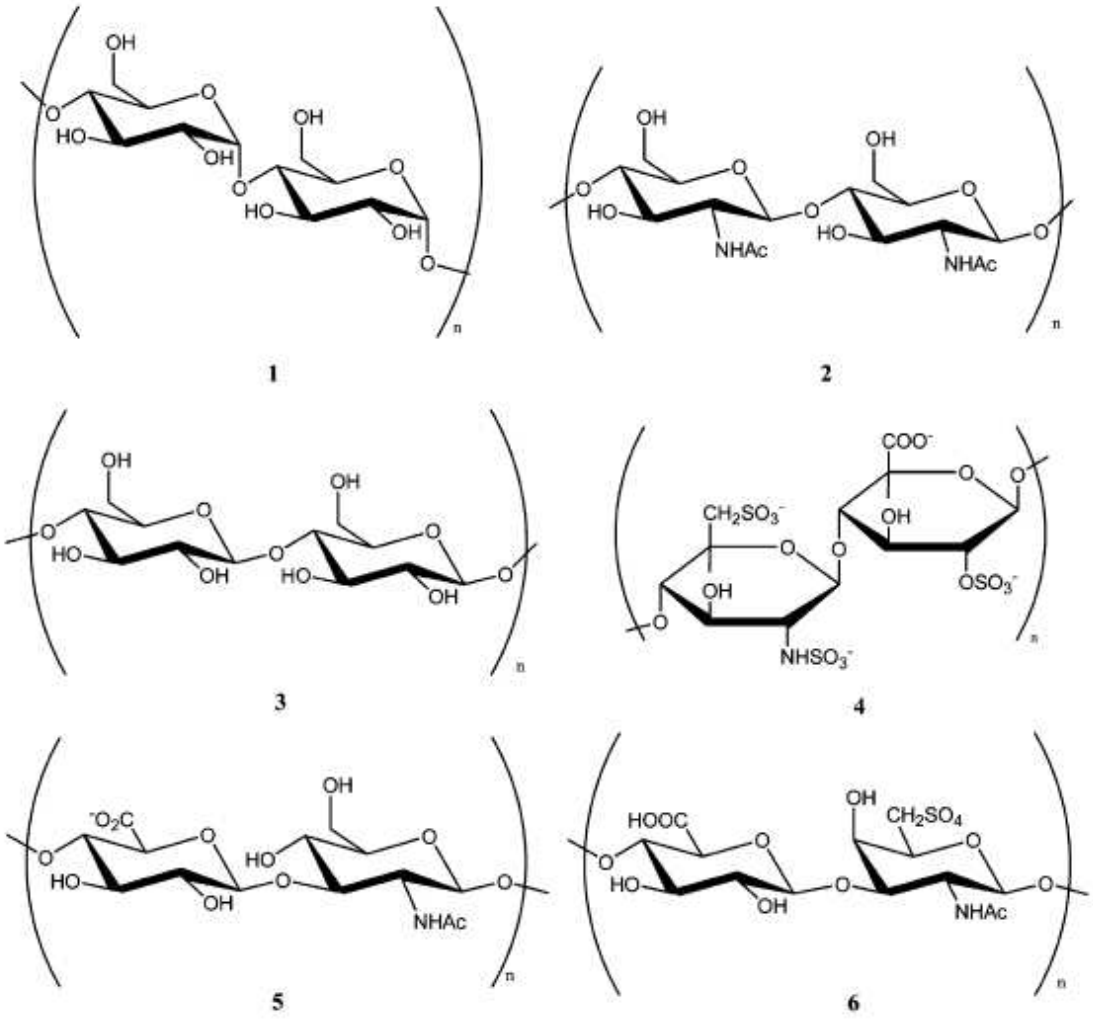


**Figure 1.1.** Structures of natural biopolymers. (1) starch; (2) chitin; (3) cellulose; (4) heparin; (5) hyaluronan; (6) chondroitin sulfate.

Polysaccharides in solution can exist as loose random coils or rigid helices. They can be anionic, cationic, nonionic, or even amphoteric depending on the chemical identity of the pendant groups on the backbones. They can be single coils, double coils, and even aggregates of coils, the nature of which can be influenced by, among other things, temperature, concentration, and addition of salts.

Polysaccharides are one of the main ingredients in the formulation of many cosmetically acceptable products. They perform countless functions in cosmetics formulations. For instance, they act as rheology modifiers, suspending agents, hair conditioners, and wound-healing agents. They moisturise, hyrdrate, emulsify, and emolliate.[5-8]

### 1.2.2.1. α,α-D-Trehalose

α,α-D-Trehalose is a symmetrical disaccharide composed of two glucose molecules bound by an alpha, alpha-1, 1 –linkage, Fig. 1.2. Trehalose occurs naturally in many living organisms, including mushroom, insects, and yeasts.[9] Trehalose has a non-reducing character and high thermostability and a wide pH-stability range compared to other sugars. Its particular physical features make it one of the promising monomers for production of linear polymers.[10-13] In this view, trehalose is an extremely attractive substance for industrial/biomedical applications.

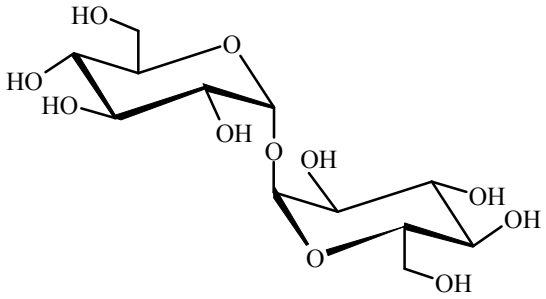


**Figure 1.2.** Structures of α,α-D-Trehalose

### 1.2.2.2. Hydroxyethyl Cellulose (HEC)

Hydroxyethyl cellulose (HEC) is derived from cellulose. Cellulose itself is a water-insoluble, long-chain molecule consisting of repeating anhydroglucose units. HEC differs from cellulose in that some or all of the hydroxyl groups of the glucose repeat unit have been replaced with hydroxyethyl ether groups, Fig. 1.3.

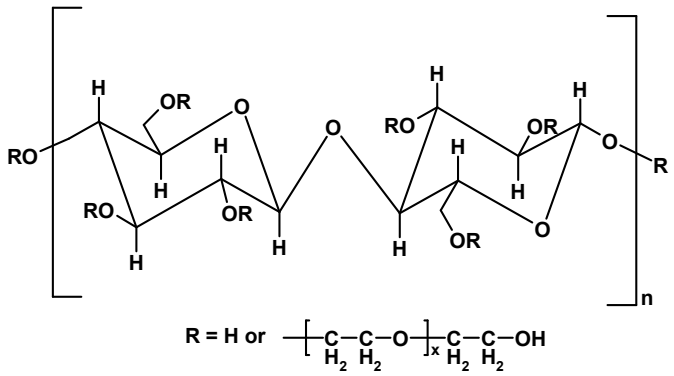


**Figure 1.3.** Structures of HEC

In the synthesis of HEC, purified cellulose is reacted with sodium hydroxide to produce swollen alkali cellulose. This alkali-treated cellulose is more chemically reactive than cellulose. By reacting the alkali cellulose with ethylene oxide, a series of hydroxyethyl cellulose ethers is produced. The hydroxyethyl groups confer water solubility to HEC. The manner in which ethylene oxide is added to cellulose can be described by two terms: Degree of substitution (DS) and molar substitution (MS). The DS designates the average number of hydroxyl positions on the anhydroglucose unit that have been reacted with ethylene oxide. Since each anhydroglucose unit of the cellulose molecule has three hydroxyl groups, the maximum value for DS is three. However, MS is defined as the average number of ethylene oxide molecules that have reacted with each anhydroglucose unit. Once a hydroxyethyl group is attached, it can further react with additional groups in an end-to-end formation. As long as ethylene oxide is available, this reaction can continue, theoretically without limit.[14]

HEC is a nonionic, water-soluble polymer that can thicken, suspend, bind, emulsify, form films, stabilise, disperse, retain water, and provide protective colloid action. HEC has a safety profile and is presently approved by FDA.[15] HEC has therefore been widely used in many applications.[16-21]

In cosmetics and personal care,[7] HEC is an effective film-former, binder, thickener, stabiliser, and dispersant in shampoos, hair sprays, neutralisers, creams and lotions. Hair shampoos must pour rich and heavy from the container and yet thin out, feel wet, and disperse easily when rubbed between the hands and applied to the hair. It also makes the soap in the shampoo less foamy, and it helps the shampoo clean better by forming colloids around dirt particles. Furthermore, it can be used to thicken underarm deodorants despite the high salt levels of such products. Because of its strong salt resistance and acid resistance, HEC can make toothpaste stable and improve water retention and emulsification power.

## 1.3. Synthetic Biopolymers

### 1.3.1. Glycopolymers

Synthetic carbohydrate-containing macromolecules are known as glycopolymers. They are attracting ever-increasing interest due to their role as biomimetic analogues. Glycobiology is the branch of biology that deals with the nature and the role of carbohydrates in biological events.[22, 23] It is now clear that carbohydrates play a major role in many recognition events. Recognition is key to a variety of biological processes and the first step in numerous phenomena based on cell–cell interactions, such as fertilisation, embryogenesis, cell migration, organ formation, immune defense, microbial and viral infection, inflammation, and cancer metastasis.[22, 24] These recognition processes are thought to proceed by specific carbohydrate–protein interaction. The proteins involved, generically named lectins, are most frequently found on cell surfaces. They have the ability to bind specifically and non-covalently to carbohydrates.[25] The mechanism of the carbohydrate–lectin interaction and the structures of the glycopolymers involved in these recognition processes are still largely unknown. Consequently, synthetic complex carbohydrates and carbohydrate-based polymers, ‘‘glycomimics’’, are emerging as an important well-defined tool for investigating glycopolymer–protein interaction.[26, 27] In addition, a number of research collaborations have begun to develop carbohydrate-containing polymers aimed at biomedical, pharmaceutical and medical applications, such as surfactants,[28] detergents,[29] texture-enhancing food additives,[30] drug release,[31, 32] scaffolds for tissue engineering,[33-35] inhibitors to avoid rejection in xenotransplantation,[36] treatment of infectious disease[37] and treatment of HIV.[38]

There are two main strategies to synthesise glycopolymers; (1) polymerisation of saccharide-containing monomers (monomeric glycosides) and (2) functionalisation of a polymer precursor. Glycopolymers have diverse architectures, such as comb polymers, dendrimers and cross-linked hydrogels.[1, 39, 40]

### 1.3.2. Aliphatic Polyesters

Aliphatic polyesters provide versatile biocompatible and biodegradable polymers possessing good mechanical properties. These advantages have seen aliphatic polyesters receive increasing attention over the last few years driven by their application as

biodegradable substitutes for conventional commodity thermoplastics and in the biomedical field. This has led to polyester homo- and co-polymers being widely used as sutures, oral implants, and microspheres for drug encapsulation and delivery.[41-43]

Aliphatic polyesters are prepared through one of two routes: the first is step-growth polymerisation of a hydroxy acid or a diacid with a diol, enabling access to a large range of monomer feedstocks. However, the molecular weights are generally limited and any minor deviations in the stoichiometry are detrimental to the chain length. Moreover, long reaction times and high temperatures are often required resulting in unfavourable side reactions.[44] The second route for the synthesis of aliphatic polyesters is *via* ring opening polymerisation (ROP), which will be discussed later in this chapter in section 1.6.2.

#### 1.3.2.1. Poly(lactic acid) (PLA)

Poly(lactic acid) or polylactide (PLA) is a biodegradable, bioabsorbable, biocompatible and renewably derived thermoplastic polyester extensively investigated over the last several decades.[45-52]

Lactic acid is produced by converting sugar or starch obtained from vegetable sources (e.g., corn, wheat, or rice) using either bacterial fermentation or a petrochemical route. Lactic acid exists as two optical isomers, L- and D-lactic acid. Lactic acid produced by petrochemical routes is an optically inactive 50/50 mixture of the D and L forms. Since the fermentation approach is more eco-friendly, it has been used more extensively since 1990.[53]

Polymerisation of lactic acid to PLA can be achieved by a direct condensation process that involves solvents under high vacuum. Alternatively, in a solvent-free process, a cyclic dimer intermediate called lactide is formed followed by catalytic ROP of the cyclic lactide. Due to the optical activity of lactic acid, lactide can be found in three different versions, i.e., D,D-lactide, L,L-lactide, and D,L-lactide (meso-lactide).[54] The stereochemical composition of lactide monomers determines the final properties of the polymer.[55] With the direct condensation route, only low molecular weight (Mw ~ 2–10 kDa) polymers can be produced, mainly due to the presence of water and impurities.[56] Typically, low molecular weight PLA has substandard mechanical properties. Therefore, it suffers from the need for use of solvents under high vacuum and temperature, water removal and increased colour and racemisation of PLA.[57]

Because of these disadvantages, the commercial manufacture of PLA commonly involves ROP of lactide.[57]

PLA degrades to form lactic acid, which is normally present in the body. The lactic acid enters the tricarboxylic acid cycle and decomposes to water and carbon dioxide. PLA degrades by hydrolysis and not by microbial attack. At higher temperatures and humidity high molecular weight PLA is not contaminated by microbes. This feature of PLA is good for applications where the polymer would be in direct contact with the human body or foods and for this reason it has been approved by FDA. PLA can also be degraded by enzymes which accelerate hydrolysis of PLA as well as other biodegradable plastics and can be incorporated into the natural cycle of organic materials.[58] If composted properly PLA takes only 3-4 weeks for complete degradation. The first stage of degradation is hydrolysis to water-soluble oligomers and lactic acid.

PLA is clear, provides good gloss and clarity, but it is brittle and thermally unstable. In addition, the lack of reactive side-chain groups and the hydrophobic character of PLA limit the successful implementation of PLA without modifications in most practical applications. Therefore, it has been a challenging task to surface/bulk modify PLA.[59]

#### 1.3.2.2. Polycaprolactone (PCL)

Polycaprolactone (PCL) is an aliphatic polyester, which has been used in biomedical applications. PCL has very similar properties to PLA but with slower rate of degradation and superior thermal properties.[60]

PCL is synthesised in a similar way to PLA; either by condensation of 6-hydroxycaproic (6-hydroxyhexanoic) acid or ROP of ε-caprolactone (ε-CL). There are a large number of compounds, either metal-based, organic or even enzymatic systems that can catalyse the ROP of ε-CL with various mechanisms such as anionic, cationic and coordination – insertion.[61-63]

### 1.3.3. Poly(ethylene glycol) (PEG)

Poly(ethylene glycol) (PEG) is a synthetic polyether compound, known as polyethylene oxide (PEO) or polyoxyethylene (POE), depending on its molecular weight. PEG is a neutral, biocompatible, water soluble, non-toxic, non-immunogenic, FDA approved and

probably the most widely used polymer in biomedical applications.[64, 65] PEG is a perfect material for many bio-applications including stealth drug carriers and protein repellent surfaces.[66, 67] PEG allows a good solubility of bioactive compounds in physiological media and prevents the adsorption of plasma proteins, which can trigger immune response.[68, 69] Nonlinear PEG analogues, which possess a vinyl backbone and multiple PEG side chains, has been used for building superior biomaterials.[70]

PEG is an excellent shielding agent for *in-vivo* delivery of various bioactive compounds and has been extensively used in delivery of low molecular weight drugs, active peptides, proteins, and genetic material. PEG conjugation chemistry, known as "PEGylation", has been widely used for the modification of biomolecules such as peptides, proteins, and enzymes, as well as of nanocarriers for drug delivery systems such as liposomes and nanoparticles. The direct covalent conjugation linkage between the active substance and PEG can be either stable (permanent PEGylation) or labile (prodrug strategy). PEGylation can improve pharmaceutical and pharmacological properties due to its increased water solubility and circulatory half-life *in-vivo*, the reduced antigenicity and immunogenicity, and the tolerance of biomolecules against degradation.[71-74]

### 1. 3.4. Polydimethylsiloxane (PDMS)

Polydimethylsiloxane (PDMS) is a polymeric organo-silicon compound that is commonly referred to as silicon rubber. PDMS is the most widely used silicon-based organic polymer and is of particular interest in biomedical applications. PDMS is a highly flexible polymer showing a very low glass transition temperature, $T_g$, (about −123 $^oC$). Moreover, it has physiological inertness, biocompatibility, low toxicity, high oxygen permeability, good thermal and oxidative stability, and anti-adhesive properties.[75, 76] Medical devices based on PDMS include blood pumps, cardiac pacemaker leads, mammary prostheses, drainage implants in glaucoma, artificial skin, contact lenses, oxygenators, medical adhesives, finger joints, catheters, drug delivery systems and denture liners.[77] In skin lotion formulations, PDMS provides a protective, breathable barrier on the skin and reduces the whitening or soaping effect typically encountered during rub-in of the lotion. In hair care products, the silicone ingredient present in the shampoo formulations causes the hair to be shiny, more spirited and slippery. It has been also used in antiperspirant and aerosol products.[7]

Polyorganosiloxanes were incorporated as soft segments into polysaccharide-based materials to improve the physical and mechanical properties for some practical applications. Organic–inorganic hybrid membranes were obtained by simultaneous grafting and crosslinking of chitosan with epoxy-terminated PDMS and γ-glycidoxypropyltrimethoxysilane. The low surface tension of siloxane polymers, which resulted from the modification of chitosan with polysiloxane enhanced the surface hydrophobicity of the materials, as indicated by the increase of water contact angles.[78]

The importance of polyorganosiloxanes is not less than that of the polysaccharides in the territory of cosmetics and personal care formulation technology.[7] Therefore, grafting/modification of polysaccharides with polysiloxane to obtain cosmetic compositions has been of great interest for the industrial research. Many patents reported different compositions based on combination of polysaccharides and silicones to produce personal care products.[79-84]

### 1.4. "Click" Chemistry

"Click" chemistry is a chemical philosophy introduced by Barry Sharpless in 2001. He defined Click chemistry as the generation of complex substances by bringing together smaller units *via* heteroatoms. This is inspired by the fact that nature also generates substances by joining small modular units. While a range of chemical reactions can in principle fulfill these criteria, successful examples often originate from five broad classes of reactions that appear to fit the framework of "Click" chemistry exceptionally well:[85]

1. Cycloaddition of unsaturated species: 1,3-dipolar cycloaddition.
2. Cycloaddition of unsaturated species: [4+2]-cycloaddition (Diels–Alder).
3. Nucleophilic substitution/ring-opening reactions.
4. Carbonyl reactions of the non-aldol type.
5. Addition to carbon–carbon multiple bonds.

Therefore, the term "Click" refers to energetically favoured, specific, and versatile chemical transformations, which lead to a single reaction product. In other words, the essence of Click chemistry is simplicity and efficiency. Yet, the last few years saw the emergence of Click toolbox, which includes, for example, Diels–Alder cycloadditions, thiol–ene additions, oxime formation, and copper(I)-catalysed Huisgen azide–alkyne cycloadditions (CuAAC).[86] However, CuAAC has rapidly become the

most popular Click reaction to date and in recent literature, the term Click chemistry has been used almost exclusively to denote these reactions.[87]

The formation of triazoles *via* the cycloaddition of azide and acetylene was first reported by Dimroth in the early 1900's but the generality, scope, and mechanism of these cycloadditions was not fully realised until the 1960's by Huisgen.[88] In the absence of a transition-metal catalyst, these reactions are not regioselective, relatively slow, and require high temperatures to reach acceptable yields. The reaction generates a mixture of 1,4- and 1,5-disubstituted triazoles, Scheme 1.1.

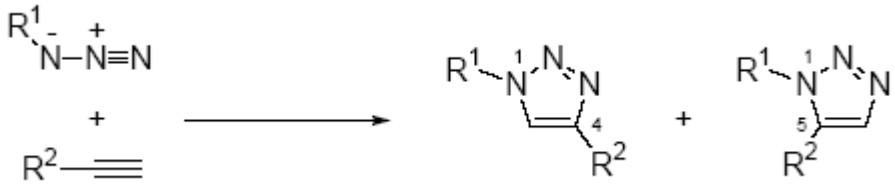

**Scheme 1.1.** Huisgen 1,3-dipolar azide–alkyne cycloaddition

Various attempts to control the regioselectivity have been reported without much success until the discovery of the copper (I)-catalysed reaction in 2002 by Sharpless and Meldal,[89, 90] which exclusively yields the 1,4-disubstituted 1,2,3-triazole. This type of Click reactions is classified as highly efficient and specific. Moreover, they are experimentally simple needing no protection from oxygen, requiring only stoichiometric amounts of starting materials, and generating virtually no by-products. Furthermore, it is a benign chemistry. It has been demonstrated, by Sharpless and Fokin,[89] that CuAAC can be successfully performed in polar media, such as tert-butyl alcohol, ethanol or pure water. Numerous authors collectively demonstrated that CuAAC is a true example of efficient and versatile Click chemistry.[91-96]

CuAAC reaction is thought to proceed in a stepwise manner starting with the generation of copper (I) acetylide (**7**). Density functional theory calculations show a preference for the stepwise addition (**7** → **8** → **9** → **10**) over the concerted cycloaddition (**7** → **10**) by approximately 12 to 15 kcal $mol^{-1}$, leading to the intriguing six-membered metallocycle (**9**), Scheme 1.2.[89]

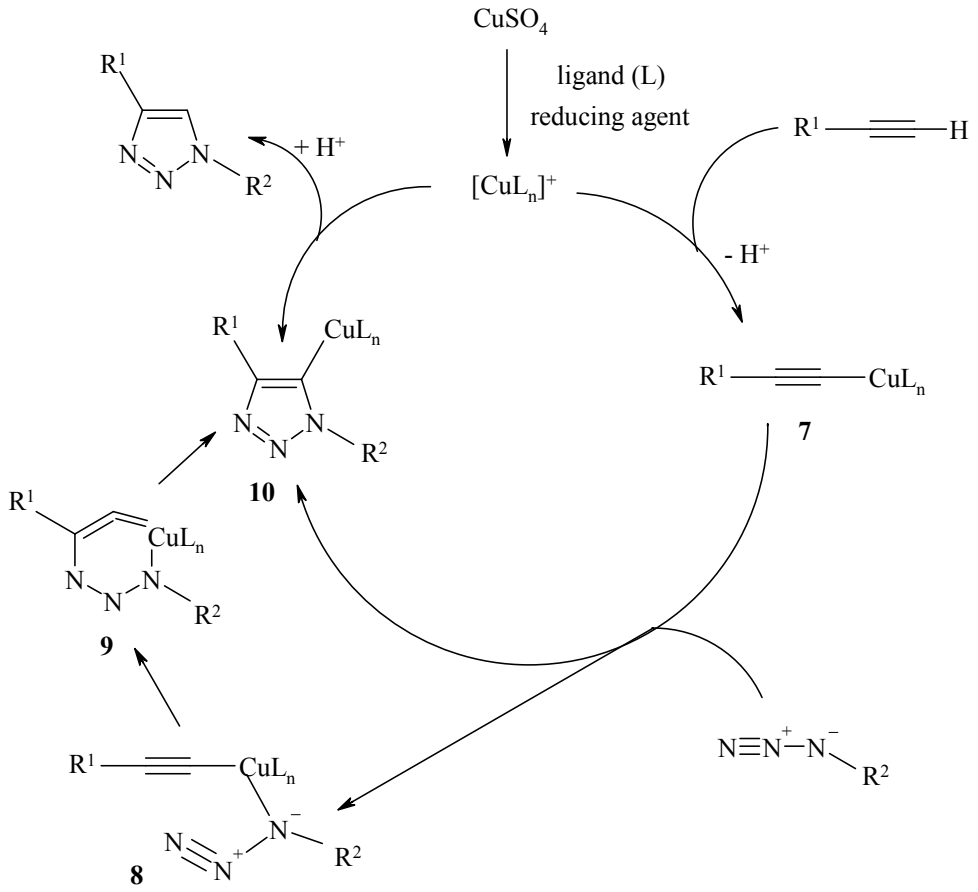


**Scheme 1.2.** Postulated mechanism for CuAAC

There are a number of methods to generate the active catalyst for the CuAAC reaction. One of the most common techniques is to reduce Cu(II) salts, such as $CuSO_4 \cdot 5H_2O$, *in-situ* to form Cu(I) salts. Sodium ascorbate is typically used as the reducing agent in a 3- to 10-fold excess,[97] but other reducing agents, including hydrazine[98] and tris(2-carboxyethyl)phosphine,[99] have been used with reasonable success. The advantages of this strategy are; it is cheap, it can be performed in water, and it does not require a deoxygenated atmosphere.[97] The main disadvantage is the reducing agent might reduce Cu(II) to Cu(0). This can generally be prevented, though, by using a proper ratio of reducing agent to catalyst and/or adding a copper stabilising agent, such as tris-(hydroxypropyltriazolylmethyl)amine.[97]

The second way to create the catalyst is to directly add Cu(I) salts. Many such compounds have been utilised over the past few years, including CuBr, CuI, $CuOTf \cdot C_6H_6$ (OTf= trifluoromethanesulfonate), $[Cu(NCCH_3)_4][PF_6]$, etc.[89] This method does not require a reducing agent, but it has to be done in a deoxygenated environment and in an organic solvent (or a mixed solvent), meaning that a base will probably be needed.[89, 100, 101] Nevertheless, Cu(I) salts are not as reliable as the procedures using Cu (II) salts.[89]

Oxidizing copper metal with an amine salt is another way to generate the catalyst.[100, 102] There are a considerable number of disadvantages with this strategy. Longer reaction times are needed as well as larger amounts of copper. It is more expensive, and requires a slightly acidic environment to dissolve the metal, which could be damaging to any acid sensitive functional groups present in the reactants.[97]

Recently, Cu(I)-modified zeolites were reported as catalysts for the CuAAC reaction.[103] Zeolites are particularly desired as catalysts because of their high concentration of active acid sites, high thermal/hydrothermal stability, and high size selectivity. In one particular CuAAC reaction, the zeolite, modified with CuI, exhibited far better results than CuCl; higher conversions and shorter reaction times.[103]

Another research group has attempted to find a replacement for copper as the catalyst. Golas et al. reacted propargyl ether with azide-terminated polystyrene to make polymers using three different catalyst: $NiCl_2$, $PtCl_2$, and $PdCl_2$.[98] Although none of them displayed catalytic activity as high or as fast as CuBr, they all produced polymerisation products. $PtCl_2$ produced polymers with the highest molecular weight, followed by $PdCl_2$, followed by $NiCl_2$.

In 2005, pentamethyl cyclopentadienyl ruthenium (II) complexes (Cp*Ru), such as $Cp^*RuCl(PPh_3)_2$, were discovered as novel catalysts for Click chemistry. Contrary to all previously mentioned catalysts, Cp*Ru complexes afford only 1,5-substituted 1,2,3-triazoles.[104] Furthermore, they can work on both terminal and internal alkynes alike.[105] Due to their recent discovery, though, limited information is available detailing the role of ruthenium (II) complexes in Click chemistry.

Finally, studies have shown that catalysts are not always required for the cycloaddition to proceed. By using electron deficient alkynes, the reaction can proceed readily at ambient conditions.[106] However, electron deficient alkynes are very reactive toward nucleophiles and can lead to side products,[107] which has kept these types of reactions estranged from the field of Click chemistry. Other studies have shown that the cycloaddition can occur rapidly if the alkyne is first incorporated into an eight-member ring, forming a cyclooctyne.[107, 108] Cyclooctynes are very unstable, due to a high degree of ring strain (18 kcal/mol), which causes them to react readily with azides.[107] While this method leaves no side products and requires no cytotoxic catalysts, it requires the prerequisite of connecting the alkyne of interest to an eight-member ring. This can be a very challenging task and is much more complicated than simply adding an acetylene functional group, as in traditional Click reactions. Moreover, in comparison to CuAAC, these cycloalkynes gave rather slow cycloaddition kinetics. However, this situation was

dramatically improved by introducing electron-withdrawing substituents on the a position of the triple bond.[107, 109] For instance, fluoro substituents were selected as they are relatively inert in a biological environment. An additional concern with the cyclooctyne method is it produces a racemic mixture of regio-isomers (Scheme 1.3).[107] This stipulation is typically consequential to pharmaceutical applications and it defies the very definition of Click chemistry, which requires Click reactions to be regio-specific.

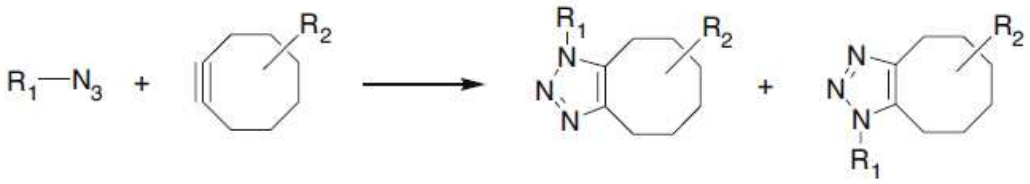


**Scheme 1.3.** Copper-free cycloaddition reaction of an azide and alkyne incorporated into an eight-member ring (cyclooctyne)

CuAAC reactions have been shown to be highly relevant for biomedical applications. Indeed, such reactions can be performed under experimental conditions, which are compatible with biological environments (e.g. aqueous medium and body temperature). Although, azide and alkyne functions are, respectively, absent or relatively rare in the biological world,[110] azide–alkyne chemistry constitutes a very interesting chemoselective platform for the functionalisation or ligation of biological systems. 1,2,3-triazole rings have been reported to be extremely water soluble, making *in-vivo* administration much easier. They are readily associated with biological targets through hydrogen bonding and dipole interactions. Their electronic properties are very similar to amide bonds, but they are not subject to the same hydrolysis reactions.[97] The triazoles are also stable in typical biological conditions, which tend to be aqueous and mildly reducing in nature.[87] For instance, CuAAC has been recently investigated for designing a wide range of biomaterials, such as stationary phases for bioseparation, site-specific modified proteins or viruses, drug- or gene- delivery carriers, protein or oligonucleotide microarrays, and functionalised cell surfaces.[111-118]

However, in some particular cases, the presence of transition metal catalysts may be a problem. Some examples of *in-vitro* copper-induced degradation of viruses or oligonucleotide strands have been reported.[117, 118] Additionally, the use of CuAAC for *in-vivo* applications is limited by the fact that, if present in more than trace quantities, copper ions are potentially toxic for living organisms. In this context, the development of metal-free Click strategies is particularly relevant to biological applications as

discussed here earlier and highlighted by Lutz.[119] Recently, we demonstrated, for the first time, the use of Cu-wire as a catalyst for Click-polymerisation of trehalose and PEG to produce temperature responsive glycopolymer.[120] The use of Cu-wire is expected to reduce / eliminate copper contamination in the glycopolymer.

### 1.5. Utilisation of Click Chemistry on Saccharides/Polysaccharides

Srinivasachari et al.[121] synthesised glycopolymers based on trehalose *via* Click-polymerisation to promote nucleic acid delivery in the presence of biological media containing serum. These structures were designed to contain a trehalose moiety **11** to promote biocompatibility, water solubility, and stability against aggregation. They reported the synthesis of diazido-trehalose monomer **14**, which was generated in three steps, Scheme 1.4. Firstly, iodination reaction of trehalose **11** to yield **12** which was then reacted with sodium azide to produce azido-derivative **13**. Finally, protection reaction was performed on **13** with acetic anhydride to produce monomer **14**.

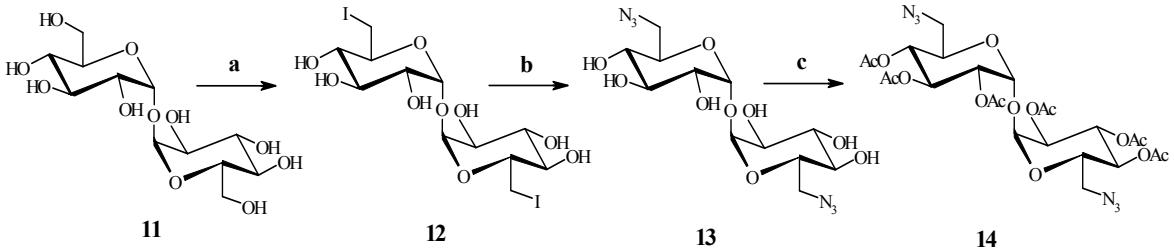


Conditions: (a) $PPh_3$, $I_2$, DMF; (b) $NaN_3$, DMF; (c) 1:1 $Ac_2O$ Pyr.

**Scheme 1.4.** Synthesis of diazido-trehalose monomer

They also reported the synthesis of series of dialkyne-oligoamine monomers (Scheme 1.5)[121] by first selectively protecting the primary amine end groups in **15** with trifluoroacetyl units ($COCF_3$) and the internal secondary amines with tert-butoxycarbonyl (Boc). The terminal $COCF_3$ moieties were then cleaved with potassium carbonate to produce **16**. The primary amines in **16** were coupled to propiolic acid *via* dicyclohexyl carbodiimide (DCC ) coupling to yield monomer **17**.

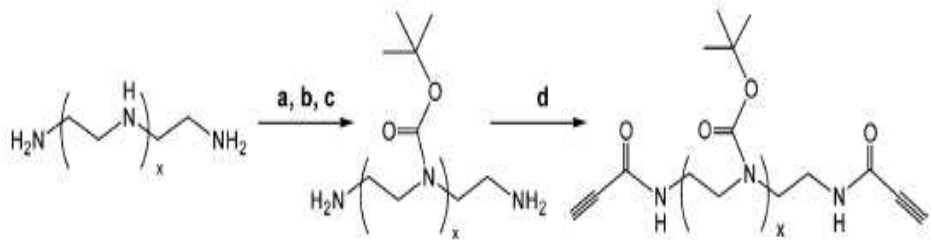


Conditions: (a) $CF_3COOEt$, $CH_2Cl_2$; (b) $(Boc)_2O$, $CH_2Cl_2$, TEA; (c) $K_2CO_3$, 20:1 MeOH/$H_2O$; (d) propiolic acid, DCC, $CH_2Cl_2$.

**Scheme 1.5.** Synthesis of dialkyne-oligoamine monomers

Monomer **14** and **17** were then coupled in equal molar ratios *via* Click-polymerisation using copper(II) sulfate pentahydrate and sodium ascorbate followed by deprotection, Scheme 1.6.[121] This was the first study demonstrating that Click-polymerisation is a highly effective means of forming biocompatible glycopolymers for biomedical applications, particularly for the cellular delivery of nucleic acids.

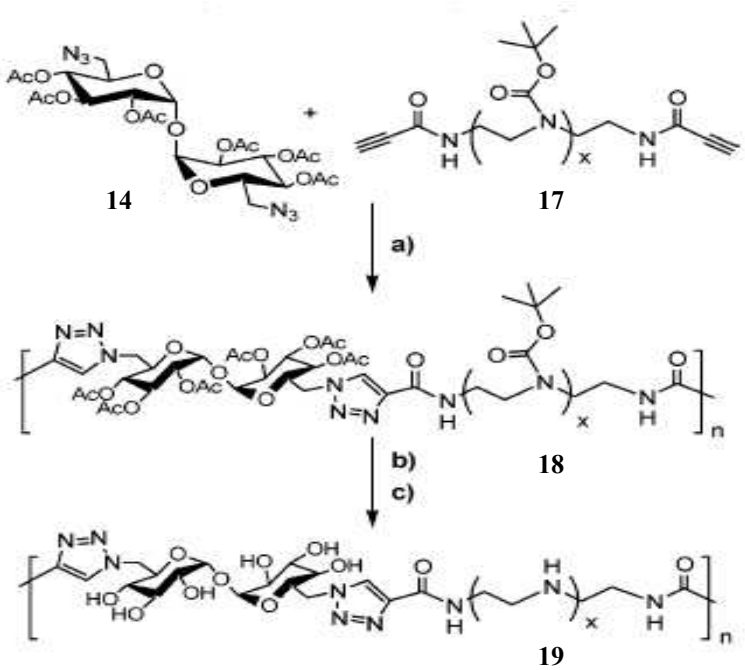


Conditions: (a) $CuSO_4$/sodium ascorbate, 1:1 t-BuOH/$H_2O$; (b) NaOMe/MeOH; (c) $CF_3COOH/CH_2Cl_2$.

**Scheme 1.6.** Click-polymerisation and polymer deprotection

Liebert et al. used Click chemistry to modify the surface of cellulose.[122] It was thought that the 1,2,3-triazoles would interact with biological targets through hydrogen bonding and dipole interactions, increasing the overall affinity of cellulose towards its desired target. The team first introduced azide functional groups into cellulose through two steps: tosylation of the primary alcohol groups followed by azidation with sodium azide. The overall yield ranged from 60 % to 99 %. Three different terminal alkyne-containing low molecular weight compounds (methylpropiolate, 2-ethynylaniline, and 3-ethynylthiophene) were then mixed with three different strands of azidified cellulose in separate reactions, using a copper(II) salt catalyst and sodium ascorbate. It was claimed that the yields of the reactions were ranging from 75 % to 98 %, depending on the reaction conditions utilised. A variety of unconventional properties were expected especially concerning the biological activity as already found for sulphated polysaccharides, e.g., curdlan- and shizophyllan sulphuric acid half esters, which are among the most promising drugs with anti-HIV and cancerostatic activities.

In that same year, Hafrén et al.[123] also modified cellulose with Click chemistry but took a slightly different approach. In one single step, terminal alkynes were introduced through the primary alcohols of cellulose using 5-hexynoic acid in a neat reaction. 3-Azido-coumarin and copper catalyst were then added. Upon reaction, the coumarin-cellulose compound began to fluoresce a bright blue colour, indicating that the reaction was successful, but no product yield was calculated. This methodology was claimed to have a great potential to prepare novel composites, printing paper, and textiles. The work of Liebert and Hafrén research teams clearly showed that polysaccharides can be modified *via* Click chemistry. Both azide and terminal alkyne functional groups can be introduced and the CuAAC reaction still occurs despite steric hindrance.

The Click coupling approach was used to develop curdlan (polysaccharide; known also as β-1,3-glucan) derivatives having various functional modules (β-lactoside, ferrocene, pyrene, and porphyrin). These biomaterials were reported to have interesting structural features (rigid and triple-stranded helical structure, etc.), pharmaceutical effects (anticancer activity, etc.), and binding properties (with polynucleotides, single-walled carbon nanotubes, etc.).[124]

Recently, Click chemistry has been used as a cross-linking reaction to obtain hydrogels based on hyaluronan, also called hyaluronic acid (HA). An azide and an alkyne derivative of HA were obtained by amidation reaction in aqueous solution of HA using an amino-azide bifunctional linker and propargylamine, respectively. The results

showed that the resulting gels are useful materials for controlled drug release of therapeutically relevant biomolecules as well as for cells scaffolding in tissue engineering. It was also claimed that the amount of Cu(I) used in this study showed not to be toxic for the yeast cells, nor for red blood cells.[125]

Polysaccharide-block-polypeptide copolymers were developed using Click chemistry. The copolymers was shown to have ability to self-assemble into small vesicles to construct a new generation of drug and gene-delivery systems with a high affinity for the surface glycoproteins of living cells.[126] In this work, dextran and poly(γ-benzyl L-glutamate) (PBLG) were used as model blocks. An alkyne group was introduced at the reducing end of dextran. PBLG that was end-functionalised with an azide group was obtained through the ring opening polymerisation of γ-benzyl L-glutamate N-carboxylic anhydride initiated by 1-azido-3-aminopropane. Dextran and PBLG were then coupled in DMSO at ambient temperature in the presence of copper(I) catalyst (CuBr) and the ligand pentamethyldiethylenetriamine (PMDETA) to produce dextran-b-PBLG copolymer.

It was also reported that Click chemistry is a facile method to incorporate a hydrophobic substitution (phenyl derivative) on β-cyclodextrin. The modified β-cyclodextrin obtained in this way exhibited self-assembly behaviour in polar solvents such as water and DMSO.[127]

CuAAC as well as metal-free coupling reaction were used for the decoration of Chitosan-*g*-PEG nanostructures with various bioactive molecules and probes under physiological conditions. The study claimed to represent a step forward in the development of environmentally friendly bioconjugation technologies for the preparation of immunonanoparticles.[128]

Click chemistry was also applied in heterogeneous conditions to prepare a biodegradable material. This approach involved the grafting of the surface of cellulose fibres by PCL macromolecular chains *via* CuAAC. The cellulose substrate bearing multiple acetylene functionalities was prepared by esterification reaction with undecynoic acid. In parallel, a commercially available PCL-diol was converted to azido-derivative. Finally, cellulose ester was reacted with azido-PCL grafts in heterogeneous conditions *via* Click chemistry to produce the biodegradable composite which was then fully characterised.[129]

### 1.6. Combination of Click Chemistry with Living Controlled Polymerisation Reactions

Living polymerisation is a chain polymerisation that proceeds in the absence of termination or chain transfer reactions. Therefore, once the monomer has been consumed, the propagating polymer chain end remains active.
The important features of living polymerisations can be summarised as following:[130]

- The polymerisation proceeds until all of the monomer has been consumed, and further addition of monomer results in continued polymerisation.
- The number average molecular weight ($M_n$) is a linear function of conversion and thus the molecular weight can be controlled by the stoichiometry of the reaction.
- The number of active centres remains constant and is independent of conversion.
- The resultant polymers have narrow molecular weight distributions.
- Block copolymers can be prepared by sequential addition of monomers.

Therefore, chain-end functionalised polymers can be prepared by the appropriate choice of initiators and terminating agents. Click chemistry has been shown to complement the different types of controlled polymerisation reactions to generate a wide range of macromolecular architectures.[131, 132]

#### 1.6.1. Radical Polymerisations

During the last decade, controlled radical polymerisation (CRP) techniques such as nitroxide mediated polymerisation (NMP),[133] atom transfer radical polymerisation (ATRP),[134, 135] and reversible addition fragmentation transfer polymerisation (RAFT),[136-138] have been proven to be very efficient techniques for the preparation of functional polymers. In particular, due to the CRP mechanism, polymer chains prepared by such techniques are end-capped by a ‘‘dormant’’ unit (a halogen atom in ATRP, an alkoxyamine moiety in NMP, a dithioester moiety in RAFT), which can be transformed into diverse functional groups, including azide and alkyne groups, after polymerisation.

NMP is a metal free polymerisation technique. This process relies on the reversible capture of the propagating species by nitroxides with formation of dormant chains (alkoxyamines) (Scheme 1.7). Whenever this equilibrium is shifted toward the dormant form, the stationary concentration of the active species is low and the irreversible chain termination is limited.[133, 139]

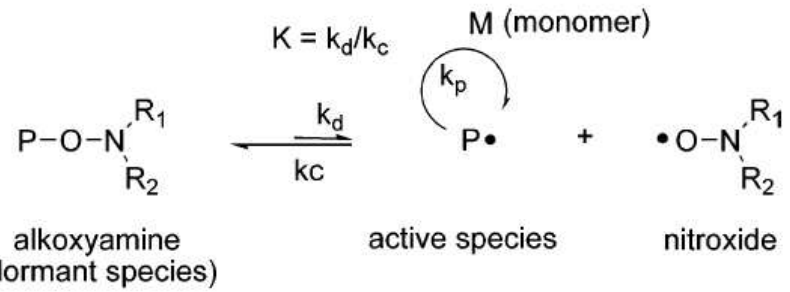


**Scheme 1.7.** Mechanism of NMP

The initiation step occurs either by bimolecular or unimolecular mechanism. The bimolecular initiation requires combining a traditional free radical initiator (e.g., benzoyl peroxide (BPO) and 2,2′-azobis(isobutyronitrile) (AIBN)) with a nitroxide (e.g., 2,2,6,6-tetramethylpiperidinyloxy (TEMPO)). On the other hand, thermolysis of a well-defined unimolecular initiator, typically an alkylated nitroxide or alkoxyamine, releases both the initiating radical and the nitroxide in a 1/1 molar ratio. NMP mediated by TEMPO was limited by slow polymerisation (25-70 h), high polymerisation temperature (125-145 °C), and a limited range of suitable monomers, mainly styrene and derivatives. Other nitroxides have been developed to extend NMP to acrylate monomers (such as *N*-*tert*-butyl-*N*-(1-diethylphosphono-2,2-dimethylpropyl)-*N*-oxyl (DEPN), 2,2,5,5-tetramethyl-4-phenyl-3-azahexane-3-oxyl (TIPNO), and *N*-*tert*-butyl-(1-*tert*-butyl-2-ethylsulfinyl)propyl nitroxide (BESN)).[133, 139]

Few examples have been reported for the combination of NMP and Click reaction.[140, 141] For instance, various copolymers (e.g., the water-soluble terpolymer **20**) were prepared by NMP to enable the direct introduction of the terminal acetylenic moieties after deprotection with tetrabutylammonium fluoride (TBAF). Subsequent attachment of azido-moieties **21** was effected using $(Ph_3)_3CuBr$ and DIPEA **22** to produce a large variety of different polymers **23** in high yields, Scheme 1.8.

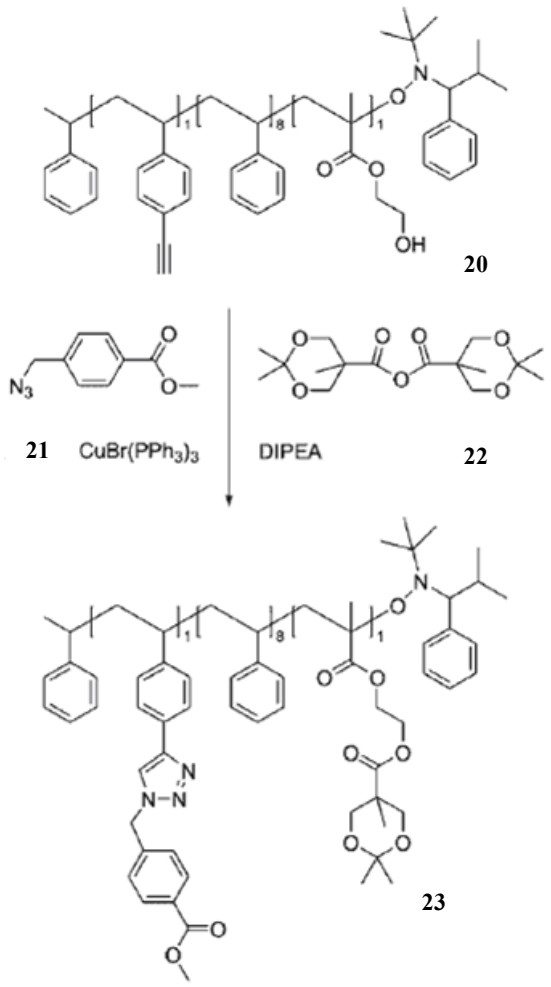


**Scheme 1.8.** Synthesis of copolymers *via* combination of NMP and Click chemistry

The general mechanism for ATRP is shown in Scheme 1.9. The radicals, or the active species, are generated through a reversible redox process catalysed by a transition metal complex ($Mt^n$−Y/Ligand, where Y may be another ligand or the counterion) which undergoes a one electron oxidation followed by abstraction of a halogen atom, X, from a dormant species, R-X. Several transition metals can catalyse the process, but Cu(I) complexes received the most attention.[134] This process occurs with a rate constant of activation, $k_{act}$, and deactivation $k_{deact}$. Polymer chains grow by the addition of the intermediate radicals to monomers in a manner similar to a conventional radical polymerisation, with the rate constant of propagation $k_p$. Termination reactions ($k_t$) also occur in ATRP, mainly through radical coupling and disproportionation; however, in a well-controlled ATRP, no more than a few percent of the polymer chains undergo termination. Other side reactions may additionally limit the achievable molecular weights. Typically, no more than 5% of the total growing polymer chains terminate during the initial, short, nonstationary stage of the polymerisation. This process generates oxidised metal complexes, $X\text{-}M_t^{n+1}$, as persistent radicals to reduce the

stationary concentration of growing radicals and thereby minimise the contribution of termination. A successful ATRP will have not only a small contribution of terminated chains, but also a uniform growth of all the chains (narrow PDI), which is accomplished through fast initiation and rapid reversible deactivation.[135]

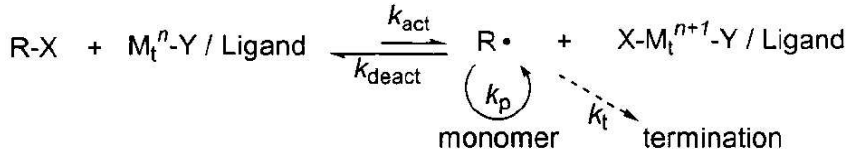


**Scheme 1.9.** Transition metal catalysed ATRP

ATRP has been extensively used in conjunction with Click chemistry. This is probably due to both techniques are mediated by Cu(I). Moreover, the chain ends of polymers prepared using ATRP containing halogen can be easily transformed into azides to form what is known as azido-telechelic polymers. One example of this approach has been reported by Lutz et al., Scheme 1.10.[70, 94] Polystyrene (PS) with PDI of 1.11 was prepared by ATRP using CuBr/PMDETA, featuring a terminal bromine end-group **24**. Subsequent nucleophilic substitution of the bromine formed azido-telechelic polymer **25**. Click reaction with various terminal acetylenes was then conducted on polymer **25** using the the CuBr/4,4′-di-(5-nonyl)-2,2′- bipyridine catalytic system in THF as solvent, giving the final polymer **26** in quantitative yield.

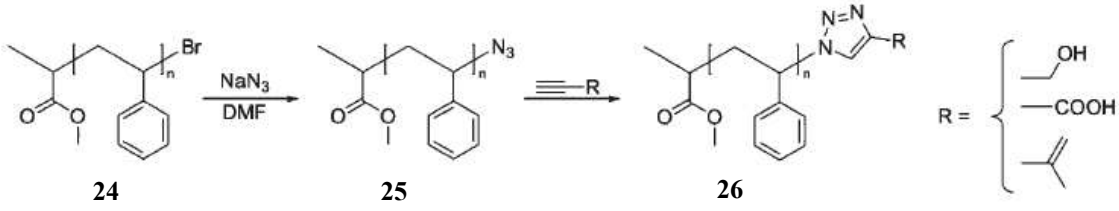


**24** **25** **26**

**Scheme 1.10.** Transformation of bromine end-functional polystyrene into various functional polymers

The incorporation of clickable functionality throughout a polymer chain is another approach to combine Click chemistry with ATRP. This can be generally accomplished by polymerising azide or alkyne functionalised monomer. One of the first examples of this strategy involved the synthesis 3-azidopropyl methacrylate **27** followed by ATRP to produce polymer **28** in a good yield and acceptable PDI of 1.33.[142] Polymer **28** was further functionalised *via* Click chemistry with several alkynes, Scheme 1.11.

However, the ATRP of commercially available propargyl methacrylate was also attempted, but this resulted in polymers with high polydispersities, which was explained by the participation of the acetylene group during polymerisation.

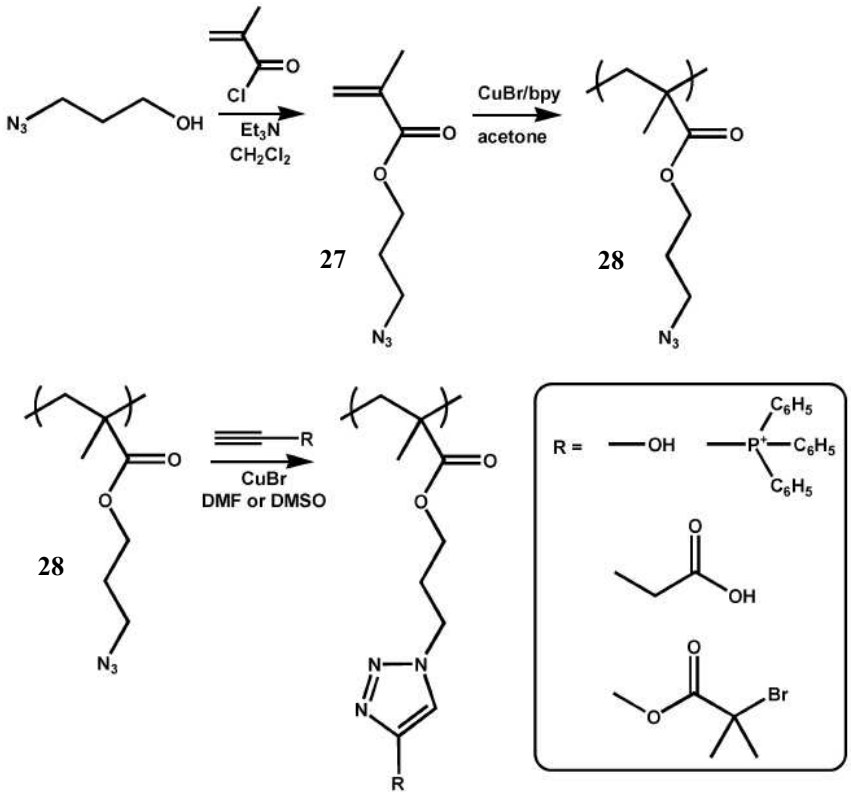


**Scheme 1.11.** ATRP of 3-azidopropyl methacrylate followed by post-polymerisation functionalisation *via* Click reaction with various alkynes

Haddleton and co-workers[143] reported a method which involves incorporation of the azide moiety in the initiator for ATRP. The azide containing ATRP initiators **31** were used to polymerise methyl methacrylate *via* the N-alkyl-2-pyridylmethanimine CuBr-initiating system, to yield polymers **32**, Scheme 1.12. The initiating efficiency of **31b** was found to be higher than those of **31a**, presumably because of steric effects. Subsequent Click reaction upon addition of terminal alkynes gave the final polymers **33** in quantitative yields, relying on the residual Cu(I) catalyst present from the ATRP reaction.

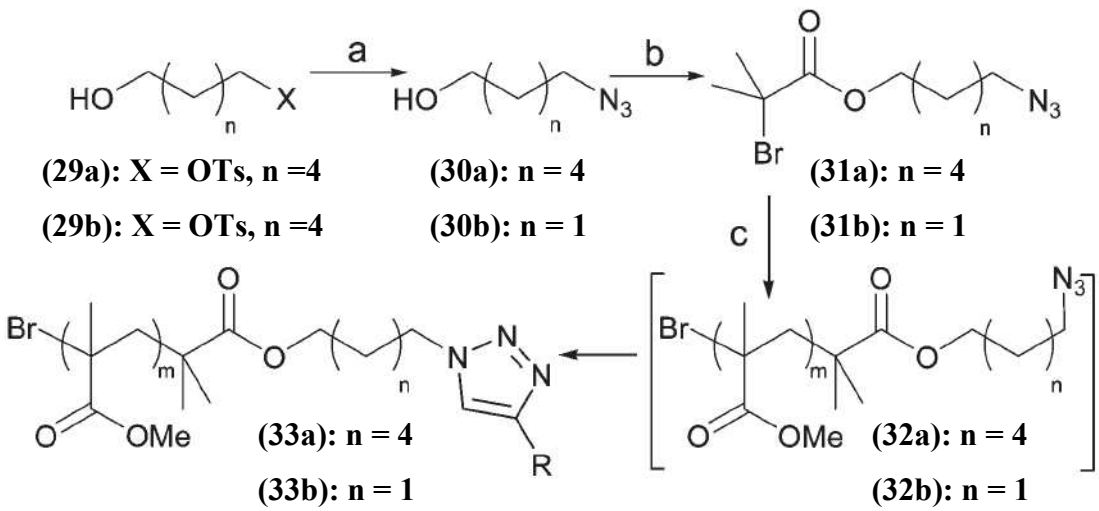


Reagents and conditions: a) $NaN_3$, acetone–water, reflux, b) 2-bromoisobutyryl bromide, $Et_3N$, $Et_2O$, 0 $^oC$ to ambient temperature, c) i. methyl methacrylate, N-alkyl-2-pyridylmethanimine–CuBr; ii.RC≡CH.

**Scheme 1.12.** Synthesis of azide functionalised ATRP initiator followed by ATRP and Click reactions

Similar strategies have been applied *via* combining ATRP and Click chemistry to produce different end-functional polymers and different polymer architectures including block, graft, star and brush polymers.[144-149]

The major limitation of the application of polymers, made by ATRP, as biomaterials has been the copper contaminations of the final product. Traditional ATRP techniques require relatively large amounts of copper catalyst (typically 0.1–1 mol% vs. monomer). Recently, considerable effort has been devoted to decrease the amount of copper catalyst used in ATRP systems.[150] The activators regenerated by electron transfer (ARGET) ATRP,[151] which involves an excess of reducing agent (such as tin octoate, ascorbic acid, or copper(0)), relative to the catalyst, is reported to continuously regenerate the activators by reduction of the copper(II) that accumulate because of unavoidable radical termination. In initiators for continuous activator regeneration (ICAR) ATRP,[152] a source of organic free radicals is employed to continuously regenerate the copper(I) activator which is otherwise consumed in termination reactions when catalysts are used at very low concentrations. These techniques have been coupled with different purification strategies such as passing through a column filled with neutral alumina, stirring with an ion exchange resin, or reprecipitation method to remove / eliminate the copper contamination at ppm level in the polymeric material.[153]

RAFT polymerisations were first reported in 1998 by the CSIRO group.[154] The general mechanism for RAFT polymerisation is shown in Scheme 1.13.[138] The first step of polymerisation is the initiation step, where a radical is created. Many different sources of initiation have been reported for RAFT polymerisation, however, the thermal decomposition of radical initiators is the most widely adopted method of initiation, due to the commercial availability of such compounds (e.g. AIBN). The oligomeric radicals produced in the initiation step react with the RAFT agent **34** in a step of initialisation (step 2). RAFT agents are organic compounds possessing a thiocarbonylthio moiety. The R group initiates the growth of polymeric chains, while the Z group activates the thiocarbonyl bond toward radical addition and then stabilises the resultant adduct radical. RAFT agents are consumed in this step before any propagation commences. This is due to the highly reactive C=S bond of the RAFT agent, which means that radical addition is favoured over the addition to any of the double bonds that are present on the monomer. The radical intermediate **35** can fragment back to the original RAFT agent **34** and an oligomeric radical or fragment to yield an oligomeric RAFT agent **36** and a reinitiating R radical. The structure of R should be such that it is a good reinitiating group. It should fragment at least as quickly as the initiator or polymer chains from the stabilised radical intermediate **35**. Following initialisation, polymer chains grow by adding monomer (step 3), and they rapidly exchange between existing growing radicals (as in the propagation step) and the thiocarbonylthio group capped species **37** (step 4). The rapid interchange in the chain transfer step ensures that the concentration of growing radical chains is kept lower than that of the stabilised radical intermediates **37**, therefore limiting termination reactions. Although limited, termination reactions still occur v*ia* combination or disproportionation mechanisms (step 5).[136-138]

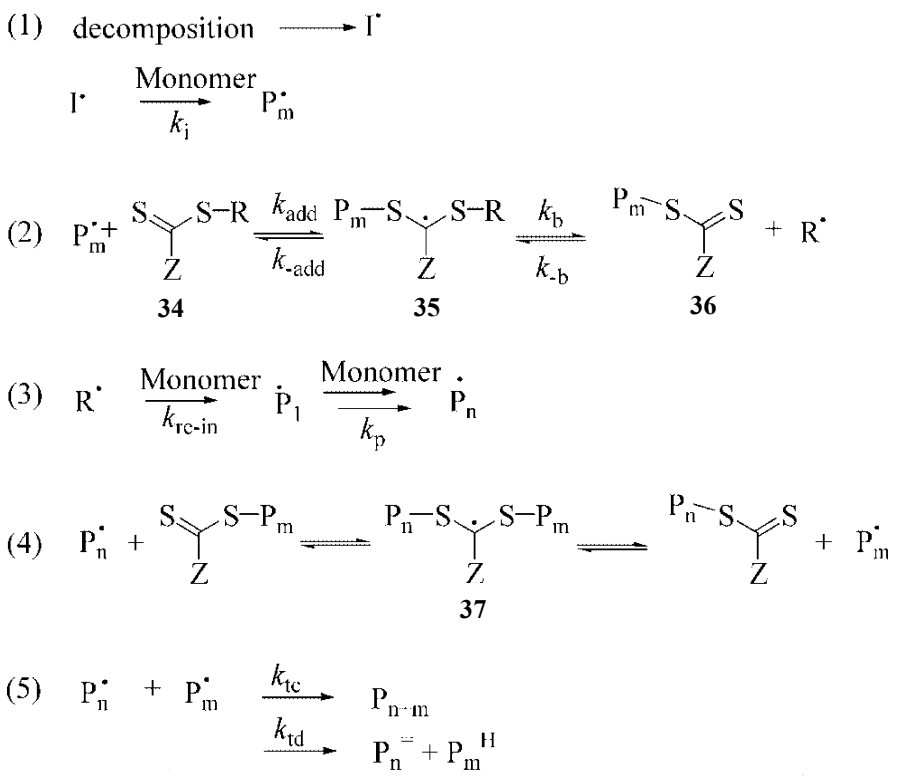

**Scheme 1.13.** The general mechanism for RAFT polymerisation

A combination of RAFT and Click reaction has been reported, taking advantage of the RAFT polymerisation process.[141] However, protection of the terminal acetylene moiety as a trimethylsilyl derivative was required. The final Click reaction resulted in the corresponding coumarin derivative within a block-copolymeric micelle.[141]

### 1.6.2. Ring Opening Polymerisation (ROP)

ROP of cyclic esters can be done in mild conditions and high molecular weight aliphatic polyesters can be prepared in short periods of time often with useful functional groups. ROP is a particularly attractive method for the synthesis of aliphatic polyesters because it uses living polymerisation which can be used to control a polymers physical properties and polydispersity index. The thermodynamic driving force for the ring opening relieves ring strain. For instance, four membered rings, such as β-propiolactone, have higher ring strain and so have a larger driving force for ROP compared with the six membered ring of lactide.[155]

The general mechanism for ROP involves either initiation by a cationic, anionic or coordination-insertion mechanism. The use of living ionic ROP is limited, due to the harsh reaction conditions required, such as an oxygen-free environment and very low

temperatures as well as the need for a high level of monomer purity.[42, 44, 61] The coordination-insertion ROP produces high molecular weight polymers. The mechanism works by the coordination of a lactone or lactide (as an example) to a Lewis acidic metal alkoxide complex, which activates and attacks the ring at the carbonyl carbon. Acyl bond cleavage results in ring opening and a new metal alkoxide species is formed which enables the cycle to reinitiate, Scheme 1.14.[155] A number of metal alkylalkoxide or metal alkoxide initiators fulfil criteria required for the living process,[156] such as $R_nAl(OR')_{3-n}$, $R_nSn(OR')_{3-n}$, $Fe(OR)_3$ and $Ti(OR)_4$.[157]

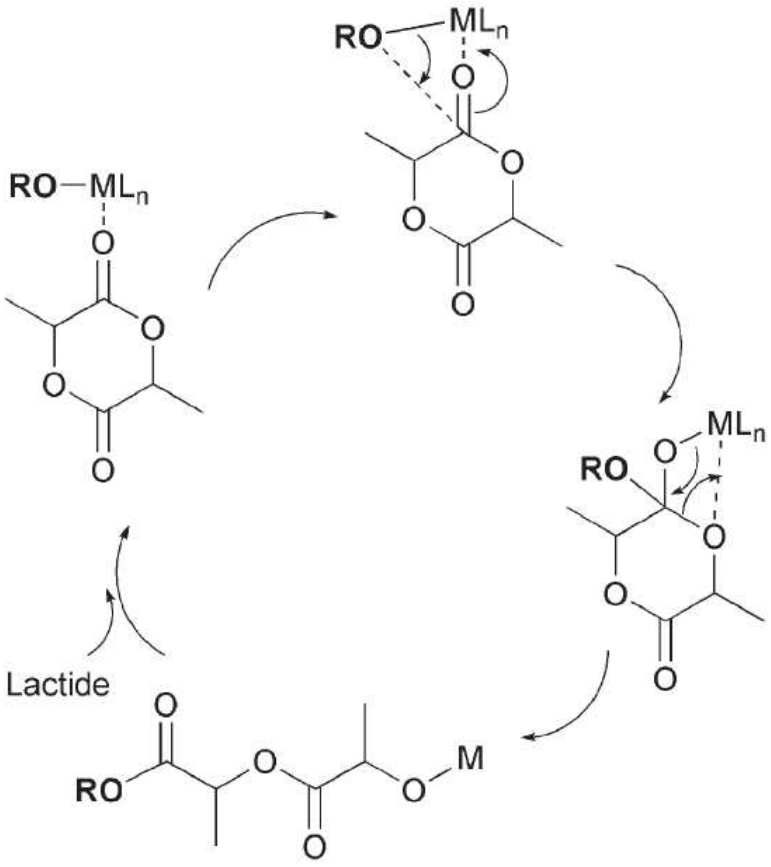


**Scheme 1.14.** Coordination–insertion mechanism for ROP of lactide

When $Sn(Oct)_2$ is used in conjunction with an alcohol, ROH, as the initiating system, the two react together *in-situ* to form a stannous alkoxide, $Sn(OR)_2$, and octanoic acid. Once formed, the final $Sn(OR)_2$ alkoxide then becomes the 'true' initiating species in the ROP of the cyclic ester monomer. The mechanism of ROP using stannous octoate is well thought to be of the coordination-insertion type.[158]

ROP has been used to prepare aliphatic polyesters bearing azides or terminal alkynes either along the chains or at the chain-ends. Different strategies have been

implemented to introduce these functionalities, such as end-group functionalisation and polymerisation of functional monomers.[159] Click chemistry methods have been subsequently applied on these functionalised polyesters to prepare a new class of degradable polymers. Moreover, Click chemistry has been proven to be a very effective strategy for derivatising biodegradable aliphatic polyesters, without degradation.[160]

The first example of derivatisation of aliphatic polyesters by Click reactions under very mild conditions has been reported by Lecomte and co-workers.[161-163] They grafted a wide range of functional groups; cationic, anionic or neutral onto PCL and PLA without any protection/deprotection reactions. This involved ROP of a functionalised caprolactone monomer followed by Click reaction with different functionalities, Scheme 1.15.

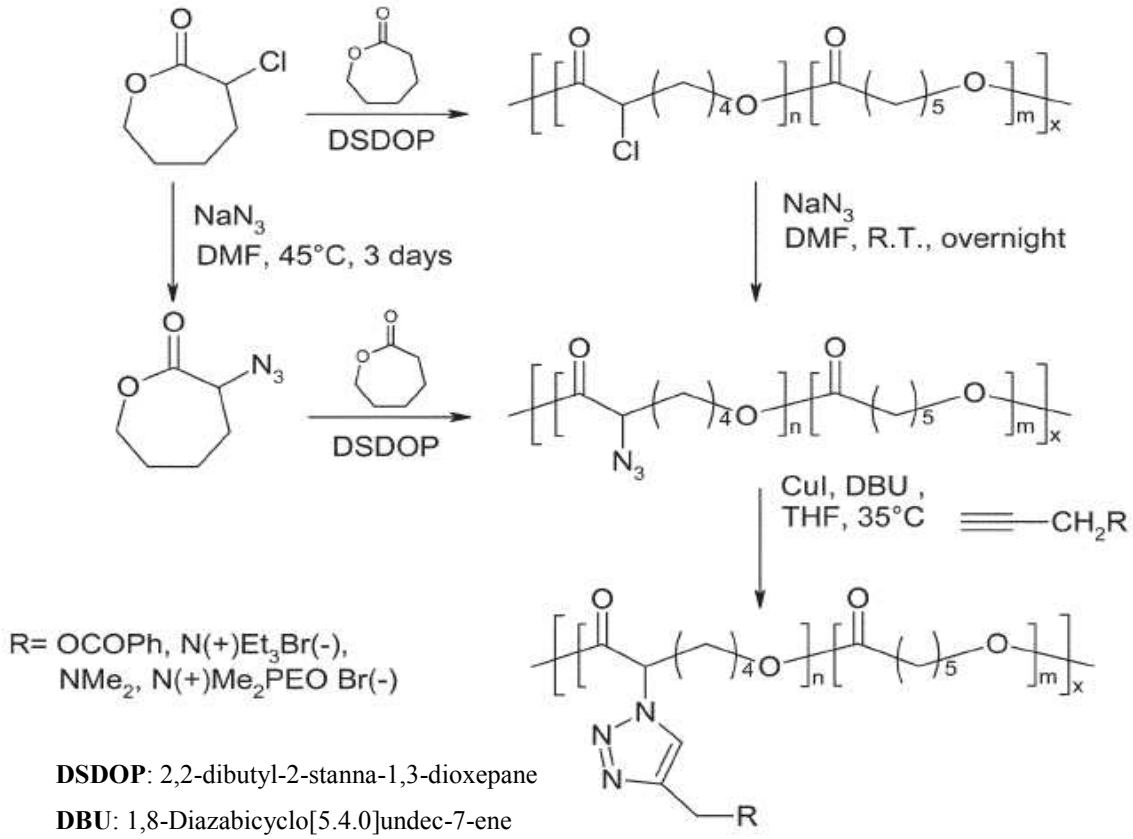


**Scheme 1.15.** Combination of ROP with Click reaction towards derivatisation of PCL

### 1.6.3. Ring Opening Metathesis Polymerisation (ROMP)

Olefin metathesis is a catalytically induced bond reorganisation process, which provides an effective pathway to the redistribution of carbon-carbon double bonds.[164-167] The metathesis reaction can be applied to all types of olefinic compounds, and the field of olefin metathesis is now categorised into four broad groups;[168] Cross Metathesis (CM) of acyclic alkenes, Ring Closing Metathesis (RCM) of acyclic dienes, Ring Opening Metathesis Polymerisation (ROMP) of cyclic olefins and Acyclic Diene Metathesis (ADMET) polymerisation, Scheme 1.16. Since its discovery, olefin metathesis has received widespread attention and has developed into a powerful technique for both organic and polymer synthesis.

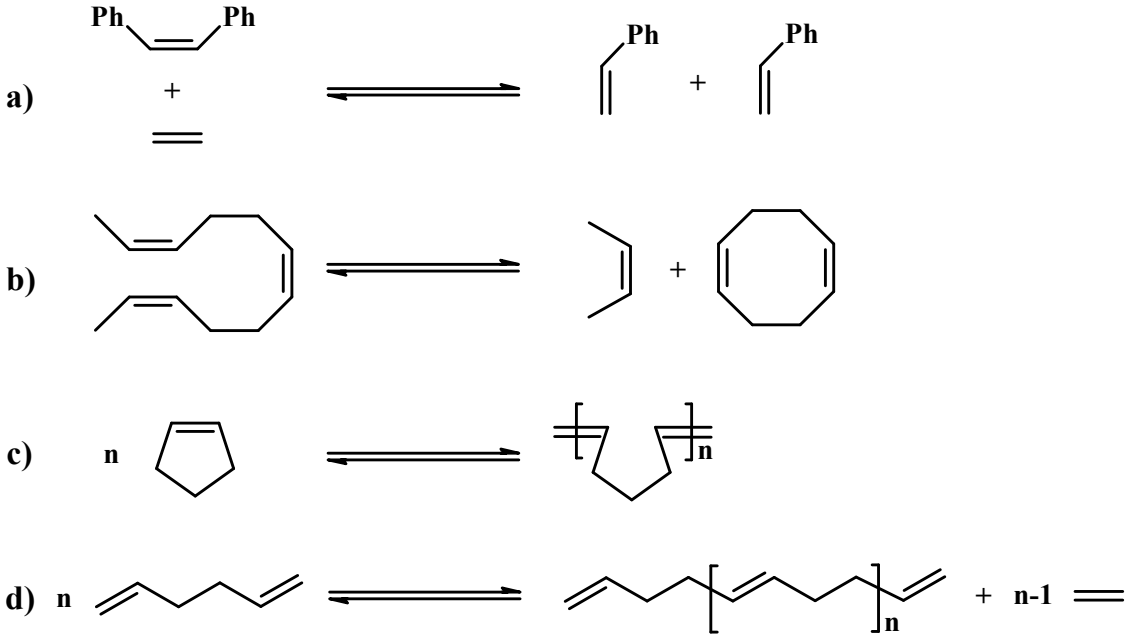


**Scheme 1.16.** Examples of a) Cross Metathesis, b) Ring Closing Metathesis (RCM), c) Ring Opening Metathesis Polymerisation (ROMP) and d) Acyclic Diene Metathesis (ADMET) polymerisation

The widely accepted mechanism for olefin metathesis has been proposed by Herisson and Chauvin in 1971.[169] The olefinic carbon-carbon double bond reacts with this metal alkylidene-species in a reversible [2+2] cycloaddition, to form a metallacyclobutane species. The four-membered ring can then open either non-productively (degeneratively) to regenerate the original reagents, or productively to form a new olefin and a new metal alkylidene species, Scheme 1.17.

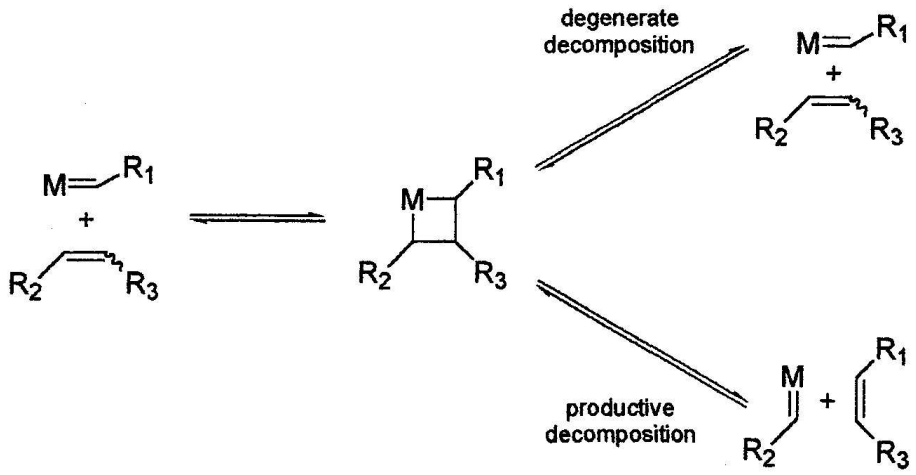


**Scheme 1.17.** Mechanism of olefin metathesis

ROMP of strained cyclic, bicyclic or multicyclic monomers result in ring scission and the formation of unsaturated linear polymers. Productive cleavage of the metallacyclobutane species formed when cyclic olefins undergo [2+2] cyclo-addition with metal-alkylidenes, leads to ring opening of the olefin, Scheme 1.18.[170]

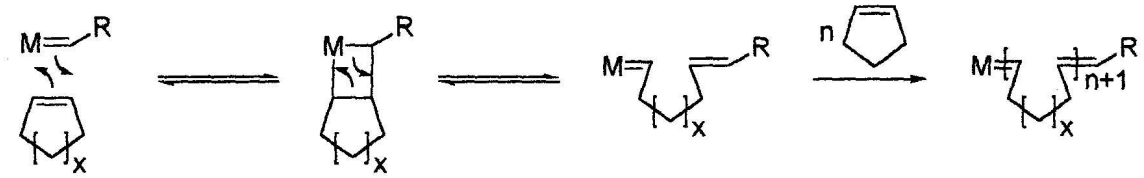

**Scheme 1.18.** Mechanism of ROMP of strained cyclic olefins

The high ring strain in norbornene derivatives means that the reactions are not reversible and the polymerisations go to completion. In some cases, secondary metathesis reactions, between the metal-alkylidene and double bonds contained within the polymer backbone, can occur intra- and/or intermolecularly (backbiting). This broadens the molecular weight distribution of the polymer and induces the formation of cyclic oligomers.

Metathesis initiators are classified in two categories; the ill-defined "classical initiators", and the more recently developed single component "well-defined initiators".

The ill-defined "classical initiators" are so named because the precise nature of the active site at the metal centre is not known, and is formed *in-situ* prior to reaction. Classical initiator systems are usually based on chlorides, oxides or oxychlorides of

transition metals, such as $WCl_6$, $MoCl_5$, $WOCl_4$ and $ReCl_5$.[164] A co-catalyst is required to activate the systems, and this is normally an organometallic compound or a Lewis acid such as $Me_4Sn$. Ill-defined systems do not provide control over molecular weight and molecular weight distribution and is further compounded by the occurrence of intra- and/or intermolecular backbiting reactions.[171] However, these catalytic systems do find applications both in industry[172] and academia,[173] due to their low cost and simple preparation.

Well-defined initiators have proved to be more successful in the field of olefin metathesis than their classical counterparts. In contrast to ill-defined initiators, the exact nature of the active site of single component well-defined initiators is fully understood.[174, 175] Different well-defined initiators have been developed based upon Molybdenum, Tungsten, Tantalum, and Ruthenium.[176-179] Therefore, it is now possible to perform living ROMP and control the polymer molecular weight distribution and tacticity.

Ruthenium initiators were found to have better functional group tolerance relative to early transition metal initiators such as titanium, tungsten and molybdenum. They have been intensively used as ROMP initiators.[180] Ruthenium complexes react preferentially with carbon-carbon double bonds over most other functionalities, which make these initiators unusually stable toward alcohols, amides, aldehydes, and carboxylic acids.

Grubbs 1$^{st}$ generation ruthenium initiator (**G-I)**, Fig. 1.4, polymerises strained cyclic olefins to produce polymers with PDI of ~1.20 and it fulfills the general criteria for a living system.[181] Grubbs 2$^{nd}$ generation initiator (**G-II)**, Fig. 1.4, displays dramatically improved thermal stability and inertness towards oxygen and moisture compared to **G-I**.[182-184] **G-II** is capable of performing ROMP of norbornene derivatives at very fast rates. However, the rate of propagation is usually far higher than that of initiation ($^1$H-NMR spectroscopy indicated that generally, less than 5% of the complex initiates before the ROMP of the monomer reaches completion) and backbiting may also occur to some degree.[185] Therefore, in some cases, polymers with broad molecular weight distributions are obtained.[186]

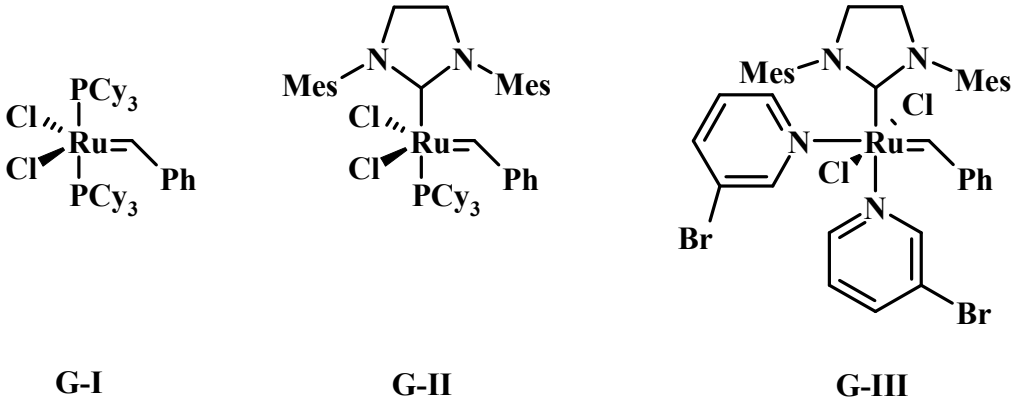


**G-I** **G-II** **G-III**

**$PCy_3$ = tricyclohexylphosphine** **Mes = 2,4,6-trimethylphenyl**

**Figure 1.4.** Structure of Grubbs ruthenium initiators **G-I − G-III**

The high steric hindrance present in macromonomers can, in some cases, hinder ROMP initiated by **G-I** resulting in slow and incomplete polymerisation.[185] Nevertheless, this steric hindrance becomes beneficial for polymerisations initiated by **G-II** because it lowers $k_p$ relative to $k_i$ and suppresses chain transfer reactions, resulting in well-controlled polymerisations.[187]

The replacement of $PCy_3$ ligand with two pyridine ligands, in particular 3-bromopyridine (3-BrPyr) in **G-II**, gave Grubbs 3$^{rd}$ generation initiator (**G-III)**, Fig. 1.4, which exhibits high reactivity, fast initiation and high functional group tolerance. In contrast to **G-II**, the polymerisations, performed by **G-III** complex, exhibit much higher values of $k_i$ relative to $k_p$ and result in the formation of polymers with narrow molecular weight distributions (PDI of ~1.05).[188, 189]

The mechanism of ROMP mediated by **G-I** to polymerise norbornene was established and followed up step-by-step using $^1$H-NMR.[190, 191] The initiation step in ROMP involves the dissociation of $PCy_3$ from **G-I** to enable the double bond of the monomer unit to react with the ruthenium-carbon double bond *via* a [2+2] cyclo-addition reaction to form a metallacyclobutane species. The productive cleavage of this four-membered ring results in the formation of a new alkylidene species, called the propagating alkylidene, Scheme 1.19. The initiation step can be clearly observed by $^1$H-NMR as the characteristic alkylidene proton resonance of the initiator (19.99 ppm) is converted into propagating alkylidene resonances, which typically appear between 19.5 and 18.0 ppm.

The propagation step involves the insertion of subsequent monomer units into the active polymer chain-end which occurs *via* a [2+2] cyclo-addition reaction, Scheme 1.19. The consumption of the monomer can be seen by the decrease of the sharp olefinic resonances of the monomer as the intensity of the broad polymeric olefinic resonances increase in the $^{1}$H-NMR spectra.

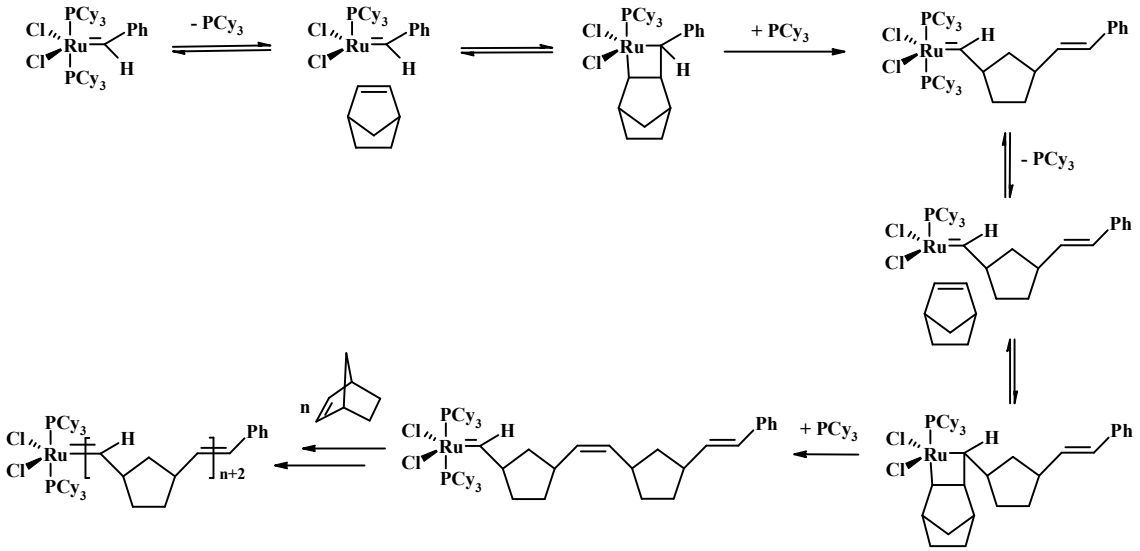


**Scheme 1.19.** The initiation and propagation steps for ROMP of norbornene using **G-I**

The reaction can be terminated by addition of an acyclic olefinic terminating agent, most commonly, ethyl vinyl ether. The reaction of propagating ruthenium alkylidene species with ethyl vinyl ether produces almost exclusive $CH_2$ end- capped polymer. Termination can be observed by $^{1}$H-NMR spectroscopy as the resonance due to the protons of the propagating alkylidene species (19.5 − 18.0 ppm) disappears and the only alkylidene species present in the system is $RuC1_2(PCy_3)_2(CHOEt)$ which typically appears at 14.58 ppm.

Few examples have been reported that combine Click chemistry with ROMP. Binder et al.[192, 193] have demonstrated an efficient method for the preparation of side chain functionalised polyoxanorbornenes. Two different approached were applied to combine Click chemistry with ROMP: (a) the attachment of functional groups, such as hydrophobic and hydrogen bonding units (supramolecular receptors) by Click reactions to 7-oxynorbornenes bearing acetylenes and subsequent ROMP yielding the final polymers; (b) the ROMP polymerisation furnishing first polyoxynorbornenes bearing acetylenic and azido moieties and subsequently attaching the functional units by use of the Click reactions onto the modified polymers, Scheme 1.20.

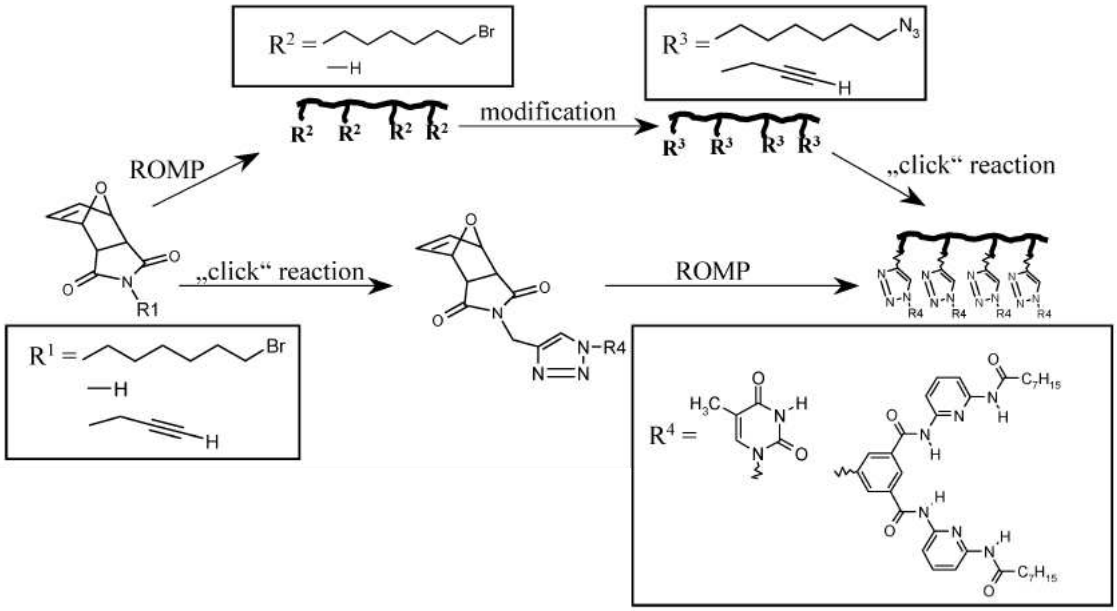


**Scheme 1.20.** The two suggested approaches to combine Click chemistry with ROMP

### 1.7. Brush Polymers

Cylindrical (bottle) brush polymers are special class of graft copolymers which have attracted considerable attention from polymer chemists due to their unique properties and potential applications.[194-197] They are one-dimensional macromolecules in which multiple polymer chains are grafted to the polymer backbone. The side chains are distributed densely enough so that they are stretched away from the backbone to form a brush-like conformation.[135, 198-205] Generally, there are three different grafting strategies: "grafting from", "grafting onto", and "grafting through", Scheme 1.21.[204, 206, 207] The "grafting from" strategy involves the growth of side chains from polymeric backbones with pendant initiation sites. This strategy has been widely used as a technique for the preparation of brush polymers.[208-213] The only downside for this strategy is the possible limited initiation efficiency from the pendant initiation sites due to their high density.[195, 214] The "grafting onto" method has the advantage of allowing for individual preparation of backbone polymers and side chains. The down side is that the grafting becomes progressively more difficult as the conversion increases, leading to limited grafting density, even when a large molar excess of side chains is used. Among these three methods, only "grafting through", known as the macromonomer approach, guarantees complete grafting (e.g., one side chain per repeating unit). Additionally, this approach can afford the most precise and easiest control of side chain and main chain lengths, provided that the polymerisation is efficient and controlled. However, synthesis of

polymacromonomers with a high DP and low PDI remains synthetically challenging, largely because of the inherently low concentration of polymerisable groups and the demanding steric hindrance of side chains.

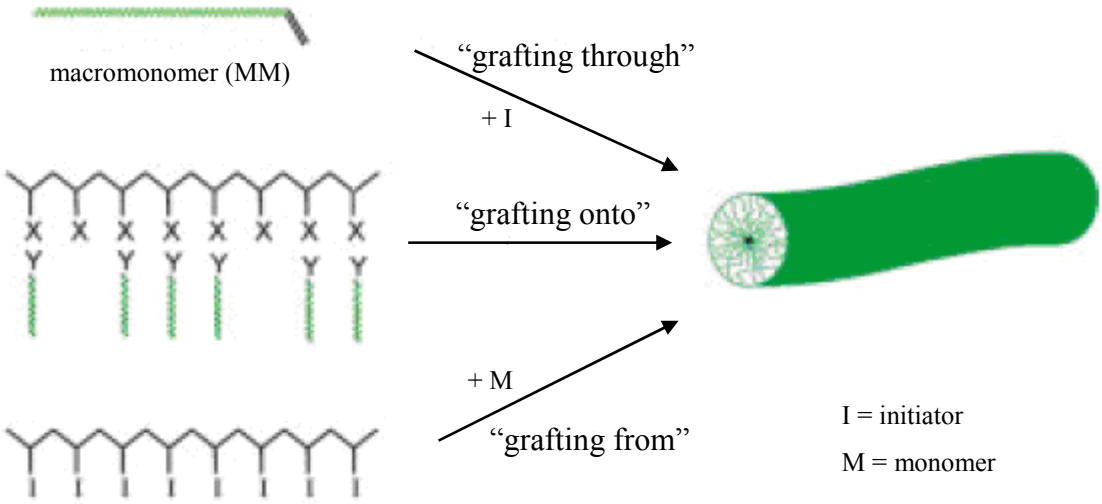


**Scheme 1.21.** Strategies for the synthesis of cylindrical polymer brushes

There are numerous examples of polymer brushes in the literature prepared *via* controlled polymerisation techniques.[215-217] However, relevant to the work presented in this thesis, Grubbs et al.[218] have recently reported the preparation of a variety of norbornenyl macromonomers by coupling azido-terminated polymers (such as PS, PMMA, P*t*BA) made by ATRP with alkyne-functionalised norbornene. The macromonomers were subsequently subjected to ROMP using Grubbs ruthenium initiators to produce various high molecular weight brush polymers with narrow PDI and broad range of functionalities, Scheme 1.22.

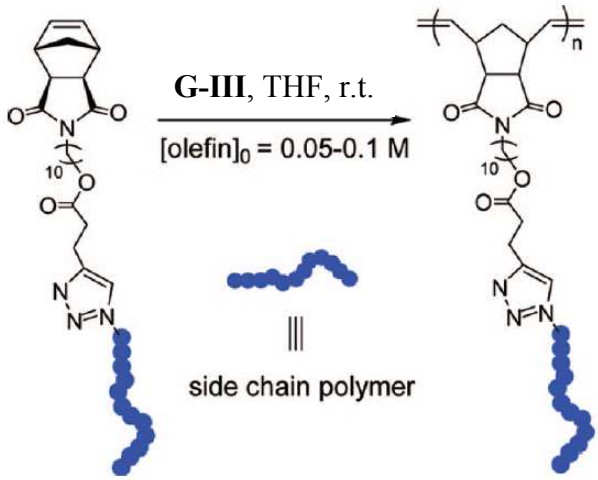


**Scheme 1.22.** Synthesis of brush polymers *via* combination of Click chemistry with ROMP

## 1.8. Stimuli Responsive Polymers

Stimuli responsive or "*smart*" polymeric systems are polymers that undergo a conformational change or phase transition in response to an external stimulus. The external stimulus can include, but is not limited to, temperature, pH, light, electrolytes (ions), other molecules (e.g. glucose) or a combination of these. The conformational changes that can be triggered in response to external stimuli usually involve ionic interactions, hydrogen bonding, hydrophobic effects, or a combination of these. The most important systems, from a biomedical point of view, are those sensitive to pH or temperature.[219] Human body presents variations on pH along the gastrointestinal tract, and also in some specific areas like certain tissues or sub-cellular compartments. Thermo-responsive polymers with critical temperature close to the physiological value offer many possibilities in the biomedical field. Therefore, the synthesis and development of these "*smart*" polymers has been the main focus of current research.[219-221]

### 1.8.1. pH-Responsive Polymers

pH-responsive polymers are polyelectrolytes that bear in their structure weak acidic or basic groups that either accept or release protons in response to changes in pH. The pendant acidic or basic groups on polyelectrolytes undergo ionisation and by generating the charge along the polymer backbone, the electrostatic repulsion between these charges results in an increase in the hydrodynamic volume of the polymer.[222] This transition between tightly coiled and expanded state is influenced by any change in pH or ionic strength.

Polyacidic polymers will be unswollen at low pH, since the acidic groups will be protonated and unionised. When increasing the pH, a negatively charged polymer will swell. The opposite behaviour is found in polybasic polymers, since the ionisation of the basic groups will increase when decreasing the pH. Typical examples of pH-sensitive polymers with anionic groups are poly(carboxylic acids) such as poly(acrylic acid) (PAA) or poly(methacrylic acid). A few examples of cationic polyelectrolytes are poly(N,N-diakyl aminoethyl methacrylates), poly(lysine), poly(ethylenimine), and chitosan.

When pH-sensitive polymeric chains are cross-linked forming hydrogels, their behaviour is not only influenced by the nature of the ionisable groups, the polymer composition, and the hydrophobicity of the polymer backbone, but also by the cross-

linking density. This affects the solute permeability in terms of bioactive compounds release in several applications; the higher the cross-linking density, the lower the permeability, especially significant in the case of high molecular weight solutes.

pH-sensitive polymers have been used in several biomedical applications, the most important being their use as drug[223, 224] and gene[225-227] delivery systems, and glucose sensors.[228]

### 1.8.2. Temperature Responsive Polymers

Polymers sensitive to temperature changes exhibit a critical solution temperature (typically in water) at which the phase of polymer and solution is changed in accordance with their composition. Those systems exhibiting one phase above certain temperature and a phase separation below it, possess an upper critical solution temperature (UCST). For instance, PAA is water soluble at ambient temperature, but will undergo phase separation upon cooling. On the other hand, polymer solutions that appear as monophasic below a specific temperature and biphasic above it, generally exhibit the so-called lower critical solution temperature (LCST). Below the LCST, the polymer chains exhibit hydrophilic state and form hydrogen bounding so they have coil conformation. However, above the LCST, the polymer chains collapse and have globule conformation, losing the hydrogen bonding and they exhibit hydrophobic state as it has been shown by Alexander et al.,[219] Fig. 1.5. These represent the type of polymers with most number of applications.[228] This *"smart"* behaviour originates from the architecture of the polymer and the balance between the hydrophilic/hydrophobic fragments.[219]

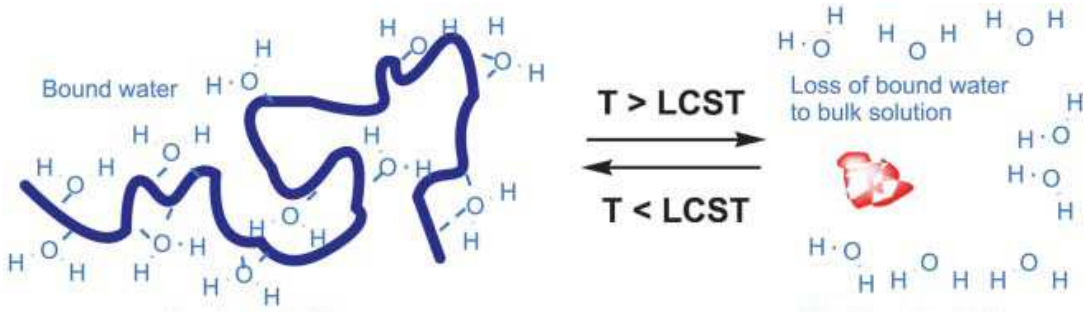


Coil Conformation
Extended Polymer Chains
Formation of H-Bonding
Hydrophilic State

Globule Conformation
Collapsed Polymer Chains
Loss of H-Bonding
Hydrophobic State

**Figure 1.5.** Schematic presentation of the phase transition in temperature responsive polymer

The temperature responsive materials with LCST in the physiological range (30 – 40 $^{o}$C) that can undergo reversible conformational or phase changes attract much attention due to their potential biomedical applications and drug delivery systems.[229, 230]

Poly(N-isopropyl acrylamide) (PNIPAM) has been the most studied temperature responsive homopolymer exhibiting a soluble-insoluble change in aqueous solution due to its molecular architecture.[231-233] However, the homopolymers of PNIPAM exhibits LCST in water around 32 $^{o}$C which is close to the lower end of the physiological range.[234] The efforts have been made to tune the LCST of PNIPAM to around 37 $^{o}$C by variation in hydrophilic or hydrophobic co-monomer content, for different biomedical applications.[235, 236] Although, PNIPAM is known to be biocompatible but strictly speaking it is not a bio-inert polymer. Indeed, the presence of multiple secondary amide functions in the molecule structure of PNIPAM may lead to the formation of cooperative H-bonding interactions with other amide containing polymers, in particular with proteins.[237, 238] Therefore, the development of new classes of temperature responsive materials for *in-vivo* delivery of various bioactive compounds remains a central challenge.

Recently, non-PNIPAM based materials have been developed to generate LCST materials.[239-243] Poly(ethylene glycol) (PEG) is a neutral, water soluble, biocompatible, non-toxic, non-immunogenic, FDA approved and probably the most widely used polymer in the biomedical applications.[65,64] Although, PEG undergoes a phase transition upon heating, the LCST ranges from 99 to 176 $^{o}$C, depending on molecular weight.[244, 245] This LCST is outside the physiological range and therefore limits its use as a temperature responsive material in medical applications.[246] However, it is possible to

tune the LCST of PEG for some applications. It has been reported that the addition of additives (such as urea, NaCl, and $KH_2PO_4$) affects the thermodynamic properties of aqueous PEG solutions.[247] Obviously, the applicability of this strategy to lower the LCST of PEG is limited because the use of external chemicals which are either undesirable or have to be removed for many applications.

In order to incorporate PEG in macromolecular constructions, two synthetic routes have been used. The first one is a macroinitiator approach, in which a PEG segment is transformed into an atom transfer radical polymerisation (ATRP) initiator.[248-252] The second route involves direct polymerisation of a radically polymerisable PEG macromonomer such as oligo(ethylene glycol) methacrylate (OEGMA).[253-255] The resulting poly(oligo(ethylene glycol) methacrylate) (POEGMA) with side chains consisting of 8/9 ethylene oxide units exhibited an LCST in water around 90 °C, which is very high for medical applications.[256] Moreover, polymers of 2-(2'-methoxyethoxy)ethyl methacrylate ($MEO_2MA$) with only two ethylene oxide units as side groups have been reported that exhibited LCST around 26 °C,[257] which is out of the physiological range and therefore, prohibits *in-vivo* applications. Recently, copolymers of $MEO_2MA$ and OEGMA have been prepared *via* ATRP with LCST in the range of 28 – 90 $^{o}$C, depending on the composition of the copolymer.[240, 258, 259] It should be noticed that all temperature responsive materials mentioned above are in fact macromolecular brushes with PEG as side chains.[204] A series of linear copolymers of ethylene and ethylene oxide has been reported with LCST in the range of 7 to 70 °C in water by controlling the hydrophobic/hydrophilic balance.[260, 261] The major disadvantage of all approaches discussed above is that PEG segments are attached through a hydrolysable ester and amide linkage, which is, in most cases, problematic for applications in aqueous media. Therefore, developing stable (non-hydrolysable) linkers is crucial if the range of applications for these polymers is to be expanded.

Recently, Click chemistry has been used to generate temperature responsive materials. Azide terminated PEG chains and 1-decyl azides have been grafted onto polyglycolide containing pendant acetylene groups. The result of the work in terms of LCST behaviour is unclear but it claimed that it was possible to produce biodegradable LCST materials with tunable transition temperatures in a range from 25 to 65 °C by adjusting the length and mole fraction of alkyl to PEG side chains.[239] Moreover, Click chemistry has been used to couple the azide containing PNIPAM with alkyne containing PEG and alkynyl-functionalised $C_{60}$ to produce self-assembled hybrid nanoparticles that retained the thermoresponsiveness of PNIPAM.[262] The work involves difficult synthesis

and produces materials, which are exactly the same as PNIPAM in terms of their temperature responsive behaviour.

We recently demonstrated, for the first time, the use of Click chemistry as a polymerisation technique to copolymerise hydrophobic and hydrophilic components based on modified trehalose and PEG to produce a linear water-soluble temperature responsive glycopolymer with LCST well within the physiological range.[120]

## 1.9. References


1. V. Ladmiral, E. Melia, D. M. Haddleton, *European polymer Journal* **2004**, *40*, 431-449.
2. Z. J. Witczak, K. A. Nieforth, *Carbohydrates in drug design*. Marcel Dekker: New York, **1997**.
3. K. L. Goa, P. Benfield, *Drugs* **1994**, *47*, 536-566.
4. T. E. McAlindon, M. P. LaValley, D. T. Felson, *Jama-Journal of the American Medical Association* **2000**, *284*, 1242-1242.
5. G. L. Brode, R. L. Kreeger, E. M. Partain, J. L. Pavlichko, *Journal of the Society of Cosmetic Chemists* **1988**, *39*, 78-78.
6. H. J. Buschmann, E. Schollmeyer, *Journal of Cosmetic Science* **2002**, *53*, 185-191.
7. E. D. Goddard, J. V. Gruber, *Principles of Polymer Science and Technology Cosmetics and Personal Care*. Dekker: New York, **1999**.
8. R. A. A. Muzzarelli, C. Muzzarelli, *Polysaccharides I: Structure, Characterization and Use*: *Advances in Polymer Science* **2005**, *186*, 151-209.
9. T. Higashiyama, *Pure and Applied Chemistry* **2002**, *74*, 1263-1269.
10. K. Kurita, N. Masuda, S. Aibe, K. Murakami, S. Ishii, S. I. Nishimura, *Macromolecules* **1994**, *27*, 7544-7549.
11. N. Teramoto, Y. Arai, M. Shibata, *Carbohydrate Polymers* **2006**, *64*, 78-84.
12. N. Teramoto, N. D. Sachinvala, M. Shibata, *Molecules* **2008**, *13*, 1773-1816.
13. N. Teramoto, M. Unosawa, S. Matsushima, M. Shibata, *Polymer Journal* **2007**, *39*, 975-981.
14. M. N. Belgacem, A. Gandini, *Monomers, polymers, composites from renewable resources*. T. Heinze, K. Petzold, *Cellulose chemistry: novel products and synthesis paths.* Elsevier, **2008**, 343–368.
15. Dow-Chemical, in *Book Union Carbide Emulsion Systems Products: Cellulosize. Available at:* http://www.dow.com/ucarlatex/prod/cello
16. S. G. Cohen, H. C. Haas, *Journal of the American Chemical Society* **1950**, *72*, 3954-3958.
17. W. E. Gloor, B. H. Mahlman, R. D. Ullrich, *Industrial and Engineering Chemistry* **1950**, *42*, 2150-2153.
18. S. Erkselius, O. J. Karlsson, *Carbohydrate Polymers* **2005**, *62*, 344-356.
19. H. Evertsson, S. Nilsson, *Carbohydrate Polymers* **1999**, *40*, 293-298.
20. K. Liedermann, L. Lapcik, *Carbohydrate Polymers* **2000**, *42*, 369-374.

21. W. B. Sun, D. J. Sun, Y. P. Wei, S. Y. Liu, S. Y. Zhang, *Journal of Colloid and Interface Science* **2007**, *311*, 228-236.
22. R. A. Dwek, *Chemical Reviews* **1996**, *96*, 683-720.
23. C. R. Bertozzi, L. L. Kiessling, *Science* **2001**, *291*, 2357-2364.
24. N. Sharon, H. Lis, *Scientific American* **1993**, *268*, 82-89.
25. N. Sharon, H. Lis, *Science* **1989**, *246*, 227-234.
26. Y. C. Lee, R. T. Lee, *Accounts of Chemical Research* **1995**, *28*, 321-327.
27. E. E. Simanek, G. J. McGarvey, J. A. Jablonowski, C. H. Wong, *Chemical Reviews* **1998**, *98*, 833-862.
28. J. Klein, M. Kunz, J. Kowalczyk, *Makromolekulare Chemie-Macromolecular Chemistry and Physics* **1990**, *191*, 517-528.
29. G. Wulff, J. Schmid, T. Venhoff, *Macromolecular Chemistry and Physics* **1996**, *197*, 259-274.
30. E. Dickinson, B. Bergenstahl, *Food colloids: proteins, lipids, and polysaccharides*. Cambridge: The Royal Society of Chemistry, **1997**, Vol. 192.
31. J. Kopecek, P. Kopeckova, H. Brondsted, R. Rathi, B. Rihova, P. Y. Yeh, K. Ikesue, *Journal of Controlled Release* **1992**, *19*, 121-130.
32. J. Murata, Y. Ohya, T. Ouchi, *Carbohydrate Polymers* **1996**, *29*, 69-74.
33. R. Bahulekar, T. Tokiwa, J. Kano, T. Matsumura, I. Kojima, M. Kodama, *Carbohydrate Polymers* **1998**, *37*, 71-78.
34. S. H. Kim, M. Goto, C. S. Cho, T. Akaike, *Biotechnology Letters* **2000**, *22*, 1049-1057.
35. J. K. F. Suh, H. W. T. Matthew, *Biomaterials* **2000**, *21*, 2589-2598.
36. H. Sashiwa, J. M. Thompson, S. K. Das, Y. Shigemasa, S. Tripathy, R. Roy, *Biomacromolecules* **2000**, *1*, 303-305.
37. M. G. Petronio, A. Mansi, C. Gallinelli, S. Pisani, L. Seganti, F. Chiarini, *Chemotherapy* **1997**, *43*, 211-217.
38. T. Yoshida, T. Akasaka, Y. Choi, K. Hattori, B. Yu, T. Mimura, Y. Kaneko, H. Nakashima, E. Aragaki, M. Premanathan, N. Yamamoto, T. Uryu, *Journal of Polymer Science Part A-Polymer Chemistry* **1999**, *37*, 789-800.
39. S. G. Spain, M. I. Gibson, N. R. Cameron, *Journal of Polymer Science Part A-Polymer Chemistry* **2007**, *45*, 2059-2072.
40. S. Slavin, J. Burns, D. M. Haddleton, C. R. Becer, *European Polymer Journal* **2010**, doi: 10.1016/j.eurpolymj.2010.09.019.

41. E. S. Place, J. H. George, C. K. Williams, M. M. Stevens, *Chemical Society Reviews* **2009**, *38*, 1139-1151.
42. A. C. Albertsson, I. K. Varma, *Biomacromolecules* **2003**, *4*, 1466-1486.
43. R. J. Pounder, A. P. Dove, *Polymer Chemistry* **2010**, *1*, 260-271.
44. A. C. Albertsson, I. K. Varma, *Degradable Aliphatic Polyesters* **2002**, *157*, 1-40.
45. C. Gottschalk, H. Frey, *Macromolecules* **2006**, *39*, 1719-1723.
46. M. Okada, *Progress in Polymer Science* **2002**, *27*, 87-133.
47. R. M. Rasal, D. E. Hirt, *Macromolecular Bioscience* **2009**, *9*, 989-996.
48. S. S. Ray, M. Okamoto, *Macromolecular Rapid Communications* **2003**, *24*, 815-840.
49. C. Schugens, C. Grandfils, R. Jerome, P. Teyssie, P. Delree, D. Martin, B. Malgrange, G. Moonen, *Journal of Biomedical Materials Research* **1995**, *29*, 1349-1362.
50. Z. P. Zhang, S. S. Feng, *Biomaterials* **2006**, *27*, 4025-4033.
51. K. J. Zhu, X. Z. Lin, S. L. Yang, *Journal of Applied Polymer Science* **1990**, *39*, 1-9.
52. R. Auras, B. Harte, S. Selke, *Macromolecular Bioscience* **2004**, *4*, 835-864.
53. B. Gupta, N. Revagade, J. Hilborn, *Progress in Polymer Science* **2007**, *32*, 455-482.
54. A. Sodergard, M. Stolt, *Progress in Polymer Science* **2002**, *27*, 1123-1163.
55. D. J. Sawyer, *Macromolecular Symposia* **2003**, *201*, 271-281.
56. D. Garlotta, *Journal of Polymers and the Environment* **2001**, *9*, 63-84.
57. E. T. H. Vink, K. R. Rabago, D. A. Glassner, P. R. Gruber, *Polymer Degradation and Stability* **2003**, *80*, 403-419.
58. K. Masaki, N. R. Kamini, H. Ikeda, H. Iefuji, *Applied and Environmental Microbiology* **2005**, *71*, 7548-7550.
59. R. M. Rasal, A. V. Janorkar, D. E. Hirt, *Progress in Polymer Science* **2010**, *35*, 338-356.
60. M. Labet, W. Thielemans, *Chemical Society Reviews* **2009**, *38*, 3484-3504.
61. K. M. Stridsberg, M. Ryner, A. C. Albertsson, *Degradable Aliphatic Polyesters* **2002**, *157*, 41-65.
62. P. Dubois, O. Coulembier, J.-M. Raquez, *Handbook of Ring-Opening Polymerization*. Wiley-VCH, **2009**, 53 - 63.
63. M. S. Kim, K. S. Seo, G. Khang, H. B. Lee, *Macromolecular Rapid Communications* **2005**, *26*, 643-648.
64. R. Duncan, *Nature Reviews Drug Discovery* **2003**, *2*, 347-360.

65. J. H. Lee, H. B. Lee, J. D. Andrade, *Progress in Polymer Science* **1995**, *20*, 1043-1079.
66. K. Knop, R. Hoogenboom, D. Fischer, U. S. Schubert, *Angewandte Chemie-International Edition* **2010**, *49*, 6288-6308.
67. J. M. Zhu, *Biomaterials* **2010**, *31*, 4639-4656.
68. K. L. Prime, G. M. Whitesides, *Journal of the American Chemical Society* **1993**, *115*, 10714-10721.
69. S. Stolnik, L. Illum, S. S. Davis, *Advanced Drug Delivery Reviews* **1995**, *16*, 195-214.
70. J. F. Lutz, H. G. Borner, K. Weichenhan, *Macromolecules* **2006**, *39*, 6376-6383.
71. R. B. Greenwald, Y. H. Choe, J. McGuire, C. D. Conover, *Advanced Drug Delivery Reviews* **2003**, *55*, 217-250.
72. S. Hiki, K. Kataoka, *Bioconjugate Chemistry* **2007**, *18*, 2191-2196.
73. F. M. Veronese, *Biomaterials* **2001**, *22*, 405-417.
74. S. Zalipsky, *Advanced Drug Delivery Reviews* **1995**, *16*, 157-182.
75. K. J. Quinn, J. M. Courtney, *British Polymer Journal* **1988**, *20*, 25-32.
76. M. Rutnakornpituk, P. Ngamdee, P. Phinyocheep, *Polymer* **2005**, *46*, 9742-9752.
77. C. R. McMillin, *Rubber Chemistry and Technology* **1994**, *67*, 417-446.
78. D. Enescu, V. Hamciuc, R. Ardeleanu, M. Cristea, A. Ioanid, V. Harabagiu, B. C. Simionescu, *Carbohydrate Polymers* **2009**, *76*, 268-278.
79. SILTECH INC. US5428142A, **1995**.
80. SHISEIDO CO LTD. JP11349450A, **1999**.
81. GIROUD, FRANCK. US20020197226A1, **2002**.
82. L'OREAL. WO2003105788A2, **2003**.
83. Unilever PLC. EP1409629B1, **2003**.
84. SHIN-ETSU CHEMICAL CO., LTD. US6066727A, **2000**.
85. H. C. Kolb, M. G. Finn, K. B. Sharpless, *Angewandte Chemie-International Edition* **2001**, *40*, 2004.
86. J. F. Lutz, H. Schlaad, *Polymer* **2008**, *49*, 817-824.
87. H. C. Kolb, K. B. Sharpless, *Drug Discovery Today* **2003**, *8*, 1128-1137.
88. R. Huisgen, *Proceedings of the Chemical Society of London* **1961**, 357.
89. V. V. Rostovtsev, L. G. Green, V. V. Fokin, K. B. Sharpless, *Angewandte Chemie-International Edition* **2002**, *41*, 2596.
90. C. W. Tornoe, C. Christensen, M. Meldal, *Journal of Organic Chemistry* **2002**, *67*, 3057-3064.

91. J. P. Collman, N. K. Devaraj, C. E. D. Chidsey, *Langmuir* **2004**, *20*, 1051-1053.
92. D. D. Diaz, S. Punna, P. Holzer, A. K. McPherson, K. B. Sharpless, V. V. Fokin, M. G. Finn, *Journal of Polymer Science Part A-Polymer Chemistry* **2004**, *42*, 4392-4403.
93. B. Helms, J. L. Mynar, C. J. Hawker, J. M. J. Frechet, *Journal of the American Chemical Society* **2004**, *126*, 15020-15021.
94. J. F. Lutz, H. G. Borner, K. Weichenhan, *Macromolecular Rapid Communications* **2005**, *26*, 514-518.
95. N. V. Tsarevsky, B. S. Sumerlin, K. Matyjaszewski, *Macromolecules* **2005**, *38*, 3558-3561.
96. P. Wu, A. K. Feldman, A. K. Nugent, C. J. Hawker, A. Scheel, B. Voit, J. Pyun, J. M. J. Frechet, K. B. Sharpless, V. V. Fokin, *Angewandte Chemie-International Edition* **2004**, *43*, 3928-3932.
97. V. D. Bock, H. Hiemstra, J. H. van Maarseveen, *European Journal of Organic Chemistry* **2006**, 51-68.
98. P. L. Golas, N. V. Tsarevsky, B. S. Sumerlin, K. Matyjaszewski, *Macromolecules* **2006**, *39*, 6451-6457.
99. W. H. Zhan, H. N. Barnhill, K. Sivakumar, T. Tian, Q. Wang, *Tetrahedron Letters* **2005**, *46*, 1691-1695.
100. H. A. Orgueira, D. Fokas, Y. Isome, P. C. M. Chan, C. M. Baldino, *Tetrahedron Letters* **2005**, *46*, 2911-2914.
101. W. S. Horne, C. D. Stout, M. R. Ghadiri, *Journal of the American Chemical Society* **2003**, *125*, 9372-9376.
102. F. Himo, T. Lovell, R. Hilgraf, V. V. Rostovtsev, L. Noodleman, K. B. Sharpless, V. V. Fokin, *Journal of the American Chemical Society* **2005**, *127*, 210-216.
103. S. Chassaing, M. Kumarraja, A. S. S. Sido, P. Pale, J. Sommer, *Organic Letters* **2007**, *9*, 883-886.
104. L. Zhang, X. G. Chen, P. Xue, H. H. Y. Sun, I. D. Williams, K. B. Sharpless, V. V. Fokin, G. C. Jia, *Journal of the American Chemical Society* **2005**, *127*, 15998-15999.
105. G. C. Tron, T. Pirali, R. A. Billington, P. L. Canonico, G. Sorba, A. A. Genazzani, *Medicinal Research Reviews* **2008**, *28*, 278-308.
106. Z. M. Li, T. S. Seo, J. Y. Ju, *Tetrahedron Letters* **2004**, *45*, 3143-3146.

107. N. J. Agard, J. A. Prescher, C. R. Bertozzi, *Journal of the American Chemical Society* **2004**, *126*, 15046-15047.

108. J. M. Baskin, J. A. Prescher, S. T. Laughlin, N. J. Agard, P. V. Chang, I. A. Miller, A. Lo, J. A. Codelli, C. R. Bertozzit, *Proceedings of the National Academy of Sciences of the United States of America* **2007**, *104*, 16793-16797.

109. N. J. Agard, J. M. Baskin, J. A. Prescher, A. Lo, C. R. Bertozzi, *Acs Chemical Biology* **2006**, *1*, 644-648.

110. S. Brase, C. Gil, K. Knepper, V. Zimmermann, *Angewandte Chemie-International Edition* **2005**, *44*, 5188-5240.

111. T. S. Seo, Z. M. Li, H. Ruparel, J. Y. Ju, *Journal of Organic Chemistry* **2003**, *68*, 609-612.

112. A. Deiters, T. A. Cropp, D. Summerer, M. Mukherji, P. G. Schultz, *Bioorganic & Medicinal Chemistry Letters* **2004**, *14*, 5743-5745.

113. A. J. Link, M. K. S. Vink, D. A. Tirrell, *Journal of the American Chemical Society* **2004**, *126*, 10598-10602.

114. S. Punna, E. Kaltgrad, M. G. Finn, *Bioconjugate Chemistry* **2005**, *16*, 1536-1541.

115. P. C. Lin, S. H. Ueng, M. C. Tseng, J. L. Ko, K. T. Huang, S. C. Yu, A. K. Adak, Y. J. Chen, C. C. Lin, *Angewandte Chemie-International Edition* **2006**, *45*, 4286-4290.

116. J. F. Lutz, H. G. Borner, *Progress in Polymer Science* **2008**, *33*, 1-39.

117. Q. Wang, T. R. Chan, R. Hilgraf, V. V. Fokin, K. B. Sharpless, M. G. Finn, *Journal of the American Chemical Society* **2003**, *125*, 3192-3193.

118. J. Gierlich, G. A. Burley, P. M. E. Gramlich, D. M. Hammond, T. Carell, *Organic Letters* **2006**, *8*, 3639-3642.

119. J. F. Lutz, *Angewandte Chemie-International Edition* **2008**, *47*, 2182-2184.

120. A. M. Eissa, E. Khosravi, *European polymer Journal* **2011**, *47 (1)*, 61-69.

121. S. Srinivasachari, Y. M. Liu, G. D. Zhang, L. Prevette, T. M. Reineke, *Journal of the American Chemical Society* **2006**, *128*, 8176-8184.

122. T. Liebert, C. Hansch, T. Heinze, *Macromolecular Rapid Communications* **2006**, *27*, 208-213.

123. J. Hafren, W. B. Zou, A. Cordova, *Macromolecular Rapid Communications* **2006**, *27*, 1362-1366.

124. T. Hasegawa, M. Umeda, M. Numata, T. Fujisawa, S. Haraguchi, K. Sakurai, S. Shinkai, *Chemistry Letters* **2006**, *35*, 82-83.

125. V. Crescenzi, L. Cornelio, C. Di Meo, S. Nardecchia, R. Lamanna, *Biomacromolecules* **2007**, *8*, 1844-1850.
126. C. Schatz, S. Louguet, J. F. Le Meins, S. Lecommandoux, *Angewandte Chemie-International Edition* **2009**, *48*, 2572-2575.
127. A. Biswas, H. N. Cheng, G. W. Selling, J. L. Willett, D. F. Kendra, *Carbohydrate Polymers* **2009**, *77*, 681-685.
128. E. Lallana, E. Fernandez-Megia, R. Riguera, *Journal of the American Chemical Society* **2009**, *131*, 5748.
129. M. Krouit, J. Bras, M. N. Belgacem, *European polymer Journal* **2008**, *44*, 4074-4081.
130. R. P. Quirk, B. Lee, *Polymer International* **1992**, *27*, 359-367.
131. W. H. Binder, R. Sachsenhofer, *Macromolecular Rapid Communications* **2008**, *29*, 952-981.
132. P. L. Golas, K. Matyjaszewski, *Chemical Society Reviews* **2010**, *39*, 1338-1354.
133. C. J. Hawker, A. W. Bosman, E. Harth, *Chemical Reviews* **2001**, *101*, 3661-3688.
134. M. Kamigaito, T. Ando, M. Sawamoto, *Chemical Reviews* **2001**, *101*, 3689-3745.
135. K. Matyjaszewski, J. H. Xia, *Chemical Reviews* **2001**, *101*, 2921-2990.
136. G. Moad, E. Rizzardo, S. H. Thang, *Australian Journal of Chemistry* **2009**, *62*, 1402-1472.
137. G. Moad, E. Rizzardo, S. H. Thang, *Polymer* **2008**, *49*, 1079-1131.
138. C. Boyer, V. Bulmus, T. P. Davis, V. Ladmiral, J. Q. Liu, S. Perrier, *Chemical Reviews* **2009**, *109*, 5402-5436.
139. V. Sciannamea, R. Jerome, C. Detrembleur, *Chemical Reviews* **2008**, *108*, 1104-1126.
140. M. Malkoch, R. J. Thibault, E. Drockenmuller, M. Messerschmidt, B. Voit, T. P. Russell, C. J. Hawker, *Journal of the American Chemical Society* **2005**, *127*, 14942-14949.
141. R. K. O'Reilly, M. J. Joralemon, C. J. Hawker, K. L. Wooley, *Chemistry-A European Journal* **2006**, *12*, 6776-6786.
142. B. S. Sumerlin, N. V. Tsarevsky, G. Louche, R. Y. Lee, K. Matyjaszewski, *Macromolecules* **2005**, *38*, 7540-7545.
143. G. Mantovani, V. Ladmiral, L. Tao, D. M. Haddleton, *Chemical Communications* **2005**, 2089-2091.
144. J. A. Opsteen, J. C. M. van Hest, *Chemical Communications* **2005**, 57-59.

145. A. J. T. Dirks, S. S. van Berkel, N. S. Hatzakis, J. A. Opsteen, F. L. van Delft, J. Cornelissen, A. E. Rowan, J. C. M. van Hest, F. Rutjes, R. J. M. Nolte, *Chemical Communications* **2005**, 4172-4174.
146. H. F. Gao, K. Matyjaszewski, *Macromolecules* **2006**, *39*, 4960-4965.
147. B. A. Laurent, S. M. Grayson, *Journal of the American Chemical Society* **2006**, *128*, 4238-4239.
148. V. Ladmiral, G. Mantovani, G. J. Clarkson, S. Cauet, J. L. Irwin, D. M. Haddleton, *Journal of the American Chemical Society* **2006**, *128*, 4823-4830.
149. J. Yin, Z. S. Ge, H. Liu, S. Y. Liu, *Journal of Polymer Science Part a-Polymer Chemistry* **2009**, *47*, 2608-2619.
150. N. V. Tsarevsky, K. Matyjaszewski, *Chemical Reviews* **2007**, *107*, 2270-2299.
151. W. Jakubowski, K. Min, K. Matyjaszewski, *Macromolecules* **2006**, *39*, 39-45.
152. W. A. Braunecker, K. Matyjaszewski, *Progress in Polymer Science* **2007**, *32*, 93-146.
153. L. Mueller, K. Matyjaszewski, *Macromolecular Reaction Engineering* **2010**, *4*, 180-185.
154. J. Chiefari, Y. K. Chong, F. Ercole, J. Krstina, J. Jeffery, T. P. T. Le, R. T. A. Mayadunne, G. F. Meijs, C. L. Moad, G. Moad, E. Rizzardo, S. H. Thang, *Macromolecules* **1998**, *31*, 5559-5562.
155. C. K. Williams, *Chemical Society Reviews* **2007**, *36*, 1573-1580.
156. A. Duda, S. Penczek, *Mechanism of aliphatic polyester formation. Biopolymers. Vol. 3b: polyesters II–properties and chemical synthesis.* Weinheim: Wiley-VCH; **2002**, 371– 430.
157. S. Penczek, M. Cypryk, A. Duda, P. Kubisa, S. Slomkowski, *Progress in Polymer Science* **2007**, *32*, 247-282.
158. A. Kowalski, A. Duda, S. Penczek, *Macromolecules* **2000**, *33*, 689-695.
159. P. Lecomte, R. Riva, C. Jerome, R. Jerome, *Macromolecular Rapid Communications* **2008**, *29*, 982-997.
160. B. Parrish, R. B. Breitenkamp, T. Emrick, *Journal of the American Chemical Society* **2005**, *127*, 7404-7410.
161. H. Y. Li, R. Riva, R. Jerome, P. Lecomte, *Macromolecules* **2007**, *40*, 824-831.
162. R. Riva, P. Schmeits, F. Stoffelbach, C. Jerome, R. Jerome, P. Lecomte, *Chemical Communications* **2005**, 5334-5336.
163. R. Riva, S. Schmeits, C. Jerome, R. Jerome, P. Lecomte, *Macromolecules* **2007**, *40*, 796-803.

164. K. J. Ivin, J. C. Mol, *Olefin Metathesis and Metathesis Polymerization, Second Edition*, **1996**.
165. R. L. Banks, G. C. Bailey, *Industrial & Engineering Chemistry Product Research and Development* **1964**, *3*, 170.
166. N. Calderon, H. Y. Chen, K. W. Scott, *Tetrahedron Letters* **1967**, 3327.
167. N. Calderon, E. A. Ofstead, J. P. Ward, W. A. Judy, K. W. Scott, *Journal of the American Chemical Society* **1968**, *90*, 4133.
168. R. H. Grubbs, *Tetrahedron* **2004**, *60*, 7117-7140.
169. J. L. Herisson, Y. Chauvin, *Makromolekulare Chemie* **1971**, *141*, 161.
170. R. H. Grubbs, *Handbook of Metathesis, Vol. 3 - Applications in Polymer Synthesis*. Wiley-VCH, **2003**.
171. U. Frenzel, O. Nuyken, *Journal of Polymer Science Part A-Polymer Chemistry* **2002**, *40*, 2895-2916.
172. J. C. Mol, *Journal of Molecular Catalysis A-Chemical* **2004**, *213*, 39-45.
173. M. McCann, E. M. Coda, *Journal of Molecular Catalysis A-Chemical* **1996**, *109*, 99-111.
174. E. O. Fischer, A. Maasbol, *Angewandte Chemie-International Edition* **1964**, *3*, 580.
175. C. P. Casey, Burkhard.Tj, *Journal of the American Chemical Society* **1973**, *95*, 5833-5834.
176. J. S. Murdzek, R. R. Schrock, *Organometallics* **1987**, *6*, 1373-1374.
177. R. R. Schrock, J. Feldman, L. F. Cannizzo, R. H. Grubbs, *Macromolecules* **1987**, *20*, 1169-1172.
178. R. R. Schrock, R. T. Depue, J. Feldman, K. B. Yap, D. C. Yang, W. M. Davis, L. Park, M. Dimare, M. Schofield, J. Anhaus, E. Walborsky, E. Evitt, C. Kruger, P. Betz, *Organometallics* **1990**, *9*, 2262-2275.
179. C. J. Schaverien, J. C. Dewan, R. R. Schrock, *Journal of the American Chemical Society* **1986**, *108*, 2771-2773.
180. T. M. Trnka, R. H. Grubbs, *Accounts of Chemical Research* **2001**, *34*, 18-29.
181. M. Ulman, R. H. Grubbs, *Journal of Organic Chemistry* **1999**, *64*, 7202-7207.
182. M. Scholl, T. M. Trnka, J. P. Morgan, R. H. Grubbs, *Tetrahedron Letters* **1999**, *40*, 2247-2250.
183. U. Frenzel, T. Weskamp, F. J. Kohl, W. C. Schattenman, O. Nuyken, W. A. Herrmann, *Journal of Organometallic Chemistry* **1999**, *586*, 263-265.
184. L. Jafarpour, S. P. Nolan, *Journal of Organometallic Chemistry* **2001**, *617*, 17-27.

185. S. Jha, S. Dutta, N. B. Bowden, *Macromolecules* **2004**, *37*, 4365-4374.
186. H. D. Maynard, S. Y. Okada, R. H. Grubbs, *Macromolecules* **2000**, *33*, 6239-6248.
187. C. W. Bielawski, R. H. Grubbs, *Macromolecules* **2001**, *34*, 8838-8840.
188. T. L. Choi, R. H. Grubbs, *Angewandte Chemie-International Edition* **2003**, *42*, 1743-1746.
189. J. A. Love, J. P. Morgan, T. M. Trnka, R. H. Grubbs, *Angewandte Chemie-International Edition* **2002**, *41*, 4035-4037.
190. M. S. Sanford, J. A. Love, R. H. Grubbs, *Journal of the American Chemical Society* **2001**, *123*, 6543-6554.
191. M. S. Sanford, M. Ulman, R. H. Grubbs, *Journal of the American Chemical Society* **2001**, *123*, 749-750.
192. W. H. Binder, C. Kluger, *Macromolecules* **2004**, *37*, 9321-9330.
193. C. Kluger, W. H. Binder, *Journal of Polymer Science Part A-Polymer Chemistry* **2007**, *45*, 485-499.
194. P. Dziezok, S. S. Sheiko, K. Fischer, M. Schmidt, M. Moller, *Angewandte Chemie-International Edition* **1997**, *36*, 2812-2815.
195. D. Neugebauer, B. S. Sumerlin, K. Matyjaszewski, B. Goodhart, S. S. Sheiko, *Polymer* **2004**, *45*, 8173-8179.
196. S. S. Sheiko, M. Moller, *Chemical Reviews* **2001**, *101*, 4099-4123.
197. S. S. Sheiko, F. C. Sun, A. Randall, D. Shirvanyants, M. Rubinstein, H. Lee, K. Matyjaszewski, *Nature* **2006**, *440*, 191-194.
198. K. Fischer, M. Schmidt, *Macromolecular Rapid Communications* **2001**, *22*, 787-791.
199. L. H. He, J. Huang, Y. M. Chen, L. P. Liu, *Macromolecules* **2005**, *38*, 3351-3355.
200. Y. Nakamura, Y. Wan, J. W. Mays, H. Iatrou, N. Hadjichristidis, *Macromolecules* **2000**, *33*, 8323-8328.
201. F. Sun, S. S. Sheiko, M. Moller, K. Beers, K. Matyjaszewski, *Journal of Physical Chemistry A* **2004**, *108*, 9682-9686.
202. M. Zamurovic, S. Christodoulou, A. Vazaios, E. Iatrou, M. Pitsikalis, N. Hadjichristidis, *Macromolecules* **2007**, *40*, 5835-5849.
203. B. Zhang, S. J. Zhang, L. Okrasa, T. Pakula, T. Stephan, M. Schmidt, *Polymer* **2004**, *45*, 4009-4015.
204. M. F. Zhang, A. H. E. Muller, *Journal of Polymer Science Part A-Polymer Chemistry* **2005**, *43*, 3461-3481.
205. Z. B. Zhang, Z. Q. Shi, X. Han, S. Holdcroft, *Macromolecules* **2007**, *40*, 2295-2298.

206. N. Hadjichristidis, M. Pitsikalis, S. Pispas, H. Iatrou, *Chemical Reviews* **2001**, *101*, 3747-3792.
207. R. C. Advincula, W. J. Brittain, K. C. Caster, J. Ruhe, *Polymer Brushes*. Wiley-VCH: Weinheim, **2004**.
208. K. L. Beers, S. G. Gaynor, K. Matyjaszewski, S. S. Sheiko, M. Moller, *Macromolecules* **1998**, *31*, 9413-9415.
209. H. G. Borner, K. Beers, K. Matyjaszewski, S. S. Sheiko, M. Moller, *Macromolecules* **2001**, *34*, 4375-4383.
210. G. L. Cheng, A. Boker, M. F. Zhang, G. Krausch, A. H. E. Muller, *Macromolecules* **2001**, *34*, 6883-6888.
211. R. M. Kriegel, W. S. Rees, M. Weck, *Macromolecules* **2004**, *37*, 6644-6649.
212. M. B. Runge, S. Dutta, N. B. Bowden, *Macromolecules* **2006**, *39*, 498-508.
213. M. F. Zhang, T. Breiner, H. Mori, A. H. E. Muller, *Polymer* **2003**, *44*, 1449-1458.
214. B. S. Sumerlin, D. Neugebauer, K. Matyjaszewski, *Macromolecules* **2005**, *38*, 702-708.
215. H. I. Lee, J. Pietrasik, S. S. Sheiko, K. Matyjaszewski, *Progress in Polymer Science* **2010**, *35*, 24-44.
216. B. Zhao, L. Zhu, *Macromolecules* **2009**, *42*, 9369-9383.
217. S. S. Sheiko, B. S. Sumerlin, K. Matyjaszewski, *Progress in Polymer Science* **2008**, *33*, 759-785.
218. Y. Xia, J. A. Kornfield, R. H. Grubbs, *Macromolecules* **2009**, *42*, 3761-3766.
219. C. D. H. Alarcon, S. Pennadam, C. Alexander, *Chemical Society Reviews* **2005**, *34*, 276-285.
220. A. B. Lowe, C. L. McCormick, *Stimuli Responsive Water-Soluble and Amphiphilic (Co)polymers*. ACS Symposium Series **2000**, Vol. 780, 1-13.
221. M. R. Aguilar, C. Elvira, A. Gallardo, B. Vázquez, J. S. Román, *Topics in Tissue Engineering, Vol. 3, Chapter 6: Smart Polymers and Their Applications as Biomaterials*. **2007**, (Eds.) Ashammakhi, N; Reis, R & Chiellini.
222. Y. Qiu, K. Park, *Advanced Drug Delivery Reviews* **2001**, *53*, 321-339.
223. M. K. Chourasia, S. K. Jain, *Drug Delivery* **2004**, *11*, 129-148.
224. M. Sauer, D. Streich, W. Meier, *Advanced Materials* **2001**, *13*, 1649-1651.
225. W. T. Godbey, A. G. Mikos, *Journal of Controlled Release* **2001**, *72*, 115-125.
226. G. Borchard, *Advanced Drug Delivery Reviews* **2001**, *52*, 145-150.
227. M. E. H. El-Sayed, A. S. Hoffman, P. S. Stayton, *Journal of Controlled Release* **2005**, *101*, 47-58.

228. K. Podual, F. J. Doyle, N. A. Peppas, *Polymer* **2000**, *41*, 3975-3983.
229. R. Yoshida, K. Sakai, T. Okano, Y. Sakurai, Y. H. Bae, S. W. Kim, *Journal of Biomaterials Science-Polymer Edition* **1991**, *3*, 155-162.
230. D. Crespy, R. N. Rossi, *Polymer International* **2007**, *56*, 1461-1468.
231. G. Bokias, D. Hourdet, I. Iliopoulos, *Macromolecules* **2000**, *33*, 2929-2935.
232. M. Heskins, J. E. Guillet, *Journal of Macromolecular Science, Part A* **1968**, *2*, 1441 – 1455.
233. X. D. Xu, X. Z. Zhang, J. Yang, S. X. Cheng, R. X. Zhuo, Y. Q. Huang, *Langmuir* **2007**, *23*, 4231-4236.
234. H. G. Schild, *Progress in Polymer Science* **1992**, *17*, 163-249.
235. Z. Cheng, Q. Zhang, S. Bauer, D.A., Polymer-Based Smart Materials — Processes, Properties and Application, Wrobleski B. Budhlall, T. Trongsatitkul, *Synthesis of Thermoresponsive Copolymers Composed of Poly(ethylene oxide) and Poly(N-isopropylacrylamide) for Cell Encapsulation*, Mater. Res. Soc. Symp. Proc., Warrendale, PA, **2009**, Vol. 1134 - BB08 - 46.
236. S. Hopkins, S. Carter, S. MacNeil, S. Rimmer, *Journal of Materials Chemistry* **2007**, *17*, 4022-4027.
237. M. Keerl, V. Smirnovas, R. Winter, W. Richtering, *Angewandte Chemie-International Edition* **2008**, *47*, 338-341.
238. J. Y. Wu, S. Q. Liu, P. W. S. Heng, Y. Y. Yang, *Journal of Controlled Release* **2005**, *102*, 361-372.
239. X. Jiang, E. B. Vogel, M. R. Smith, G. L. Baker, *Macromolecules* **2008**, *41*, 1937-1944.
240. J. F. Lutz, A. Hoth, *Macromolecules* **2006**, *39*, 893-896.
241. T. Shimokuri, T. Kaneko, M. Akashi, *Journal of Polymer Science Part A-Polymer Chemistry* **2004**, *42*, 4492-4501.
242. Y. Tachibana, M. Kurisawa, H. Uyama, S. Kobayashi, *Biomacromolecules* **2003**, *4*, 1132-1134.
243. F. A. Plamper, A. Schmalz, M. Ballauff, A. H. E. Muller, *Journal of the American Chemical Society* **2007**, *129*, 14538.
244. S. Bekiranov, R. Bruinsma, P. Pincus, *Physical Review E* **1997**, *55*, 577-585.
245. E. E. Dormidontova, *Macromolecules* **2004**, *37*, 7747-7761.
246. S. Saeki, N. Kuwahara, M. Nakata, M. Kaneko, *Polymer* **1976**, *17*, 685-689.
247. S. Nozary, H. Modarress, A. Eliassi, *Journal of Applied Polymer Science* **2003**, *89*, 1983-1990.

248. Y. L. Cai, S. P. Armes, *Macromolecules* **2004**, *37*, 7116-7122.
249. M. H. Dufresne, M. A. Gauthier, J. C. Leroux, *Bioconjugate Chemistry* **2005**, *16*, 1027-1033.
250. S. B. Lee, A. J. Russell, K. Matyjaszewski, *Biomacromolecules* **2003**, *4*, 1386-1393.
251. S. Y. Liu, J. V. M. Weaver, Y. Q. Tang, N. C. Billingham, S. P. Armes, K. Tribe, *Macromolecules* **2002**, *35*, 6121-6131.
252. S. Perrier, D. M. Haddleton, *European Polymer Journal* **2004**, *40*, 2277-2286.
253. L. Tao, G. Mantovani, F. Lecolley, D. M. Haddleton, *Journal of the American Chemical Society* **2004**, *126*, 13220-13221.
254. X. S. Wang, S. P. Armes, *Macromolecules* **2000**, *33*, 6640-6647.
255. X. S. Wang, S. F. Lascelles, R. A. Jackson, S. P. Armes, *Chemical Communications* **1999**, 1817-1818.
256. M. Mertoglu, S. Garnier, A. Laschewsky, K. Skrabania, J. Storsberg, *Polymer* **2005**, *46*, 7726-7740.
257. S. Han, M. Hagiwara, T. Ishizone, *Macromolecules* **2003**, *36*, 8312-8319.
258. H. Kitano, T. Hirabayashi, M. Gemmei-Ide, M. Kyogoku, *Macromolecular Chemistry and Physics* **2004**, *205*, 1651-1659.
259. J. F. Lutz, *Journal of Polymer Science Part a-Polymer Chemistry* **2008**, *46*, 3459-3470.
260. M. Rackaitis, K. Strawhecker, K. Manias, *Journal of Polymer Science Part B-Polymer Physics* **2002**, *40*, 2339-2342.
261. L. D. Taylor, L. D. Cerankowski, *Journal of Polymer Science Part A-Polymer Chemistry* **1975**, *13*, 2551-2570.
262. C. H. Li, J. M. Hu, J. Yin, S. Y. Liu, *Macromolecules* **2009**, *42*, 5007-5016.

# Chapter 2

# Click Chemistry on Model Compounds

## 2.1. Introduction

This chapter addresses the applicability of Click chemistry as a powerful, highly reliable, and selective reaction on model compounds (3-methylbenzyl alcohol and phenol). In order to employ Click chemistry, an azide and a terminal alkyne have to be prepared individually and then reacted together to form 1,2,3-triazole ring. It is therefore important to investigate the ease of the chemical transformations for azide and alkyne functionalities on organic compounds. Azide derivatives can be prepared by nucleophilic substitution reaction between sodium azide and alkyl halide or esters of sulphonic acid. On the other hand, terminal alkynes can be prepared by Williamson's etherification reaction between alcohol and alkyl halide. It has been reported that both azides and alkynes can tolerate oxygen, water, common organic synthesis conditions, biological molecules, a large range of solvents and pH's, and the reaction conditions of living systems (reducing environment, hydrolysis, etc.).[1,2,3] Even though the decomposition of aliphatic azides is thermodynamically favoured, a kinetic barrier exists that allows them to be stable in the aforementioned conditions.[4] Moreover, Click reaction is unaffected by steric factors. Variously substituted primary, secondary, tertiary, and aromatic azides readily participate in this transformation.

The work on model compounds was initiated in order to get familiar with the chemistry of Click reactions, the methodology of chemical modification and the systematic characterisation. It was anticipated that the chemistry and the mechanistic pathways will be closely related to those for the polymeric materials. However, there will be some differences between model compounds and macromolecules in terms of reactions' work up, products' isolation and characterisation tools.

## 2.2. Experimental

### 2.2.1. Materials

All chemicals and reagents used in the synthesis were purchased from Sigma – Aldrich and used without further purification. All dry solvents were obtained from the Solvent Purification System (SPS), Chemistry Department, Durham University.

### 2.2.2. Instrumentation and Measurements

$^{1}$H-NMR spectra were recorded using deuteriated solvent lock on a Varian Mercury 400 or a Varian Inova 500 spectrometer at 400 MHz and 500 MHz, respectively. Chemical shifts are quoted in ppm, relative to tetramethylsilane (TMS), as the internal reference. $^{13}$C-NMR spectra were recorded at 101 MHz or 126 MHz (2000 scans) using continuous broad band proton decoupling and a 3 S recycle dely, and therefore not quantitative; chemical shifts are quoted in ppm, relative to $CDCl_3$ (77.55 ppm). The following abbreviations are used in listing NMR spectra: s = singlet, d = doublet, t = triplet, q = quartet, m = multiplet, b = broad. DEPT (Distortionless Enhancement by Polarisation Transfer) experiment allows to determine multiplicity of carbon atom substitution with hydrogens. It differentiates between CH, $CH_2$ and $CH_3$ groups. The spectrum gives all CH and $CH_3$ in a phase opposite to $CH_2$. Signals from quaternary carbons and other carbons with no attached protons are always absent. NOESY (Nuclear Overhauser effect spectroscopy) experiment is a two-dimensional proton NMR spectrum. It is used to establish the correlations through space.

Electron Impact (EI) and Electrospray ($ES^{+}$) mass spectra were recorded on a Thermo Finnigan LTQ FT spectrometer operating at 70 eV with the ionisation mode as indicated.

### 2.2.3. Synthesis of 3-Methyl Benzyl Mesylate 2.1

3-Methyl benzyl alcohol (5 g, 0.041 mol) was added to $CH_2Cl_2$ (50 mL) in a dry three-necked round-bottom flask, equipped with magnetic stirrer, dropping funnel and kept under $N_2$ atmosphere at −30 $^{o}$C (acetone and dry ice bath). The mixture was stirred for 30 min and $MeSO_2Cl$ (6.5 mL, 0.082 mol) was added. The reaction mixture was stirred for 15 min and triethylamine (17.5 mL, 0.125 mol) was added drop-wise over a period

of 15 min. The mixture was warmed up to 0 $^{o}$C and left for 30 min. Diethyl ether (200 mL) was added to extract the product. The organic layer was washed with water (3 x 75 mL), dilute HCl (5 %) and then with Brine. The organic layer was dried over anhydrous $MgSO_4$, and the solvent was evaporated under reduced pressure to give the product **2.1**, yield 59 % (4.8 g, 0.024 mol). bp of **2.1** reported to be 354.7 ± 21.0 $^{o}$C at 760 Torr.[5]

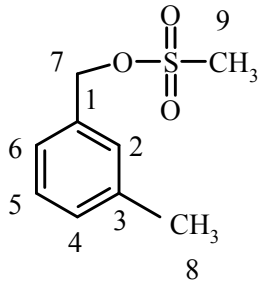


**2.1**

**Figure 2.1.** Structure of 3-methyl benzyl alcohol with numerical assignment for NMR

$^{1}$H-NMR (400 MHz, $CDCl_3$): δ 7.25 (m, 4H, $H_{2,4,5,6}$), 5.23 (s, 2H, $H_7$), 2.93 (s, 3H, $H_9$), 2.39 (s, 3H, $H_8$).

$^{13}$C-NMR (101 MHz, $CDCl_3$): δ 138.73 ($C_1$), 133.30 ($C_3$), 130.14 ($C_5$), 129.54 ($C_4$), 128.79 ($C_2$), 125.92 ($C_6$), 71.66 ($C_7$), 38.33 ($C_9$), 21.29 ($C_8$).

### 2.2.4. Synthesis of 3-Methyl Benzyl Azide 2.2

Sodium azide (0.65 g, 0.01 mol) was added to a solution of the mesylate **2.1** (2 g, 0.01 mol) in DMF (55 mL) in a dry three-necked round-bottom flask, equipped with magnetic stirrer, rubber seal septum and kept under $N_2$ atmosphere. The mixture was stirred at ambient temperature for 15 min in an oil bath at 85 $^{o}$C for 6 hr. The course of the reaction was monitored by TLC. The mixture was cooled to ambient temperature and NaOH (5 % aq., 25 mL) was added followed by water (100 mL). The addition of NaOH was to make sure that there is no hydrazoic acid, which is very toxic. The product was extracted with ethyl acetate / hexane (1:1, 3 x 25 mL). The organic layer was washed with water (3 x 25 mL), brine solution, and the organic layer was dried over anhydrous $MgSO_4$. The solvent was removed under reduced pressure to give azide derivative product **2.2**, yield 89 % (1.3 g, 0.0089 mol).

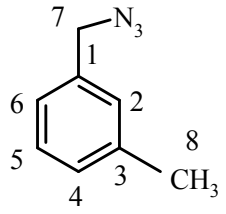


**2.2**

**Figure 2.2.** Structure of 3-methyl benzyl azide with numerical assignment for NMR

$^{1}$H-NMR (400 MHz, $CDCl_3$): δ 7.21 (m, 4H, $H_{2,4,5,6}$), 4.35 (s, 2H, $H_7$), 2.40 (s, 3H, $H_8$).
$^{13}$C-NMR (101 MHz, $CDCl_3$): δ 138.58 ($C_1$), 135.30 ($C_3$), 129.05 ($C_5$), 128.93 ($C_4$), 128.71 ($C_2$), 125.26 ($C_6$), 54.85 ($C_7$), 21.36 ($C_8$).

### 2.2.5. Synthesis of Phenyl Propargyl Ether 2.3

Potassium carbonate (20.75 g, 0.3 mol) was added to a solution of phenol (~99%) (12.7 g, 0.135 mol) in DMF (125 mL) in a dry three-necked round-bottom flask, equipped with magnetic stirrer, dropping funnel and kept under $N_2$ atmosphere. The mixture was stirred at ambient temperature for 30 min. Propargyl bromide (80 wt % in toluene, 15 mL, 0.135 mol) was added and the mixture was stirred at ambient temperature for 18 hr. Ethyl acetate (300 mL) was added and the precipitate was filtered. The filtrate was washed with water (4 x 150 mL) followed by brine. The organic layer was dried over anhydrous $MgSO_4$ and the solvent was removed under reduced pressure to give phenol propargyl ether product **2.3**, yield 88 % (15.7 g, 0.119 mol). bp of **2.3** reported to be 97-99 $^{o}$C at 20 Torr.[6]

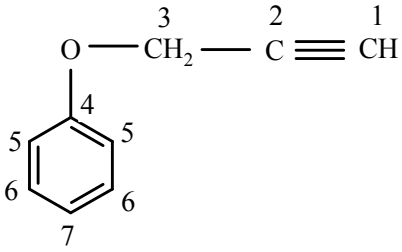


**2.3**

**Figure 2.3.** Structure of phenyl propargyl ether with numerical assignment for NMR

$^{1}$H-NMR (400 MHz, $CDCl_3$): δ 7.15 (m, 5H, $H_{5,6,7}$), 4.74 (dd, $J$ = 13.8 Hz, 15.9 Hz, 2H, $H_3$), 2.52 (t, $J$ = 2.4 Hz, 1H, $H_1$).
$^{13}$C-NMR (101 MHz, $CDCl_3$): δ 157.56 ($C_4$), 129.46 ($C_6$), 121.58 ($C_7$), 114.92 ($C_5$), 78.64 ($C_2$), 75.41 ($C_1$), 55.76 ($C_3$).

### 2.2.6. Click Reaction between 3-Methyl Benzyl Azide and Phenyl Propargyl Ether 2.4

In a two-necked round-bottom flask, equipped with magnetic stirrer and rubber seal septum, 3-Methyl benzyl azide **2.2** (1 g, 6.8 mmol) and phenyl propargyl ether **2.3** (0.9 g, 6.8 mmol) were stirred in t-BuOH / water (1:1, 10 mL) at ambient temperature. Sodium ascorbate (0.068 g, 0.34 mmol) in water (2.5 mL) was added. This was followed by the addition of copper sulphate pentahydrate (0.017 g, 0.068 mmol) in water (2.5 mL). The mixture was stirred vigorously at ambient temperature for 18 hr. The reaction mixture was diluted with water (50 mL), cooled in ice, and the precipitate was collected. The precipitate was washed with water (3 x 25 mL) and dried under reduced pressure overnight to produce product **2.4**, mp 75 – 77 $^{o}$C, yield 90 % (1.7 g, 6.1 mmol).

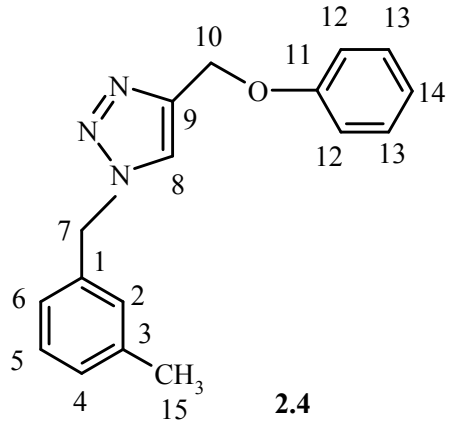


**2.4**

**Figure 2.4.** Structure of the product with numerical assignment for NMR

$^{1}$H-NMR (500 MHz, $CDCl_3$): δ 7.51 (s, 1H, $H_8$), 7.14 (m, 9H, $H_{2,4,5,6,12,13,14}$), 5.50 (s, 2H, $H_{10}$), 5.20 (s, 2H, $H_7$), 2.35 (s, 3H, $H_{15}$).

$^{13}$C-NMR (126 MHz, $CDCl_3$): δ 158.45 ($C_{11}$), 144.84 ($C_9$), 139.20 ($C_1$), 134.66 ($C_3$), 129.77 ($C_{13}$), 129.24 − 129.07 ($C_{5,4,2}$), 125.43 ($C_6$), 122.97 ($C_8$), 121.48 ($C_{14}$), 115.01 ($C_{12}$), 62.23 ($C_{10}$), 54.44 ($C_7$), 21.58 ($C_{15}$).

ESI-MS: calcd for $C_{17}H_{17}N_3O$ + H = 280.34954; found for $[M + H]^+$ = 280.3.

## 2.3. Results and Discussion

### 2.3.1. General Synthetic Strategy

The general strategy for the application of Click chemistry on model compounds is shown in Scheme 2.1.

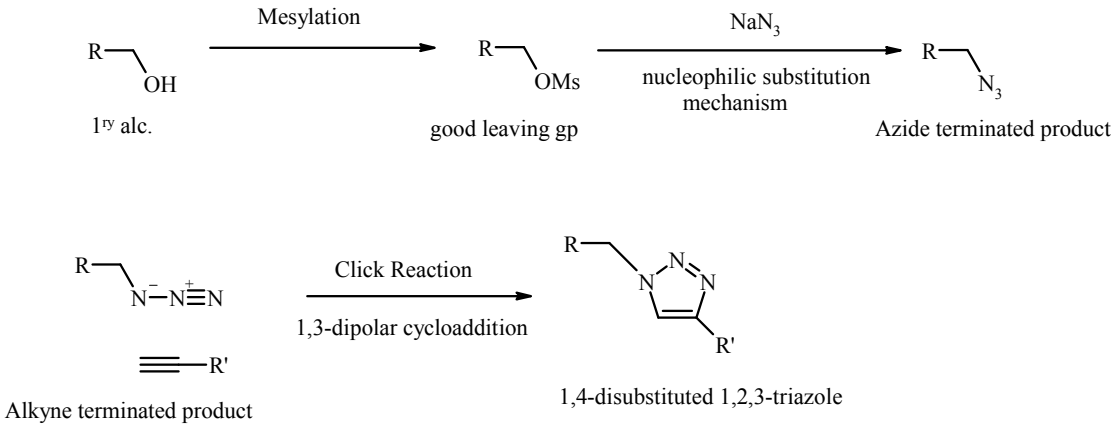


**Scheme 2.1.** General synthetic strategy for the application of Click chemistry on model compounds

The first step involved the conversion of the hydroxyl of a primary alcohol to mesylate group (yield ~ 59%). The mesylated product was then reacted with $NaN_3$ to form the azide terminated product (yield ~ 89%). On the other hand, the alkyne terminated compound was prepared by Williamson etherification reaction between alcohol and alkyl halide (yield ~ 88%). The Click product containing 1,2,3-triazole ring was finally produced with high yield ( ~ 90 %) *via* 1,3-cycloaddition between azide and alkyne terminated products.

### 2.3.2. Formation of Azide Terminated Product

The first step is the mesylation reaction of 3-methyl benzyl alcohol. The reaction was carried out using methane sulphonyl chloride (mesyl chloride), in the presence of triethylamine to trap the formed HCl and hence favour the production of the ester, Scheme 2.2.

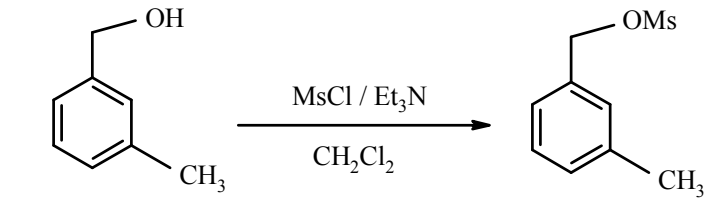


**3-methyl benzyl alcohol** **2.1**

**Scheme 2.2.** Synthesis of 3-methyl benzyl mesylate

The product **2.1** was fully characterised by $^{1}$H-, $^{13}$C- and DEPT-NMR. The comparison of the $^{1}$H-NMR spectra of the starting material and the product **2.1** showed that the mesylation reaction of 3-methyl benzyl alcohol was carried out successfully. The peak due to hydroxyl proton ($H_8$) at 1.78 ppm disappeared (Fig. 2.5.A and B) and a significant peak appeared at 2.93 ppm, corresponding to the protons of the mesyl group ($H_{10}$) (Fig. 2.5.B). In addition, there was a shift to higher δ-value, 5.23 ppm, for the peak of the benzyl $CH_2$ ($H_7$) (Fig. 2.5.A and B), indicating the attachment to the mesylate group. Moreover, the $^{13}$C-NMR spectrum of **2.1** (Fig. 2.6.A and B) showed appearance of a new peak at 38.33 ppm, characteristic for the $CH_3$ of the mesyl group ($C_{10}$).

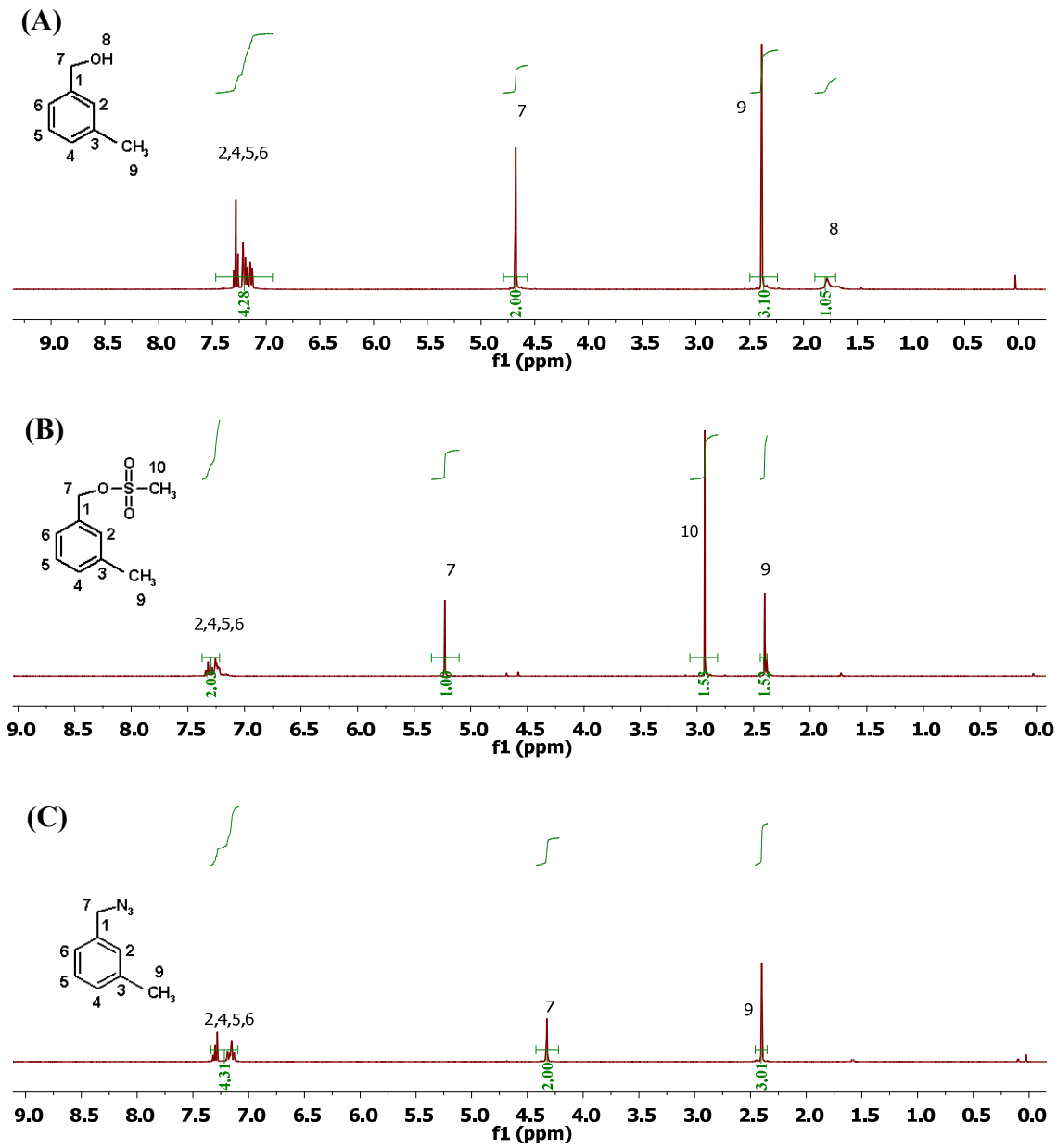


**Figure 2.5.** $^{1}$H-NMR spectra in $CDCl_3$ of (A) 3-methyl benzyl alcohol, (B) 3-methyl benzyl mesylate **2.1**, and (C) 3-methyl benzyl azide **2.2**.

The second step is the nucleophilic substitution reaction between **2.1** and sodium azide to form the azide terminated product **2.2**, Scheme 2.3.

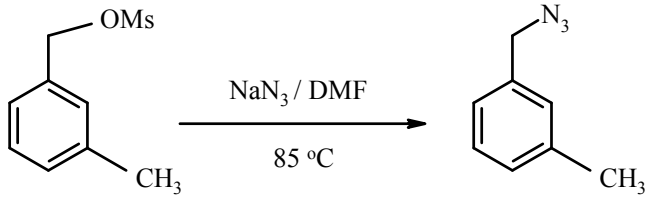


**2.1** **2.2**

**Scheme 2.3.** Synthesis of 3-methyl benzyl azide

The product **2.2** was fully characterised by $^{1}$H-, $^{13}$C- and DEPT-NMR. The $^{1}$H-NMR spectrum of **2.2** showed a complete disappearance of the peak corresponding to the mesyl protons ($H_{10}$), Fig. 2.5.B and C. It also showed a clear shift to lower δ-value, 4.35 ppm, for the adjacent benzyl $CH_2$ ($H_7$), indicating the successful azidation reaction. Moreover, the $^{13}$C-NMR spectrum of **2.2** showed the complete disappearance of the peak corresponding to the $CH_3$ of the mesyl group ($C_{10}$) at 38.33 ppm, Fig. 2.6.B and C.

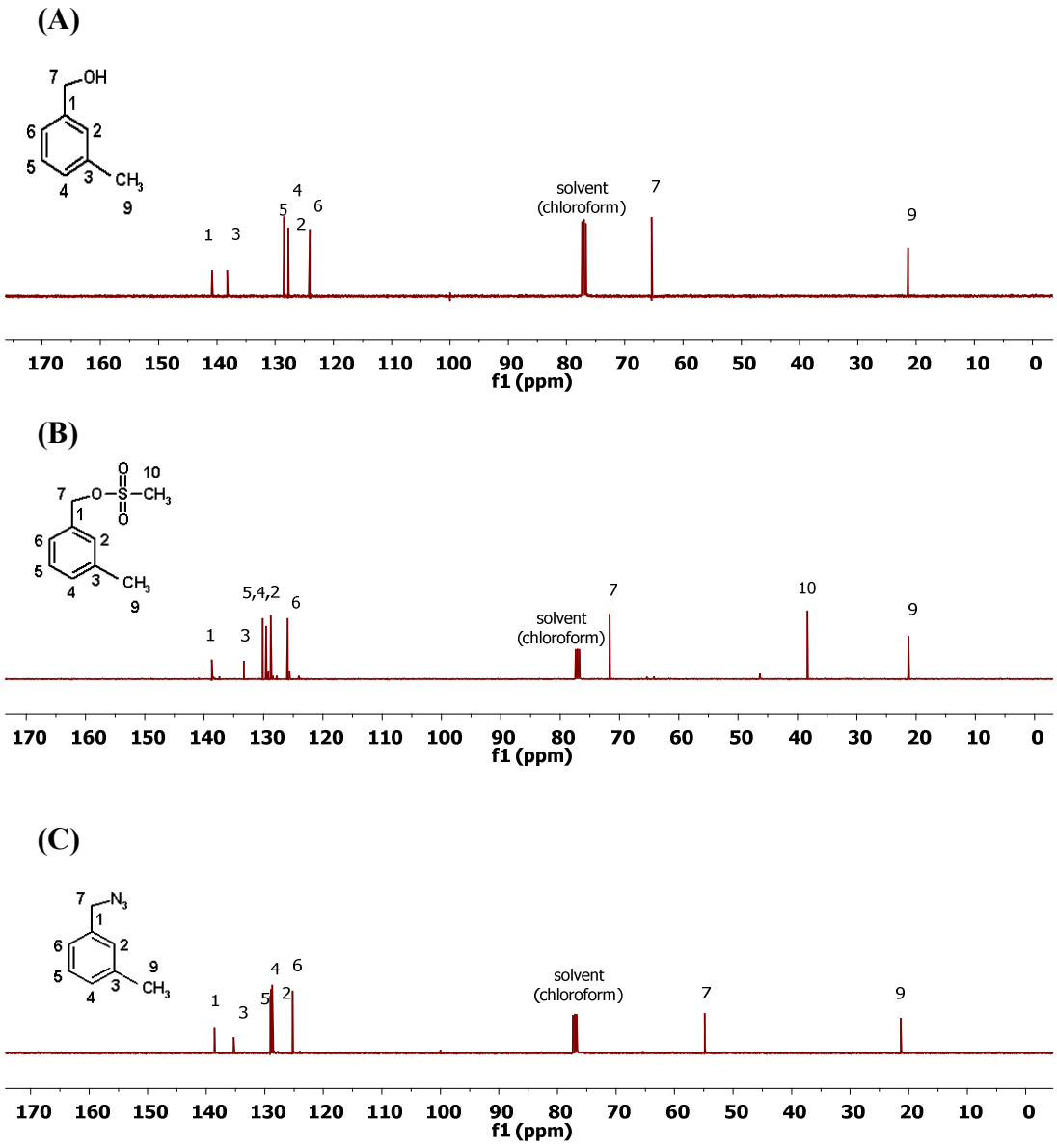


**Figure 2.6.** $^{13}$C-NMR spectra in $CDCl_3$ of (A) 3-methyl benzyl alcohol, (B) 3-methyl benzyl mesylate **2.1**, and (C) 3-methyl benzyl azide **2.2**.

The shift of the benzyl $CH_2$ can easily be seen in the DEPT- NMR spectra in Fig. 2.7. The benzyl $CH_2$ peak ($C_7$) shifted to higher δ-value, 71.66 ppm, Fig. 2.7.A and B. However, the same benzyl $CH_2$ peak shifted to the lower δ-value, 54.85 ppm, as it became adjacent to azide group, Fig. 2.7.C.

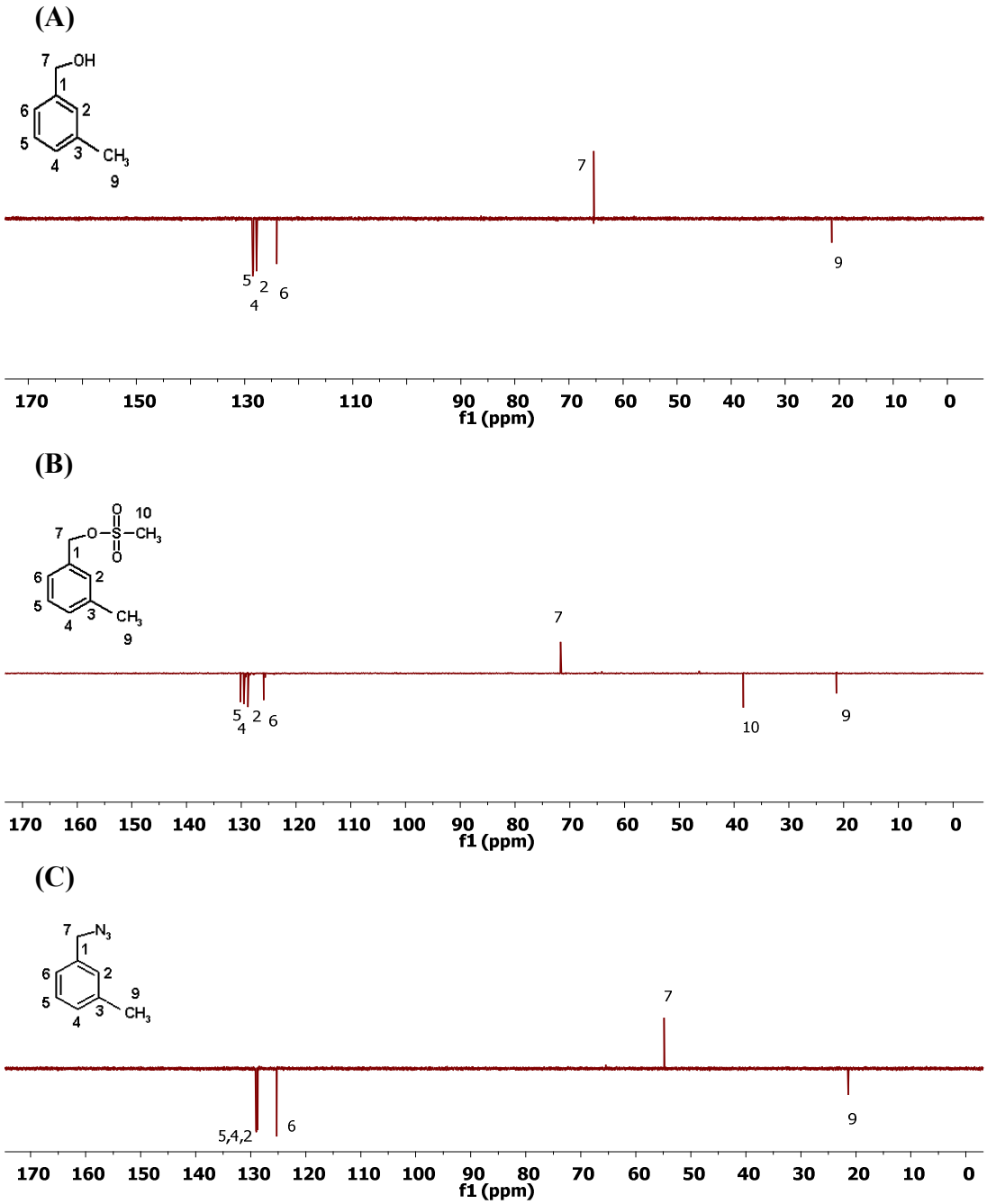


**Figure 2.7.** DEPT-NMR spectra in $CDCl_3$ of (A) 3-methyl benzyl alcohol, (B) 3-methyl benzyl mesylate **2.1**, and (C) 3-methyl benzyl azide **2.2**

### 2.3.3. Formation of Alkyne Terminated Product

Formation of alkyne terminated compound was carried out by reacting phenol with propargyl bromide to produce phenyl propargyl ether **2.3**, Scheme 2.4.

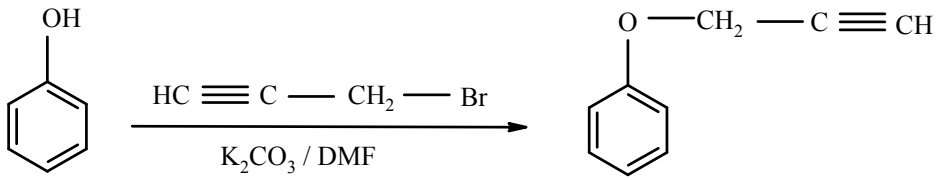


**2.3**

**Scheme 2.4.** Synthesis of phenyl propargyl ether

**2.3** was fully characterised by $^{1}$H-, $^{13}$C- and DEPT- NMR. The peak for the $CH_2$ protons of propargyl bromide ($H_3$) at 3.91 ppm (Fig. 2.8.A) shifted to higher δ-value, 4.74 ppm, for the $CH_2$ protons of the product **2.3** ($H_3$), Fig. 2.8.B.

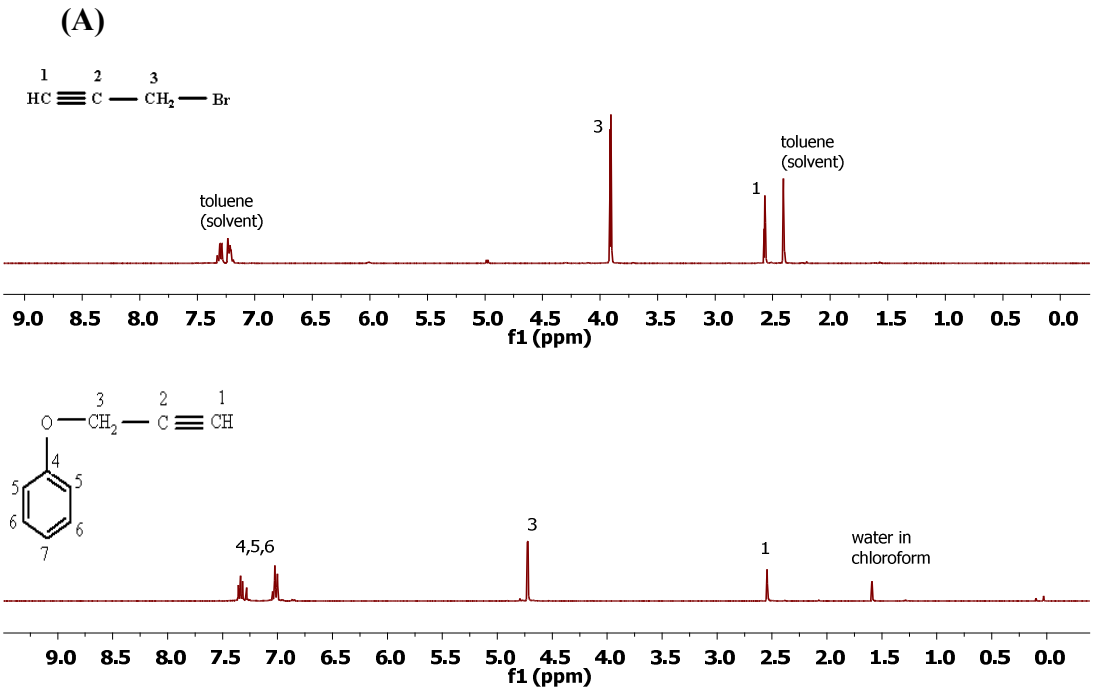


**Figure 2.8.** $^{1}$H-NMR spectra in $CDCl_3$ of (A) propargyl bromide, and (B) phenyl propargyl ether **2.3**

Moreover, the fully assigned $^{13}$C-NMR spectrum of **2.3** (Fig. 2.9) confirmed the successful reaction.

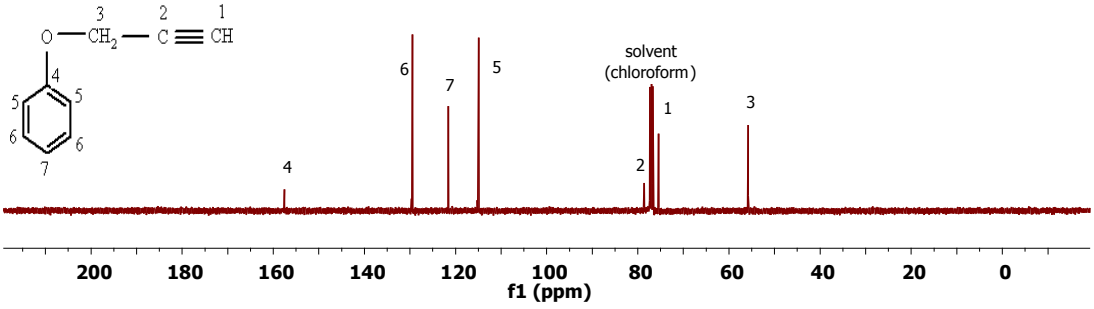


**Figure 2.9.** $^{13}$C-NMR spectrum of phenyl propargyl ether **2.3** in $CDCl_3$

### 2.3.4. Click Reaction

The azide – alkyne cycloaddition reaction was successfully carried out to form 1,2,3-triazole ring through 1,3-diopolar cycloaddition mechanism, Scheme 2.5.

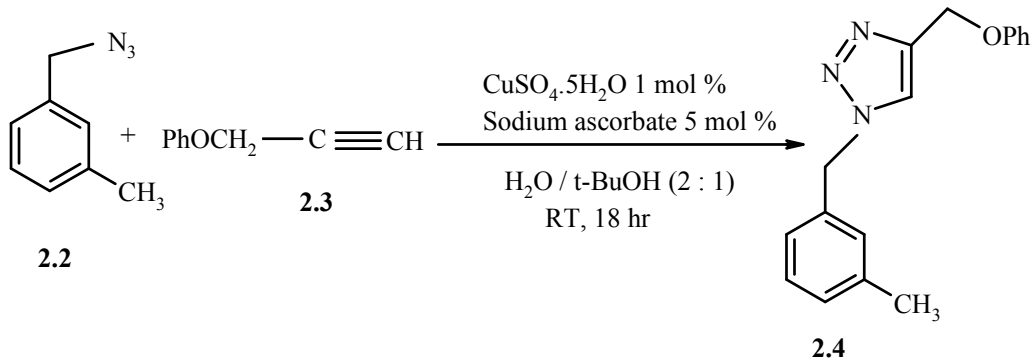


**Scheme 2.5.** Click reaction between 3-methyl benzyl azide and phenyl propargyl ether

The Click product **2.4** was fully characterised by $^{1}$H-, $^{13}$C-, and NOSEY-NMR and MS. The formation of 1,2,3-triazole ring was confirmed by the appearance of a clear characteristic peak in the $^{1}$H-NMR spectrum at 7.43 ppm for the triazole's proton ($H_8$), Fig. 2.10. Moreover, $^{13}$C-NMR spectrum of **2.4** showed two new peaks at 143.76 and 122.97 ppm, assigned to the triazole's double bond carbons, ($C_9$) and ($C_8$), respectively, Fig. 2.11.

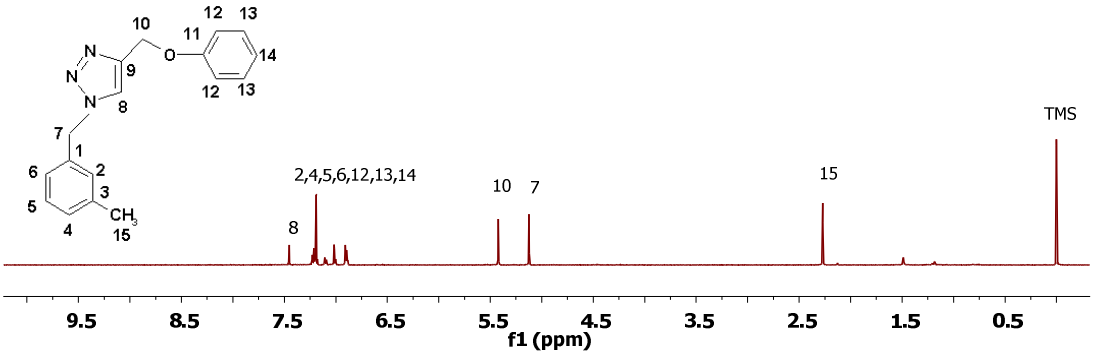


**Figure 2.10.** $^{1}$H-NMR spectrum of product **2.4** in $CDCl_3$

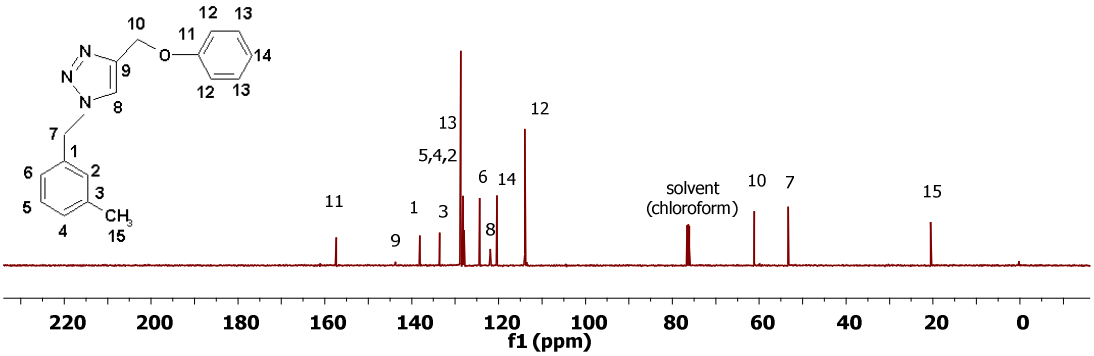


**Figure 2.11.** $^{13}$C-NMR spectrum of product **2.4** in $CDCl_3$

NOSEY-NMR technique was used to verify the regio-selectivity of the cycloaddition reaction under the copper catalytic condition. NOESY-NMR spectrum of **2.4** showed an obvious interaction between the triazole's proton ($H_8$) and the protons of both methylene groups attached to the triazole ring ($H_7$ and $H_{10}$), Fig. 2.12. Moreover, no interaction was observed between $H_7$ and $H_{10}$, indicating the presence of the triazole proton between two methylene groups. This established the formation of the 1,4-disubstituted isomer.

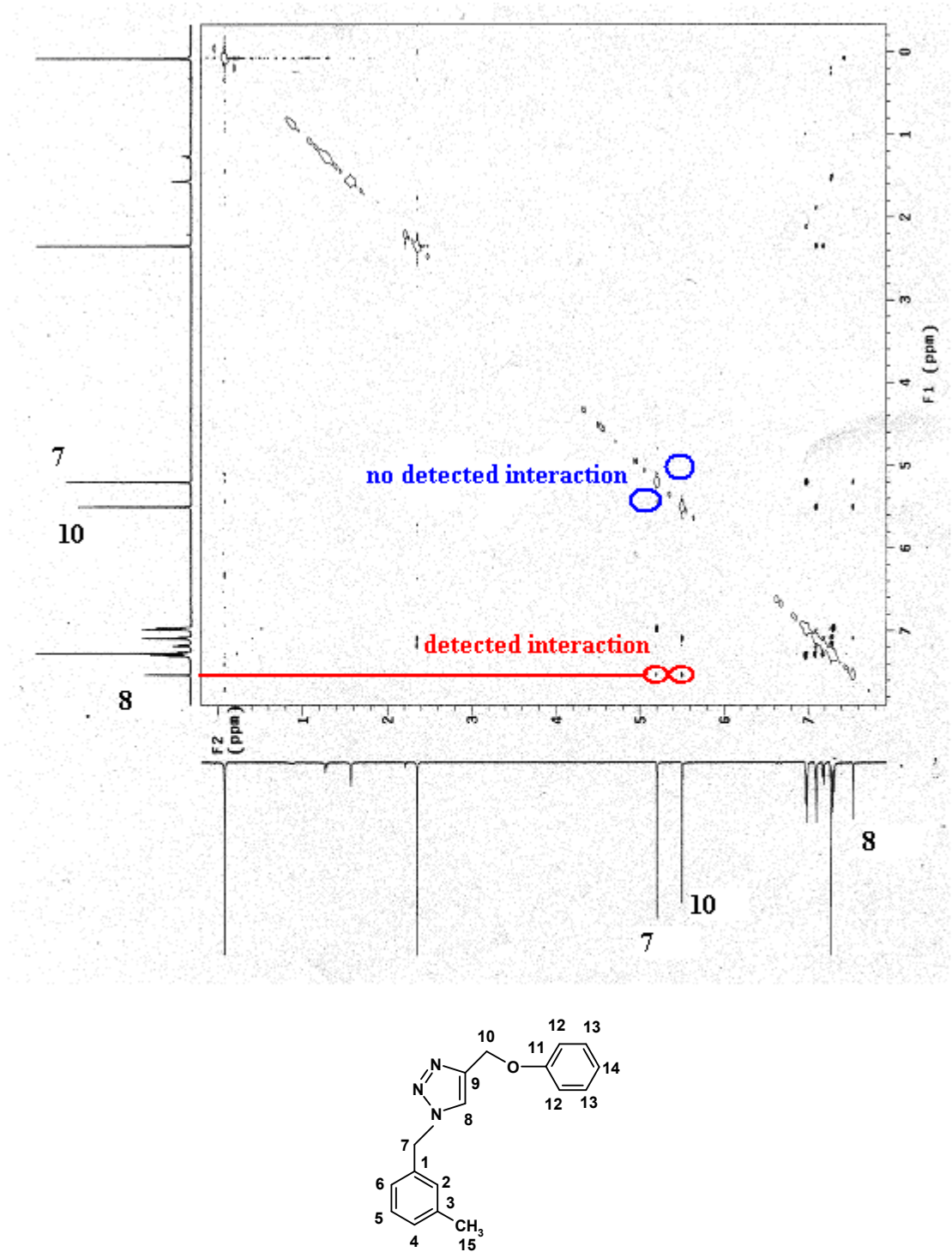


**Figure 2.12.** NOSEY-NMR spectrum of product **2.4** in $CDCl_3$

ESI-MS results of **2.4** showed a base peak at 280.3, which is in a good agreement with the theoretical calculation for $[M + H]^+$.

## 2.4. Summary

Click chemistry was successfully utilised on model compounds to produce the model product **2.4**. NMR spectroscopy was found to be a good choice for characterisation of the resulting products. The process involved in the reactions and their full characterisations provided extremely useful knowledge and understanding, which will be applied in the following chapters.

## 2.5. References


1. H. C. Kolb, and K. B. Sharpless, *Drug Discov. Today* **2003**, *8*, 1128–1137.
2. W. H. Zhan, H. N. Barnhill, K. Sivakumar, H. Tian, and Q. Wang, *Tetrahedron Letters* **2005**, *46*, 1691–1695.
3. V. V. Rostovtsev, L. G. Green, V. V. Fokin, and K. B. Sharpless, *Angewandte Chemie International Edition English* **2002**, *41*, 2596–2599.
4. V. D. Bock, H. Hiemstra, and J. H.-V. Maarseveen, *European Journal of Organic Chemistry* **2006**, 51–68.
5. X. Creary, T. L. Underiner, *Journal of Organic Chemistry* **1985**, *50 (12)*, 2165-70.
6. A. Shafiee, S. Toghraie, F. Aria, G. Mortezaei-Zandjani, *Journal of Heterocyclic Chemistry* **1982**, *19*, 1305 – 1308.

# Chapter 3

# Click Chemistry on α,α-D-Trehalose

## 3.1. Introduction

Trehalose is a symmetrical disaccharide composed of two glucose molecules bound by an alpha, alpha-1,1-linkage. It occurs naturally in many living organisms, including mushroom, insects, and yeasts. The usefulness of trehalose has been recognised and produced on an industrial scale since 1994.[1] Trehalose has a good sweetness property like sucrose. Compared to glucose, trehalose has virtually no immediate or long term effect on blood glucose levels. It shows poor reactivity against amino compounds in food, because it has high thermostability, wide pH-stability range, and no reducing power. Trehalose masks unpleasant tastes and odours in food. Therefore, it is superb for the maintenance of food quality.[2]

It has been reported that trehalose is capable of suppressing degradation of lipids. The oxidation products of lipids have a bad influence on human health and aging. It is also known that the typical odour from seniors skins which increases with age, especially after 55 years is due to unsaturated aldehydes which are produced by the degradation of unsaturated fatty acid (palmitoleic acid). Therefore, trehalose has a great potential in personal care and cosmetic applications.[3]

A recent physiological study on mice bones suggested that trehalose might have a kind of suppressive effect on the development of osteoporosis.[4] These results further imply that the daily ingestion of trehalose-containing foods could be useful for both bone metabolism and prevention of osteoporosis. Furthermore, it has been shown that trehalose could protect corneal epithelial cells in culture from death by desiccation and suppress tissue denaturalisation.[5,6] Hence, trehalose has been considered as a potential new drop for dry eyes syndrome and for effective preservation of organs.

The overview of this chapter is to illustrate the applicability of Click chemistry on trehalose. The interest in trehalose steamed not only from its unique properties but also from the fact that trehalose is a saccharide model compound which has the same functionalities as the core skeleton of polysaccharides, in particular 2-hydroxyethyl cellulose (HEC), which will be discussed in details in chapter 5. Investigation of Click reactions on trehalose and characterisation of the products would provide a valuable knowledge for evaluating Click reactions on HEC.

Ester, acrylate and epoxy functionalities are introduced on trehalose. The di-acrylate functionalised trehalose shows a cross-linking ability in the polymerisation of 2-hydroxyethyl methacrylate (HEMA).

## 3.2. Experimental

### 3.2.1. Materials

α,α-D-Trehalose dihydrate was purchased from Sigma – Aldrich and fully characterised by NMR spectroscopy.

All other chemicals and reagents used in the synthesis were also purchased from Sigma – Aldrich and used without further purification. All dry solvents were obtained from the Solvent Purification System (SPS), Chemistry Department, Durham University.

### 3.2.2. Instrumentation and Measurements

$^{1}$H-NMR spectra were recorded using deuteriated solvent lock on a Varian Mercury 400 or a Varian Inova 500 spectrometer at 400 MHz and 500 MHz, respectively. Chemical shifts are quoted in ppm, relative to tetramethylsilane (TMS), as the internal reference. $^{13}$C-NMR spectra were recorded at 101 MHz or 126 MHz (2000 scans) using continuous broad band proton decoupling and a 3 S recycle delay, and therefore not quantitative; chemical shifts are quoted in ppm, relative to $CDCl_3$ (77.55 ppm). The following abbreviations are used in listing NMR spectra: s = singlet, d = doublet, t = triplet, q = quartet, m = multiplet, b = broad. DEPT (Distortionless Enhancement by Polarization Transfer) experiment allows to determine multiplicity of carbon atom substitution with hydrogens. It differentiates between CH, $CH_2$ and $CH_3$ groups. The spectrum gives all CH and $CH_3$ in a phase opposite to $CH_2$. Signals from quaternary carbons and other carbons with no attached protons are always absent.

Electron Impact (EI) and Electrospray ($ES^+$) mass spectra were recorded on a Thermo Finnigan LTQ FT spectrometer operating at 70 eV with the ionisation mode as indicated.

FT-IR spectra were recorded on a Perkin Elmer 1600 series FT-IR spectrometer fitted with a golden gate. The samples were used as solids or liquids.

Molecular weight analysis was carried out by gel permission chromatography (GPC) on a Viscotek TDA 302 with refractive index, viscosity and light scattering detector (with a 690 nm wavelength laser), unless otherwise stated. Two 300 mm PLgel 5 μm mixed C columns (with a linear range of molecular weight from 200 to 2 000 000 $gmol^{-1}$) were used. THF or DMF was used as the eluent with a flow rate of 1.0 $mLmin^{-1}$ at 30 $^{o}$C.

### 3.2.3. Synthesis of 2,3,4,2′,3′,4′-Hexa-*O*-Acetyl-6,6′-Ditosyl-6,6′-Dideoxy-D-Trehalose 3.1

The product **3.1** was prepared using the following literature procedure and the characterisation results were in a good agreement.[7,8]

In a dry three-necked round-bottom flask, equipped with magnetic stirrer, thermometer and condenser, trehalose dihydrate (4 g, 11 mmol) was dissolved in pyridine (56 mL) and kept under $N_2$ atmosphere. The colour of the solution changed from lime green to pale yellow with the slow addition of ρ-toluenesulfonyl chloride (10 g, 53 mmol) during which heat was emitted. The reaction was stirred for 1 hr, the mixture quenched with acetic anhydride (56 mL) and stirred for further 18 hr. The resulting dark solution was poured over ice water (600 mL) and the precipitate was collected. The crude product was recrystallised from methanol three times. The crystals was dried in an oven at 40 $^{o}$C under reduced pressure to give the product **3.1** as a white solid, mp 170 – 172 °C, yield 14 % (1.39 g, 1.54 mmol).

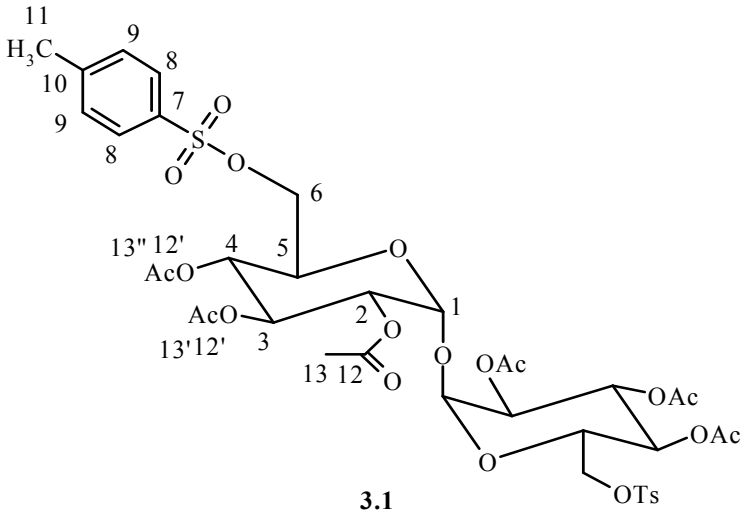


**3.1**

**Figure 3.1.** Structure of 2,3,4,2′,3′,4′-hexa-*O*-acetyl-6,6′-ditosyl-6,6′-dideoxy-D-trehalose with numerical assignment for NMR

$^{1}$H-NMR (400 MHz, $CDCl_3$): δ 7.69 (d, $J$ = 8.3 Hz, 4H, $H_8$), 7.30 (d, $J$ = 8.0 Hz, 4H, $H_9$), 5.35 (t, $J$ = 5.4 Hz, 2H, $H_3$), 4.96 – 4.79 (m, 6H, $H_{1,6}$), 4.12 – 3.90 (m, 6H, $H_{5,2,4}$), 2.40 (s, 6H, $H_{11}$), 2.03 (s, 6H); 1.98 (s, 6H); 1.96 (s, 6H) ($H_{13,13',13''}$).

$^{13}$C-NMR (101 MHz, $CDCl_3$): δ 168.88; 168.53; 168.50 ($C_{12,12',12''}$), 144.28; 131.53; 128.88; 127.06 ($C_{7,8,9,10}$), 91.81 ($C_1$), 68.84; 68.26; 67.62; 67.20 ($C_{2\text{-}5}$), 66.58 ($C_6$), 20.64 ($C_{11}$), 19.61; 19.55 ($C_{13,13',13''}$).

HRMS: calcd for $C_{38}H_{46}O_{21}S_2$ + Na = 925.18652; found for $(M + Na)^+$ = 925.18563.

Anal. Calc for $C_{38}H_{46}O_{21}S_2$: C 50.55, H 5.14, S 7.10. Found: C 50.69, H 5.14, S 7.02.

### 3.2.4. Synthesis of 2,3,4,2′,3′,4′-Hexa-*O*-Acetyl-6,6′-Di-azide functionalised-6,6′-Dideoxy-D-Trehalose 3.2

The product **3.2** was prepared using the following literature procedure and the characterisation results were in a good agreement.[7,8]

Sodium azide (154 mg, 2 mmol) was added to a solution of the protected ditosylated trehalose **3.1** (1 g, 1 mmol) in 1,3-dimethyl-3,4,5,6-tetrahydro-2-(1H)-pyrimidinone (DMPU) (7 mL) in a dry three-necked round-bottom flask, equipped with magnetic stirrer, condenser, and kept under $N_2$ atmosphere. The mixture was stirred in an oil bath at 90°C for 6 hr. The maroon-coloured reaction mixture was quenched with water and the resulting precipitate was isolated. Repeated recrystallisations (2 times) of the precipitate from methanol was performed. The crystals were dried in an oven at 40 $^{o}$C under reduced pressure to give the product **3.2**, mp 114 – 116 °C, yield 64 % (0.6 g, 0.64 mmol).

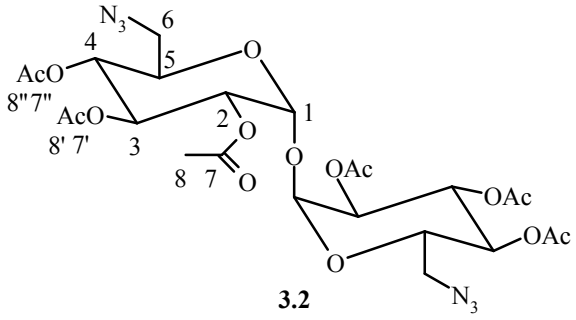


**3.2**

**Figure 3.2.** Structure of 2,3,4,2′,3′,4′-hexa-*O*-acetyl-6,6′-di-azide functionalised-6,6′-dideoxy-D-trehalose with numerical assignment for NMR

$^{1}$H-NMR (400 MHz, $CDCl_3$): δ 5.44 (t, *J* = 5.5 Hz, 2H, $H_3$), 5.30 (d, *J* = 3.9 Hz, 2H, $H_1$), 5.06 (dd, *J* = 3.9 Hz, 3.9 Hz, 2H, $H_2$), 4.96 (t, *J* = 5.0 Hz, 2H, $H_4$), 4.12 – 4.00 (m, 2H, $H_5$), 3.34 (dd, *J* = 7.3 Hz, 13.3 Hz, 2H, $H_6$), 3.14 (dd, *J* = 2.4 Hz, 13.3 Hz, 2H, $H_{6'}$), 2.10 (s, 6H); 2.04 (s, 6H); 2.00 (s, 6H) ($H_{8,8',8''}$).

$^{13}$C-NMR (101 MHz, $CDCl_3$): δ 168.95; 168.65; 168.60 ($C_{7,7',7''}$), 92.00 ($C_1$), 68.92; 68.84; 68.74; 68.68 ($C_{2\text{-}5}$), 51.01 ($C_6$), 24.39; 19.64; 19.62 ($C_{8,8',8''}$).

Anal. Calcd for: $C_{24}H_{32}N_6O_{15}$: C 44.72, H 4.97, N 13.04. Found: C 44.72, H 5.06, N12.94.

FT-IR: 2097cm$^{-1}$ (C-$N_3$)

### 3.2.5. Synthesis of Protected Trehalose Clicked with Ethyl Propiolate 3.3

In a vial, protected di-azide functionalised trehalose **3.2** (0.133 g, 0.2 mmol), ethyl propiolate (0.04 mL, 0.4 mmol), copper (II) sulfate pentahydrate (11 mg, 0.04 mmol)

and sodium ascorbate (16 mg, 0.08 mmol) were added to t-butanol / water (1:1, 3 mL). The mixture was stirred and heated up to 50 $^{o}$C in an oil bath for 6 hr. The mixture was then cooled down in an ice bath. The resulting mixture consisted of a blue solution and a white precipitate. The white precipitate was collected and washed three times by water. The solid was dried in an oven at 40 $^{o}$C under reduced pressure to give the product **3.3**, mp 133 – 135 $^{o}$C, yield 90 % (0.15 g, 0.18 mmol).

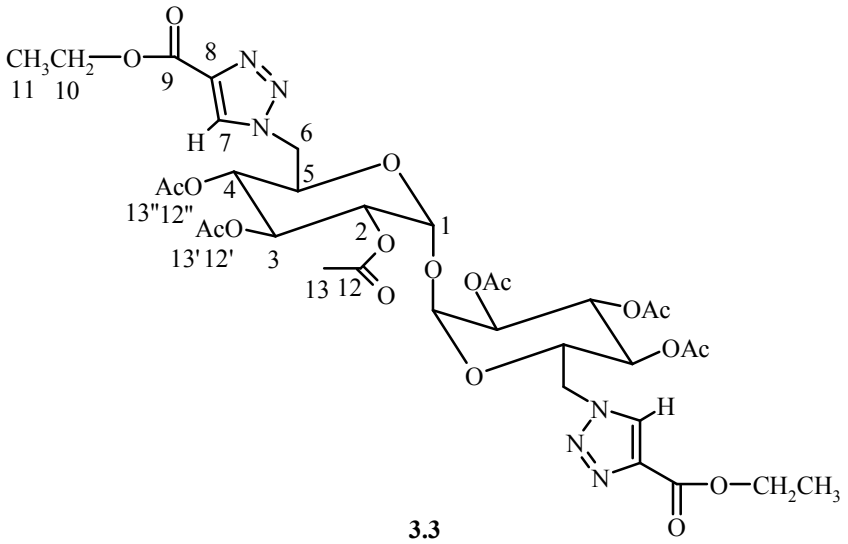


**3.3**

**Figure 3.3.** Structure of protected trehalose clicked with ethyl propiolate with numerical assignment for NMR

$^{1}$H-NMR (400 MHz, $CDCl_3$): δ 8.13 (s, 2H, $H_7$), 5.48 (t, $J$ = 5.4 Hz, 2H, $H_3$), 4.87 − 4.21 (m, 16H, $H_{1,2,4,5,6,10}$), 2.11 (s, 6H, $H_{13}$), 2.07 (s, 6H, $H_{13'}$), 2.00 (s, 6H, $H_{13''}$), 1.43 (t, $J$ = 7.09 Hz , 6H, $H_{11}$).

$^{13}$C-NMR (101 MHz, $CDCl_3$): δ 170.01; 169.98; 169.50 ($C_{12,12',12''}$), 160.77 ($C_9$), 129.13 ($C_7$), 92.03 ($C_1$), 69.97; 69.60; 69.06; 68.98 ($C_{2\text{-}5}$), 61.75 ($C_{10}$), 51.17 ($C_6$), 20.91; 20.83; 20.74 ($C_{13,13',13''}$), 14.57 ($C_{11}$).

Anal. Calcd for: $C_{34}H_{44}N_6O_{19}$: C 48.57, H 5.29, N 10.00. Found: C 49.15, H 5.11, N 8.77.

### 3.2.6. Deacetylation (Deprotection) Reaction of Protected Trehalose Clicked with Ethyl Propiolate 3.4

In a vial, protected trehalose clicked with ethyl propiolate **3.3** (0.1 g, 0.12 mmol) and a solution of NaOMe (0.04 g, 0.72 mmol) in MeOH (5 mL) were mixed and stirred at ambient temperature for 18 hr. Acetone and methanol washed Dowex MR-3 mixed bed

ion-exchange resin (~ 1 g) was added. The mixture was stirred until a pH of 7 was attained. The neutralised solution was filtered and the solvent was removed under reduced pressure. The resulting solid was dried in an oven at 40 $^{o}$C under reduced pressure to give the product **3.4**, yield 94 % (0.065 g, 0.11 mmol).

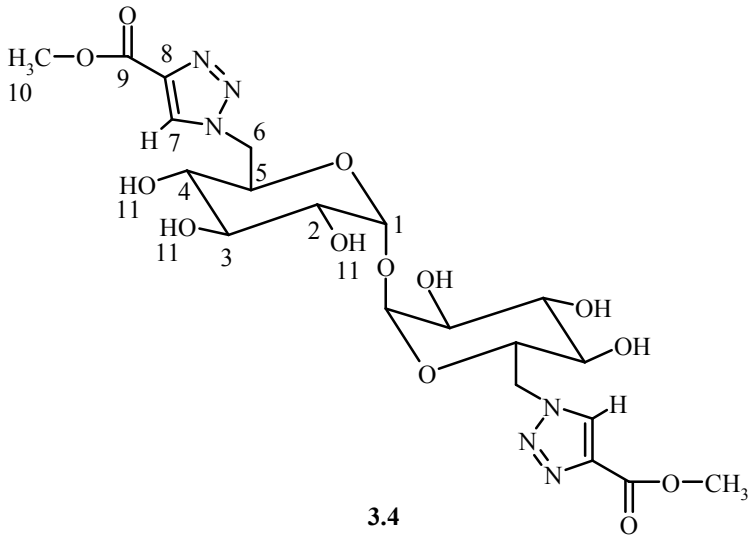


**3.4**

**Figure 3.4.** Structure of deprotected trehalose clicked with ethyl propiolate with numerical assignment for NMR

$^{1}$H-NMR (400 MHz, DMSO-$d_6$): δ 8.55 (s, 2H, $H_7$), 5.35 (s, 2H, $H_3$), 4.97 – 4.54 (m, 12 H, $H_{1,2,4,5,6}$), 4.07 (bs, 6H, $H_{11}$), 3.82 (s, 6H, $H_{10}$).
$^{13}$C-NMR (101 MHz, DMSO-$d_6$): δ 161.26 ($C_9$), 138.85 ($C_8$), 130.17 ($C_7$), 94.38 ($C_1$), 72.96; 71.60; 71.42; 70.06 ($C_{2\text{-}5}$), 52.24 ($C_{10}$), 51.28 ($C_6$).

### 3.2.7. Synthesis of Protected Trehalose Clicked with Propargyl Acrylate 3.5

In a vial, protected di-azide functionalised trehalose **3.2** (500 mg, 0.775 mmol), propargyl acrylate (170 mg, 1.55 mmol), copper (II) sulfate pentahydrate (40 mg, 0.155 mmol), sodium ascorbate (65 mg, 0.31 mmol) were added to THF / water (5:1, 6 mL). The mixture was heated to 50 $^{o}$C in an oil bath for 24 hr and then water (5 mL) was added. The resulting yellowish precipitate was collected by filtration and washed with water (x 3). The solid was dried under reduced pressure to give the pale yellow product **3.5**, mp 139 – 141 $^{o}$C, yield 92 % (620 mg, 0.713 mmol).

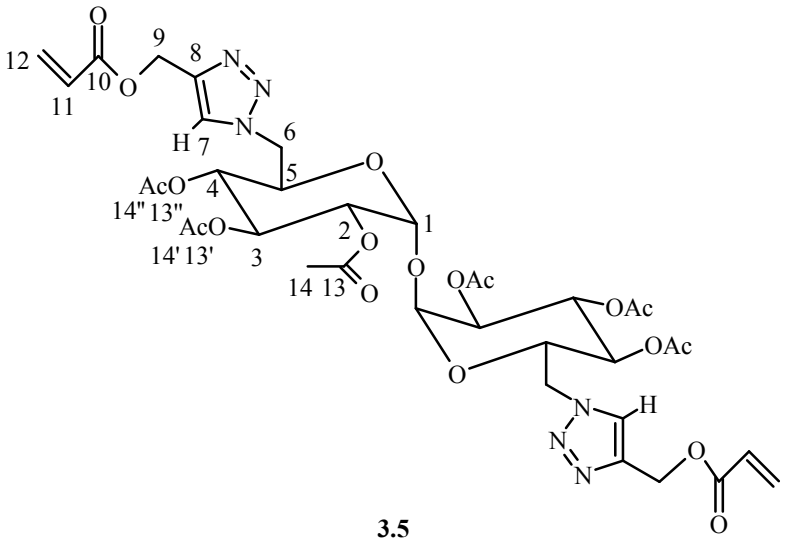

**3.5**

**Figure 3.5.** Structure of protected trehalose clicked with propargyl acrylate with numerical assignment for NMR

$^{1}$H-NMR (400 MHz, $CDCl_3$): δ 7.72 (s, 2H, $H_7$), 6.45 (d, *J* = 17.43 Hz, 2H, $H_{12}$), 6.15 (dd, *J* = 10.45 Hz, 17.31 Hz, 2H, $H_{11}$), 5.88 (d, *J* = 10.39 Hz, 2H, $H_{12}$), 5.43 (s, 2H, $H_3$), 5.31 (s, 4H, $H_9$), 4.94 (s, 2H, $H_1$), 4.88 (s, 2H, $H_2$), 4.86 (s, 2H, $H_4$), 4.57 (d, *J* = 13.27 Hz, 2H, $H_6$), 4.28 (d, *J* = 8.86 Hz, 2H, $H_6$), 4.20 (m, 2H, $H_5$), 2.19 (s, 6H); 2.01 (s, 12H) ($H_{14,14',14''}$).

$^{13}$C-NMR (101 MHz, $CDCl_3$): δ 169.55; 169.01 ($C_{13,13',13''}$), 165.80 ($C_{10}$), 143.00 ($C_8$), 131.19 ($C_{12}$), 127.89 ($C_{11}$), 125.04 ($C_7$), 91.58 ($C_1$), 69.58 ($C_3$), 69.36 ($C_2$), 68.82 ($C_5$), 68.51 ($C_4$), 57.39 ($C_9$), 50.47 ($C_6$), 20.45; 20.35; 20.23 ($C_{14,14',14''}$).

HRMS: calcd for $C_{36}H_{44}N_6O_{19}$ + K = 903.22928; found for $(M + K)^+$ = 903.22905.

### 3.2.8. Synthesis of Protected Trehalose Clicked with Glycidyl Propargyl Ether 3.6

In a dry three-necked round-bottom flask, equipped with magnetic stirrer and rubber seal septum, protected di-azide functionalised trehalose **3.2** (200 mg, 0.31 mmol), glycidyl propargyl ether (70 mg, 0.62 mmol) and CuBr (44 mg, 0.31 mmol) were added to dry THF (15 mL) under $N_2$ atmosphere. Pentamethyldiethylenetriamine (PMDETA) (54 mg, 0.31 mmol) was then injected to the mixture using a syringe and the mixture was stirred at 35 $^{o}$C for 24 hr. The mixture was filtered and the filtrate was stirred in amberlite IRC 748 sodium form (resin exchanger) for 3 hr. The solvent was removed under reduced pressure to produce viscous liquid product **3.6**, yield 74 % (200 mg, 0.23 mmol).

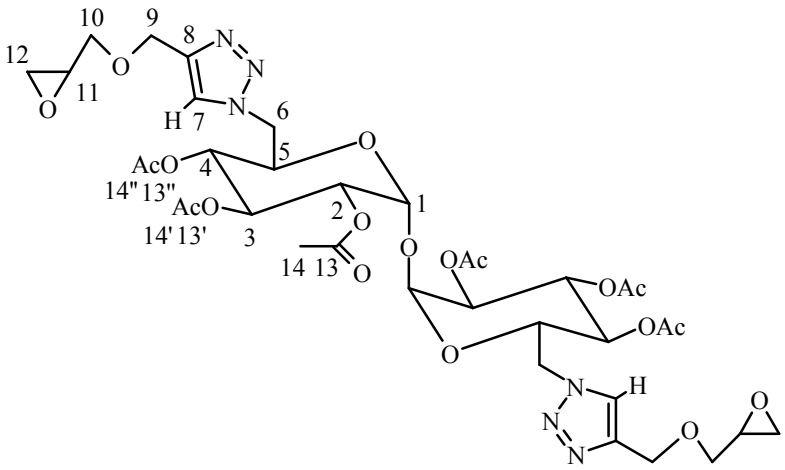

**3.6**

**Figure 3.6.** Structure of protected trehalose clicked with glycidyl propargyl ether with numerical assignment for NMR

$^{1}$H-NMR (400 MHz, $CDCl_3$): δ 7.65 (s, 2H, $H_7$), 5.44 (t, *J* = 9.7 Hz, 2H, $H_3$), 4.98 (d, *J* = 10.2 Hz, 2H, $H_1$), 4.86 (m, 4H, $H_2$), 4.70 (s, 4H, $H_9$), 4.55 (m, 2H, $H_4$), 4.25 (m, 2H, $H_5$), 3.87 (m, 2H, $H_{11}$), 3.45 (m, 4H, $H_6$), 3.19 (d, *J* = 2.2 Hz, 2H, $H_{10}$), 2.82 (t, *J* = 4.4 Hz, 2H, $H_{12}$), 2.65 (m, 2H, $H_{12}$), 2.12 (s, 6H, $H_{14}$), 2.05 (s, 6H, $H_{14'}$), 2.01 (s, 6H, $H_{14''}$).
$^{13}$C-NMR (101 MHz, $CDCl_3$) δ 169.74; 169.72; 169.35 ($C_{13,13',13''}$), 145.37 ($C_8$), 124.00 ($C_7$), 91.71 ($C_1$), 67.94 ($C_{10}$), 64.58 ($C_9$), 50.69 ($C_6$), 50.41 ($C_{11}$), 44.19 ($C_{12}$), 20.64; 20.56; 20.50 ($C_{14,14',14''}$).
ESI-MS: calcd for $C_{36}H_{48}N_6O_{19}$ + Na = 891.79592; found for $[M + Na]^+$ = 891.3.

### 3.2.9. Synthesis of Poly(2-hydroxyethyl methacrylate) (HEMA) 3.7

In a dry ampoule, 2-hydroxyethyl methacrylate (HEMA) (1 g, 7.7 mmol) and azobisisobutyronitrile (AIBN) (31 mg, 0.19 mmol) were dissolved in dry DMF (2 mL). The solution was degassed three times by freeze pump thaw technique. The ampoule was sealed under vacuum and placed in an oil bath at 70 °C. The mixture was stirred for 2 hr. The polymer was precipitated into toluene and reprecipitated from DMF into toluene. The polymer was dried in an oven at 40 $^{o}$C under reduced pressure to produce the product **3.7**, yield 95 % (0.95 g).

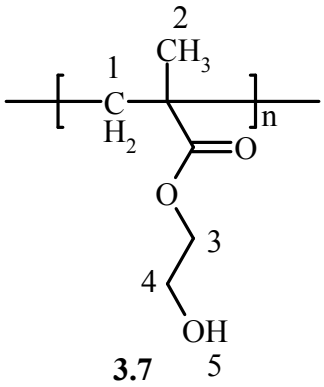


**3.7**

**Figure 3.7.** Structure of PHEMA with numerical assignment for NMR

$^1$H-NMR (400 MHz, DMSO): δ 4.82 (bs, 1H, $H_5$), 3.90 (bs, 2H, $H_3$), 3.58 (bs, 2H, $H_4$), 0.94; 0.77 (bs, 3H, $H_2$ two isomers).
GPC: $M_n$ = 108,400 gmol$^{-1}$, PDI of 1.8.

### 3.2.10. Synthesis of Cross-linked PHEMA 3.8

In an NMR tube fitted with young's tap, 2-hydroxyethyl methacrylate (HEMA) (200 mg, 1.54 mmol), azobisisobutyronitrile (AIBN) (6.5 mg, 0.04 mmol) and propargyl acrylate clicked protected trehalose **3.5** (6.7 mg, 0.077 mmol) were dissolved in dry DMF-$d_6$ (0.8 mL). The solution was degassed three times by freeze pump thaw technique. The tube was sealed under vacuum and placed in an NMR machine at fixed temperature of 70 °C. The NMR machine was programmed to run a $^1$H spectrum every 15 min. The experiment was stopped after 45 min. The resulting gel was removed from the tube, extracted with DMF (100 mg of the sample / 2 mL of DMF) at 60 $^o$C for 24 hr and the gel content was calculated (90 %).

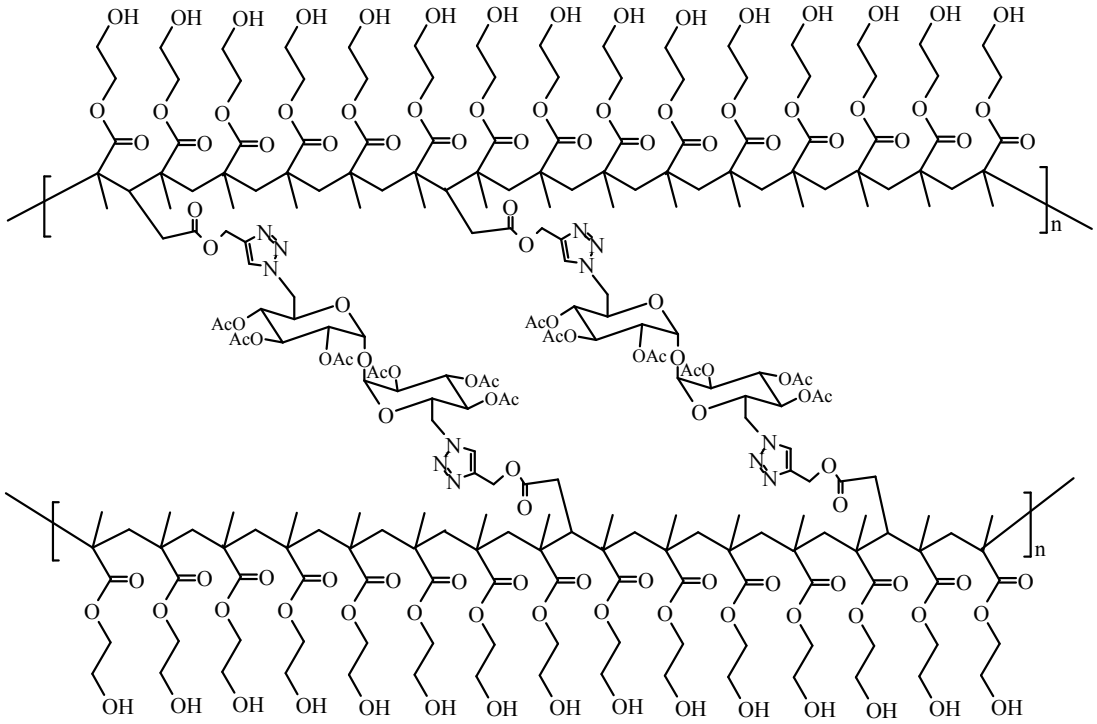

**cross-linked material**

**3.8**

**Figure 3.8.** Structure of cross-linked PHEMA

### 3.3. Results and Discussion

#### 3.3.1. Azide Functionalisation of Trehalose

The azide functionalisation strategy of trehalose, as a bi-functional saccharide model compound, is based on two steps. Intermediate **3.1** was prepared by selective tosylation of the two primary hydroxyl groups followed by protection of the secondary hydroxyl groups by acetic anhydride. The protection of the secondary hydroxyl groups induced the hydrophobicity in trehalose and facilitated the isolation of the product. The azidification reaction of **3.1** *via* nucleophilic substitution produced the protected di-azide functionalised trehalose **3.2**, Scheme 3.1.[7,8]

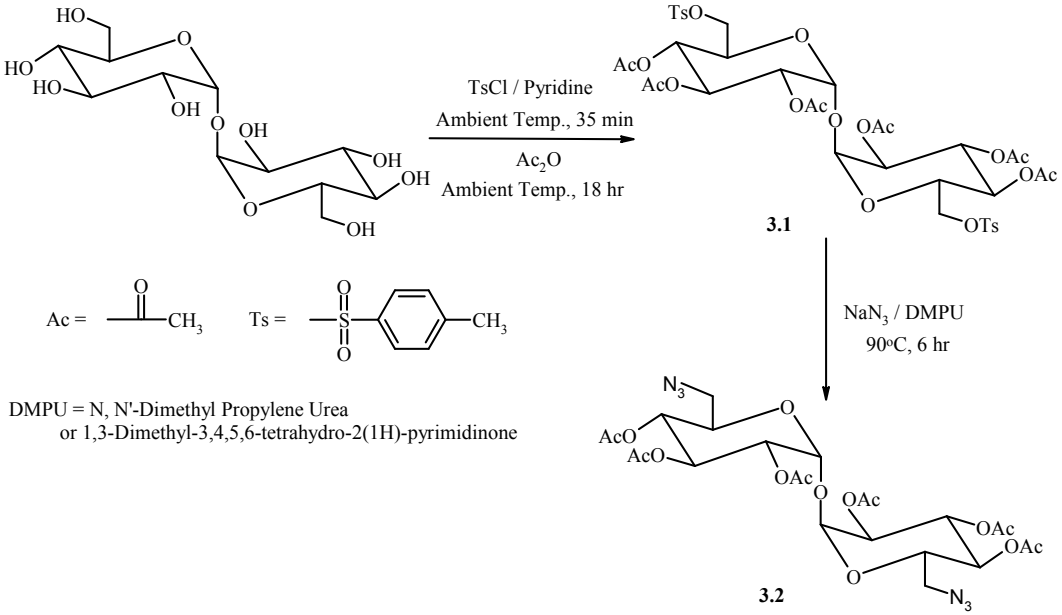


**Scheme 3.1.** Synthesis of the protected di-azide functionalised trehalose

The structures of **3.1** and the final product **3.2** were fully characterised by NMR, MS and IR. Tosylation occurred preferentially on $C_6$ (primary alcohol) while the secondary alcohols were all acetylated. $^1$H-NMR spectrum of **3.1** (Fig. 3.9.B) in comparison with that of trehalose (Fig. 3.9.A) showed appearance of new peaks for aromatic ($H_{8,9}$) and methyl hydrogens ($H_{11}$) of tosylate groups and the methyl hydrogens of the acetate groups ($H_{13,13',13''}$). The $^1$H-NMR spectrum of **3.1** also showed the right integration ratios for two tosylate groups and six acetate groups per trehalose unit.

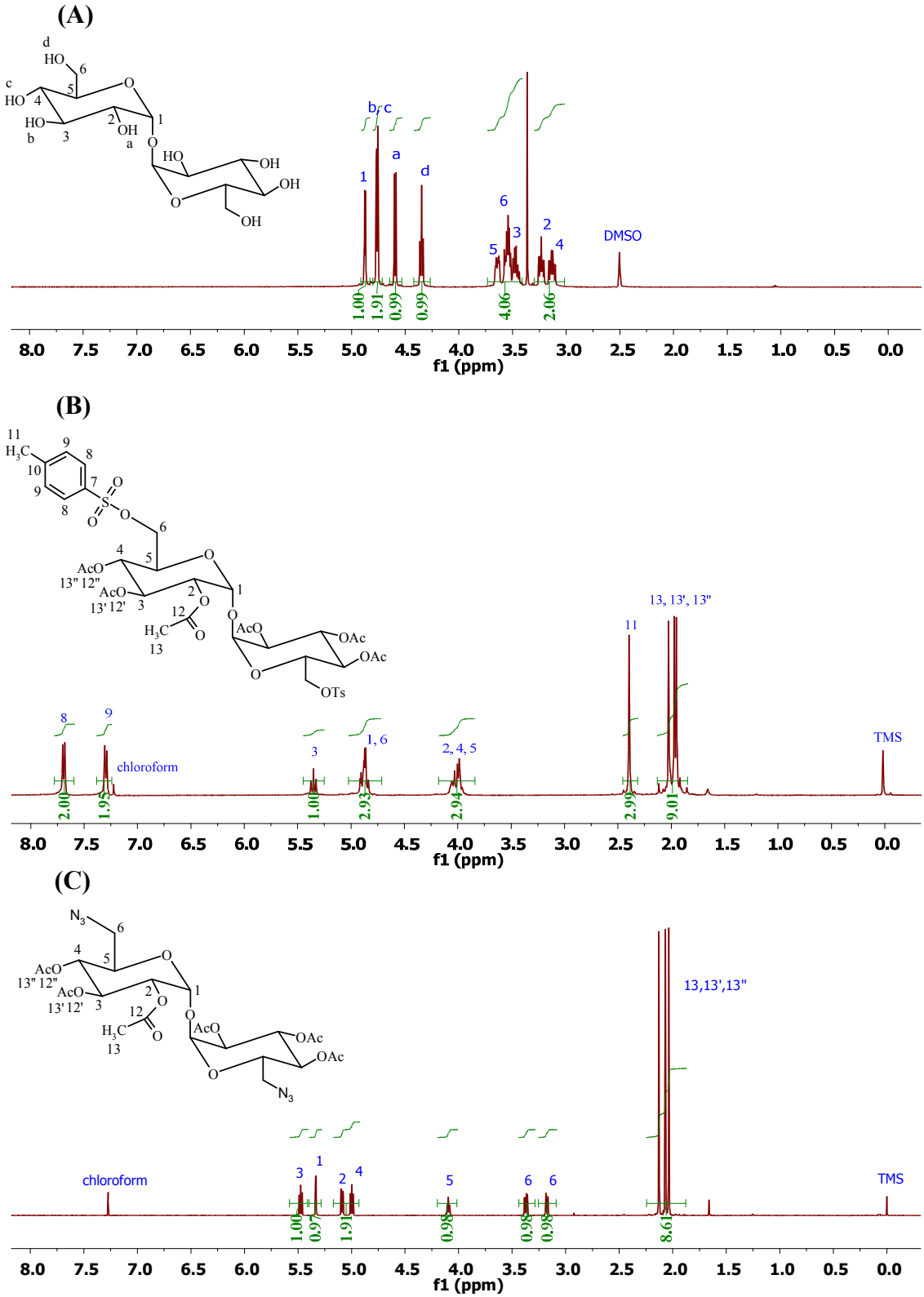


**Figure 3.9.** $^{1}$H-NMR spectra of (A) trehalose in DMSO-$d_6$, (B) protected ditosylated trehalose **3.1** in $CDCl_3$ and (C) protected di-azide functionalised trehalose **3.2** in $CDCl_3$

The $^{13}$C-NMR spectrum of **3.1** (Fig. 3.10.B) in comparison with that of trehalose (Fig. 3.10.A) showed the appearance of all the peaks for the carbons of the tosylate groups ($C_{7,8,9,10,11}$) and those of the acetate groups ($C_{12,12',12'',13,13',13''}$). Moreover, the

resonance due to $CH_2$ ($C_6$) was observed at higher δ-value, 66.58 ppm, (Fig. 3.10.B) in comparison with that of trehalose (Fig. 3.10.A). This provided a strong evidence for attachment of the $CH_2$ ($C_6$) to the tosyl group and the formation of the intermediate **3.1**. Although the spectrum of trehalose could not be taken in $CDCl_3$ due to its insolubility, the shift of the $CH_2$ peak ($C_6$) to higher δ-value is expected due to the higher electronegativity of the tosylate group compared to that for hydroxyl group.

After the successful tosylation and acetylation of trehalose, azidation was performed. In the comparison $^1$H-NMR spectra of **3.1** and **3.2** (Fig. 3.9.B and C), the peaks for aromatic hydrogens ($H_{8,9}$) and methyl hydrogens ($H_{11}$) of tosylate groups disappeared, however, those for the acetate hydrogens ($H_{13,13',13''}$) remained. This indicated the detachment of the tosylate groups. The comparison $^{13}$C-NMR spectra of **3.1** and **3.2** (Fig. 3.10.B and C) also showed disappearance of the peaks for aromatic carbons ($C_{7,8,9,10}$) and methyl carbons ($C_{11}$) of tosylate groups. Moreover, the shift to lower δ-value, 51.01 ppm, for the $CH_2$ peak ($C_6$) confirmed the attachment to azide group.

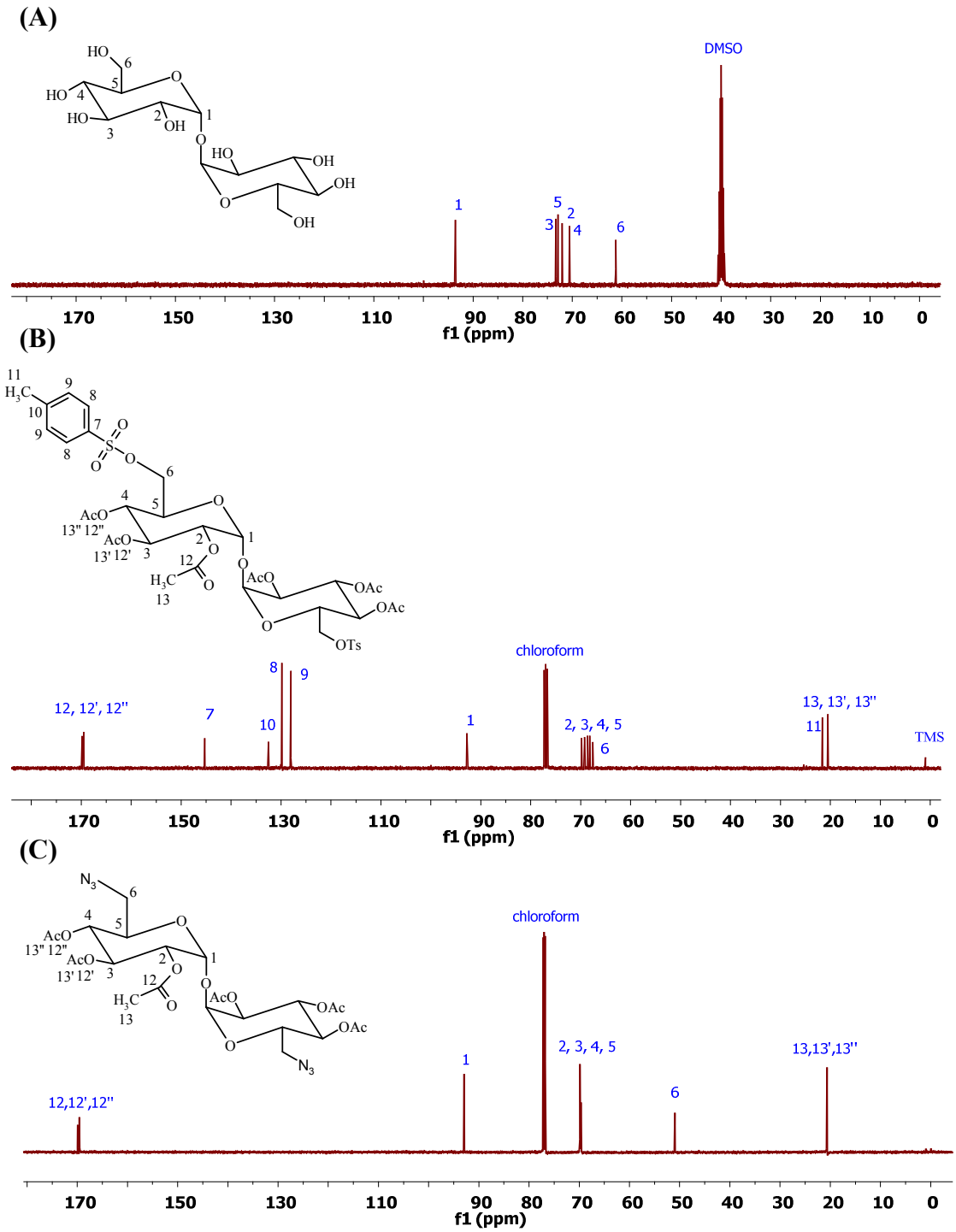


**Figure 3.10.** $^{13}$C-NMR spectra of (A) trehalose in DMSO-$d_6$, (B) protected di-tosylated trehalose **3.1** in $CDCl_3$ (C) protected di-azide functionalised trehalose **3.2** in $CDCl_3$

DEPT-NMR was found to be an efficient and easy way to follow up the azide functionalisation reaction of trehalose. The comparison DEPT-NMR spectra of trehalose, **3.1** and **3.2** (Fig. 3.11.A, B and C) showed the different chemical shifts for the inverted $CH_2$ peak ($C_6$) depending on the attached group. These obvious shifts illustrated the successful development of these functionalisation reactions.

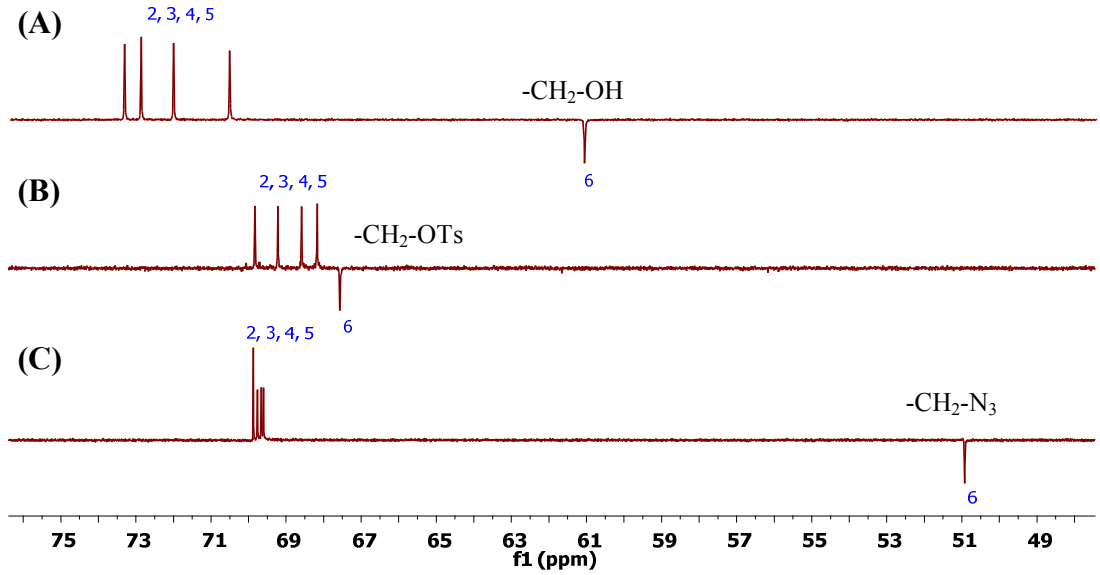


**Figure 3.11.** DEPT-NMR spectra of (A) trehalose in DMSO-$d_6$, (B) the protected ditosylated trehalose **3.1** in $CDCl_3$ and (C) the protected di-azide functionalised trehalose **3.2** in $CDCl_3$

FT-IR spectroscopy presented another useful tool for the characterisation of the reaction products. The IR spectra showed the presence of a strong peak at 1742 $cm^{-1}$ for the carbonyl groups in **3.1** and **3.2**, Fig. 3.12.B and C. The IR spectrum for **3.2** showed the presence of a strong absorption at 2097$cm^{-1}$ due to the azide group, Fig. 3.12.C.

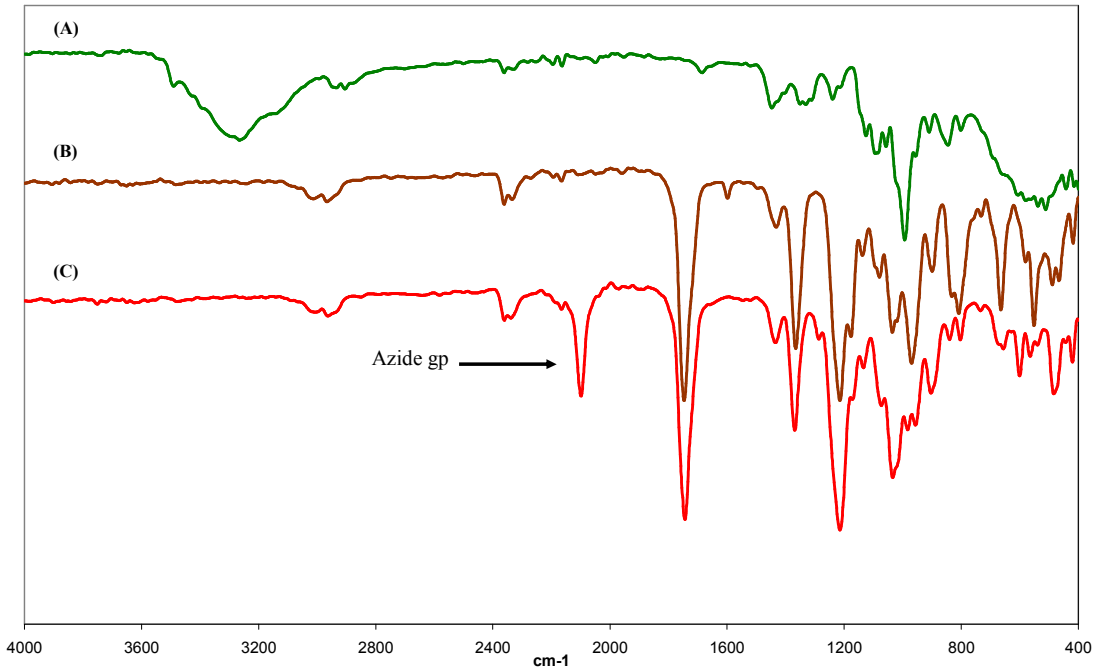


**Figure 3.12.** FT-IR spectra of (A) trehalose, (B) the protected di-tosylated trehalose **3.1**, and (C) the protected di-azide functionalised trehalose **3.2**

Although the tosylation and subsequent azidation of trehalose was successful, the overall yield of the tosylation followed by acetylation reaction was 14 %. However, the yield of tosylation followed by acetylation reactions for trehalose was reported to be low, about 14 %.[7,8] This could be attributed to several recrystallisation steps required for the purification of the final product. It could also be due to the formation of presently unknown different side reactions. Therefore, alternative routes for producing azide functionalised trehalose were sought and attempted. One alternative route was to perform chlorination on the primary alcohols, instead of tosylation, followed by acetylation for the secondary alcohols. The yield of chlorination followed by acetylation reactions was reported to be 88 %,[9] however, when the same procedure was repeated here, the yield was found to be 54 %. Although the yield is higher for the chlorination route, the following step, which is the azidation reaction, required high temperature (135 $^{o}$C) which was reported to cause partial deacetylation of the product.[9] The other alternative route was to perform iodination on the primary alcohols followed by azidation and then acetylation for the secondary alcohols. The yield of the iodination, azidation, and acetylation steps was reported to be 71, 60, and 23 %, respectively.[10] Therefore, the overall yield to produce the acetylated azide functionalised trehalose is not that different to the route used in this work. When the procedure was followed, it was found that the handling and the isolation of the iodinated product was even more complicated than reported previously.[10]

### 3.3.2. Functionalisation of Trehalose *via* Click Chemistry

A series of Click reactions on the protected di-azide functionalised trehalose **3.2** with different molecules containing potentially useful functional groups was performed to produce bi-functional trehalose derivatives. The method was used to introduce different functionalities such as ester, acrylate and epoxide groups.

#### 3.3.2.1. Introduction of Ester Functionality

Click reaction between the protected di-azide functionalised trehalose **3.2** and ethyl propiolate was carried out successfully, using copper sulphate pentahydrate and sodium ascorbate in a mixture of water and t-butanol (1:1) solvents, to yield the ester clicked product **3.3**, Scheme 3.2.

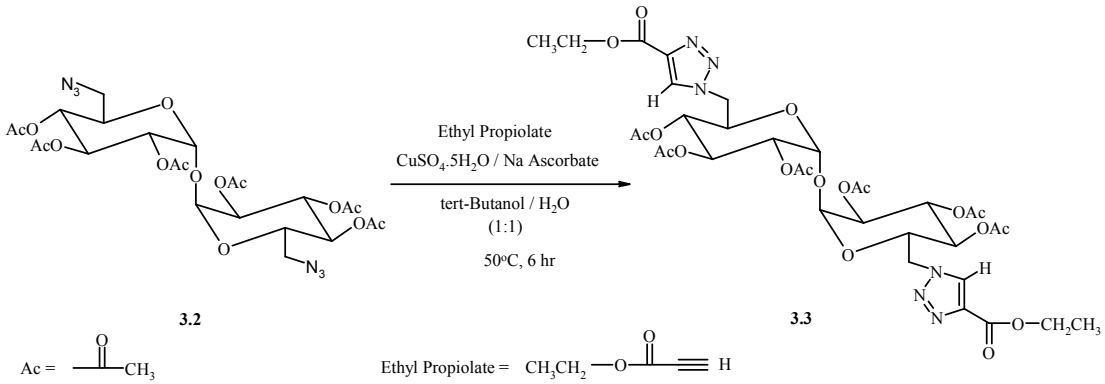


**Scheme 3.2.** Synthesis of protected trehalose clicked with ethyl propiolate

The structure of **3.3** was confirmed by $^{1}$H- and $^{13}$C-NMR spectroscopy. The $^{1}$H-NMR spectrum of **3.3** (Fig. 3.13) showed appearance of a peak at 8.13 ppm, assigned for the triazole proton ($H_7$). This provided a good evidence for the formation of 1,2,3-triazole ring. The spectrum also showed appearance of all peaks corresponding to the trehalose ($H_{1,2,3,4,5,6,13,13',13''}$) as well as the clicked ethyl propiolate ($H_{10,11}$). $^{13}$C-NMR spectrum of **3.3** (Fig. 3.14) also showed a peak at 129.13 ppm, corresponding to the double bond carbon of the triazole ring ($C_7$).

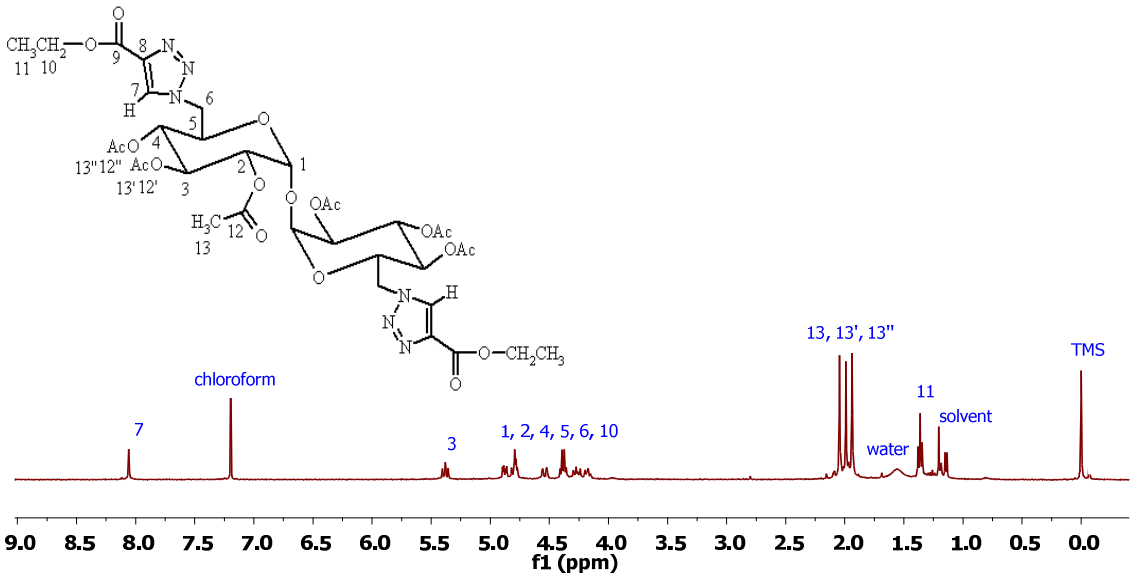


**Figure 3.13.** $^{1}$H-NMR spectrum of protected trehalose clicked with ethyl propiolate **3.3** in $CDCl_3$

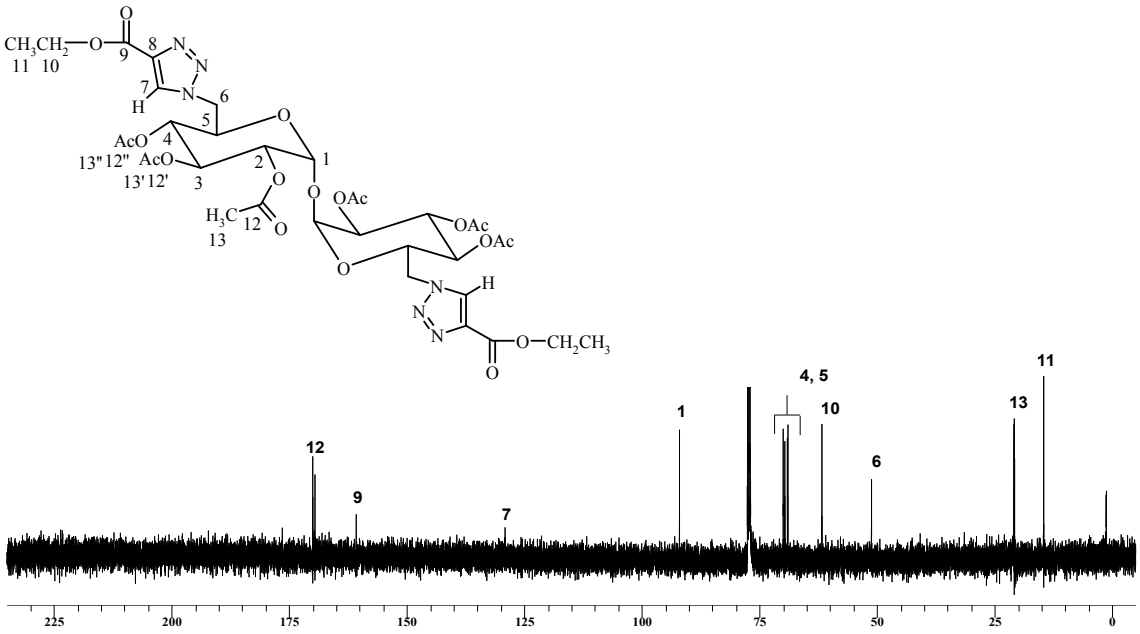


**Figure 3.14.** $^{13}$C-NMR spectrum of protected trehalose clicked with ethyl propiolate **3.3** in $CDCl_3$

FT-IR spectrum of **3.3** (Fig. 3.15.B) in comparison with **3.2** (Fig. 3.15.A) showed a complete disappearance of the azide peak at 2097 $cm^{-1}$, confirming the successful Click reaction and full conversion from azide to triazole ring.

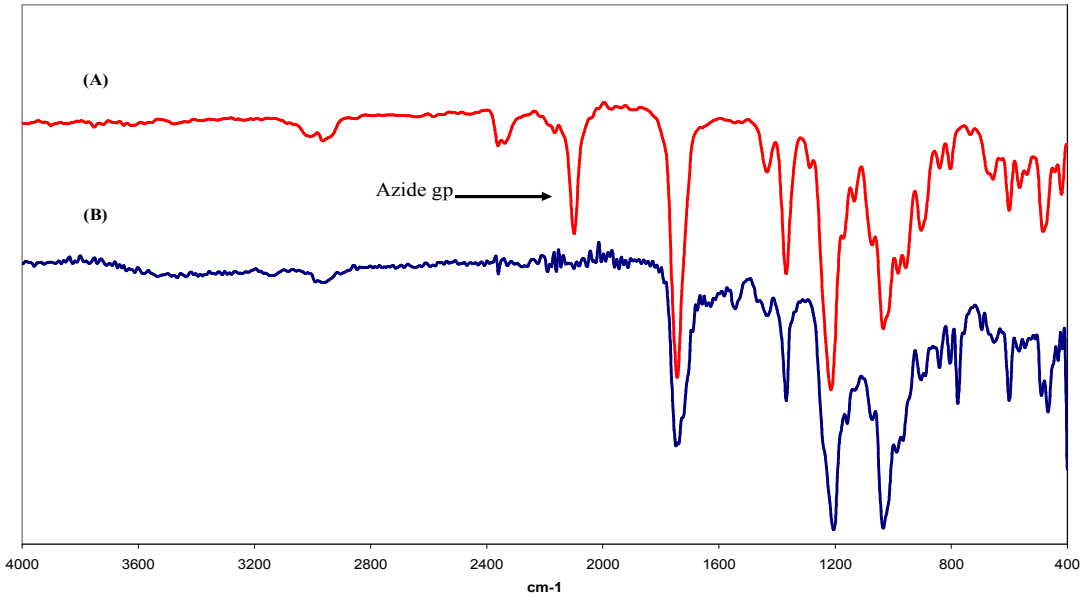


**Figure 3.15.** FT-IR spectra of (A) protected di-azide functionalised trehalose **3.2** and (B) protected trehalose clicked with ethyl propiolate **3.3**

The deprotection of the secondary hydroxyl groups in **3.3** was successfully carried out by using sodium methoxide in methanol to produce the deacetylated product **3.4**, Scheme 3.3.

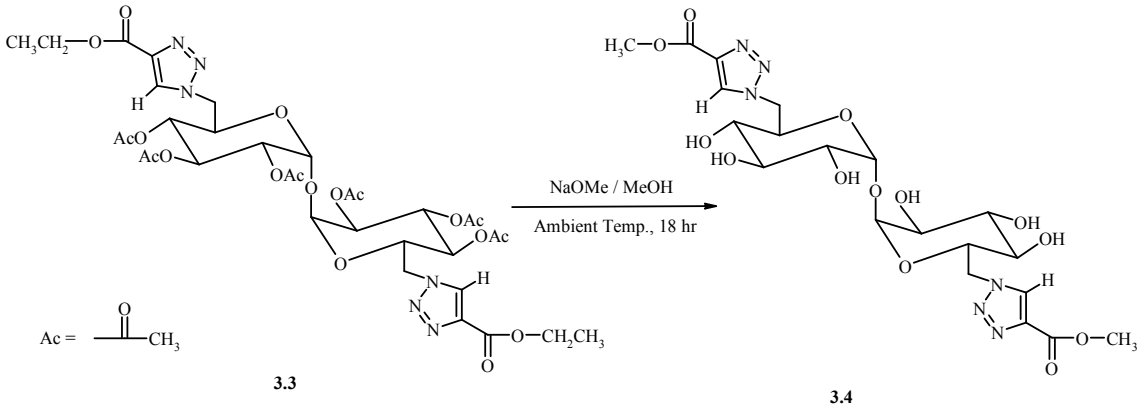


**Scheme 3.3.** Deprotection of protected trehalose clicked with ethyl propiolate

$^{1}$H- and $^{13}$C-NMR spectra of **3.4** showed clearly the absence of all the peaks corresponding to hydrogens and carbons of the acetate groups (Fig. 3.16 and 3.17) when compared with those of **3.3** (Fig. 3.13 and 3.14). In addition, because of the use of sodium methoxide / methanol as a deprotecting agent, the trans-esterification of ethyl ester in triazole ring was observed. The $^{13}$C-NMR spectrum of **3.3** (Fig. 3.14) showed two peaks at 51.74 and 62.27 ppm, corresponding to $CH_2$ groups adjacent to triazole ring ($C_6$) and $CH_2$ in the ester group ($C_9$), respectively. However, the $^{13}$C-NMR spectrum of **3.4** (Fig. 3.17) showed the disappearance of the peak at 62.27 ppm and appearance of a peak at 53.10 ppm, corresponding to the carbon of the methyl group ($C_{14}$). Furthermore, the DEPT-NMR spectrum also showed only one inverted peak at 51.74 ppm, assigned for the $CH_2$ adjacent to triazole ring ($C_6$) (Fig. 3.18). This confirmed the occurrence of the trans-esterification from ethyl to methyl group.

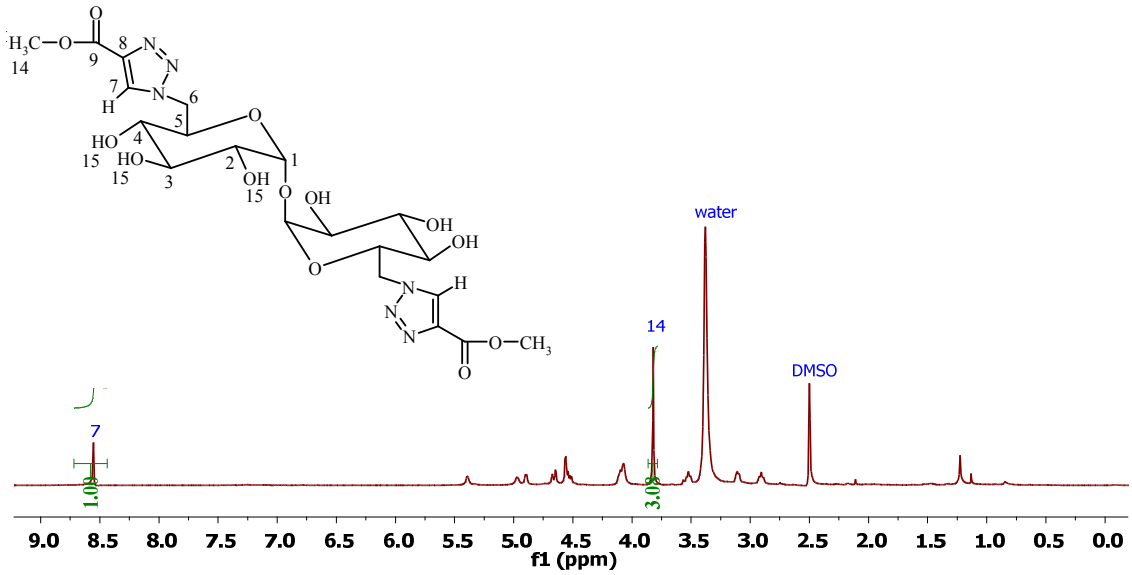


**Figure 3.16.** $^{1}$H-NMR spectrum of the deprotected adduct **3.4** in DMSO-$d_6$

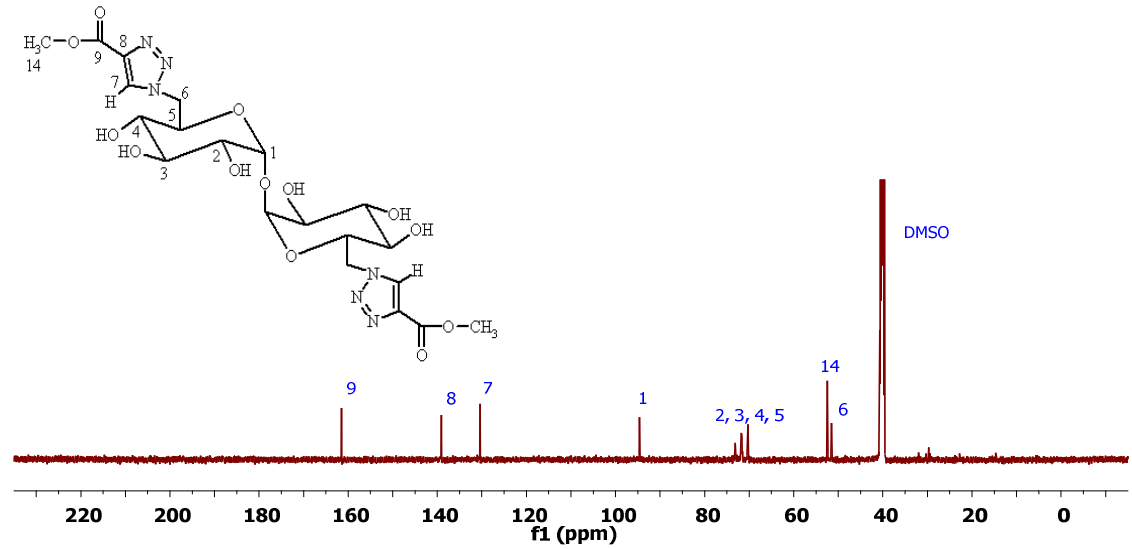


**Figure 3.17.** $^{13}$C-NMR spectrum of the deprotected adduct **3.4** in DMSO-$d_6$

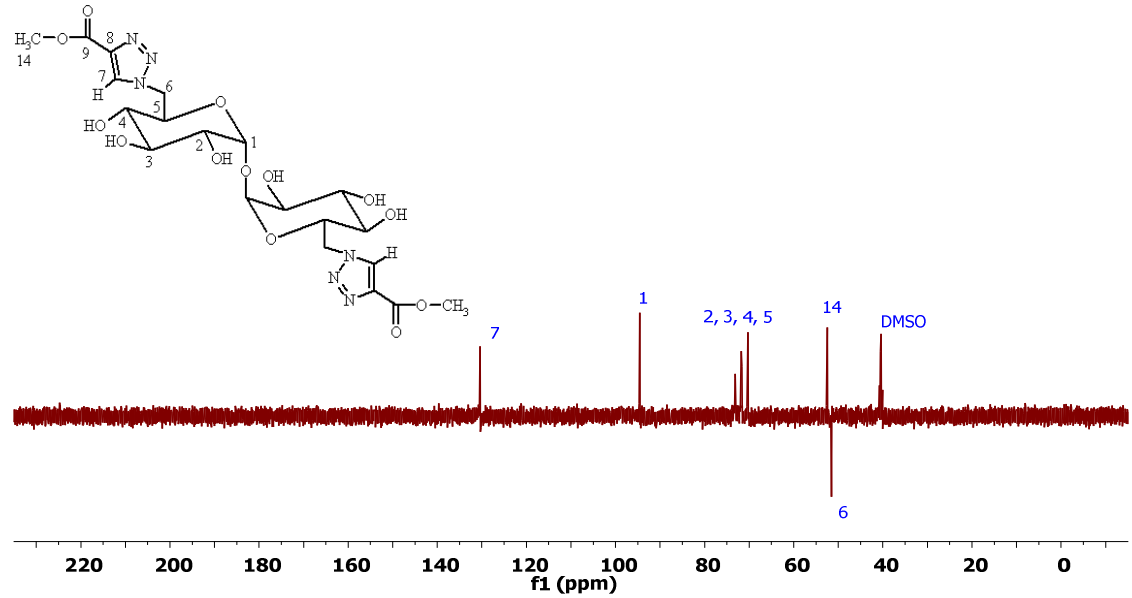


**Figure 3.18.** DEPT-NMR spectrum of the deprotected adduct **3.4** in DMSO-$d_6$

### 3.3.2.2. Introduction of Acrylate Functionality

Click reaction between the protected di-azide functionalised trehalose **3.2** and propargyl acrylate was carried out successfully, using copper sulphate pentahydrate and sodium ascorbate in a mixture of water and THF solvents, to yield the acrylate clicked product **3.5**, Scheme 3.4.

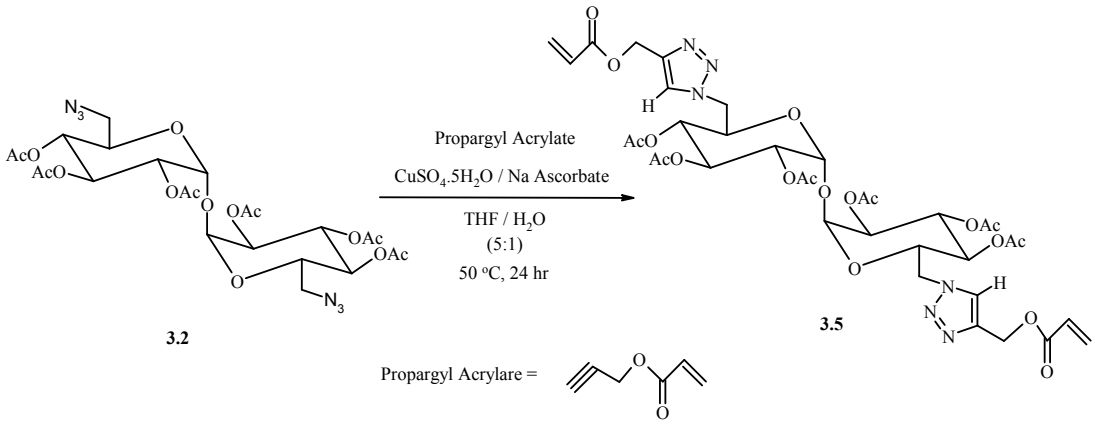


**Scheme 3.4.** Synthesis of protected trehalose clicked with propargyl acrylate

The structure of **3.5** was confirmed by $^{1}$H-, $^{13}$C- and DEPT-NMR spectroscopy. The appearance of a peak at 7.72 ppm in $^{1}$H-NMR spectrum (Fig. 3.19), assigned for the triazole proton ($H_7$), provided an evidence for the formation of 1,2,3-triazole ring. The spectrum also showed appearance of all peaks corresponding to the trehalose ($H_{1,2,3,4,5,6,14,14',14''}$) as well as the obvious set of double doubles at the region 6.45 - 5.88 ppm which are characteristic for the acrylate double bond protons ($H_{11}$ and $H_{12}$). These peaks showed the correct integration ratios with the rest of the trehalose protons, confirming the attachment of two acrylate molecules per one trehalose unit.

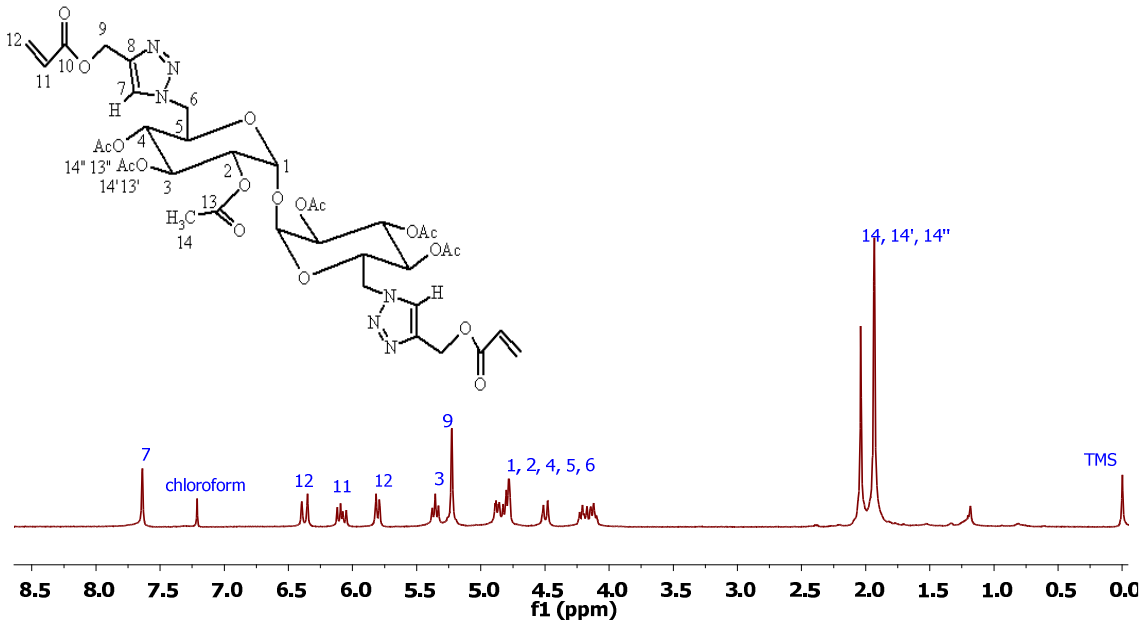


**Figure 3.19.** $^{1}$H-NMR spectrum of protected trehalose clicked with propargyl acrylate **3.5** in $CDCl_3$

$^{13}$C-NMR spectrum of **3.5** showed the peaks corresponding to the triazole double bond carbons at 125.04 ppm ($C_7$) and 142.57 ppm ($C_8$) as well as the peaks for the acrylate double bond carbons at 127.89 ppm ($C_{11}$) and 131.19 ppm ($C_{12}$) (Fig. 3.20 and 3.21).

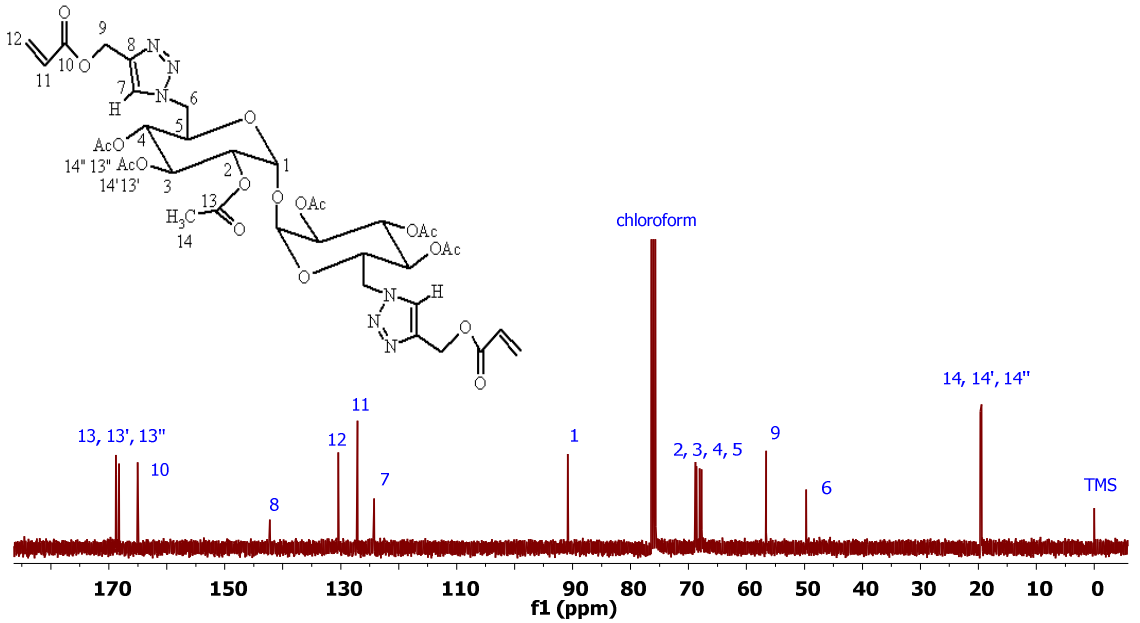


**Figure 3.20.** $^{13}$C-NMR spectrum of protected trehalose clicked with propargyl acrylate **3.5** in $CDCl_3$

DEPT-NMR spectrum of **3.5** also showed three inverted peaks at 131.19, 58.23 and 51.35 ppm, assigned for the $CH_2$ of the acrylate double bond ($C_{12}$), $CH_2$ of acrylate adjacent to triazole ($C_9$), and $CH_2$ of trehalose adjacent to triazole ($C_6$), respectively, (Fig. 3.21). This confirmed the successful Click reaction.

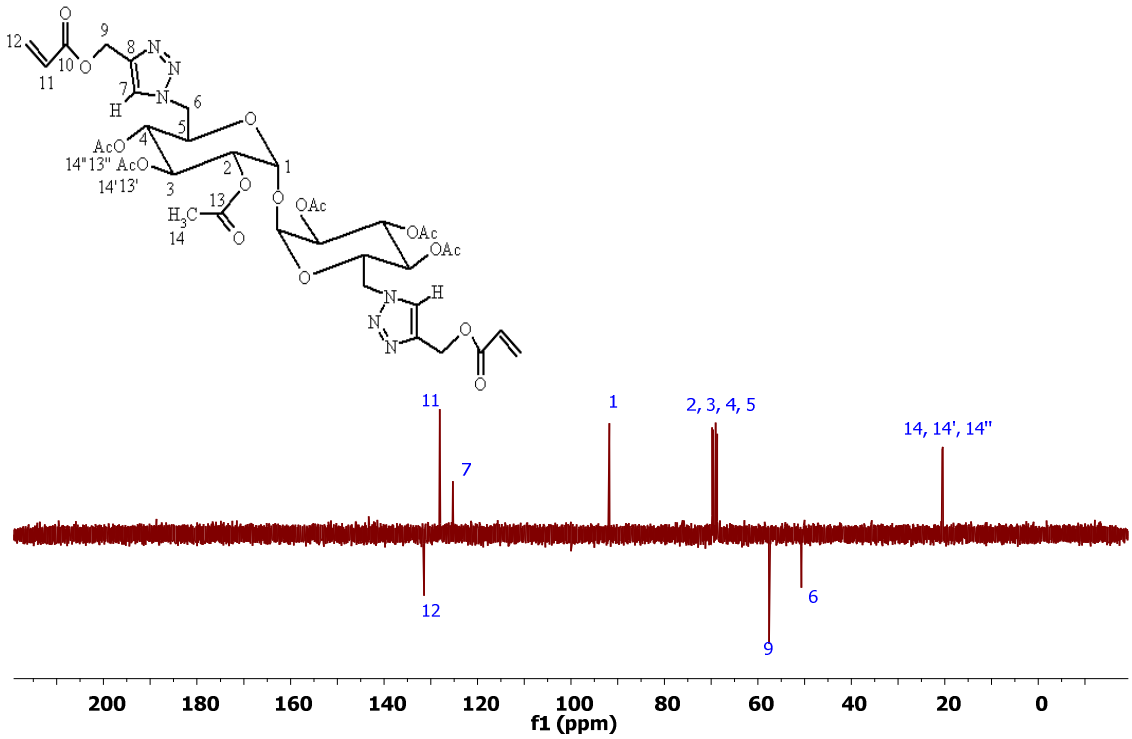


**Figure 3.21.** DEPT-NMR spectrum of protected trehalose clicked with propargyl acrylate **3.5** in $CDCl_3$

Figure 3.22 shows the FT-IR spectra of **3.2** (A) and **3.5** (B). The complete disappearance of the azide peak at 2096 $cm^{-1}$ in the IR spectrum of **3.5** indicated the quantitative conversion to the clicked product. The high resolution MS results showed a very good agreement between the calculated and the found molecular weight values.

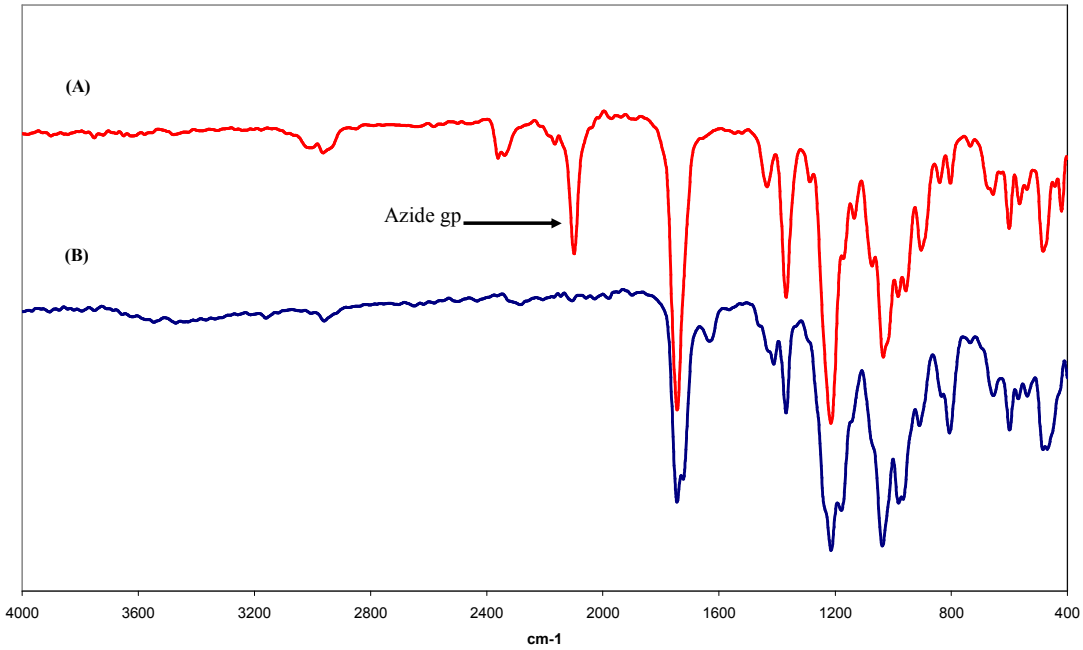


**Figure 3.22.** FT-IR spectra of (A) protected di-azide functionalised trehalose **3.2** and (B) protected trehalose clicked with propargyl acrylate **3.5**

### 3.3.2.3. Introduction of Epoxy Functionality

Unlike the Click reactions with ethyl propiolate (refer to section 3.3.2.1) or propargyl acrylate (refer to section 3.3.2.2), the use of Cu(II) salt / sodium ascorbate (reducing agent) as a catalytic system for the introduction of glycidyl propargyl ether is inappropriate. This is because in such catalytic system, water has to be used as a solvent or cosolvent, which is expected to ring open the epoxide ring. Therefore, Cu(I) was used as an alternative catalytic system, Scheme 3.5. Pentamethyldiethylenetriamine (PMDETA) was used as a ligand to solubilise the Cu(I) ions in the polar aprotic solvent (DMF). The reaction also needed to be carried out under $N_2$ atmosphere to avoid any moisture contamination. Amberlite IRC 748 sodium form was used to remove any Cu ion contaminations from the product.

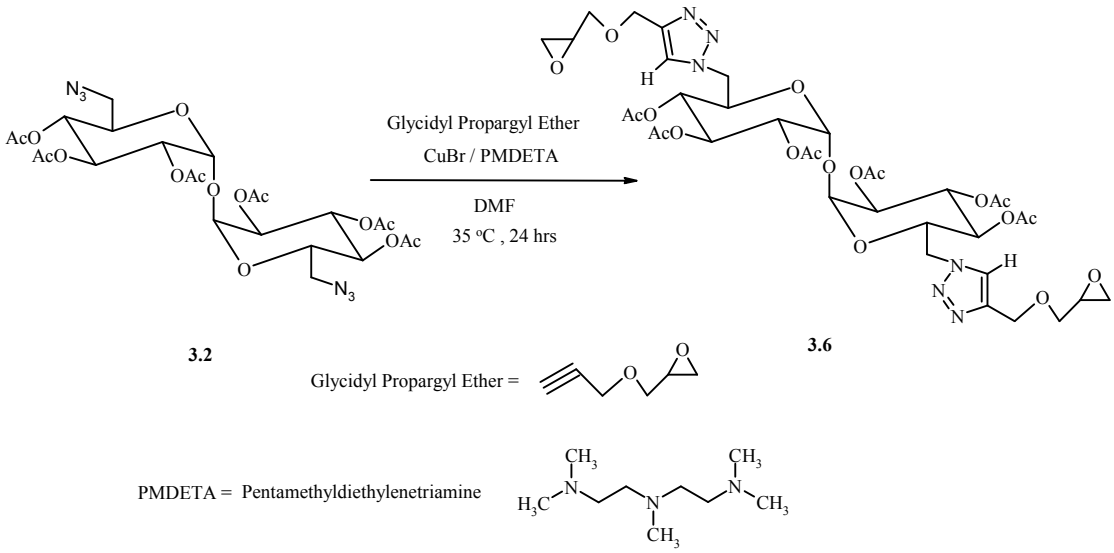


**Scheme 3.5.** Synthesis of protected trehalose clicked with glycidyl propargyl ether

The successful functionalisation of trehalose with epoxy groups was confirmed by $^{1}$H- and $^{13}$C-NMR. $^{1}$H-NMR spectrum of **3.6** showed a peak at 7.65 ppm, assigned for the triazole proton ($H_7$) (Fig. 3.23). The spectrum also showed appearance of all peaks corresponding to the trehalose ($H_{1,2,3,4,5,6,14,14',14''}$) as well as the clicked glycidyl propargyl ether ($H_{9,10,11,12}$), especially the ones for the epoxy ring at 3.78 ppm ($H_{11}$) and 2.82 and 2.65 ppm ($H_{12}$). Moreover, $^{13}$C-NMR spectrum showed the peaks corresponding to the triazole double bond carbons ($C_7$ and $C_8$) at 124.00 and 145.37 ppm, respectively (Fig. 3.24).

ESI-MS results of **3.6** showed a base peak at 891.3, which is in a good agreement with the theoretical calculation for $[M + Na]^{+}$.

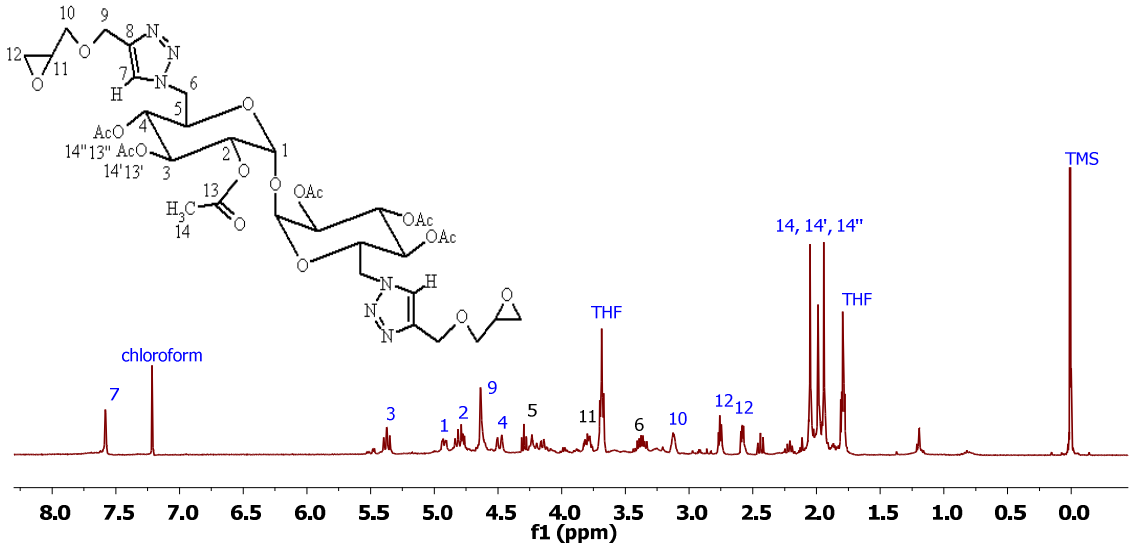


**Figure 3.23.** $^{1}$H-NMR spectrum of protected trehalose clicked with glycidyl propargyl ether **3.6** in $CDCl_3$

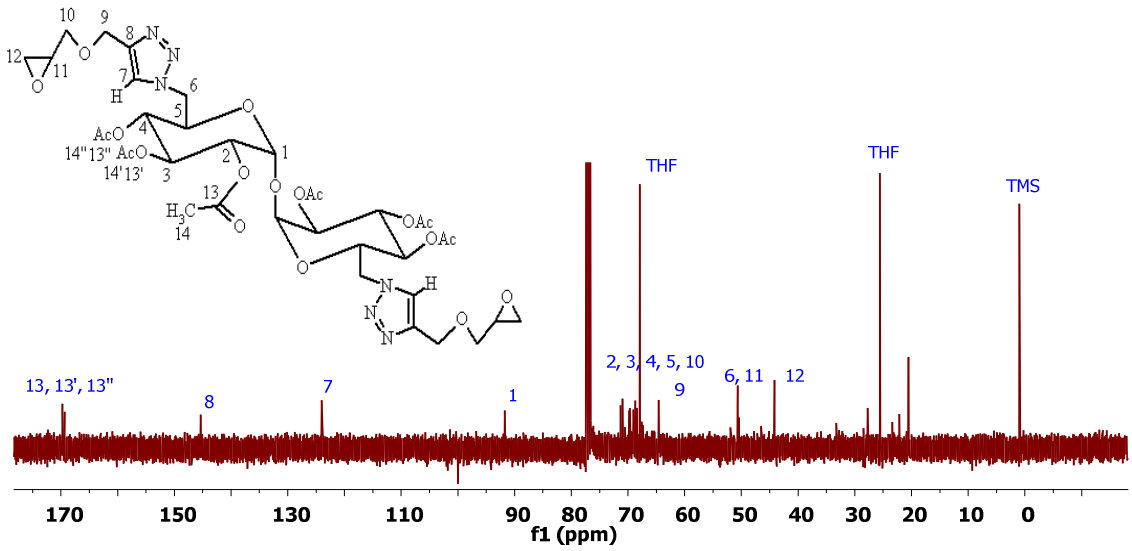


**Figure 3.24.** $^{13}$C-NMR spectrum of protected trehalose clicked with glycidyl propargyl ether **3.6** in $CDCl_3$

The di-epoxide functionalised trehalose derivative **3.6** is an interesting bi-functionalised monomer. It contains two epoxy rings and could be cured with a di-amine compound to produce resins containing trehalose.

### 3.3.3. Di-acrylate Functionalised Trehalose 3.5

#### 3.3.3.1. Thermal Polymerisation

The polymerisability of the protected trehalose clicked with propargyl acrylate **3.5** was illustrated by a simple thermal polymerisation experiment. A sample of **3.5** was dissolved in DMSO-$d_6$ and placed in NMR tube. The tube was kept in an oil bath at 120 $^{o}$C for 12 hr. A visual increase in the viscosity of the solution was observed. The comparison $^{1}$H-NMR spectra of **3.5** and the polymerisation product showed a complete disappearance of the double bond peaks ($H_{11}$ and $H_{12}$) as well as broadened peaks (Fig. 3.25.A and B). These observations indicated the occurrence of the polymerisation process.

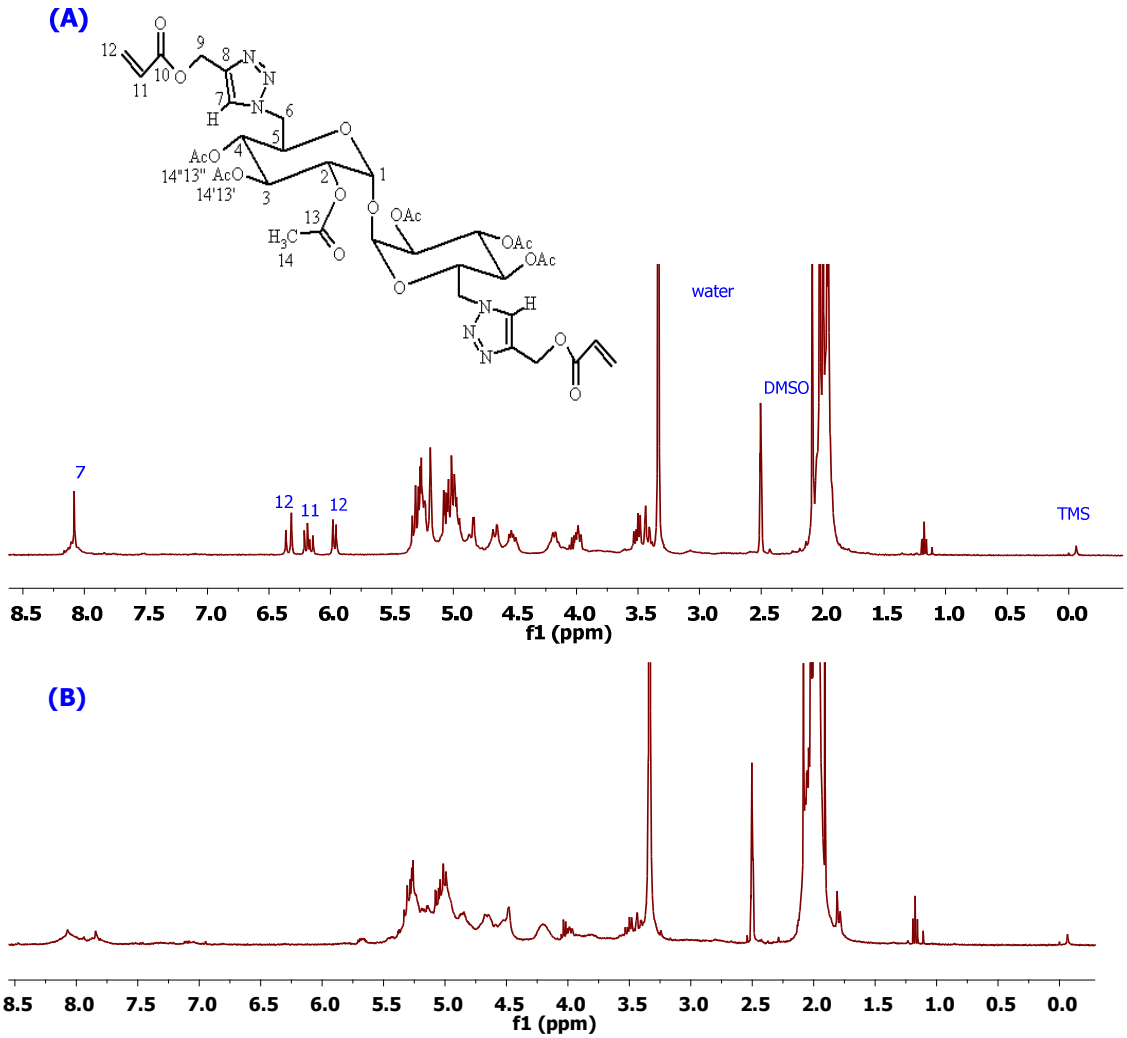


**Figure 3.25.** $^{1}$H-NMR spectra of (A) protected trehalose clicked with propargyl acrylate **3.5** and (B) poly(protected trehalose clicked with propargyl acrylate) in DMSO-$d_6$

### 3.3.3.2. As a Cross-linking Agent in the polymerisation of 2-Hydroxyethyl Methacrylate (HEMA)

In the present section, the possibility of using the prepared di-acrylate functionalised trehalose **3.5** as a saccharide cross-linker to produce three-dimensional networks (hydrogels) was investigated. Poly(2-hydroxyethyl methacrylate) (PHEMA) was used as the linear polymer chain, since it is a biocompatible and FDA approved polymer. The presence of trehalose moiety in the cross-linked polymer is expected to, not only, render the biocompatibility of PHEMA, but also promote the biodegradability.

Free radical polymerisation of HEMA using azobisisobutyronitrile (AIBN) as an initiator was utilised to produce PHEMA, Scheme 3.6. The crude polymer was purified by reprecipitated from DMF into toluene. The used molar ratio of the initiator to monomer was 2.5 mol% (i.e. [M]/[I] = 41).

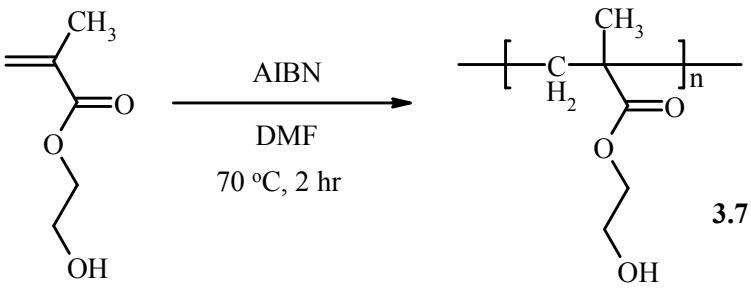


**Scheme 3.6.** Synthesis of PHEMA

The pure polymer was characterised by $^{1}$H-NMR and GPC. The $^{1}$H-NMR spectra of PHEMA **3.7** compared with HEMA (Fig. 3.26.A and B) showed complete disappearance of the double bond peaks for HEMA protons ($H_1$) and ($H_{1'}$). All the peaks were assigned to the corresponding protons in both spectra. Broadening of the peaks in the spectrum of **3.7** (Fig. 3.26.B) indicated the formation of polymeric material.

The GPC result showed $M_n$ of 108,400 gmol$^{-1}$ with PDI of 1.8. Although the GPC measurments was carried out using the three detector system, but $d_n/d_c$ used for the calculation of $M_n$ and $M_w$ was based on polystyrene standard. Therefore, the molecular weight was not absolute.

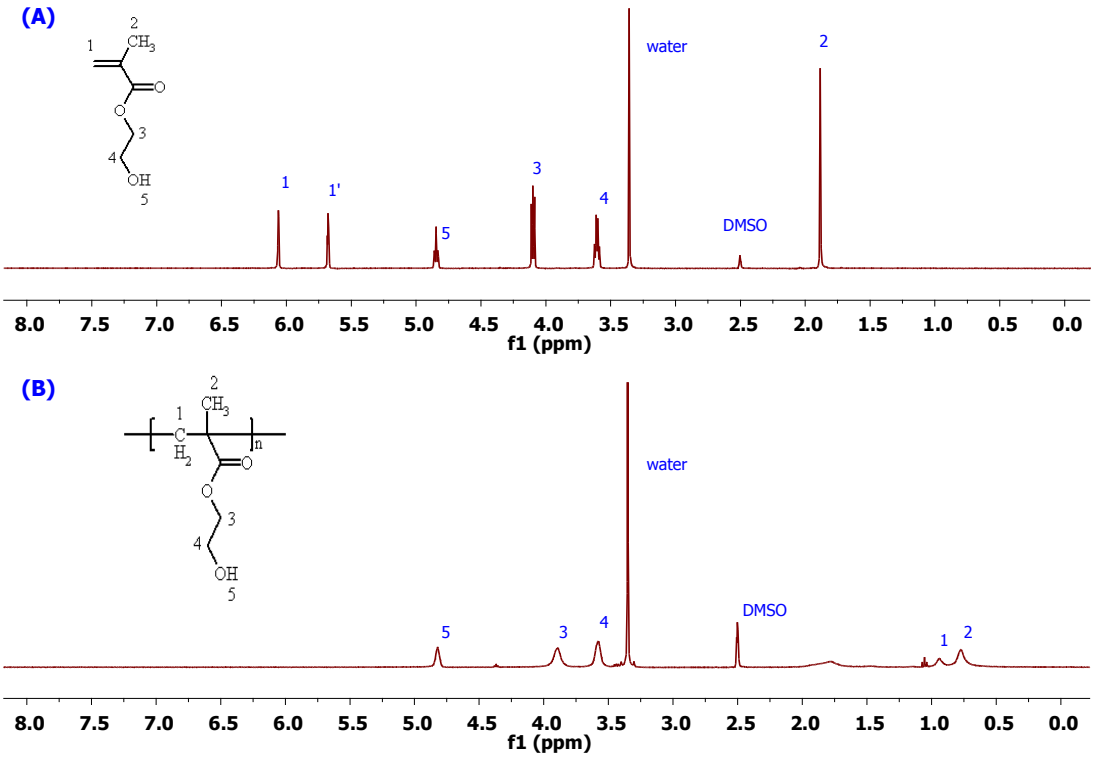


**Figure 3.26.** $^{1}$H-NMR spectra of (A) HEMA and (B) PHEMA **3.7** in DMSO-$d_6$

The cross-linked PHEMA was prepared successfully *via* free radical polymerisation using AIBN with the addition of 5 mol % of propargyl acrylate clicked protected trehalose **3.5** as a cross-linker, Scheme 3.7.

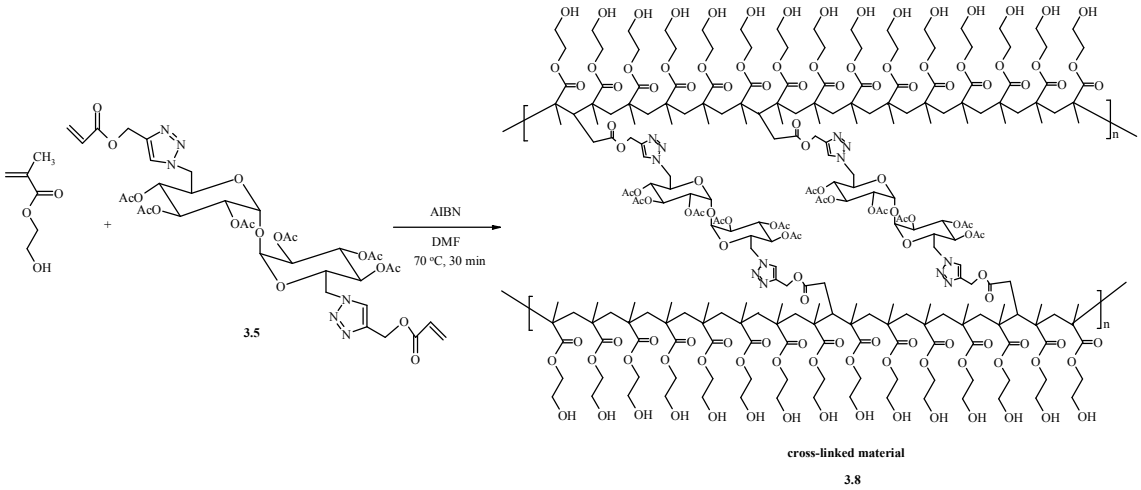


**Scheme 3.7.** Synthesis of cross-linked PHEMA

The reaction was performed in an NMR tube fitted with a young's tap in deuterated DMF (DMF-$d_6$) as a reaction solvent. The NMR tube was placed in an NMR machine equipped with a heated probe and programmed to run NMR experiment every 15 min. The $^1$H-NMR spectra of the reaction mixture is shown in Fig. 3.27. Gel was formed after 30 min and the reaction was terminated after 45 min. $^1$H-NMR spectra of the cross-linking polymerisation reaction mixture showed complete disappearance of the peaks corresponding to the double bonds broadening of the peaks after 30 min.

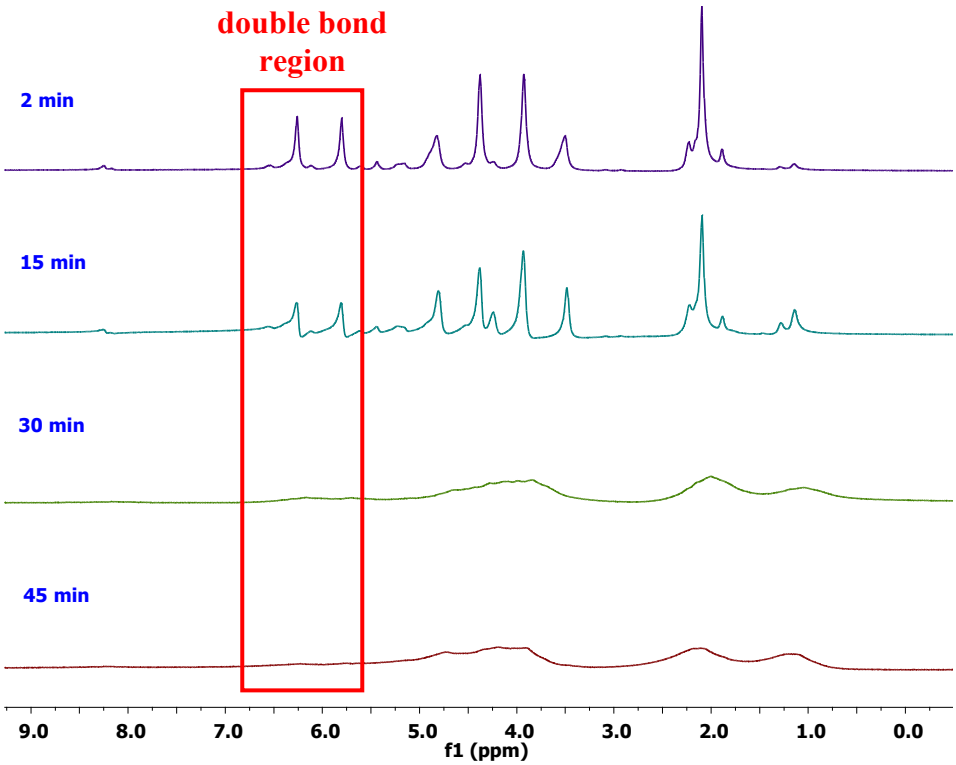


**Figure 3.27.** Monitoring the course of the cross-linking polymerisation of HEMA with **3.5** by $^{1}$H-NMR spectroscopy at 70 $^{o}$C in DMF-$d_6$

The gel content (insoluble fraction) was determined by extracting the soluble fraction with DMF at 60 $^{o}$C. The gel content was found to be 90 %, indicating high and efficient cross-linking behaviour.

### 3.4. Summary

Hexa-acetylated (protected) di-azide functionalised trehalose **3.2** was synthesised *via* tosylation followed by acetylation and subsequent reaction with sodium azide. Click chemistry was successfully utilised on **3.2** to introduce different functionalities such as ester, acrylate and epoxide groups. NMR and FT-IR spectroscopies were found to be efficient characterisation tools to follow up the Click modification reactions. The di-acrylate functionalised trehalose **3.5** was used as a cross-linking agent in the free radical polymerisation of HEMA to produce three-dimensional networks.

### 3.5. References


1. K. Maruta, T. Nakada, M. Kubota, H. Chaen, T. Sugimoto, M. Kurimoto, Y. Tsjisaka, *Bioscience, Biotechnology, and Biochemistry* **1995**, *59*, 1829–1834.
2. T. Arakawa, S. J. Prestrelski, W. C. Kenney, J. F. Carpenter, *Advanced Drug Delivery Reviews* **2001**, *46*, 307-326.
3. T. Higashiyama, *Pure and Applied Chemistry* **2002**, *74*, 1263.
4. Y. Nishizaki, C. Yoshizane, Y. Toshimori, N. Arai, S. Akamatsu, T. Hanaya, S. Arai, M. Ikeda, M. Kurimoto, *Nutrition Research* **2000**, 20, 653–664.
5. T. Matsuo, *British Journal of Ophthalmology* **2001**, 85, 610–612.
6. T. Hirata, T. Fukuse, C. J. Liu, K. Muro, H. Yokomise, K. Yagi, K. Inui, S. Hitomi, H. Wada. *Surgery* **1994**, 115, 102–107.
7. G. Birch, A. Richards, *Carbohydrate Research* **1968**, *8*, 411.
8. F. M. Menger, B. N. A. Mbadugha, *Journal of the American Chemical Society* **2001**, *123*, 875-885.
9. A. Liav, M. B. Goren, *Carbohydrate Research* **1980**, *87*, 287-293.
10. S. Srinivasachari, Y. M. Liu, G. D. Zhang, L. Prevette, T. M. Reineke, *Journal of the American Chemical Society* **2006**, *128*, 8176-8184.

# Chapter 4

# Synthesis of Glycopolymers

## 4.1. Introduction

Due to their biomimic and recognition properties, glycopolymers are attracting ever-increasing attention from both chemistry and biology communities.[1-3] The control of the chain length, composition and topology of the glycopolymer has been highly relevant to biological sciences.[4] The more popular route for the synthesis of glycopolymers is based on the polymerisation of monomers containing carbohydrate moieties by free radical, controlled radical, anionic, cationic, ring opening and ring opening metathesis polymerisation techniques. The other possible route to synthesise glycopolymers is to react a functional polymeric backbone with a carbohydrate. This synthetic route usually suffers from the difficulty of introducing sufficiently reactive pendant groups onto the polymer backbone to react with the carbohydrates and / or the accessibility of these pendant groups by the carbohydrate molecules.[5,6] However, the employment of Click chemistry in the synthesis of glycopolymers allows highly efficient post polymerisation modifications and hence a more controlled structures.[7]

Trehalose has a non-reducing character and high thermostability and a wide pH-stability range compared to other sugars.[8] The unique combination of biocompatibility and biodegradability makes trehalose a promising monomer for the production of linear polymers and an attractive substance for industrial / medical applications. [9-12]

In this chapter, the interest in trehalose is extended to generate trehalose-based glycopolymers (biomaterials) for a potential wide range of applications. Click chemistry is combined with ring opening polymerisation (ROP) to synthesise materials containing trehalose as a spacer between two poly(aliphatic ester) chains. Moreover, the use of copper wire catalysed Click chemistry is demonstrated as a polymerisation technique to polymerise PEG and trehalose to produce a new class of linear temperature responsive glycopolymers. These glycopolymers are fully characterised and evaluated as a smart materials.

## 4.2. Experimental

### 4.2.1. Materials

Tin(II) 2-ethylhexanoate (stannous octoate), 3,6-Dimethyl-1,4-dioxane-2,5-dione (D-,L-lactide), ε-caprolactone and poly(ethylene glycol) (PEG) with $M_n$ = 200, 600, and 1000 $gmol^{-1}$ were purchased from Sigma – Aldrich and fully characterised by NMR spectroscopy.

All other chemicals and reagents used in the synthesis were also purchased from Sigma – Aldrich and used without further purification. All dry solvents were obtained from the Solvent Purification System (SPS), Chemistry Department, Durham University.

### 4.2.2. Instrumentation and Measurements

$^1$H-NMR spectra were recorded using deuteriated solvent lock on a Varian Mercury 400 or a Varian Inova 500 spectrometer at 400 MHz and 500 MHz, respectively. Chemical shifts are quoted in ppm, relative to tetramethylsilane (TMS), as the internal reference. $^{13}$C-NMR spectra were recorded at 101 MHz or 126 MHz (2000 scans) using continuous broad band proton decoupling and a 3 S recycle dely, and therefore not quantitative; chemical shifts are quoted in ppm, relative to $CDCl_3$ (77.55 ppm). The following abbreviations are used in listing NMR spectra: s = singlet, d = doublet, t = triplet, q = quartet, m = multiplet, b = broad.

Electron Impact (EI) and Electrospray ($ES^+$) mass spectra were recorded on a Thermo Finnigan LTQ FT spectrometer operating at 70 eV with the ionisation mode as indicated.

FT-IR spectra were recorded on a Perkin Elmer 1600 series FT-IR spectrometer fitted with a golden gate. The samples were used as solids or liquids.

Molecular weight analysis was carried out by gel permission chromatography (GPC) on a Viscotek TDA 302 with refractive index, viscosity and light scattering detector (with a 690 nm wavelength laser), unless otherwise stated. Two 300 mm PLgel 5 μm mixed C columns (with a linear range of molecular weight from 200 to 2 000 000 $gmol^{-1}$) were used. THF or DMF was used as the eluent with a flow rate of 1.0 $mLmin^{-1}$ at 30 $^oC$.

The cloud point of the polymer was determined by using a Varian Cary – 100 UV-Vis spectrophotometer attached with temperature controller.

The optical micrographs of the aqueous polymer solution were taken by Olympus BX50WI microscope with 50x optical zoom lens, cross polarizers, 589nm tint plate and TMS 93 controller linked to T600 hotstage connect to a Pixelink A60z firewire camera through a Linkam linksys32 software.

### 4.2.3. Synthesis of Alkyne End Capped PLA 4.1

Using the ratio of lactide (LA) : propargyl alcohol (10:1); PLA DP = 20 ($PLA_{20}$):

LA (10 g, 69.4 mmol) was dissolved in degassed THF (25 mL) in a three-necked round-bottom flask, equipped with magnetic stirrer, reflux condenser and rubber seal septum. Propargyl alcohol (0.389 g, 6.94 mmol) and $Sn(Oct)_2$ (0.140 g, 0.347 mmol) dissolved in a minimum amount of toluene were added under $N_2$ atmosphere. The mixture was heated to reflux for 30 hr. The polymer was precipitated from hexane, filtered and reprecipitated from $CH_2Cl_2$ into hexane. The polymeric material was filtered and dried in an oven at 40 $^oC$ under reduced pressure for a minimum of 24 hr. The polymer product was brittle off-white powder ($PLA_{20}$) **4.1**, yield 69 % (6.9 g).

Using the ratio of LA : propargyl alcohol (50:1); PLA DP = 100 ($PLA_{100}$):

In a similar procedure, LA (10 g, 69.4 mmol), propargyl alcohol (0.078 g, 1.39 mmol) and $Sn(Oct)_2$ (0.140 g, 0.347 mmol) were used. The polymer was reprecipitated from $CH_2Cl_2$ into methanol. The polymer product was brittle off-white powder ($PLA_{100}$) **4.1**, yield 73 % (7.3 g).

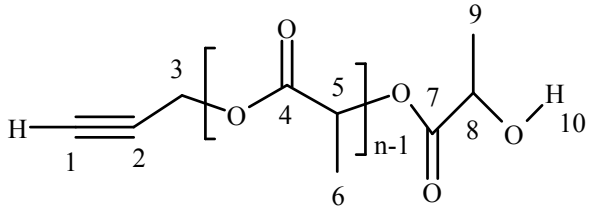


**4.1**

**Figure 4.1.** Structure of PLA with numerical assignment for NMR

$PLA_{20}$

$^1$H-NMR (400 MHz, $CDCl_3$) δ 5.13 (m, 21H, $H_5$), 4.65 (m, 1H, $H_8$), 4.30 (m, 2H, $H_3$), 2.93 (bs, 1H, $H_{10}$), 2.45 (t, $J$ = 2.4 Hz, 1H, $H_1$), 1.48 (m, 66H, $H_{6,9}$).

$^{13}$C-NMR (101 MHz, $CDCl_3$): δ 169.56 – 169.12 ($C_{4,7}$), 75.60 ($C_2$), 69.42 – 68.99 ($C_{5,8}$), 66.65 ($C_1$), 52.87 ($C_3$), 16.71 – 15.77 ($C_{6,9}$).

GPC: $M_n$ = 2650 gmol$^{-1}$, $M_w$ = 3940 gmol$^{-1}$, PDI =1.5.

$PLA_{100}$

$^1$H-NMR (400MHz, $CDCl_3$): δ 5.25 – 5.15 (m, 65H, $H_5$), 4.70 (m, 1H, $H_8$), 4.35 (m, 2H, $H_3$), 2.83 (bs, 1H, $H_{10}$), 2.50 (t, $J$ = 2.5 Hz, 1H, $H_1$), 1.70 – 1.45 (m, 198H, $H_{6,9}$).

GPC: $M_n$ = 5120 gmol$^{-1}$, $M_w$= 7900 gmol$^{-1}$, PDI = 1.5.

### 4.2.4. Synthesis of Alkyne End Capped PCL 4.2

ε-Caprolactone (CL) (10.0g, 87.6 mmol) was dissolved in degassed toluene in a three-necked round-bottom flask, equipped with magnetic stirrer, reflux condenser and rubber seal septum. Propargyl alcohol (0.0491g, 0.876mmol) and $Sn(Oct)_2$ (0.147g, 0.438mmol) were added under $N_2$ atmosphere. The mixture was heated to 110 $^oC$ for 30 hr. The polymer was precipitated from methanol, filtered and reprecipitated from $CH_2Cl_2$ into methanol. The polymeric material was filtered and dried in an oven at 40 $^oC$ under reduced pressure for a minimum of 24 hr. The polymer product was a colourless powder, which was ground down to give a fine colourless powder, ($PCL_{100}$) **4.2**, yield 90 % (9.0 g).

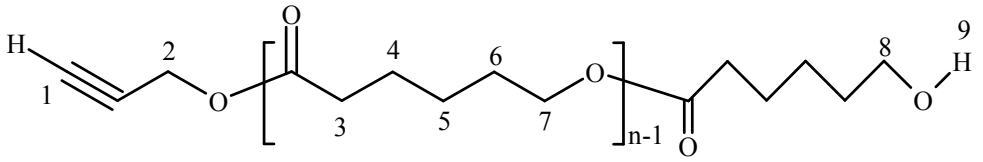


**4.2**

**Figure 4.2.** Structure of PCL with numerical assignment for NMR

$PCL_{100}$

$^1$H-NMR (400 MHz, $CDCl_3$) δ 4.61 (d, *J* = 2.5 Hz, 2H, $H_2$), 3.99 (t, *J* = 6.7 Hz, 198H, $H_7$), 3.58 (t, *J* = 6.5 Hz, 2H, $H_8$), 2.42 (t, *J* = 2.5 Hz, 1H, $H_1$), 2.24 (t, *J* = 7.5 Hz, 200H, $H_3$), 1.75 (bs, 1H, $H_9$), 1.58 (m, 400H, $H_{4,6}$), 1.32 (m, 200H, $H_5$).

$^{13}$C-NMR (101MHz, $CDCl_3$): δ 173.5 (C=O), 64.14 ($C_7$), 34.12 ($C_3$), 28.35 ($C_6$), 25.53 ($C_4$), 24.58 ($C_5$)

GPC: $M_n$ = 11,160 $gmol^{-1}$, $M_w$ = 15,830 $gmol^{-1}$, PDI =1.4.

### 4.2.5. Synthesis of Glycopolymer 4.3 Containing PCL

In a vial, protected di-azide functionalised trehalose **3.2** (refer to chapter 3) (0.05 g, 0.078 mmol) was dissolved in a mixture of acetone and water (1:1, 6 mL). Alkyne end capped $PCL_{100}$ **4.2** (1.78 g, 0.156 mmol), $CuSO_4.5H_2O$ (0.004 g, 0.0156 mmol) and sodium ascorbate (0.006 g, 0.0312 mmol) were added. The mixture was heated at 60°C for 20 hr. The product was extracted with ethyl acetate (200 mL) and washed with water (3 x 20 mL). The solvent was removed and the solid was dried in an oven at 40 $^oC$ under reduced pressure to give a pale yellow solid product **4.3**, yield 88 % (0.18 g).

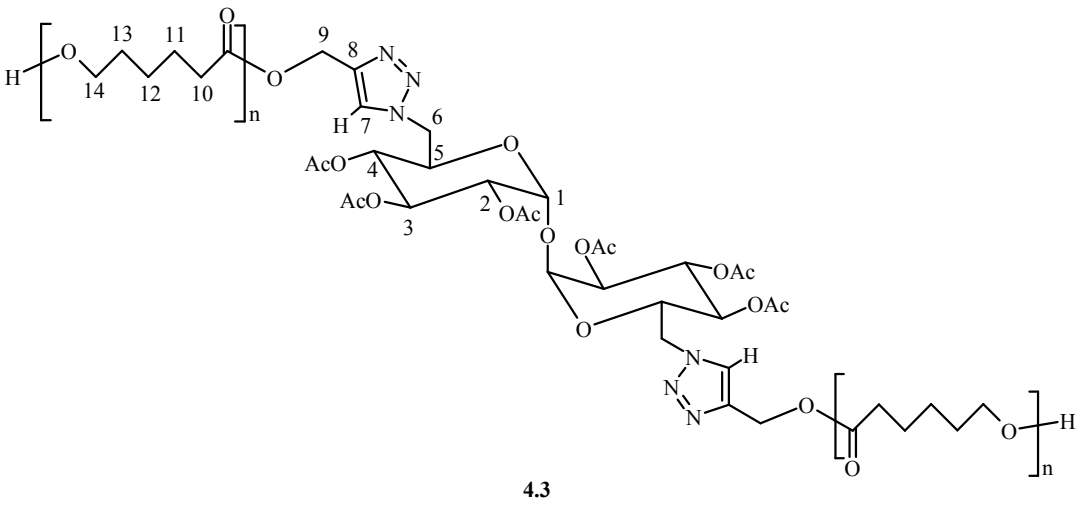

4.3

**Figure 4.3.** Structure of glycopolymer containing PCL with numerical assignment for NMR

$^{1}$H-NMR (400 MHz, $CDCl_3$): δ 7.7 (s, 2H, $H_7$), 5.5 (t, $J$ = 9.7 Hz, 2H, $H_3$), 5.2 (d, $J$ = 5.7 Hz, 2H, $H_1$), 4.96 – 4.86 (m, 4H, $H_{2,4}$), 4.69 (d, $J$ = 2.47 Hz, 4H, $H_9$), 4.55 (m, 2H, $H_5$), 4.24 (d, $J$ = 6.65 Hz, 4H, $H_6$), 4.06 (t, $J$ = 6.70 Hz, 396H, $H_{14}$), 3.69 (t, $J$ = 6.49 Hz, 4H, $H_{14}$ terminal), 2.31 (t, $J$ = 7.49 Hz, 400H, $H_{10}$), 1.65 (m, 800H, $H_{11,13}$), 1.39 (m, 400H, $H_{12}$).

$^{13}$C-NMR (101 MHz, $CDCl_3$): δ 171.2 (C=O), 70.1 ($C_9$), 63.9 ($C_{14}$), 34.0 ($C_{10}$), 29.9 ($C_{13}$), 26.5 ($C_{11}$), 24.1 ($C_{12}$) 20.3 ($CH_3$ Acetate).

FT-IR: new peak at 1750.1 $cm^{-1}$ (C=O).

GPC: $M_n$ = 23,120 $gmol^{-1}$, $M_w$ = 36,460 $gmol^{-1}$, PDI = 1.6.

### 4.2.6. Synthesis of Di-alkyne Terminated PEG (DAT-PEG) 4.4

A solution of PEG ($M_n$ ~600 $gmol^{-1}$) (5.00 g, 8.3 mmol) in dry THF (20 mL) was added dropwise at 0 $^{o}$C to a slurry of NaH (0.432 g, 18 mmol) in dry THF (10 mL) in a three-necked round-bottom flask, equipped with magnetic stirrer, thermometer, addition funnel and rubber seal septum, under $N_2$ atmosphere. The mixture was stirred for 30 min and propargyl bromide (80 % in toluene, 2.00 mL, 18 mmol) was added *via* a syringe at 0 $^{o}$C. The mixture was kept at 0 $^{o}$C for further 30 min and then stirred at ambient temperature for 24 hr. The reaction mixture was filtered and the solvent was removed under reduced pressure to produce **4.4**, yield 95 % (5.40 g, 7.9 mmol).

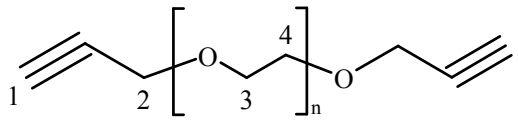

**4.4**

**Figure 4.4.** Structure of di-alkyne terminated PEG (DAT-PEG) with numerical assignment for NMR

$^1$H-NMR (400 MHz, $CDCl_3$): δ 4.12 (d, $J$ = 2.4 Hz, 4H, $H_2$), 3.64 – 3.52 (m, 60H, $H_{3,4}$), 2.40 (t, $J$ = 2.4 Hz, 2H, $H_1$).
GPC: $M_n$ = 520 gmol$^{-1}$, $M_w$ = 620 gmol$^{-1}$, PDI = 1.2.

### 4.2.7. Synthesis of Glycopolymer 4.5 Containing PEG

In a vial containing Cu-wire, protected di-azide functionalised trehalose **3.2** (refer to chapter 3) (0.477 g, 0.74 mmol), DAT-PEG **4.4** (0.5 g, 0.74 mmol) and THF / water (1:1, 5 mL) were mixed. The mixture was stirred and heated to 60 $^o$C in an oil bath for 24 hr. The polymer was reprecipitated from THF into toluene. The polymer was dried in an oven at 40 $^o$C under reduced pressure to produce the glycopolymer **4.5**, yield 99 % (0.97 g).

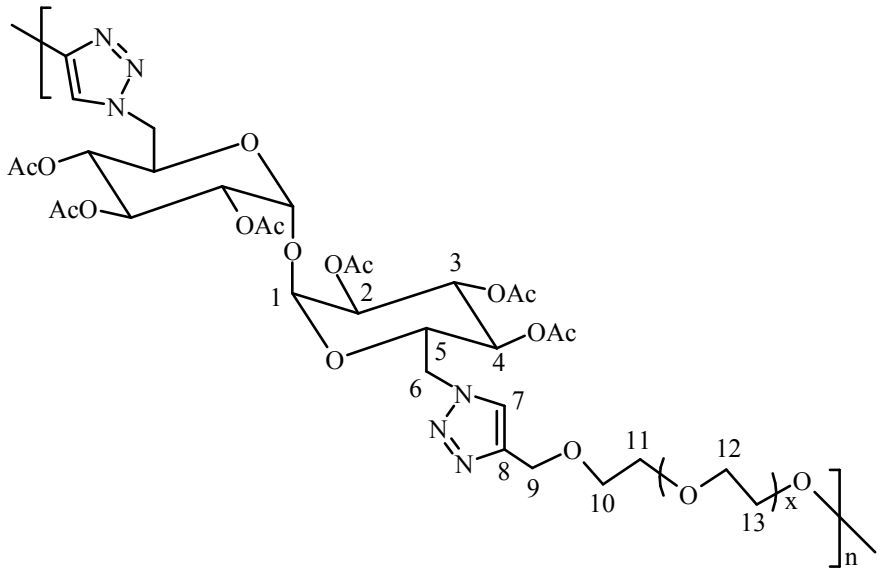

**4.5**

**Figure 4.5.** Structure of glycopolymer containing PEG with numerical assignment for NMR

$^1$H-NMR (400 MHz, $CDCl_3$) δ 7.57 (s, 1H, $H_7$), 5.41 (t, *J* = 9.7 Hz, 1H, $H_3$), 5.30 (d, *J* = 4.2 Hz, 1H, $H_1$), 4.95 (dd, *J* = 3.8 Hz, 10.2, 1H, $H_4$), 4.85 (t, *J* = 9.5 Hz, 1H, $H_2$), 4.79 (d, *J* = 3.5 Hz, 1H, $H_6$), 4.64 (s, 2H, $H_9$), 4.49 (d, *J* = 12.8 Hz, 1H, $H_6$), 4.28 – 4.18 (m, 1H, $H_5$), 3.92 – 3.36 (m, 64H, $H_{10,11,12,13}$), 2.07 (s, 3H, Ac), 2.02 (s, 3H, Ac), 1.97 (s, 3H, Ac).

GPC: $M_n = 3.4x10^4$ gmol$^{-1}$, $M_w = 5.1x10^4$ gmol$^{-1}$, PDI = 1.5.

Glycopolymers **4.6** and **4.7** were similarly synthesised and characterised using different PEG segments with $M_n$ of ~200 and ~1000 gmol$^{-1}$, respectively.

### 4.2.8. Deacetylation (Deprotection) of Glycopolymer 4.5 Containing PEG

In a vial, glycopolymer **4.5** (0.1 g) was added to a solution of NaOMe (0.04 g) in MeOH (5 mL) and stirred at ambient temperature for 24 hr. Acetone and methanol washed Dowex MR-3 mixed bed ion-exchange resin (~1 g) was added and the mixture was stirred until a pH of 7 was attained. The neutralised solution was filtered. The solvent was removed, and the resulting solid was dried under reduced pressure to give the deacetylated glycopolymer product.

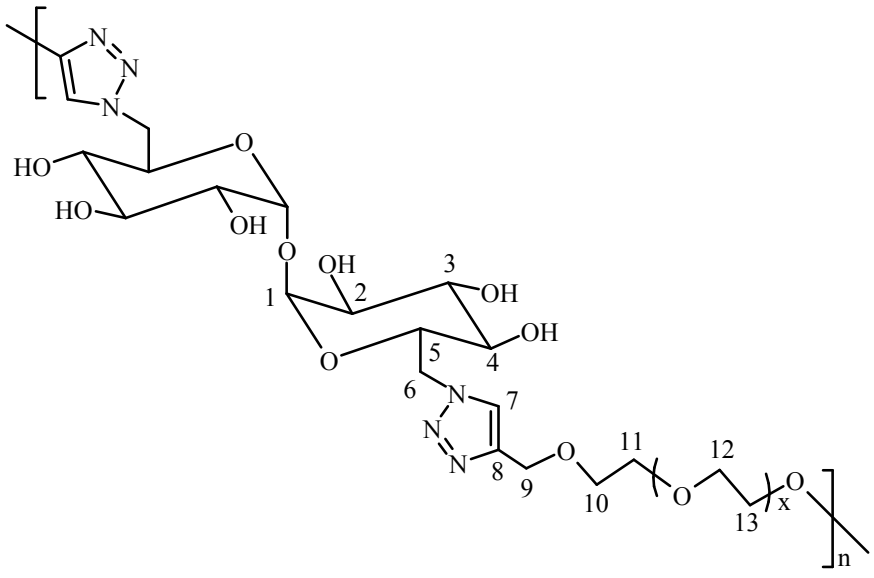


**Figure 4.6.** Structure of deacetylated glycopolymer containing PEG with numerical assignment for NMR

$^1$H-NMR spectrum showed complete disappearance of the acetate groups.

## 4.3. Results and Discussion

### 4.3.1. Glycopolymer Containing Polyaliphatic Esters

For the past decade, steadily increasing attention was paid to environmentally friendly thermoplastics and biomaterials. Aliphatic polyesters, such as poly(glycolide), PLA, and PCL, combine biodegradability and biocompatibility and are produced at the industrial scale as sutures, drug delivery carriers, and implants.[13-16] Nevertheless, lack of pendent functional groups along these polyester chains is a major limitation to a large range of applications. In order to tackle these limitations by a non-conventional method, ring opening polymerisation (ROP) and Click chemistry were combined to facilitate the attachments of functional groups onto aliphatic polyesters for modification of their properties, predominantly the chemical reactivity, in order to attach drugs, improve biocompatibility, control the biodegradation rate, increase bio-adhesion, and induce hydrophilicity. Therefore, trehalose was used, as a disaccharide spacer, into the PLA and PCL polymer chains to prepare functional materials.

The alkyne end capped PLA and PCL were prepared by ROP mechanism using propargyl alcohol as an initiator. Stannous octoate, also known as tin(II) 2-ethylhexanoate, $Sn(Oct)_2$, was chosen as catalyst for three reasons. First, $Sn(Oct)_2$ is one of the most widely used compounds for initiating the ROP of various lactones and lactides.[17, 18] It is easy to handle and is soluble in common organic solvents. Second, this catalyst is highly efficient and allows almost complete conversions even at low concentration.[19] Finally, $Sn(Oct)_2$ has been accepted as a food additive by the FDA because its toxicity is extremely low compared to other heavy metal salts. Click reaction was then performed between di-azide functionalised trehalose **3.2** (refer to chapter 3) and alkyne end capped PLA or PCL.

#### 4.3.1.1. ROP of Lactide (LA)

ROP of LA using stannous octoate and propargyl alcohol as the initiating system was carried out to produce an alkyne end capped PLA, Scheme 4.1. ROP of LA was performed with varying ratios of LA:Alcohol (10:1, 50:1), to give PLA chains of varying lengths, DP = 20 and 100, respectively, ($PLA_{20}$ and $PLA_{100}$).

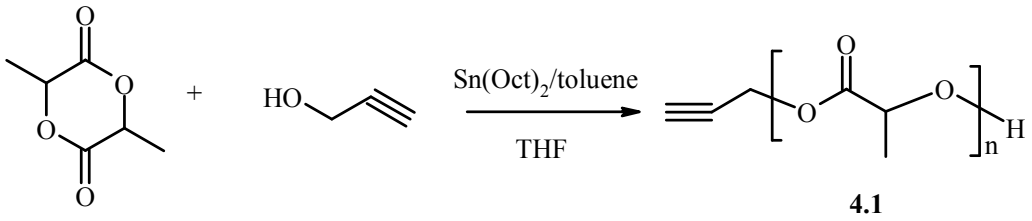


**4.1**

**Scheme 4.1.** Synthesis of alkyne end capped PLA

The polymers were fully characterised by $^{1}$H- and $^{13}$C-NMR spectroscopy. The $^{1}$H-NMR spectrum of $PLA_{20}$ (Fig. 4.7) showed the peaks corresponding to the hydrogens of the alkyne chain end ($H_1$) and ($H_3$) at 2.45 and 4.30 ppm as well as those for the PLA repeat unit ($H_5$) and ($H_6$) at 5.13 and 1.48 ppm, respectively.

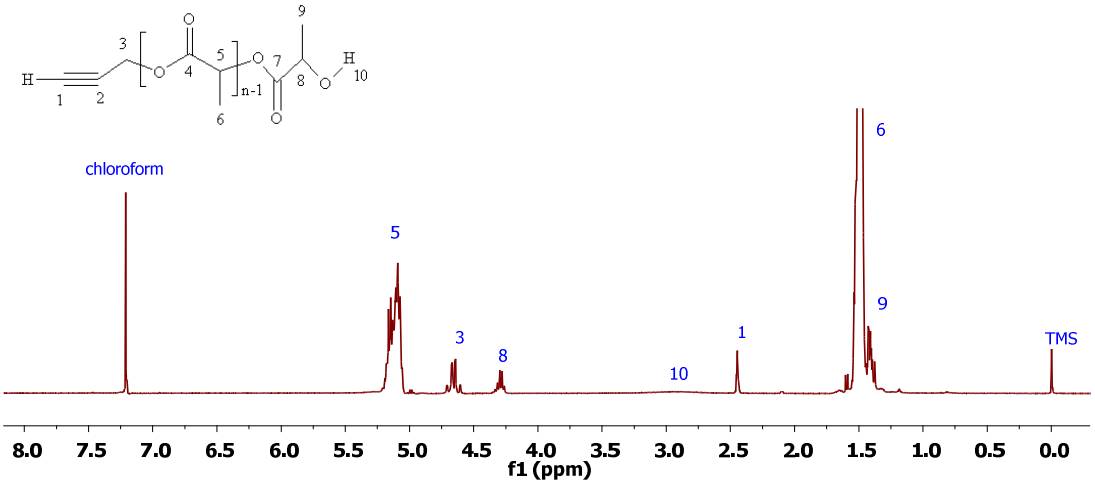


**Figure 4.7.** $^{1}$H-NMR spectrum of the alkyne end capped PLA ($PLA_{20}$) **4.1** in $CDCl_3$

The $^{13}$C-NMR spectrum of $PLA_{20}$ showed also all the peaks corresponding to the carbons of the alkyne chain end ($C_1$), ($C_2$) and ($C_3$) at 66.63, 75.59 and 52.86 ppm, respectively (Fig. 4.8). Moreover, it showed all the peaks for the polymer chain.

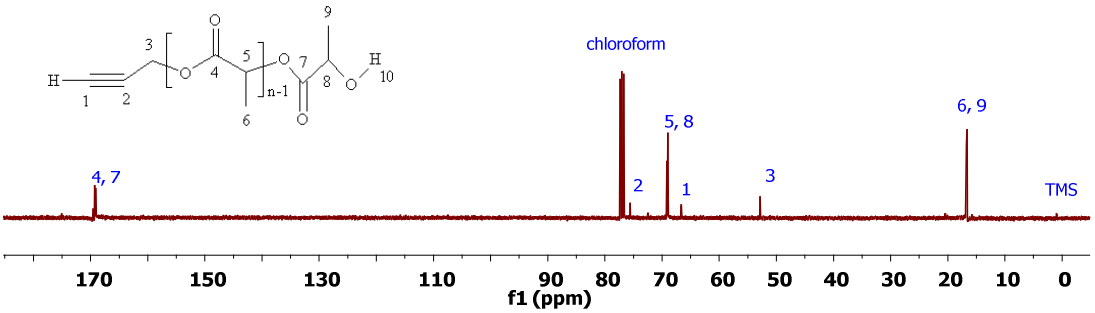


**Figure 4.8.** $^{13}$C-NMR spectrum of the alkyne end capped PLA ($PLA_{20}$) **4.1** in $CDCl_3$

The GPC results showed a polydispersity index (PDI) about 1.5 for both $PLA_{20}$ and $PLA_{100}$. $^1$H-NMR spectroscopy was also used to investigate the molecular weight and hence the chain length of the polymers. The theoretical and practical values for the molecular weights of alkyne end capped $PLA_{20}$ and $PLA_{100}$ are summarised in Table 4.1. The CH peak of the PLA ($H_5$) was integrated against the terminal CH alkyne peak ($H_1$) to give an approximate ratio of 21:1 for the $PLA_{20}$ and 65:1 for the $PLA_{100}$.

**Table 4.1.** Determination of the approximate chain lengths of the alkyne end capped PLA

| **Lactide to Alcohol Ratio** | **Theoretical Calculations** | | **$^1$H-NMR Results** | | | **GPC Results** | | |
|---|---|---|---|---|---|---|---|---|
| | **DP** (n) | **$M_n$** $gmol^{-1}$ | **Integration Ratio $H_5$:$H_1$** | **DP** (n) | **$M_n$** $gmol^{-1}$ | **$M_w$** $gmol^{-1}$ | **$M_n$** $gmol^{-1}$ | **PDI** |
| 10 : 1 | 20 | 1,570 | 21 : 1 | 22 | 1,710 | 3,940 | 2,650 | 1.5 |
| 50 : 1 | 100 | 7,260 | 65 : 1 | 66 | 4,810 | 7,900 | 5,120 | 1.5 |

The lack of agreement between molecular weights measured by GPC and those calculated from $^1$H-NMR results is believed to be due to the method of analysis used in GPC. The $M_n$ values reported here were measured by GPC with refractive index detector and were relative to polystyrene standard. Therefore, they are not absolute values. This is due to the difference between the hydrodynamic volumes of alkyne end capped PLA and that of polystyrene. The PDI is broader than expected which is believed to be due to the presence of alkyne uncapped PLA chains in the product. Impurities such as water or 2-ethylhexanoic acid, which are always present in commercial $Sn(Oct)_2$, are known to act as co-initiators to form uncapped PLA chains, Scheme 4.2.[14]

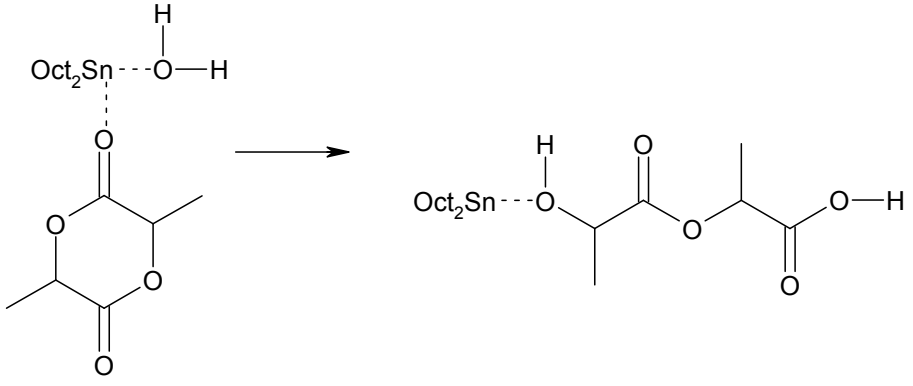


**Scheme 4.2.** Synthesis of uncapped PLA

### 4.3.1.2. ROP of ε-Caprolactone (CL)

The same method used for ROP of LA was applied to synthesise the alkyne end capped PCL **4.2**, Scheme 4.3. The reaction was carried out successfully using stannous octoate and propargyl alcohol as an initiating system. The ratio of the CL to alcohol was 100:1 to produce PCL chains with DP = 100 ($PCL_{100}$).

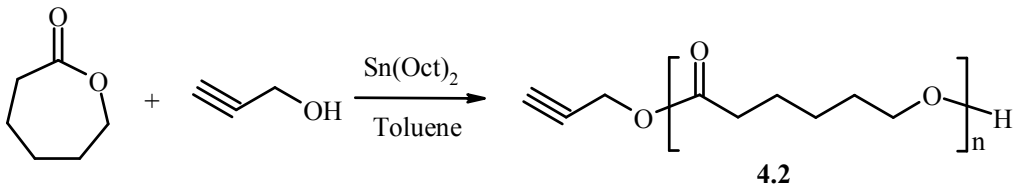


**4.2**

**Scheme 4.3.** Synthesis of alkyne end capped PCL

The polymer was fully characterised by $^1$H-NMR spectroscopy. The $^1$H-NMR spectrum of $PCL_{100}$ (Fig. 4.9) showed the peaks corresponding to the hydrogens of the alkyne chain end ($H_1$) and ($H_2$) at 2.42 and 4.61 ppm, respectively, as well as those for the PCL repeat unit ($H_3$, $H_4$, $H_5$, $H_6$ and $H_7$).

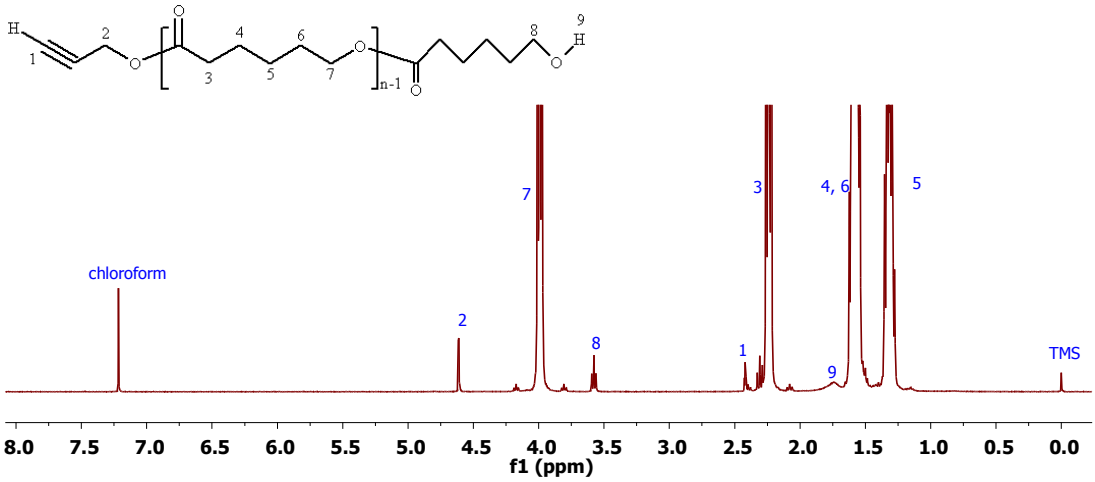


**Figure 4.9.** $^1$H-NMR spectrum of the alkyne end capped PCL ($PCL_{100}$) **4.2** in $CDCl_3$

The molecular weight of the $PCL_{100}$ was determined by $^1$H-NMR and GPC and the results are shown in Table 4.2. In the $^1$H-NMR spectrum of $PCL_{100}$ (Fig. 4.9), the $CH_2$ peak of the PCL ($H_7$) was integrated against the terminal CH alkyne peak ($H_1$) to give an approximate ratio of 99:1. The molecular weight was determined using GPC with refractive index detector. Therefore, the $M_n$ value measured was relative to polystyrene standard and the hydrodynamic volume of alkyne end capped PCL will be

expected to be very different to that of polystyrene. The PDI is broader than expected which is believed to be due to the presence of alkyne uncapped PCL chains in the product. Therefore, the $M_n$ value measured by GPC is not reliable.

**Table 4.2:** Determination of the approximate chain lengths of the alkyne end capped PCL

| Caprolactone to Alcohol Ratio | Theoretical Calculations | | $^1$H-NMR Results | | | GPC Results | | |
|---|---|---|---|---|---|---|---|---|
| | DP (n) | $M_n$ gmol$^{-1}$ | Integration Ratio $H_7$:$H_1$ | DP (n) | $M_n$ gmol$^{-1}$ | $M_w$ gmol$^{-1}$ | $M_n$ gmol$^{-1}$ | PDI |
| 100 : 1 | 100 | 11,460 | 99 : 1 | 100 | 11,460 | 15,830 | 11,160 | 1.4 |

### 4.3.1.3. Glycopolymer Containing PCL

Click reaction was successfully carried out between the alkyne end capped PCL ($PCL_{100}$) **4.2** and the protected di-azide functionalised trehalose **3.2** (refer to chapter 3) using copper sulphate pentahydrate and sodium ascorbate in a mixture of acetone and water (1:1) solvents to produce the glycopolymer **4.3** containing PCL, Scheme 4.4.

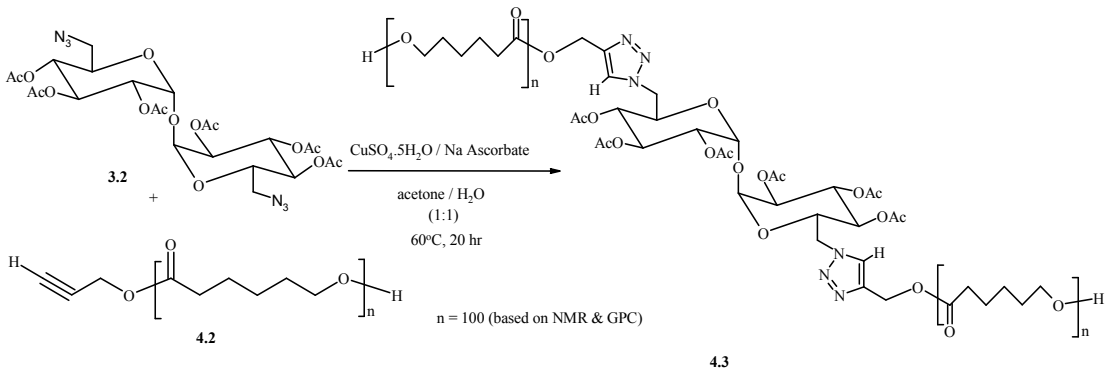


**Scheme 4.4.** Synthesis of glycopolymer containing PCL

The $^1$H-NMR spectrum of the clicked product **4.3** showed the appearance of the triazole proton ($H_7$) peak at 7.67 ppm (Fig. 4.10) as well as all the peaks corresponding to both PCL and trehalose segments. Moreover, the FT-IR spectra of **4.3** (Fig. 4.11.B) compared to that of **3.2** (Fig. 4.11.A) showed complete disappearance of the azide peak

at 2096 $cm^{-1}$ and appearance of a new peak at 1722 $cm^{-1}$, corresponding to the carbonyl of the PCL, slightly lower than the absorbance of the carbonyl of the acetate groups of trehalose.

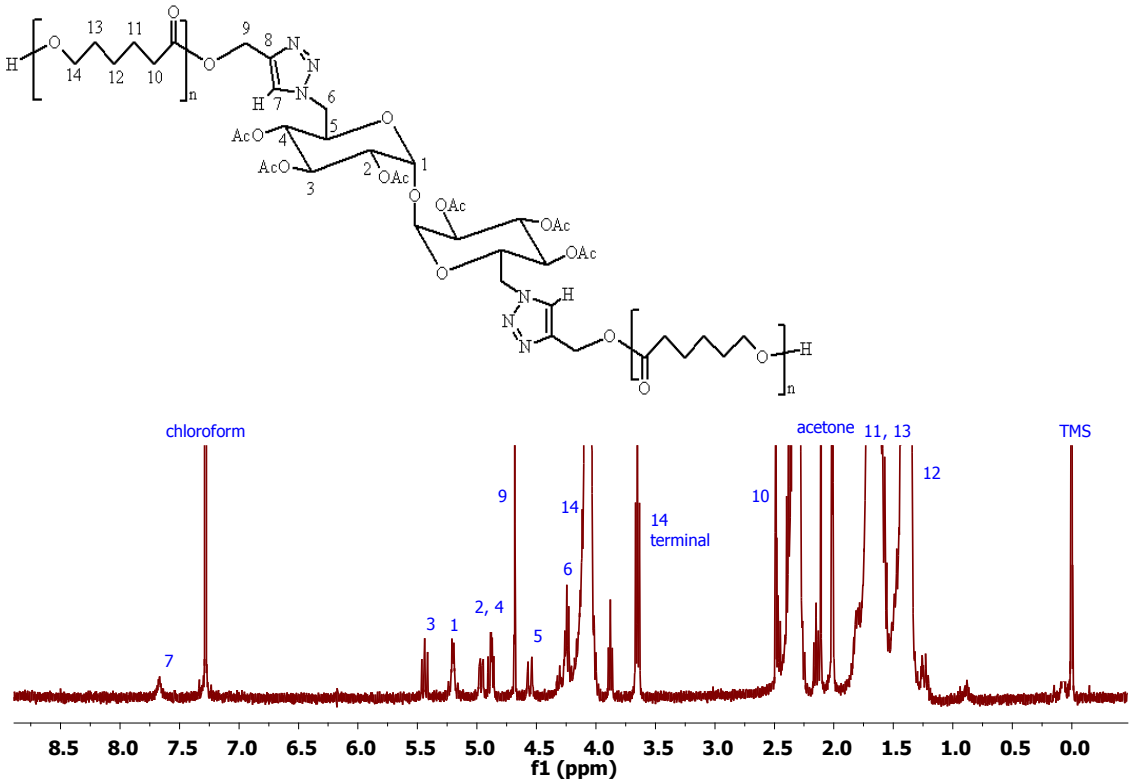


**Figure 4.10.** $^{1}$H-NMR spectra of glycopolymer **4.3** containing PCL in $CDCl_3$

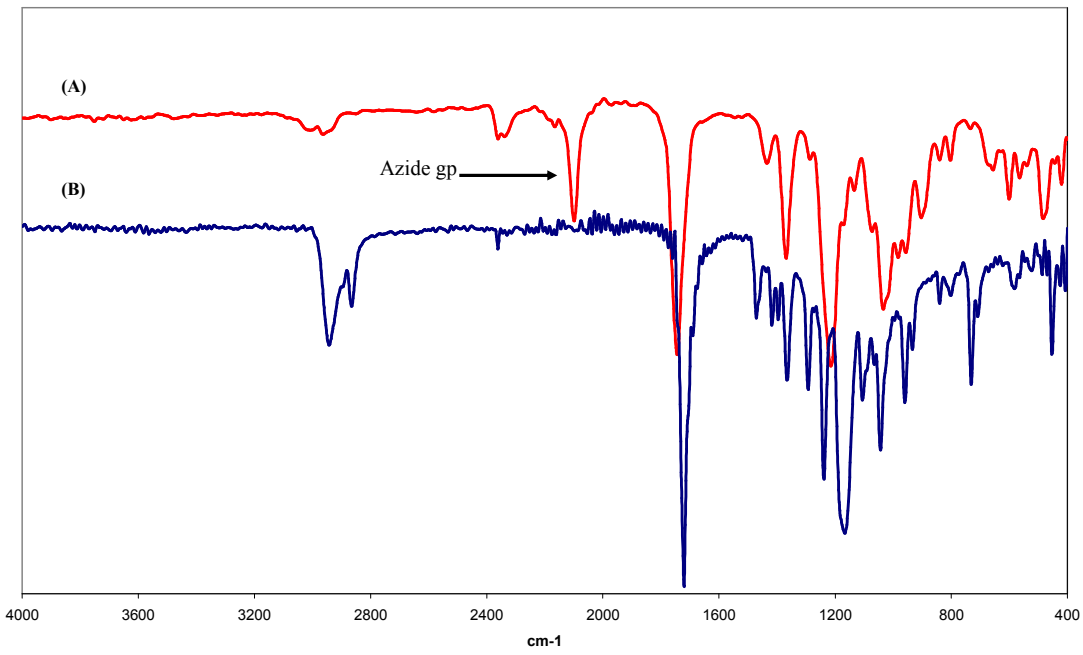


**Figure 4.11.** FT-IR spectra of (A) di-azide functionalised protected trehalose **3.2** and (B) glycopolymer **4.3** containing PCL

The molecular weight measurement was carried out using GPC with refractive index detector and the results are shown in Table 4.3. For the same reason discussed earlier, the $M_n$ values are not absolute. It can clearly be seen that $M_n$ and $M_w$ values were doubled after the reaction, indicating successful Click reactions between one trehalose unit and two PCL chains.

**Table 4.3:** GPC results for PCL and glycopolymer containing PCL

| Polymer | GPC Results | | |
|---|---|---|---|
| | $M_w$ $gmol^{-1}$ | $M_n$ $gmol^{-1}$ | PDI |
| $PCL_{100}$ **4.2** | 15,830 | 11,160 | 1.4 |
| Glycopolymer **4.3** containing PCL | 36,460 | 23,120 | 1.6 |

### 4.3.2. Glycopolymer Containing PEG Segments as Smart Temperature Responsive Material

Click chemistry was successfully utilised to prepare a new class of temperature responsive amphiphilic water-soluble glycopolymers. A commercially available di-hydroxyl terminated PEG (DHT-PEG) was quantitatively alkyne end-capped to yield di-alkyne terminated PEG (DAT-PEG). Click-polymerisation reaction between DAT-PEG and the protected di-azide functionalised trehalose **3.2** (refer to chapter 3) was successfully carried out to produce a novel linear alternating glycopolymer with triazole rings as linkers in high yield. Cu-wire was demonstrated to be an efficient alternative catalyst for Click reaction.

The presence of PEG segments is expected to render the biocompatibility of the prepared glycopolymer. Moreover, the incorporation of trehalose in the backbone is believed to induce the biodegradability. Therefore, the material has a high potential in biomedical applications.

### 4.3.2.1. Synthesis of Di-Alkyne Terminated PEG (DAT-PEG)

DAT-PEG **4.4** was successfully prepared by etherification reaction between commercially available di-hydroxyl terminated PEG (DHT-PEG) ($M_n$ ~600 $gmol^{-1}$) and propargyl bromide, Scheme 4.5.

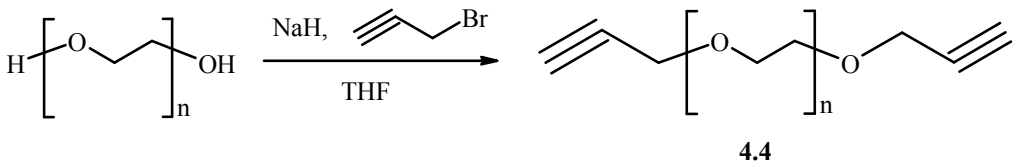


**4.4**

**Scheme 4.5.** Synthesis of di-alkyne terminated PEG (DAT-PEG)

The hydroxyl groups of DHT-PEG were quantitatively converted into alkyne functionality to produce DAT-PEG **4.4**, according to $^1$H-NMR spectroscopy. This was shown by the complete disappearance of the peak due to the hydroxyl groups in PEG at 2.92 ppm (Fig. 4.12.A). Moreover, peaks due to the alkyne proton ($H_1$) and the $CH_2$ protons adjacent to the alkyne group ($H_3$) at 2.40 and 4.12 ppm, respectively, were observed (Fig. 4.12.B).

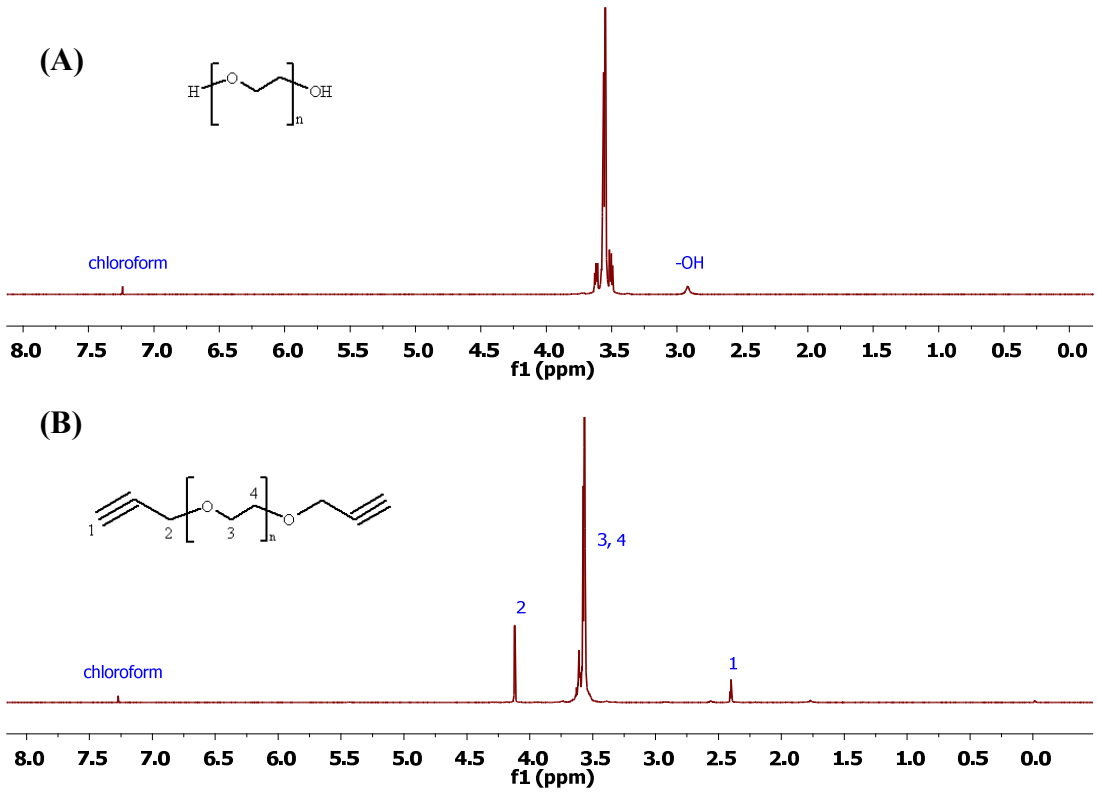


**Figure 4.12.** $^1$H-NMR spectra of (A) DHT-PEG and (B) DAT-PEG **4.4** in $CDCl_3$

#### 4.3.2.2. Click-Polymerisation of Protected Di-azide Functionalised Trehalose with DAT-PEG

The protected di-azide functionalised trehalose **3.2** (refer to chapter 3) and DAT-PEG **4.4** were polymerised *via* Click reaction using copper wire as a catalyst to produce the glycopolymer **4.5**, Scheme 4.6.

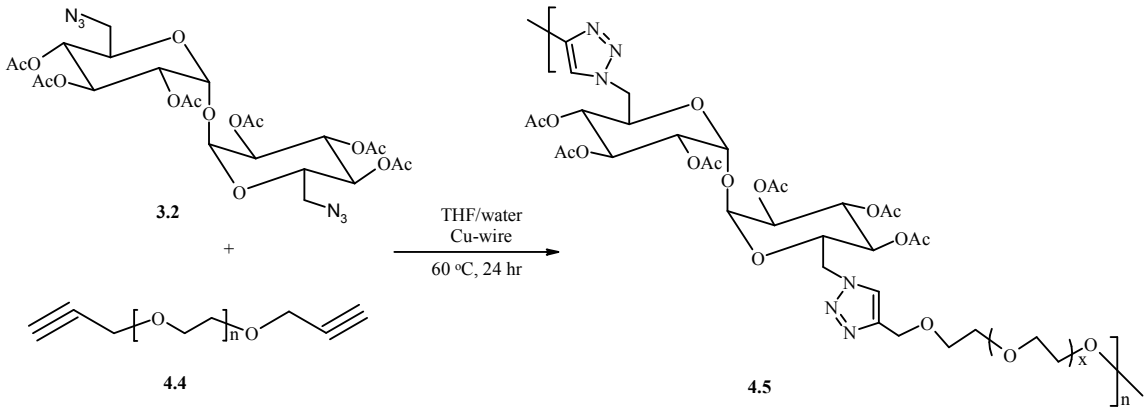


**Scheme 4.6.** Synthesis of glycopolymer containing PEG segments

The successful Click polymerisation reaction was confirmed by $^{1}$H-NMR and FT-IR spectroscopy. $^{1}$H-NMR spectrum showed appearance of a new peak at 7.57 ppm, assigned to the triazole protons ($H_7$) (Fig. 4.14). It also showed all the peaks, corresponding to both trehalose and PEG segments. The IR spectra of **4.5** (Fig. 4.15.B) compared to that of **3.2** (Fig. 4.15.A) showed disappearance of the azide peak at 2096 $cm^{-1}$.

The $M_n$ value for DHT-PEG is ~600 $gmol^{-1}$. The average molecular weight of DAT-PEG **4.4** is expected to be close to that of DHT-PEG. The molecular weight measurement for the glycopolymer **4.5** was carried out using GPC with triple detector in THF. The GPC analysis of glycopolymer **4.5** showed $M_n = 3.4x10^4$ $gmol^{-1}$ with PDI of 1.50, which was indicative of the formation of high molecular weight polymer with reasonably narrow PDI, Fig. 4.13.A.

The same synthetic strategy was used to prepare glycopolymers **4.6** and **4.7** containing PEG segments with $M_n$ of ~200 and ~1000 $gmol^{-1}$, respectively. The GPC analysis of glycopolymer **4.6** showed $M_n = 6.25x10^3$ $gmol^{-1}$ with PDI of 1.68, Fig. 4.13.B. The glycopolymer **4.7** was not completely soluble in THF and therefore it was not analysed by GPC. However, the analysis indicated that as the molecular weight of the PEG segment was increased, the $M_n$ of the resulting glycopolymer was also increased, while the PDI remained relatively the same.

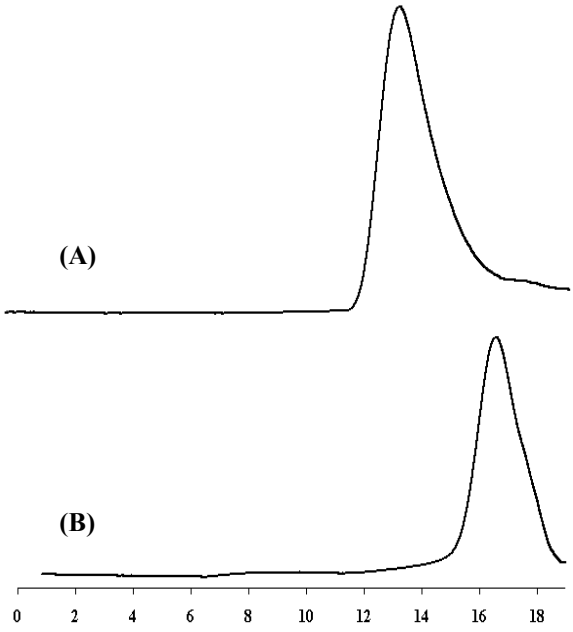


**Figure 4.13.** GPC traces of (A) glycopolymer **4.5** and (B) glycopolymer **4.6**

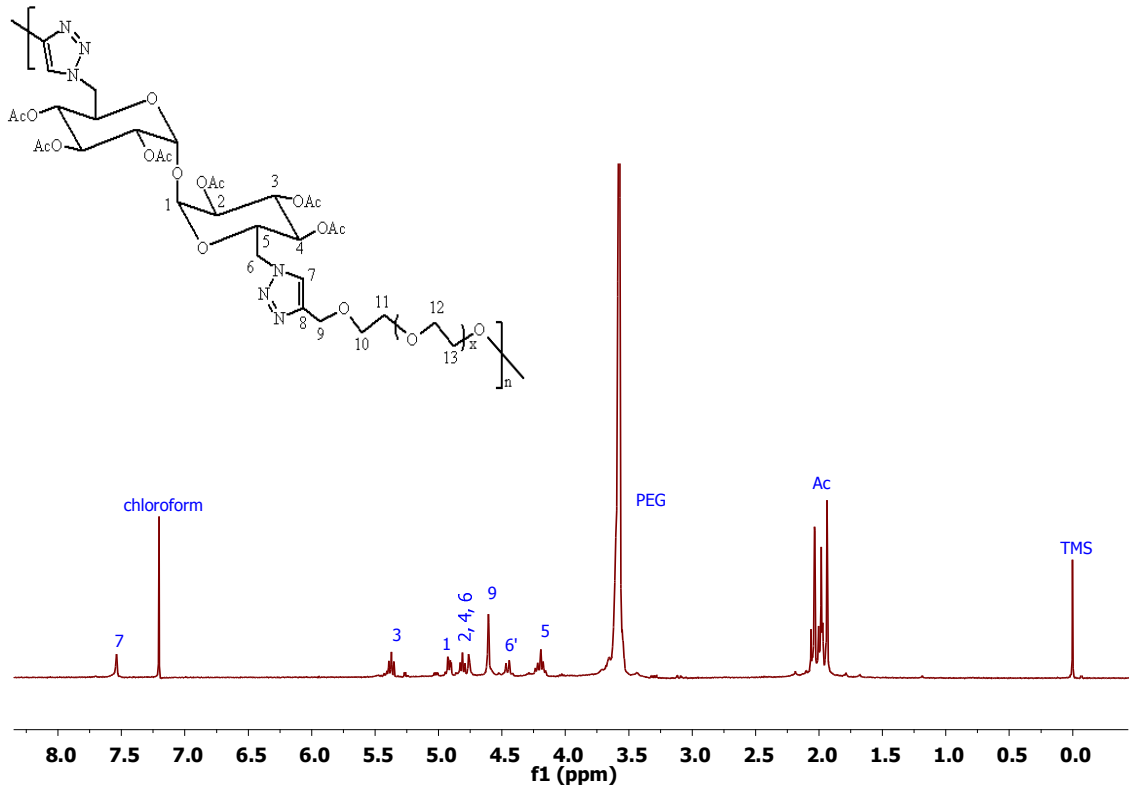


**Figure 4.14.** $^{1}$H-NMR spectrum of glycopolymer **4.5** containing PEG in $CDCl_3$

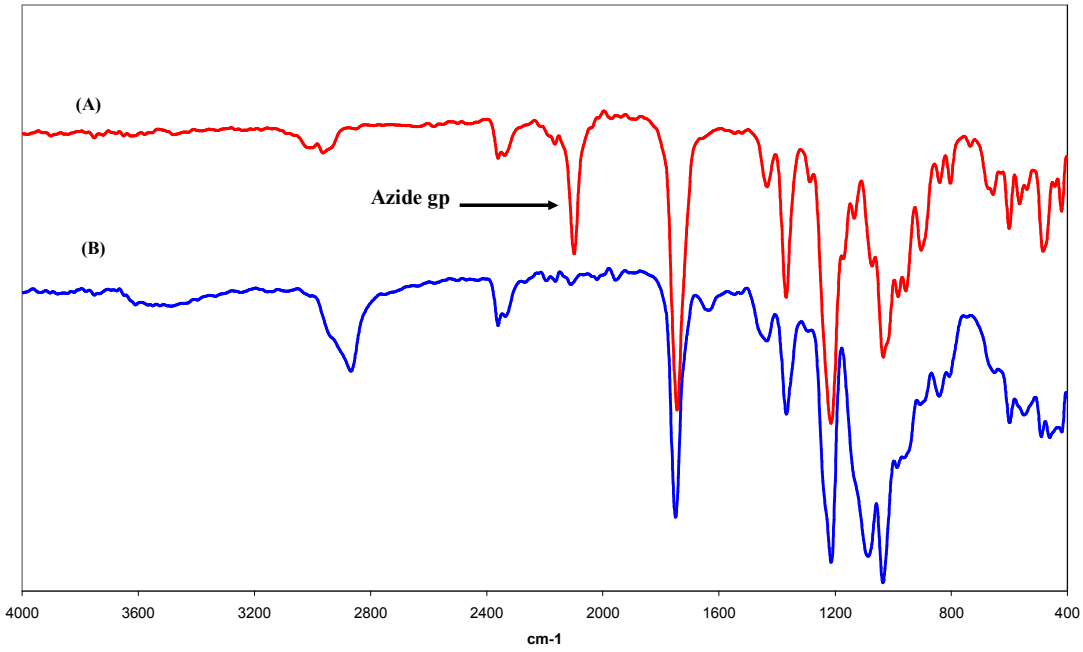


**Figure 4.15.** FT-IR spectra of (A) di-azide functionalised protected trehalose **3.2** and (B) glycopolymer **4.5** containing PEG

### 4.3.2.3. Thermal Studies

The thermogravimetric analysis (TGA) of the glycopolymer **4.5** showed that the polymer started decomposing at 320 $^{o}$C, which was lower than the decomposition temperature of PEG (355 $^{o}$C). This slight decrease in the thermal stability was attributed to the incorporation of trehalose moiety in the polymer backbone. TGA analysis of fully protected (acetylated) trehalose showed a decomposition temperature of 295 $^{o}$C.

The differential scanning calorimerty (DSC) analysis of PEG sample showed a $T_g$ at −61 $^{o}$C and a $T_m$ at +21 $^{o}$C, Fig. 4.16.A. However, the DSC analysis of glycopolymer **4.5** showed only a peak at −22 $^{o}$C, corresponding to $T_g$, Fig. 4.16.B. This is believed to be due to the incorporation of trehalose, which increased the stiffness, and the disorder of PEG segments resulting in a relatively amorphous rigid material.

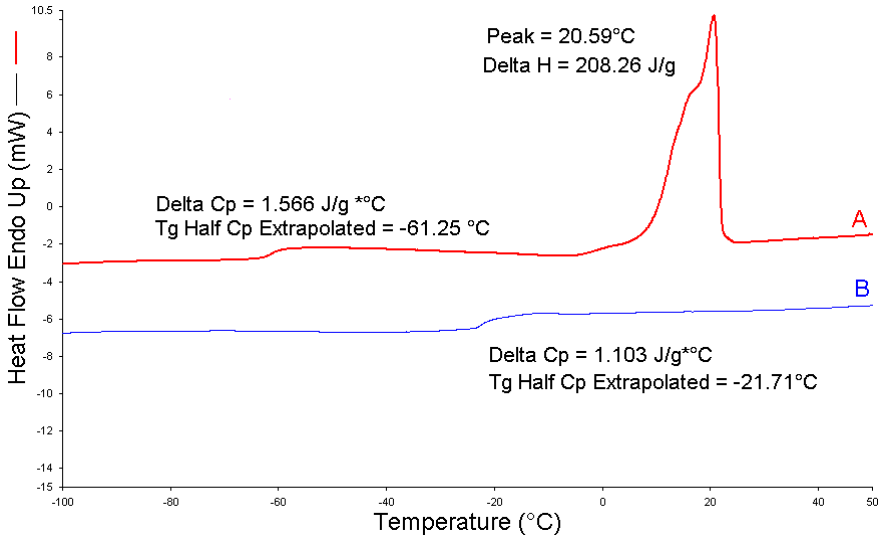


**Figure 4.16.** Differential Scanning Calorimerty (DSC) measurements for; (A) PEG and (B) glycopolymer **4.5**

### 4.3.2.4. Cloud Point Measurements

The aqueous solution of glycopolymer **4.5** showed turbidity upon heating and it became clear and homogeneous once the temperature was decreased, Fig. 4.17. There are several physical techniques reported to investigate the phase transition behaviour of aqueous polymer solutions, such as turbidimetry,[20-22] neutron scattering,[23] microcalorimetric study,[24] low-angle light scattering measurements,[25] laser beam scattering methods,[26] and UV-Vis spectroscopy.[27]

In the work reported here, the cloud point of the glycopolymer was measured by UV-Vis spectroscopy equipped with temperature controller and confirmed by optical microscopy. The measurements showed that the material exhibits a reversible phase transition at about 39 $^{o}$C.

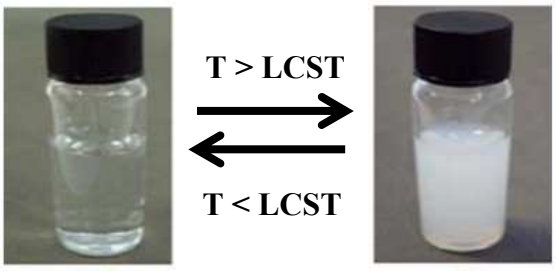


**Figure 4.17.** Photographs of the aqueous solution of the glycopolymer **4.5**

#### 4.3.2.4.1. UV-Vis Spectroscopy

The turbidimetry curve was drawn by measuring the absorbance of the aqueous polymer solution ($\lambda_{max}$= 357 nm) at a fixed concentration (2mg $mL^{-1}$) as a function of temperature (Figure 4.18.A). The rate of temperature increase was 1 $^{o}$C/min and the polymer solution was stirred and kept at the same temperature for 1 minute before each measurement. The absorbance of the polymer solution remained steady upon heating up to 39 $^{o}$C, which means that the solution was homogeneous and clear. Beyond 39 $^{o}$C, the polymer solution started to demix and became cloudy. At this point, the absorbance increased dramatically and then it became constant. The measurements were repeated on cooling and superimposable curve was obtained, indicating a reversible phase transition with $\Delta$T of ~ 10 $^{o}$C, under the measurement conditions mentioned above.

#### 4.3.2.4.2. Optical Microscopy

The optical micrograph of the aqueous solution of glycopolymer **4.5** showed that the polymer undergoes a reversible change in conformation, i.e. from hydrated coil to collapsed globule while the quality of the solvent was decreased upon heating, Fig. 4.18.B. Below the LCST, the polymer chains display a hydrophilic state whereas above it they collapse and show a hydrophobic state.

### 4.3.2.5. Effect of Deacetylation (Deprotection) of Trehalose

When the secondary hydroxyl groups of the trehalose units in glycopolymer **4.5** were deprotected, the polymer did not show phase transition behaviour under similar conditions. One explanation for this observation was that the polymer became completely hydrophilic and hence remained water-soluble at elevated temperatures. The other possibility was that the strong hydrogen bonding between the polymer chains formed a network, which prevented the collapse of the chains. The effect of the hydrogen bonding has also been observed for PNIPAM.[28]

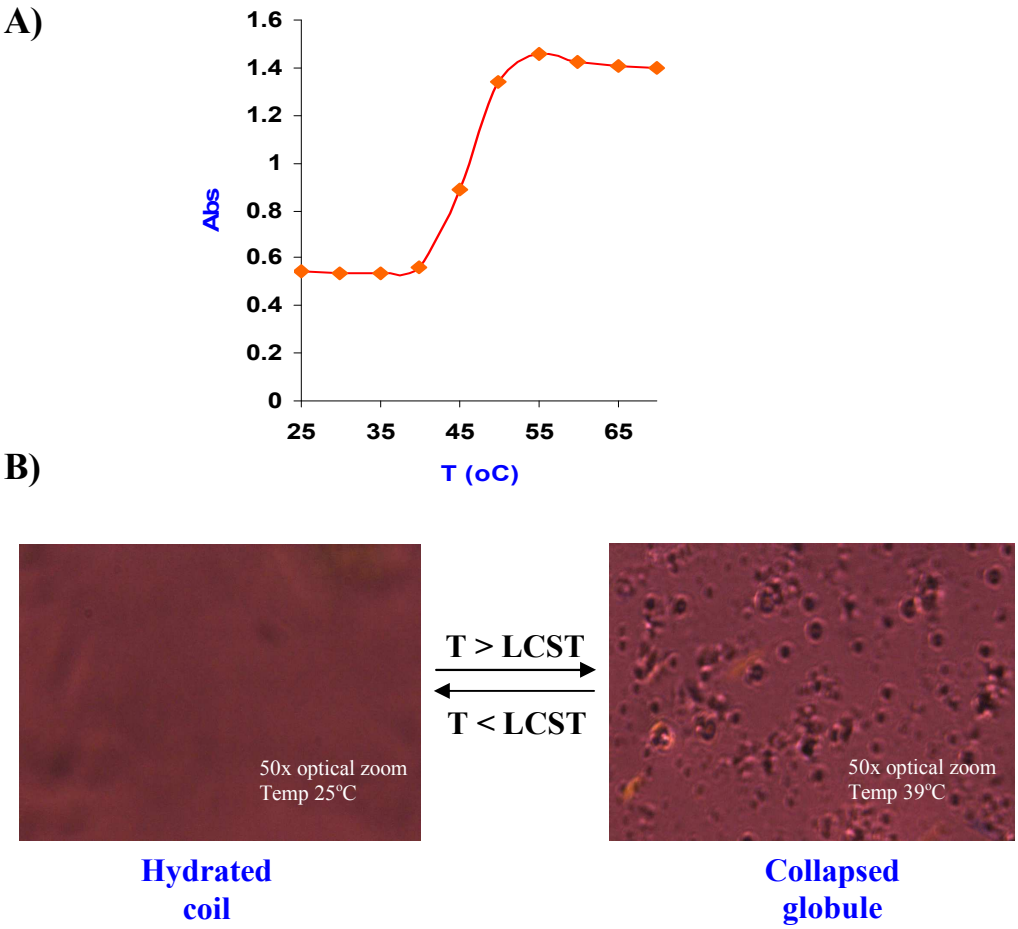


**Figure 4.18.** Cloud point measurements of the aqueous solution of glycopolymer **4.5** (A) turbidimetry profile and (B) optical micrographs below and above the LCST

### 4.3.2.6. Effect of $M_n$ of PEG

Glycopolymer **4.6** did not dissolve in water. Glycopolymer **4.7** dissolved in water but it did not show any phase transition up to 90 °C. These results were expected due to changing the balance between the hydrophilic and hydrophobic components.[29] The results indicated that the ideal molecular weight of PEG to produce glycopolymer exhibiting phase transition at ~39 °C, known as fever temperature, was ~600 $gmol^{-1}$. This is very close to the molecular weight of the hydrophobic saccharide component (protected di-azide functionalised trehalose **3.2**) of ~644 $gmol^{-1}$.

## 4.4. Summary

ROP of lactide and ε-caprolactone, using stannous octoate and propargyl alcohol, was shown to be a good method to synthesise alkyne end capped PLA and PCL. ROP and Click chemistry were combined for the synthesis of biodegradable glycopolymers containing PCL or PLA. NMR, IR and GPC were used to prove the structure of the materials.

Copper wire catalysed Click chemistry was utilised to prepare a new class of temperature responsive amphiphilic water-soluble glycopolymers. The material is an alternating linear glycopolymer composed of PEG and trehalose segments with triazole linkers. The material was fully characterised by NMR, IR and GPC. The cloud point of the aqueous polymer solution was evaluated and the LCST of the smart material was shown to be about 39 $^{o}$C, which is known as fever temperature. The phase transition of the glycopolymer was shown to be reversible. The protection (acetylation) of the secondary hydroxyl groups in trehalose was shown to be essential to promote the hydrophobic character of the glycopolymer, in order to create the hydrophobic/hydrophilic interactions, which is the origin of the phase transition. The results indicated that the ideal average molecular weight of PEG to produce glycopolymer exhibiting phase transition at the fever temperature is 600 gmol$^{-1}$, which is very close to the molecular weight of the hydrophobic component (protected trehalose), 644 gmol$^{-1}$.

## 4.5. References


1. C. R. Bertozzi, L. L. Kiessling, *Science* **2001**, *291(5512)*, 2357 – 2364.
2. J. Geng, G. Mantovani, L. Tao, J. Nicolas, G. J. Chen, R. Wallis, D. A. Mitchell, B. R. G. Johnson, S. D. Evans, D. M. Haddleton, *Journal of the American Chemical Society* **2007**, *129(49)*, 15156 – 15163.
3. S. G. Spain, M. I. Gibson, N. R. Cameron, *Journal of Polymer Science Part A: Polymer Chemistry* **2007**, *45*, 2059 – 2072.
4. B. Voit, D. Appelhans, *Macromolecular Chemistry and Physics* **2010**, *211(7)*, 727 – 735.
5. M. Okada, *Progress in Polymer Science* **2001**, *26(1)*, 67 – 104.
6. V. Ladmiral, E. Melia, D. M. Haddleton, *European Polymer Journal* **2004**, *40(3)*, 431 – 449.
7. S. Slavin, J. Burns, D. M. Haddleton, C. R. Becer, *European Polymer Journal* **2010**, doi: 10.1016/j.eurpolymj.2010.09.019
8. K. Kurita, N. Masuda, S. Aibe, K. Murakami, S. Ishii, and S. Nishimura, *Macromolecules* **1994**, *27*, 7544.
9. N. Teramoto, Y. Arai, Y. Shibassaki, and Shibata, *Carbohydrate Polymers* **2004**, *56*, 1.
10. N. Teramoto, Y. Abe, A. Enomoto, D. Watanabe, and M. Shibata, *Carbohydrate Polymers* **2005**, *59*, 217.
11. N. Teramoto, Y. Arai, and M. Shibata, *Carbohydrate Polymers* **2006**, *64*, 78.
12. N. Teramoto, M. Unosawa, S. Matsushima, and M. Shibata, *Polymer Journal* **2007**, *39 (9)*, 975.
13. K. A. Athanasiou, G. G. Niederauer, C. M. Agrawal, *Biomaterials* **1996**, *17*, 93-102.
14. T. J. Corden, I. A. Jones, C. D. Rudd, P. Christian, S. Downes, K. E. McDougall, *Biomaterials* **2000**, *21*, 713-724.
15. J. C. Middleton, A. J. Tipton, *Biomaterials* **2000**, *21*, 2335-2346.
16. M. Vert, S. M. Li, G. Spenlehauer, P. Guerin, *Journal of Materials Science-Materials in Medicine* **1992**, *3*, 432-446.
17. A. C. Albertsson, M. Gruvegard, *Polymer* **1995**, *36*, 1009-1016.
18. D. K. Gilding, A. M. Reed, *Polymer* **1979**, *20*, 1459-1464.
19. A. J. Nijenhuis, D. W. Grijpma, A. J. Pennings, *Macromolecules* **1992**, *25*, 6419-6424.
20. C. Boutris, E. G. Chatzi, C. Kiparissides, *Polymer* **1997**, *38*, 2567-2570.
21. C. Friedrich, C. Schwarzwalder, R. E. Riemann, *Polymer* **1996**, *37*, 2499-2507.

22. V. Jarm, S. Sertic, N. Segudovic, *Journal of Applied Polymer Science* **1995**, *58*, 1973-1979.
23. P. Thiyagarajan, D. J. Chaiko, R. P. Hjelm, *Macromolecules* **1995**, *28*, 7730-7736.
24. H. G. Schild, D. A. Tirrell, *Journal of Physical Chemistry* **1990**, *94*, 4352-4356.
25. L. P. Rebelo, W. A. Vanhook, *Journal of Polymer Science Part B-Polymer Physics* **1993**, *31*, 895-897.
26. S. Nozary, H. Modarress, A. Eliassi, *Journal of Applied Polymer Science* **2003**, *89*, 1983-1990.
27. F. Fernandez-Trillo, J. C. M. van Hest, J. C. Thies, T. Michon, R. Weberskirch, N. R. Cameron, *Advanced Materials* **2009**, *21*, 55-59.
28. H. G. Schild, *Progress in Polymer Science* **1992**, *17*, 163-249.
29. M. Rackaitis, K. Strawhecker, K. Manias, *Journal of Polymer Science Part B-Polymer Physics* **2002**, *40*, 2339-2342.

# Chapter 5

# Modification of 2-Hydroxyethyl Cellulose (HEC)

## 5.1. Introduction

Polysaccharides are classified as "eco-materials", since they are biodegradable and abundant in nature. They are also the most potential candidates for biomaterials, since they are biocompatible and many of them are known to have biological and pharmaceutical functions.[1-5] Because of their inherent chiralities, polysaccharides are capable of forming helical superstructures,[6] which emphasises their potential as scaffolds for tissue engineering. Based on their unique multifunctionality, polysaccharides play a very important role in personal care and cosmetic formulations. For example, they act as thickeners, suspending agents, hair conditioners, moisturisers, emulsifiers, emollients, and even wound-healing agents.[7-10] Polysaccharides are also classified, based on their electrochemical charges, into non-ionic (neutral), anionic, cationic, and amphoteric (zwitterionic) polysaccharides. Special interest has been paid to polysaccharide-based polysiloxanes, known as glyco-silicones. Such amphiphilic structures have been used as transdermal penetration enhancers,[11] surfactants,[12-16] and surface modifiers in cosmetics and detergent formulations.[17,18] Polydimethylsiloxane (PDMS) is of particular interest for this purpose due to its unique properties. It has low glass transition temperature, high flexibility, low toxicity, good biocompatibility, high oxygen permeability and good thermal stability.[19-21] Polysaccharide-based poly(aliphatic esters) (PLA and PCL) are another interesting example of the hydrophobic polysaccharides. However, the limited mixing affinity between these hydrophobic polymers (PDMS, PLA and PCL) and hydrophilic polysaccharides has been a practical barrier in the synthesis of these materials. In contrast, the incorporation of PEG into polysaccharides to produce hydrophilic polysaccharides is expected to suffer less from this poor compatibility issue. However, the regio-selective and quantitative chemical modifications of native polysaccharide backbones have been hardly accomplished and usually involve tedious synthetic routes due to the similar reactivity of the hydroxy-groups of the polysaccharides toward electrophiles.[22,23] Therefore, efficient and facile strategies to modify polysaccharides into polysaccharide-based materials are highly desired.

Recently, the synthesis of well-defined glyco-polyorganosiloxanes by Click chemistry has been reported.[24] The alkyne functionality was only introduced at the glycoside end of the polysaccharide, xyloglucan, and hence a limited amount of the azide functionalised PDMS can be coupled with the polysaccharide moiety. Nevertheless, it was claimed that the produced material exhibit a good surfactant properties.[24] Moreover, Click chemistry has been used to graft PCL onto cellulose fibres. The method involved merely

surface grafting in heterogeneous condition and a spacer molecule needed to move away the reactive functions from the fibre's surface and, consequently, makes them more accessible for PCL grafts.[25]

Akzo Nobel (formerly known as ICI National Starch) is currently supplying a cationic polysaccharide product, which consists of quaternary ammonium salt modified 2-hydroxyethyl cellulose (HEC). This product has been used in cosmetics and personal care formulations, since it has the unique advantage to bind tightly to proteins (negatively charged) of the human skin and hair and therefore acts as a damage-repairing agent. Therefore, the development of novel HEC-based materials with different charges as well as hydrophobic/hydrophilic grafts has been an attractive research target.

This chapter describes the exploitation of Click chemistry on HEC to generate novel polysaccharide based materials. To the best of our knowledge, there are no reports, up to date, on modification of HEC *via* Click chemistry. Sequential Click reactions are used to functionalise and graft HEC with different molecules and/or macromolecules to generate materials with interesting features for possible industrial / medical applications. The knowledge and experience gained from the previous work on the model compounds (chapter 2) and trehalose (chapters 3 and 4) is used in the synthesis and characterisation methods. However, due to the complex structural nature of HEC, solid-state $^{13}$C-NMR spectroscopy is also used as characterisation tool to follow up the modification reactions.

The chemical modification strategy carried out in this chapter should significantly broaden the structural diversity of polysaccharide-based materials. The utilisation of Click chemistry would yield compounds, which are not accessible *via* the commonly applied modification reactions such as etherification and esterification.

## 5.2. Experimental

### 5.2.1. Materials

2-Hydroxyethyl cellulose (HEC) ($M_w$ of ~250,000 $gmol^{-1}$, DS=1, MS=2) was purchased from Sigma – Aldrich and fully characterised by $^{13}$C-NMR spectroscopy before usage. Poly(ethylene glycol) (PEG) was also purchased from Sigma – Aldrich and fully characterised by NMR spectroscopy. Monocarbinol terminated polydimethylsiloxanes (hydroxy terminated PDMS) ($M_w$ of ~1000 $gmol^{-1}$) and Monoepoxy terminated polydimethylsiloxanes (epoxy terminated PDMS) ($M_w$ of ~1000 $gmol^{-1}$) were purchased from Gelest and fully characterised by $^1$H-NMR spectroscopy before usage.

All other chemicals and reagents used in the synthesis were purchased from Sigma – Aldrich and used without further purification. All dry solvents were obtained from the Solvent Purification System (SPS), Chemistry Department, Durham University.

### 5.2.2. Instrumentation and Measurements

$^1$H-NMR spectra were recorded using deuteriated solvent lock on a Varian Mercury 400 or a Varian Inova 500 spectrometer at 400 MHz and 500 MHz, respectively. Chemical shifts are quoted in ppm, relative to tetramethylsilane (TMS), as the internal reference. $^{13}$C-NMR spectra were recorded at 101 MHz or 126 MHz (2000 scans) using continuous broad band proton decoupling and a 3 S recycle dely, and therefore not quantitative; chemical shifts are quoted in ppm, relative to $CDCl_3$ (77.55 ppm). The following abbreviations are used in listing NMR spectra: s = singlet, d = doublet, t = triplet, q = quartet, m = multiplet, b = broad.

Solid-state NMR spectra were obtained using either a Varian VNMRS spectrometer operating at 100.56 MHz for $^{13}$C (399.88 MHz for $^1$H) or a Varian Unity Inova instrument operating at 75.40 MHz for $^{13}$C (299.82 MHz for $^1$H). They were obtained under magic-angle spinning conditions with spin-rates in the range 10000 to 14000 Hz. Carbon spectra were recorded with cross-polarisation (typically with a recycle delay of 1.0 s and a contact time of 1.00 ms) or direct excitation (typically with a recycle delay of 1.0 s) and with $^1$H decoupling. $^1$H spectra were obtained with direct excitation. Samples were run as-prepared and spectral referencing is with respect to external, neat tetramethylsilane.

FT-IR spectra were recorded on a Perkin Elmer 1600 series FT-IR spectrometer fitted with a golden gate. The samples were used as solids or liquids.

Silicon analysis was carried out by Atomic Absorbance Spectrometry using Varian Spectra AA 220 FS with $N_2$/acetylene flame. Digestion of samples were carried out by adding 3 ± 0.1 mL of concentrated $HNO_3$ to each sample in a 20 mL volumetric flask. Samples were then heated to 90 ± 5 $^oC$ for 15 min, allowed to cool and made up to the 20 mL mark with deionised water.

A Digital Instruments Nanoscope IV AFM was used to record tapping mode micrographs of the irradiated polymers. 256 x 256 line images were recorded at a scanning speed of 1 Hz, and an integrated hot stage was used to carry out annealing steps between scans. Annealing was carried out for 1800 s at 110, 121.5, and 132.2 $^oC$. Surface height versus cross-section was measured for each AFM image with the Nanoscope V6 online software.

### 5.2.3. Synthesis of Azide Functionalised HEC 5.1

HEC (10 g, 0.04 mmol; approximately 60 mmol of $1^{ry}$ OH), sodium azide (15.6 g, 240 mmol) and dry DMF (400 mL) were added to an oven-dried $N_2$-flushed three-neck round bottomed flask equipped with a stir bar, dropping funnel and thermometer. The reaction mixture was heated to 100 $^oC$ under $N_2$ atmosphere for 1 hr. The reaction mixture was then cooled in an ice water bath and triphenyl phosphine (47.2 g, 180 mmol) was added. Carbon tetrabromide (59.7g, 180 mmol) dissolved in dry DMF (50 mL) was added slowly. The reaction was allowed to warm up to ambient temperature and left for 18 hr under positive $N_2$ pressure. The colour of the reaction mixture turned from off-white to brownish yellow. Methanol (50 mL) was added to quench the reaction, and the polymer was precipitated by addition of ethanol. The precipitated polymer was recovered by filtration and washed with a mixture of ethanol / water solution (7:3) followed by ethanol. The polymer was then dried under reduced pressure in an oven at 50 $^oC$ for 24 hr to give the product **5.1**, yield 70 % (8.1 g, 0.028 mmol).

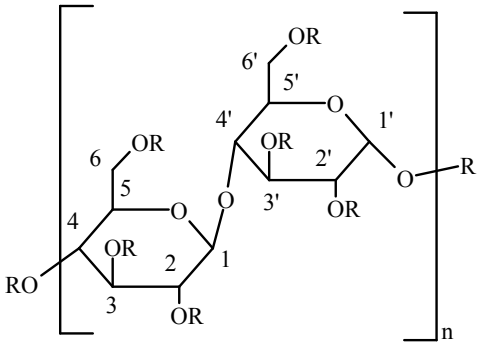


**5.1**

R = H or $-\left[\begin{matrix}7 & 8\\ C & C\\ H_2 & H_2\end{matrix}-O\right]_x-\begin{matrix}7 & 9\\ C & C\\ H_2 & H_2\end{matrix}-N_3$

x = 0 or 1

**Figure 5.1.** Structure of azide functionalised HEC with numerical assignment for NMR

Key resonance in $^{13}$C-NMR (126 MHz, DMSO-$d_6$, at 80 $^{o}$C): δ 51.04 ($C_9$).

Anal. Calc for HEC ($C_{20}H_{33}O_{14}$): C 48.29, H 6.64. Found: C 45.07, H 6.76.

Anal. Calc for azide functionalised HEC ($C_{20}H_{30}O_{11}N_9$): C 41.96, H 5.24, N 22.03. Found: C 40.93, H 5.55, N 23.05.

Key absorbance for FT-IR: ~2090 cm$^{-1}$ (C-$N_3$ stretching vibration).

### 5.2.4. Synthesis of HEC Clicked with Ethyl Propiolate 5.2

In a vial, azide functionalised HEC **5.1** (0.5 g, 0.0017 mmol; approximately 2.6 mmol of $N_3$ groups) was dissolved in DMSO (20 mL) at 70 $^{o}$C. Ethyl propiolate (3 mL, 3.0 mmol), copper (II) sulphate pentahydrate (65 mg, 0.26 mmol, in 1 mL of water) and sodium ascorbate (103 mg, 0.52 mmol, in 1 mL of water) were added and the mixture was stirred at 70 $^{o}$C for 24 hr. The polymer was precipitated in methanol (200 mL), filtered and washed three times with a mixture of ethanol / water solution (7:3) followed by methanol. The polymer was then dried under reduced pressure in an oven at 50 $^{o}$C for 24 hr to give the product **5.2**, yield 87 % (0.61 g, 0.0014 mmol).

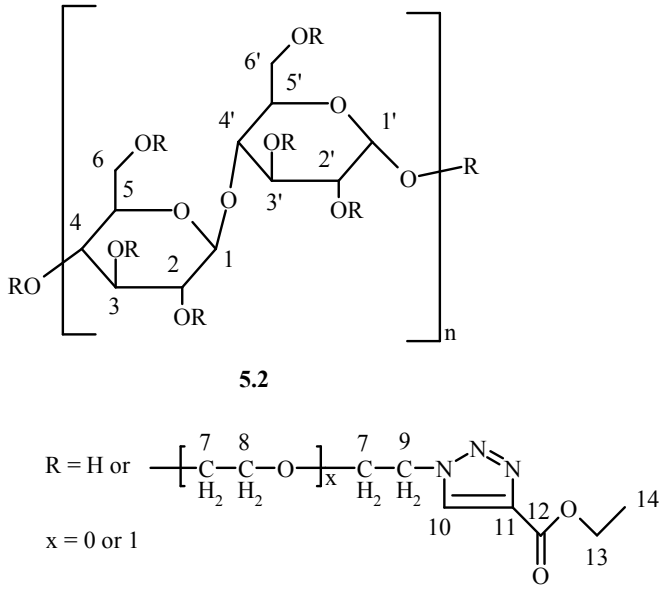


**Figure 5.2.** Structure of HEC clicked with ethyl propiolate with numerical assignment for NMR

Key resonances in $^{13}$C-NMR (126 MHz, DMSO-$d_6$, at 80 $^{o}$C): δ 161.01 ($C_{12}$), 139.97 ($C_{11}$), 129.73 ($C_{10}$), 50.53 ($C_9$), 14.75 ($C_{14}$), the rest of the resonances remained the same as the HEC backbone.

FTIR spectrum showed disappearance of azide peak at ~2090 cm$^{-1}$

### 5.2.5. Synthesis of HEC Clicked with 3-Trimethylsiloxy-1-propyne 5.3

In a vial, azide functionalised HEC **5.1** (0.5 g, 0.0017 mmol; approximately 2.6 mmol of $N_3$ groups) was dissolved in DMSO (20 mL) at 70 $^{o}$C. 3-Trimethylsiloxy-1-propyne (0.5 mL, 3.1 mmol), copper (II) sulphate pentahydrate (65 mg, 0.26 mmol, in 1 mL of water) and sodium ascorbate (103 mg, 0.52 mmol, in 1 mL of water) were added and the mixture was stirred at 70 $^{o}$C for 24 hr. The polymer was precipitated in methanol (200 mL), filtered and washed three times with a mixture of ethanol / water solution (7:3) followed by methanol. The polymer was then dried under reduced pressure in an oven at 50 $^{o}$C for 24 hr to give the product **5.3**, yield 73 % (0.6 g, 0.0012 mmol).

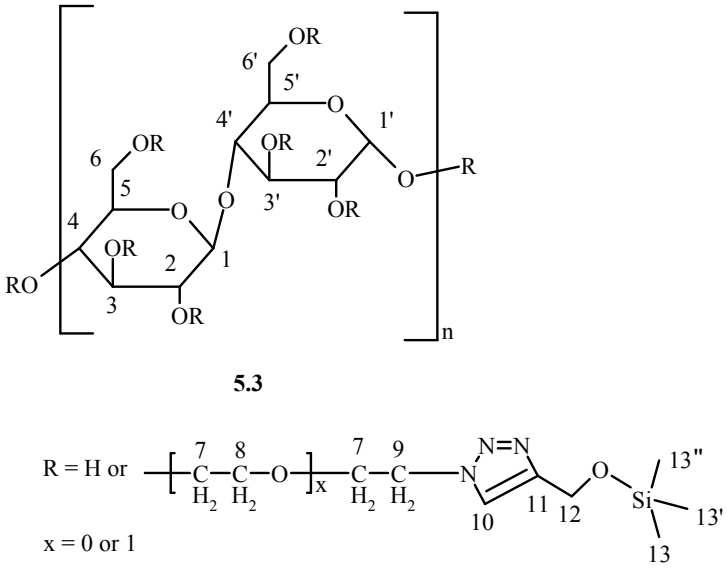

**5.3**



**Figure 5.3.** Structure of HEC clicked with 3-trimethylsiloxy-1-propyne with numerical assignment for NMR

Key resonances in $^{1}$H NMR (500 MHz, DMSO-$d_6$, at 80 $^{o}$C): δ 7.95 ($H_{10}$)
Key resonances in $^{13}$C-NMR (126 MHz, DMSO-$d_6$, at 80 $^{o}$C): δ 148.90 ($C_{11}$), 123.68 ($C_{10}$), 55.92 ($C_{12}$), 50.13 ($C_9$), the rest of the resonances remained the same as the HEC backbone.
FTIR spectrum showed disappearance of azide peak at ~2090 cm$^{-1}$

### 5.2.6. Synthesis of HEC Clicked with Propargyl Acrylate 5.4

In a vial, azide functionalised HEC **5.1** (0.5 g, 0.0017 mmol; approximately 2.6 mmol of $N_3$ groups) was dissolved in DMSO (20 mL) at 70 $^{o}$C. Propargyl acrylate (0.35 mL, 3.2 mmol), copper (II) sulphate pentahydrate (65 mg, 0.26 mmol, in 1 mL of water) and sodium ascorbate (103 mg, 0.52 mmol, in 1 mL of water) were added and the mixture was stirred at 70 $^{o}$C for 24 hr. The polymer was precipitated in methanol (200 mL), filtered and washed three times with a mixture of ethanol / water solution (7:3) followed by methanol. The polymer was then dried under reduced pressure in an oven at 50 $^{o}$C for 24 hr to give the product **5.4**, yield 86 % (0.68 g, 0.0015 mmol).

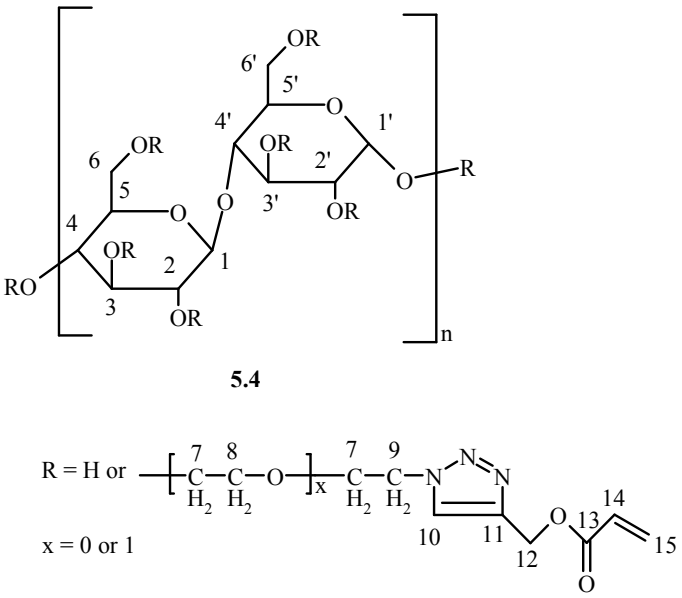

**5.4**

**Figure 5.4.** Structure of HEC clicked with propargyl acrylate with numerical assignment for NMR

Key resonances in solid-state $^{13}$C-NMR (101 MHz, cross polarisation technique): δ 165.99 ($C_{13}$), 142.57 ($C_{11}$), 128.29 ($C_{10}$), 58.77 ($C_{12}$), 51.66 ($C_9$), the rest of the resonances remained the same as the HEC backbone.
FTIR spectrum showed disappearance of azide peak at ~2090 cm$^{-1}$

### 5.2.7. Attempted Synthesis of HEC Clicked with Glycidyl Propargyl Ether

In a vial, azide functionalised HEC **5.1** (0.5 g, 0.0017 mmol; approximately 2.6 mmol of $N_3$ groups) was dissolved in DMSO (20 mL) at 70 $^{o}$C. Glycidyl propargyl ether (0.35 mL, 3.2 mmol), copper (II) sulphate pentahydrate (65 mg, 0.26 mmol, in 1 mL of water) and sodium ascorbate (103 mg, 0.52 mmol, in 1 mL of water) were added and the mixture was stirred at 70 $^{o}$C for 24 hr. The product could not be isolated.

### 5.2.8. Synthesis of HEC Clicked with 5-Hexynoic Acid 5.5

In a vial, azide functionalised HEC **5.1** (1 g, 0.0034 mmol; approximately 5.2 mmol of $N_3$ groups) was dissolved in DMSO (30 mL) at 70 $^{o}$C. 5-Hexynoic acid (0.7 mL, 6.2 mmol), copper (II) sulphate pentahydrate (130 mg, 0.52 mmol, in 1 mL of water) and sodium ascorbate (206 mg, 1.04 mmol, in 1 mL of water) were added and the mixture was stirred at 70 $^{o}$C for 24 hr. The polymer was precipitated in methanol (200 mL), filtered and washed three times with a mixture of ethanol / water solution (7:3) followed

by methanol. The polymer was then dried under reduced pressure in an oven at 50 $^{o}$C for 24 hr to give the product **5.5**, yield 79 % (1.23 g, 0.0027 mmol).

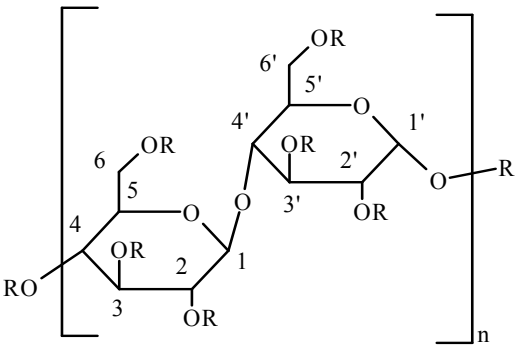


**5.5**

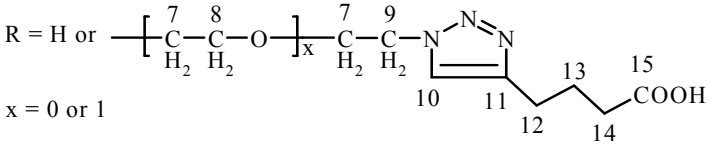


**Figure 5.5.** Structure of HEC clicked with 5-hexynoic acid with numerical assignment for NMR

Key resonances in solid-state $^{13}$C-NMR (101 MHz, cross polarisation technique): δ 176.03 ($C_{15}$), 147.39 ($C_{11}$), 125.31 ($C_{10}$), 51.54 ($C_9$), 40.58 ($C_{11}$), 33.82 ($C_{14}$), 25.55 ($C_{13}$), the rest of the resonances remained the same as the HEC backbone.
FTIR spectrum showed disappearance of azide peak at ~2090 cm$^{-1}$

### 5.2.9. Synthesis of HEC Clicked with Propargyl Amine 5.6

In a vial, azide functionalised HEC **5.1** (1 g, 0.0034 mmol; approximately 5.2 mmol of $N_3$ groups) was dissolved in DMSO (30 mL) at 70 $^{o}$C. Propargyl amine (0.4 mL, 6.2 mmol), copper (II) sulphate pentahydrate (130 mg, 0.52 mmol, in 1 mL of water) and sodium ascorbate (206 mg, 1.04 mmol, in 1 mL of water) were added and the mixture was stirred at 70 $^{o}$C for 24 hr. The polymer was precipitated in methanol (200 mL), filtered and washed three times with a mixture of ethanol / water solution (7:3) followed by methanol. The polymer was then dried under reduced pressure in an oven at 50 $^{o}$C for 24 hr to give the product **5.6**, yield 81 % (1 g, 0.0028 mmol).

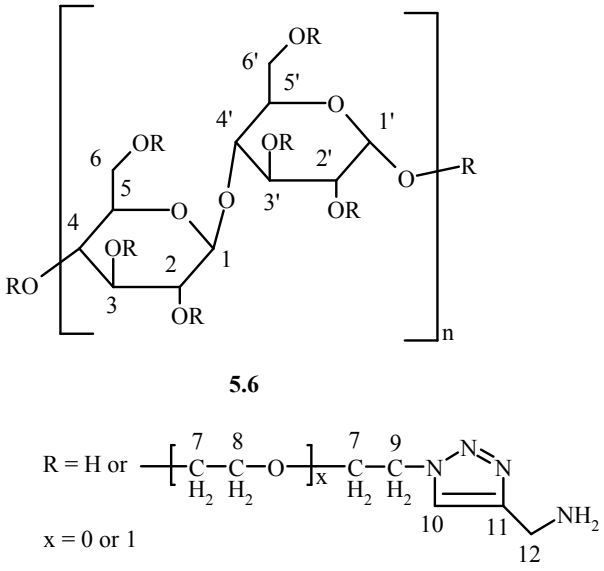


**5.6**




**Figure 5.6.** Structure of HEC clicked with propargyl amine with numerical assignment for NMR

Key resonances in solid-state $^{13}$C-NMR (101 MHz, cross polarisation technique): δ 144.26 ($C_{11}$), 125.46 ($C_{10}$), 51.59 ($C_9$), 41.21 ($C_{12}$), the rest of the resonances remained the same as the HEC backbone.

FTIR spectrum showed disappearance of azide peak at ~2090 $cm^{-1}$

### 5.2.10. Synthesis of HEC Clicked with a Mixture of 5-Hexynoic Acid and Propargyl Amine 5.7

In a vial, azide functionalised HEC **5.1** (0.5 g, 0.0017 mmol; approximately 2.6 mmol of $N_3$ groups) was dissolved in DMSO (20 mL) at 70 $^oC$. 5-Hexynoic acid (0.17 mL, 1.5 mmol), propargyl amine (0.1 mL, 1.5 mmol), copper (II) sulphate pentahydrate (65 mg, 0.26 mmol, in 1 mL of water) and sodium ascorbate (103 mg, 0.52 mmol, in 1 mL of water) were added and the mixture was stirred at 70 $^oC$ for 24 hr. The polymer was precipitated in methanol (200 mL), filtered and washed three times with a mixture of ethanol / water solution (7:3) followed by methanol. The polymer was then dried under reduced pressure in an oven at 50 $^oC$ for 24 hr to give the product **5.7**, (0.6 g).

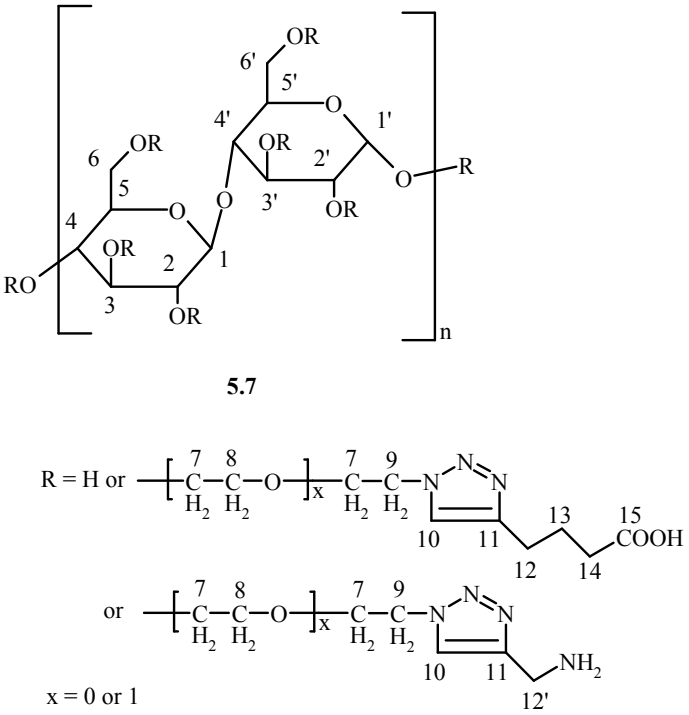

**5.7**

**Figure 5.7.** Structure of HEC clicked with a mixture of 5-hexynoic acid and propargyl amine with numerical assignment for NMR

Key resonances in solid-state $^{13}$C-NMR (101 MHz, cross polarisation technique): δ 174.80 ($C_{15}$), 147.59 ($C_{11}$), 123.11 ($C_{10}$), 51.54 ($C_9$), 40.58 ($C_{12}$), 35.39 ($C_{14}$), 25.60 ($C_{13}$), the rest of the resonances remained the same as the HEC backbone.

### 5.2.11. Attempted Synthesis of Mono-alkyne Terminated PDMS from Mono-hydroxy Terminated PDMS

A solution of mono-hydroxy terminated PDMS ($M_n$ ~1000) (20 g, 20 mmol) in dry THF (80 mL) was added dropwise at 0 $^oC$ to a slurry of NaH (720 mg, 30 mmol) in dry THF (20 mL) in a three-necked round-bottom flask, equipped with magnetic stirrer, thermometer, addition funnel and rubber seal septum, under $N_2$ atmosphere. The mixture was stirred for 30 min and propargyl bromide (80 % in toluene, 2.7 mL, 30 mmol) was added *via* a syringed at 0 $^oC$. The mixture was stirred at 0 $^oC$ for further 30 min and then at ambient temperature for 24 hr. The reaction mixture was filtered and DCM was added to the filtrate which was then washed with HCl (1N aqueous solution) followed by distilled water (x 3). The organic layer was dried over anhydrous $MgSO_4$ and the solvent was removed under reduced pressure to give a product (16 g).

### 5.2.12. Synthesis of Mono-alkyne Terminated PDMS from Mono-epoxy Terminated PDMS 5.8

In an ampoule equipped with a young's tap, mono-epoxy terminated PDMS (2 g, 2 mmol) and propargyl amine (PAm) (2 mL, 31 mmol) were mixed and the ampoule was sealed. The mixture was stirred in an oil bath at 83 $^{o}$C for 18 hr. The excess PAm was removed under reduced pressure to give the product **5.8**, yield 100 % (2.1 g, 2 mmol).

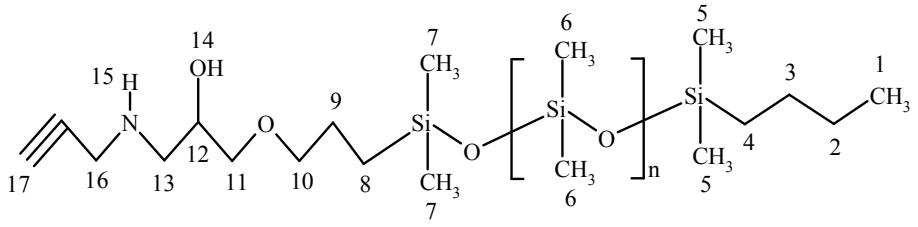


**5.8**

**Figure 5.8.** Structure of mono-alkyne terminated PDMS with numerical assignment for NMR

$^{1}$H-NMR (400 MHz, $CDCl_3$) δ 3.89 (m, 1H, $H_{12}$), 3.46 (m, 6H, $H_{10,11,16}$), 2.85 (dd, $J$ = 3.8 Hz, 12.0 Hz, 1H, $H_{13}$), 2.75 (dd, $J$ = 7.7 Hz, 12.1 Hz, 1H, $H_{13}$), 2.24 (t, $J$ = 2.43 Hz, 1H, $H_{17}$), 1.71 (bs, 1H, $H_{15}$), 1.63 (m, 2H, $H_9$), 1.33 (m, 4H, $H_{2,3}$), 0.91 (m, 3H, $H_1$), 0.55 (m, 4H, $H_{4,8}$), 0.08 (m, 72H, $H_{5,6,7}$).

### 5.2.13. Synthesis of HEC Clicked with PDMS Followed by Ethyl Propiolate 5.9

In a vial, azide functionalised HEC **5.1** (1 g, 0.0034 mmol; approximately 5.2 mmol of $N_3$ groups) was dissolved in DMSO (30 mL) at 70 $^{o}$C. Mono-alkyne terminated PDMS **5.8** (275 mg, 0.26 mmol), copper (II) sulphate pentahydrate (130 mg, 0.52 mmol, in 1 mL of water) and sodium ascorbate (206 mg, 1.04 mmol, in 1 mL of water) were added and the mixture was stirred at 70 $^{o}$C for 24 hr. Ethyl propiolate (0.53 mL, 5.2 mmol) was added and the mixture was stirred at 70 $^{o}$C for further 24 hr. The polymer was precipitated in ethanol (300 mL), filtered and washed three times with a mixture of ethanol / water solution (7:3) followed by ethanol. The polymer product was extracted with diethyl ether to remove any unreacted PDMS. The polymer was finally dried under reduced pressure in an oven at 50 $^{o}$C for 24 hr to give the product **5.9** (1.5 g).

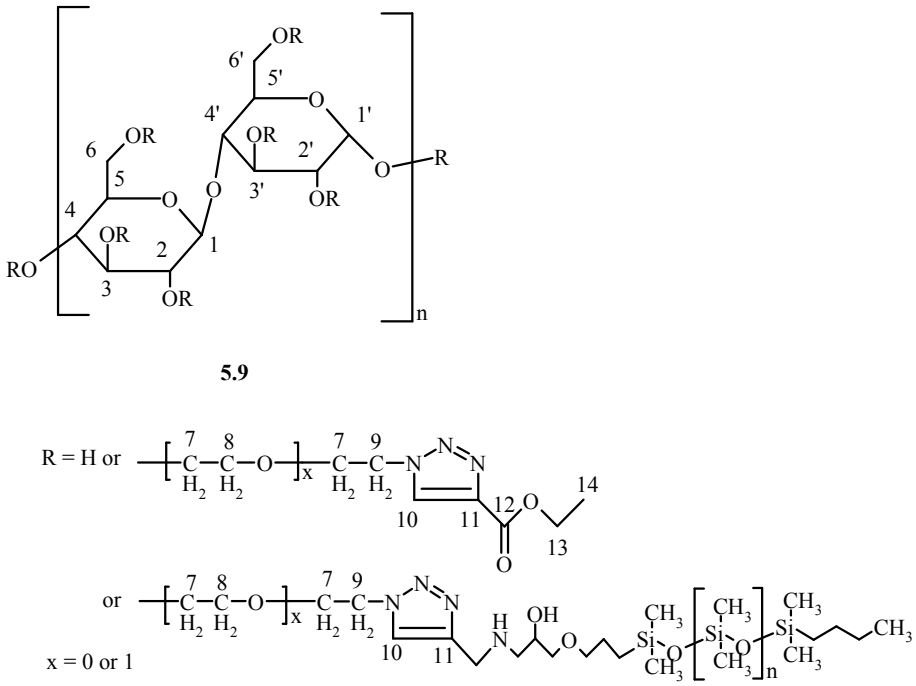

**Figure 5.9.** Structure of HEC clicked with PDMS and ethyl propiolate with numerical assignment for NMR

Key resonances in solid-state $^{13}$C-NMR (101 MHz, cross polarisation technique): δ 161.17 ($C_{12}$), 139.78 ($C_{11}$), 129.45 ($C_{10}$), 14.75 ($C_{14}$), 1.39 ($CH_3$-Si), the rest of the resonances remained the same as the HEC backbone.

Si elemental analysis (concentration of Si): theoretically (estimated calc.) = 6.4 %; practically found = 8.15 %

FTIR spectrum showed disappearance of azide peak at ~2090 cm$^{-1}$

### 5.2.14. Synthesis of HEC Clicked with PDMS Followed by Propargyl Amine 5.10

In a vial, azide functionalised HEC **5.1** (1 g, 0.0034 mmol; approximately 5.2 mmol of $N_3$ groups) was dissolved in DMSO (30 mL) at 70 $^{o}$C. Mono-alkyne terminated PDMS **5.8** (275 mg, 0.26 mmol), copper (II) sulphate pentahydrate (130 mg, 0.52 mmol, in 1 mL of water) and sodium ascorbate (206 mg, 1.04 mmol, in 1 mL of water) were added and the mixture was stirred at 70 $^{o}$C for 24 hr. Propargyl amine (0.33 mL, 5.2 mmol) was added and the mixture was stirred at 70 $^{o}$C for further 24 hr. The polymer was precipitated in ethanol (300 mL), filtered and washed three times with a mixture of ethanol / water solution (7:3) followed by ethanol. The polymer product was extracted with diethyl ether to remove any unreacted PDMS. The polymer was finally dried under reduced pressure in an oven at 50 $^{o}$C for 24 hr to give the product **5.10** (1.4 g).

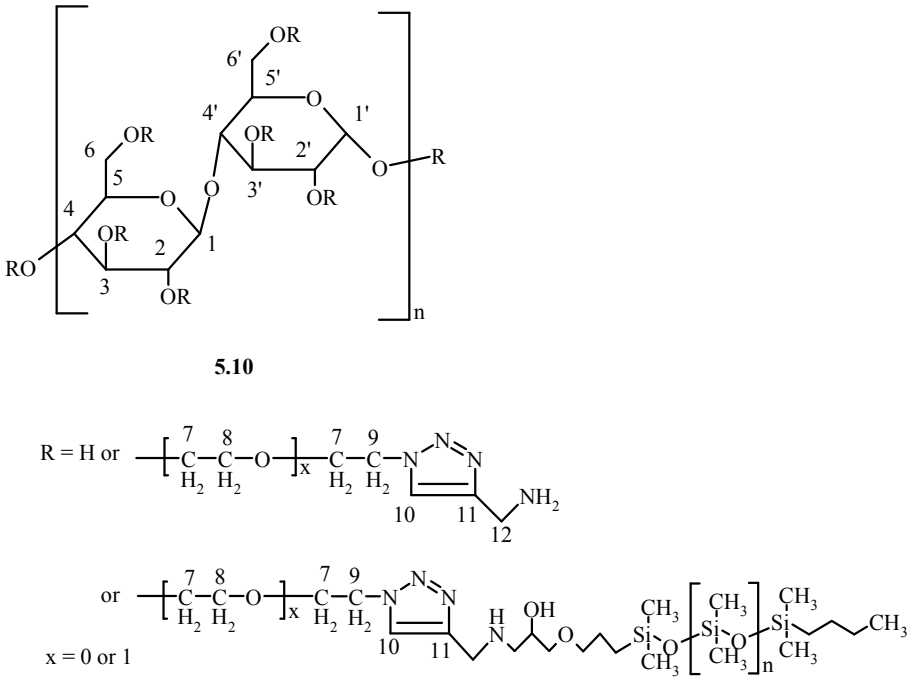

**5.10**

**Figure 5.10.** Structure of HEC clicked with PDMS and propargyl amine with numerical assignment for NMR

Key resonances in solid-state $^{13}$C-NMR (101 MHz, cross polarisation technique): δ 142.57 ($C_{11}$), 124.46 ($C_{10}$), 51.91 ($C_9$), the rest of the resonances remained the same as the HEC backbone.

Key resonances in solid-state $^{13}$C-NMR (101 MHz, direct polarisation technique): δ 40.26 ($C_{12}$), 1.49 ($CH_3$-Si), weak resonances for HEC backbone.

Si elemental analysis (concentration of Si): theoretically (estimated calc.) = 6.4 %; practically found = 4.02 %

FTIR spectrum showed disappearance of azide peak at ~2090 cm$^{-1}$

### 5.2.15. Synthesis of HEC Clicked with PDMS Followed by 5-Hexynoic Acid 5.11

In a vial, azide functionalised HEC **5.1** (1 g, 0.0034 mmol; approximately 5.2 mmol of $N_3$ groups) was dissolved in DMSO (30 mL) at 70 $^{o}$C. Mono-alkyne terminated PDMS **5.8** (275 mg, 0.26 mmol), copper (II) sulphate pentahydrate (130 mg, 0.52 mmol, in 1 mL of water) and sodium ascorbate (206 mg, 1.04 mmol, in 1 mL of water) were added and the mixture was stirred at 70 $^{o}$C for 24 hr. 5-Hexynoic acid (0.57 mL, 5.2 mmol) was added and the mixture was stirred at 70 $^{o}$C for further 24 hr. The polymer was precipitated in ethanol (300 mL), filtered and washed three times with a mixture of

ethanol / water solution (7:3) followed by ethanol. The polymer product was extracted with diethyl ether to remove any unreacted PDMS. The polymer was finally then dried under reduced pressure in an oven at 50 $^{o}$C for 24 hr to give the product **5.11** (1.3 g).

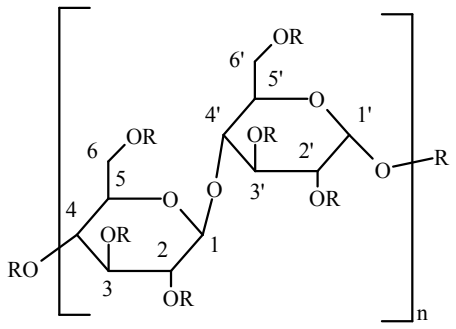

**5.11**

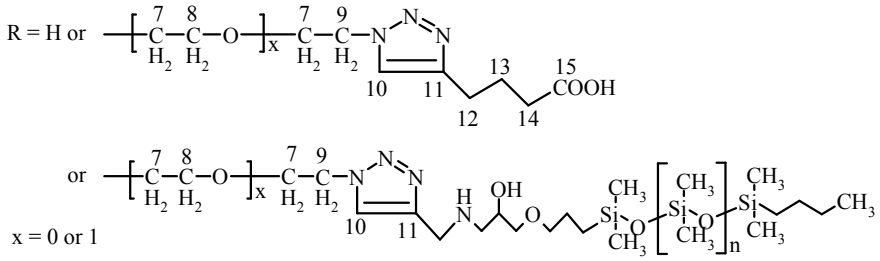

**Figure 5.11.** Structure of HEC clicked with PDMS and 5-hexynoic acid with numerical assignment for NMR

Key resonances in solid-state $^{13}$C-NMR (101 MHz, cross polarisation technique): δ 148.03 ($C_{11}$), 124.26 ($C_{10}$), 51.52 ($C_9$), 41.24 ($C_{12}$), 34.48, 25.96, the rest of the resonances remained the same as the HEC backbone.

Key resonances in solid-state $^{13}$C-NMR (101 MHz, direct polarisation technique): δ 51.42 ($C_9$), 40.75 ($C_{12}$), 33.89, 26.06, 18.42, 14.31, 1.49 ($CH_3$-Si), weak resonances for HEC backbone.

Si elemental analysis (concentration of Si): theoretically (estimated calc.) = 6.4%; practically found = 5.22%

FTIR spectrum showed disappearance of azide peak at ~2090 cm$^{-1}$

### 5.2.16. Synthesis of HEC Clicked with PDMS Followed by a Mixture of Propargyl Amine and 5-Hexynoic Acid 5.12

In a vial, azide functionalised HEC **5.1** (0.5 g, 0.0017 mmol; approximately 2.6 mmol of $N_3$ groups) was dissolved in DMSO (15 mL) at 70 $^{o}$C. Mono-alkyne terminated

PDMS **5.8** (137 mg, 0.13 mmol), copper (II) sulphate pentahydrate (65 mg, 0.26 mmol, in 0.5 mL of water) and sodium ascorbate (103 mg, 0.52 mmol, in 0.5 mL of water) were added and the mixture was stirred at 70 $^{o}$C for 24 hr. 5-Hexynoic acid (0.15 mL, 1.3 mmol) and propargyl amine (0.1 mL, 1.3 mmol) were added and the mixture was stirred at 70 $^{o}$C for further 24 hr. The polymer was precipitated in ethanol (200 mL), filtered and washed three times with a mixture of ethanol / water solution (7:3) followed by ethanol. The polymer product was extracted with diethyl ether to remove any unreacted PDMS. The polymer was finally dried under reduced pressure in an oven at 50 $^{o}$C for 24 hr to give the product **5.12** (0.65 g).

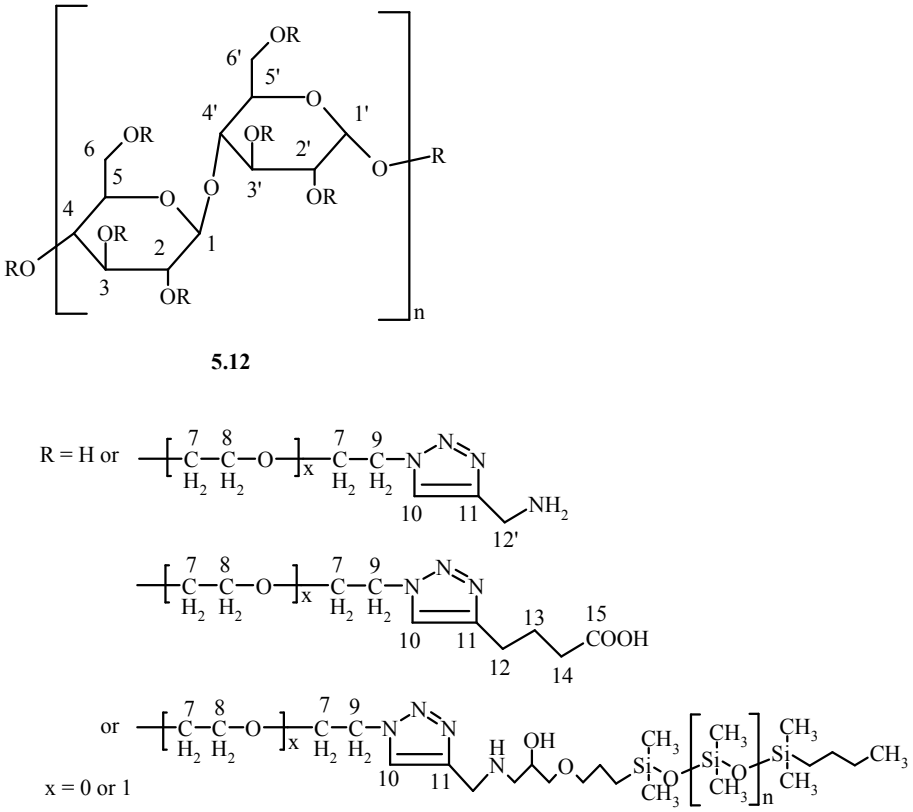


**Figure 5.12.** Structure of HEC clicked with PDMS and a mixture of propargyl amine and 5-hexynoic acid with numerical assignment for NMR

Key resonances in solid-state $^{13}$C-NMR (101 MHz, cross polarisation technique): δ 161.17 ($C_{15}$), 147.19 ($C_{11}$), 125.85 ($C_{10}$), 51.54 ($C_9$), 41.16 ($C_{12}$), 35.68 ($C_{14}$), 25.60 ($C_{13}$), 1.51 ($CH_3$-Si), the rest of the resonances remained the same as the HEC backbone.

Key resonances in solid-state $^{13}$C-NMR (101 MHz, direct polarisation technique): δ 1.41 ($CH_3$-Si), weak resonances for HEC backbone.

### 5.2.17. Synthesis of HEC Clicked with PLA Followed by Ethyl Propiolate 5.13

In a vial, azide functionalised HEC **5.1** (0.5 g, 0.0017 mmol; approximately 2.6 mmol of $N_3$ groups) was dissolved in DMSO (15 mL) at 70 $^oC$. Mono-alkyne end capped PLA (chapter 4) (0.5 g, 0.1 mmol), copper (II) sulphate pentahydrate (65 mg, 0.26 mmol, in 0.5 mL of water) and sodium ascorbate (103 mg, 0.52 mmol, in 0.5 mL of water) were added and the mixture was stirred at 70 $^oC$ for 24 hr. Ethyl propiolate (0.26 mL, 2.6 mmol) was added and the mixture was stirred at 70 $^oC$ for further 24 hr. The polymer was precipitated in ethanol (200 mL), filtered and washed three times with a mixture of ethanol / water solution (7:3) followed by ethanol. The polymer product was extracted with THF to remove any unreacted PLA. The polymer was finally then dried under reduced pressure in an oven at 50 $^oC$ for 24 hr to give the product **5.13** (1.1 g).

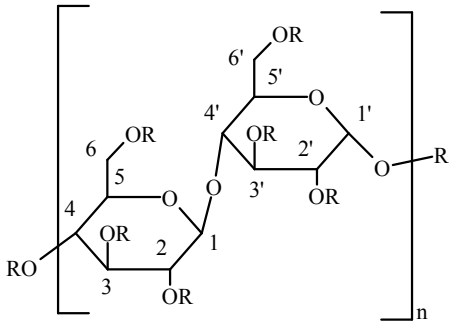


**5.13**

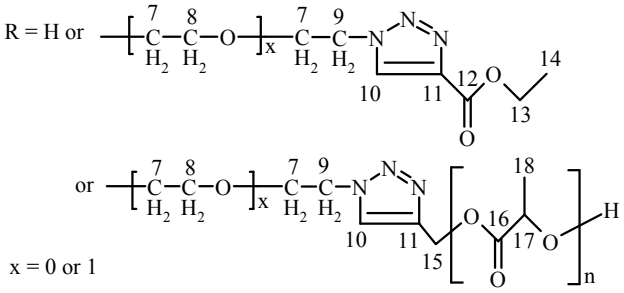


**Figure 5.13.** Structure of HEC clicked with PLA and ethyl propiolate with numerical assignment for NMR

Key resonances in solid-state $^{13}C$-NMR (101 MHz, cross polarisation technique): δ 169.88 ($C_{16}$), 161.10 ($C_{12}$), 140.41 ($C_{11}$), 130.79 ($C_{10}$), 51.64 ($C_9$), 41.17 ($C_{15}$), 17.17 ($C_{18}$), 14.96 ($C_{14}$), the rest of the resonances remained the same as the HEC backbone. FTIR spectrum showed disappearance of azide peak at ~2090 $cm^{-1}$

### 5.2.18. Synthesis of HEC Clicked with PCL Followed by Ethyl Propiolate 5.14

In a vial, azide functionalised HEC **5.1** (0.2 g, 0.00068 mmol; approximately 1.04 mmol of $N_3$ groups) was dissolved in DMSO (15 mL) at 70 $^oC$. Mono-alkyne end capped PCL (chapter 4) (0.2 g, 0.0174 mmol), copper (II) sulphate pentahydrate (26 mg, 0.104 mmol, in 0.5 mL of water) and sodium ascorbate (41 mg, 0.208 mmol, in 0.5 mL of water) were added and the mixture was stirred at 70 $^oC$ for 24 hr. Ethyl propiolate (0.11 mL, 1.04 mmol) was added and the mixture was stirred at 70 $^oC$ for further 24 hr. The polymer was precipitated in ethanol (200 mL), filtered off and washed three times with a mixture of ethanol / water solution (7:3) followed by ethanol. The polymer product was extracted with THF to remove any unreacted PCL. The polymer was finally then dried under reduced pressure in an oven at 50 $^oC$ for 24 hr to give the product **5.14** (0.43 g).

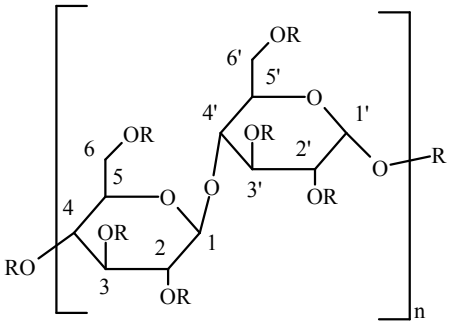

**5.14**

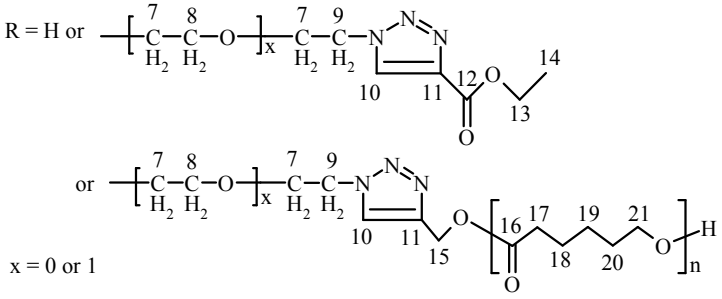


**Figure 5.14.** Structure of HEC clicked with PCL and ethyl propiolate with numerical assignment for NMR

Key resonances in solid-state $^{13}C$-NMR (101 MHz, cross polarisation technique): δ 173.82 ($C_{16}$), 161.10 ($C_{12}$), 139.75 ($C_{11}$), 131.53 ($C_{10}$), 65.74 ($C_{21}$), 51.83 ($C_9$), 41.10 ($C_{15}$), 33.62 ($C_{17}$), 29.61 ($C_{18,20}$), 26.18 ($C_{19}$), 14.83 ($C_{14}$), the rest of the resonances remained the same as the HEC backbone.

FTIR spectrum showed disappearance of azide peak at ~2090 $cm^{-1}$

### 5.2.19. Synthesis of Mono-alkyne Terminated PEG methyl ether 5.15

A solution of mono-hydroxy terminated PEG methyl ether ($M_n$ ~550) (10 g, 0.0182 mol) in dry THF (20 mL) was added dropwise to a slurry of NaH (458 mg, 19.1 mmol) in dry THF (20 mL) at 0 $^oC$ in a three-necked round-bottom flask, equipped with magnetic stirrer, thermometer, addition funnel and rubber seal septum, under $N_2$ atmosphere. The mixture was stirred for 30 min and propargyl bromide (80 % in toluene, 2.1 mL, 0.0191 mol) was added *via* a syringe. The mixture was kept at 0 $^oC$ for further 30 min and then stirred at ambient temperature for 24 hr. The reaction mixture was filtered and DCM was added to the filtrate which was then washed with HCl (1N aqueous solution) followed by distilled water (x 3). The organic layer was dried over anhydrous $MgSO_4$ and the solvent was removed under reduced pressure to give the product **5.15**, yield 89 % (9.315 g, 0.0162 mol).

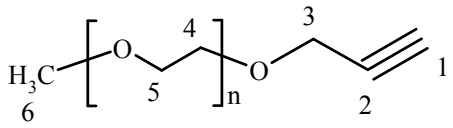


**5.15**

**Figure 5.15.** Structure of mono-alkyne terminated PEG methyl ether with numerical assignment for NMR

$^1H$ NMR (400 MHz, $CDCl_3$) δ 4.14 (d, $J$ = 2.4 Hz, 2H, $H_3$), 3.59 (m, 48H, $H_{4,5}$), 3.32 (s, 3H, $H_6$), 2.41 (t, $J$ = 2.4 Hz, 1H, $H_1$).

### 5.2.20. Synthesis of HEC Clicked with PEG 5.16

In a vial, azide functionalised HEC **5.1** (0.2 g, 0.00068 mmol; approximately 1.04 mmol of $N_3$ groups) was dissolved in DMSO (30 mL) at 70 $^oC$. Mono-alkyne terminated PEG methyl ether **5.15** (0.612 g, 1.04 mmol), copper (II) sulphate pentahydrate (26 mg, 0.104 mmol, in 0.5 mL of water) and sodium ascorbate (41 mg, 0.208 mmol, in 0.5 mL of water) were added and the mixture was stirred at 70 $^oC$ for 24 hr. The polymer was precipitated in ethanol (150 mL), filtered and washed three times with a mixture of ethanol / water solution (9:1) followed by ethanol. The polymer was finally then dried under reduced pressure in an oven at 50 $^oC$ for 24 hr to give the product **5.15**, yield 78 % (0.63 g).

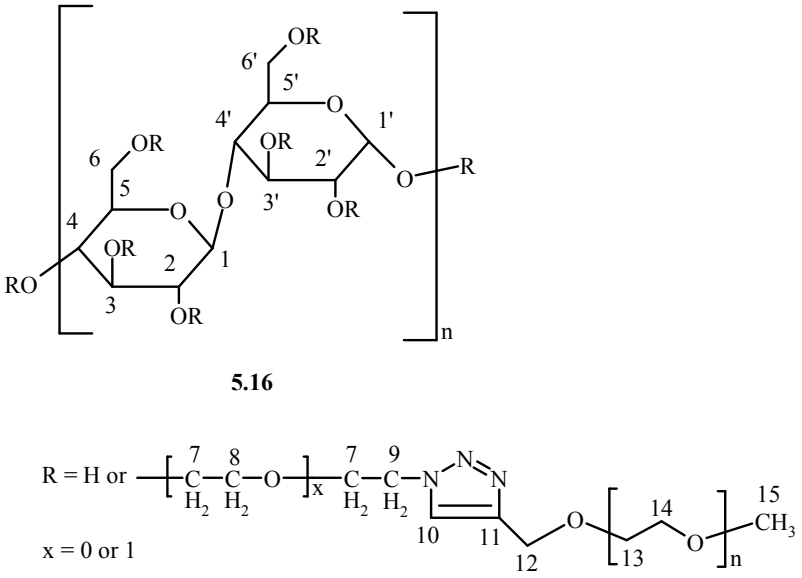

**5.16**

**Figure 5.16.** Structure of HEC clicked with PEG with numerical assignment for NMR

Key resonances in $^{1}$H-NMR (500 MHz, DMSO-$d_6$, at 80 $^{o}$C): δ 7.95 ($H_{10}$).

Key resonances in $^{13}$C-NMR (126 MHz DMSO-$d_6$, at 80 $^{o}$C): δ 144.88 ($C_{11}$), 124.66 ($C_{10}$), 64.48 ($C_{13,14}$), 58.61 ($C_{15}$), 50.14 ($C_9$), 40.71 ($C_{12}$), the rest of the resonances remained the same as the HEC backbone.

FTIR spectrum showed disappearance of azide peak at ~2090 cm$^{-1}$

## 5.3. Results and Discussion

### 5.3.1. The Choice of HEC

Akzo Nobel is currently supplying a personal care product based on quaternary ammonium modified HEC with $M_w$ of 250,000 $gmol^{-1}$ which also contains some physically mixed polydimethylsiloxane (PDMS). We initially carried out modification reactions on HEC with $M_w$ = 90,000 $gmol^{-1}$ in order to follow the reactions by NMR. However, we faced some difficulties during the recovery process of the final products due to their good solubility behaviour (water and DMSO). We therefore decided to use HEC with $M_w$ of ~250,000 $gmol^{-1}$.

### 5.3.2. Azide Functionalisation of HEC

The azidation of HEC was performed for the first time in a one pot reaction following the work reported by Cimecioglu et al.[26] and Shey et al.[27]

Cimecioglu et al.[28] found that lithium salts such as LiBr and LiCl can assist in the dissolving of polysaccharides in DMF. They also found the same improvement in the dissolution by using lithium azide in the azide derivatisation of amylose and pullulan.[26] However, because lithium salts are very hygroscopic, the use of these salts resulted in low conversions. Recently, Shey et al. suggested the use of sodium azide as an alternative source of azide in the azidation reaction of starch.[27]

The selective azidation reaction of the primary hydroxyl groups of HEC using sodium azide was successfully carried out as shown in Scheme 5.1. Sodium azide facilitated the dissolution of HEC in DMF. Homogeneous solution was obtained within 1 hr at 100°C, and this remained clear upon cooling to ambient temperature. Treatment of this solution with $Ph_3P/CBr_4$, caused a slight exotherm and a colour change from off-white to brownish yellow. The reaction mixture otherwise remained homogeneous throughout.

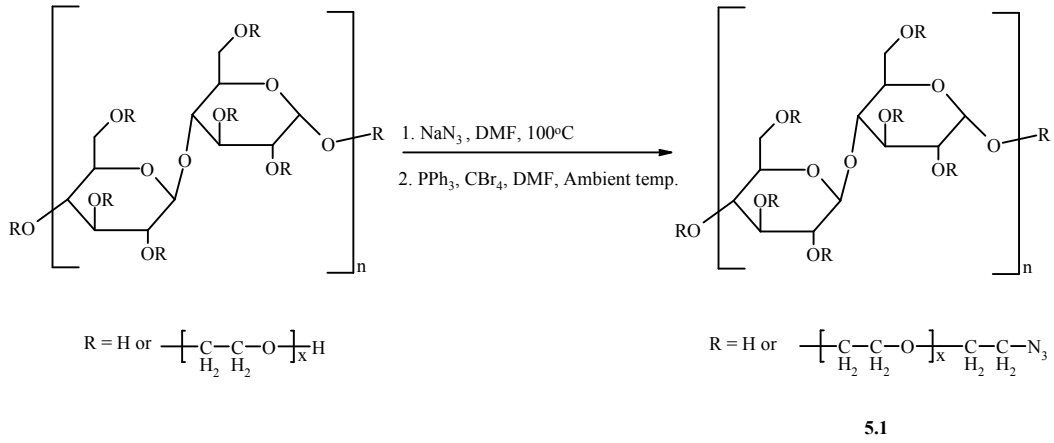


5.1

**Scheme 5.1.** Synthesis of fully azide functionalised HEC

It is believed that the one pot azidation reaction proceeds *via* a mechanistic pathway similar to the well-established Appel reaction.[29] The general postulated mechanism for this reaction is presented in Scheme 5.2.

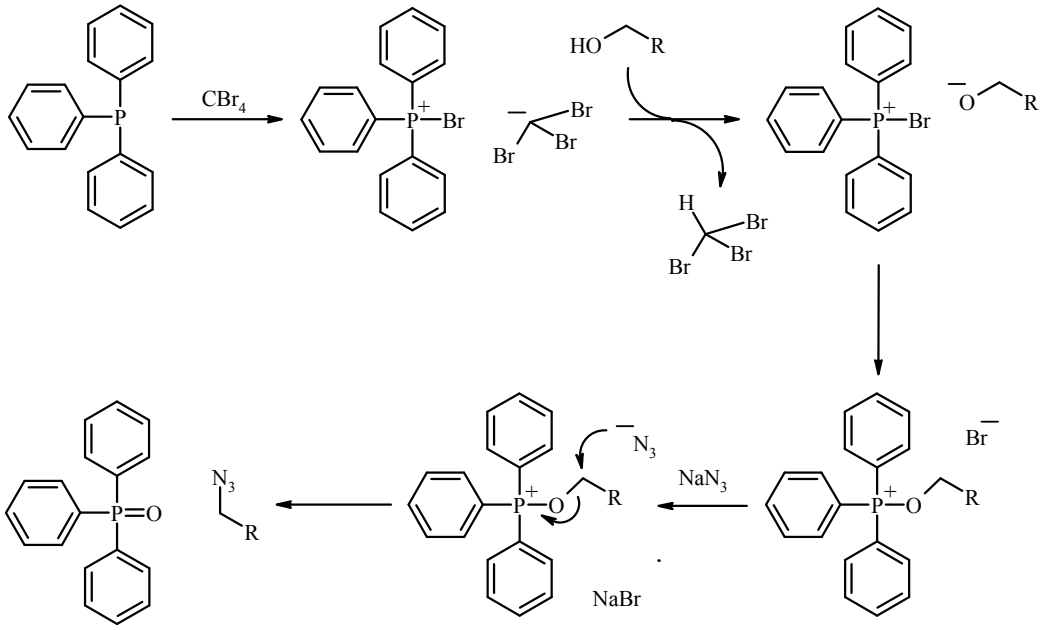


**Scheme 5.2.** Postulated mechanism for one pot azidation reaction

The FT-IR spectra of the azide functionalised HEC **5.1** (Fig. 5.17.B) compared to that of HEC (Fig. 5.17.A) showed a strong absorption at 2090 $cm^{-1}$, corresponding to C-$N_3$ stretching vibration. Moreover, there is a dramatic decrease in the intensity of the broad OH peak at ~3360 $cm^{-1}$, indicating the qualitative decrease of the hydroxyl functionalities of the HEC.

The elemental analysis obtained for HEC and product **5.1** were inaccurate, due to the presence of significant amount of moisture in the samples, which was difficult to remove even after extensive drying in oven at reduced pressure. However, the elemental analysis of **5.1** showed the existence of a high level of nitrogen in the sample.

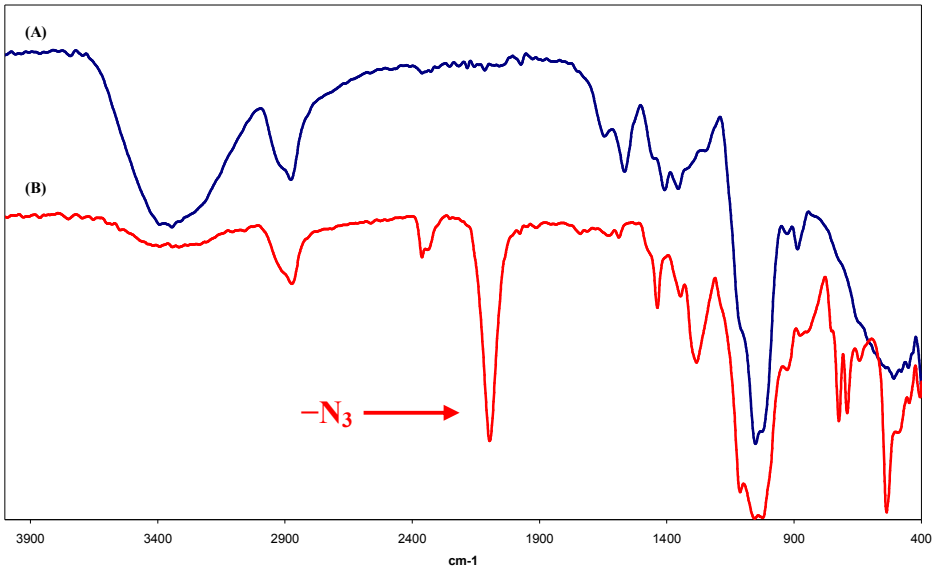


**Figure 5.17.** FT-IR spectra of (A) HEC and (B) fully azide functionalised HEC **5.1**

The $^{13}$C-NMR spectrum of the used HEC was fully assigned[30] (Fig. 5.3.A). The $^{13}$C-NMR spectra of **5.1** (Fig. 5.18.B) compared to that of HEC (Fig. 5.18.A) showed a shift to lower δ-value for the $CH_2$ peak ($C_9$) from 60.70 to 50.87 ppm, indicating the attachment of the azide group to the $CH_2$. The absence of any residual peak for the $CH_2$ attached to OH also indicated the full azide functionalisation of HEC.

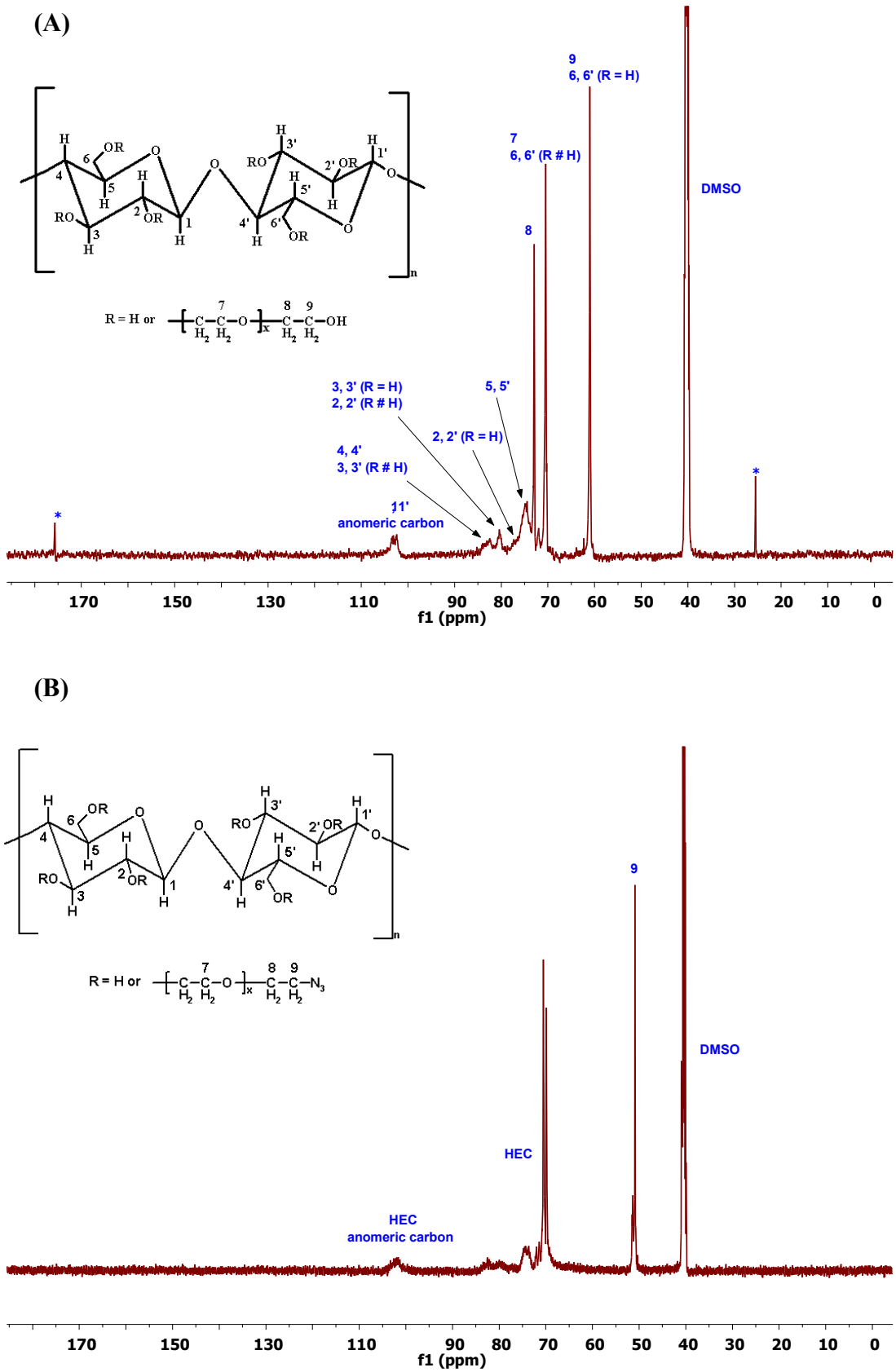


**Figure 5.18.** $^{13}$C-NMR spectra of (A) HEC and (B) fully azide functionalised HEC **5.1** in DMSO-$d_6$ at 80 $^{o}$C

The $^{1}$H-NMR spectrum of **5.1** showed a small peak at 7.78 ppm believed to be due to trace amount of triphenylphosphine oxide. This contaminant was very hard to remove completely, despite repeated reprecipitations.

The control of the degree of azidation of HEC was investigated by varying the molar equivalents of $NaN_3$, $Ph_3P$ and $CBr_4$. $^{13}$C-NMR spectroscopy was used to measure the approximate degree of conversion from primary alcohol to azide functionality. The approximate percentage of azidation was calculated from the ratios of the integration of the unreacted $–CH_2–OH$ peak to the new formed $–CH_2–N_3$ peak (Figure 5.19). Although, the integration in $^{13}$C-NMR spectra is not common, it is possible to compare the area under the peaks for the carbons of the same number of hydrogens.

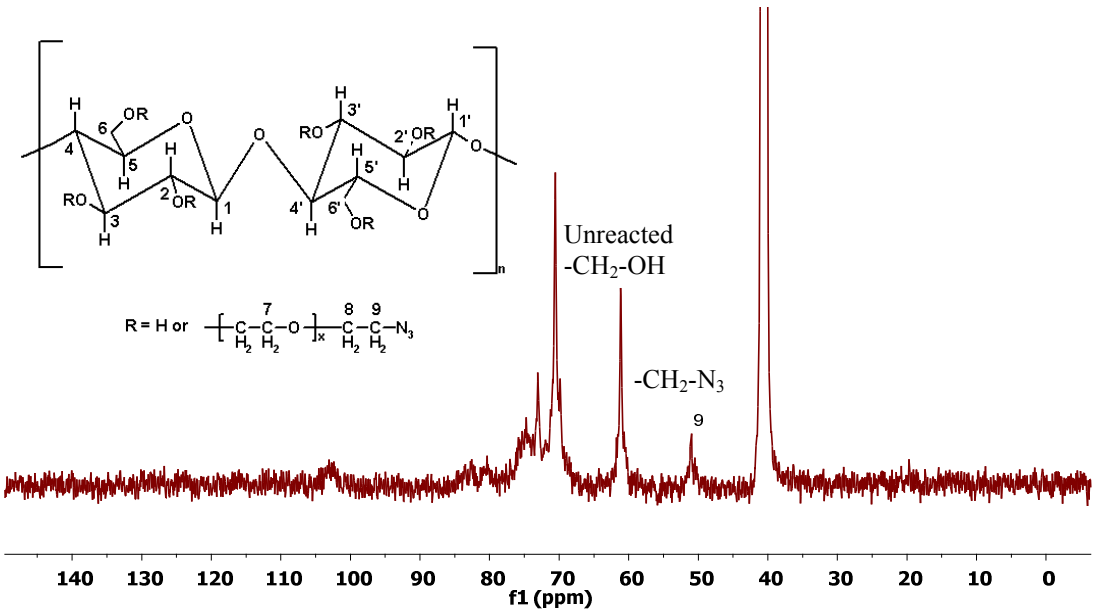


**Figure 5.19.** $^{13}$C-NMR spectrum of azide functionalised HEC with 20 % conversion to azide functionality in DMSO-$d_6$ at 80 $^{o}$C

Table 5.1 shows the effect of the molar excess of the reagents per the HEC primary OH groups on the degree of azidation. The results showed that the complete azide functionalisation was achieved by treatment with 4-fold molar excess of $NaN_3$ and 2-fold molar excess of $Ph_3P$ and $CBr_4$, each. The excess of $NaN_3$ was needed to assist the solubility as discussed earlier and to compensate the loss due to presence of moisture. The results also showed that the degree of azidation is directly proportional to the molar quantities of the reagents. Furthermore, the presented values were not reproducible. This was not too surprising because the calculated molar quantity of the primary OH groups on HEC was approximate. Moreover, it was very difficult to keep

the system away from moisture even with drying of HEC in oven at 110 $^{o}$C under reduced pressure before usage. It is believed that this moisture deactivates the intermediates and hence affects the degree of conversion.

**Table 5.1.** Effect of the molar quantities of reagents on the degree of azidation

| **Molar excess / the HEC primary OH groups** | | | **Degree of azidation %** |
|---|---|---|---|
| **$NaN_3$** | **$Ph_3P$** | **$CBr_4$** | |
| 4 | 2 | 2 | 100 |
| 2 | 1 | 1 | 25 |
| 1 | 0.5 | 0.5 | 11 |
| 1 | 0.25 | 0.25 | 0 |

### 5.3.3. Application of Click Chemistry on HEC

#### 5.3.3.1. Synthesis of HEC with Neutral Compositions

Click chemistry was utilised to introduce different neutral functionalities on HEC backbone such as ester, siloxyl, acrylate and epoxide groups.

##### 5.3.3.1.1. Synthesis of HEC with Ester Functionality

Click reaction between fully azide functionalised HEC **5.1** and ethyl propiolate was successfully carried out in DMSO containing $CuSO_4.5H_2O$ and sodium ascorbate at 70 $^{o}$C for 24 hr to afford the product **5.2**, Scheme 5.3.

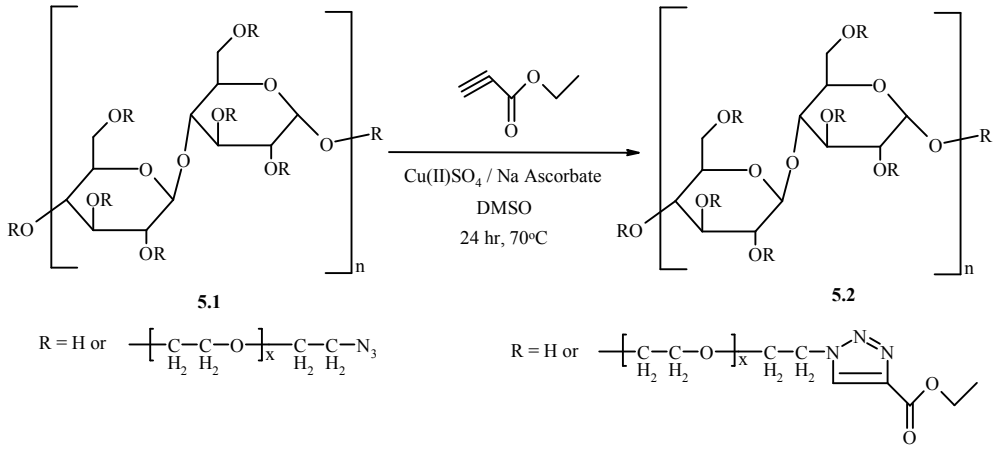


**Scheme 5.3** Synthesis of HEC with ester functionality

$^{13}$C-NMR spectrum of **5.2** showed the appearance of two new peaks at 139.62 and 129.71 ppm, assigned to the triazole carbons ($C_{11}$ and $C_{10}$), respectively. It also showed peaks due to the carbons of ethyl ester functional group ($C_{12}$, $C_{13}$ and $C_{14}$) (Fig. 5.20). Moreover, the peaks due to the HEC backbone carbons were observed in the same regions and no other unassignable peaks were seen in the spectrum.

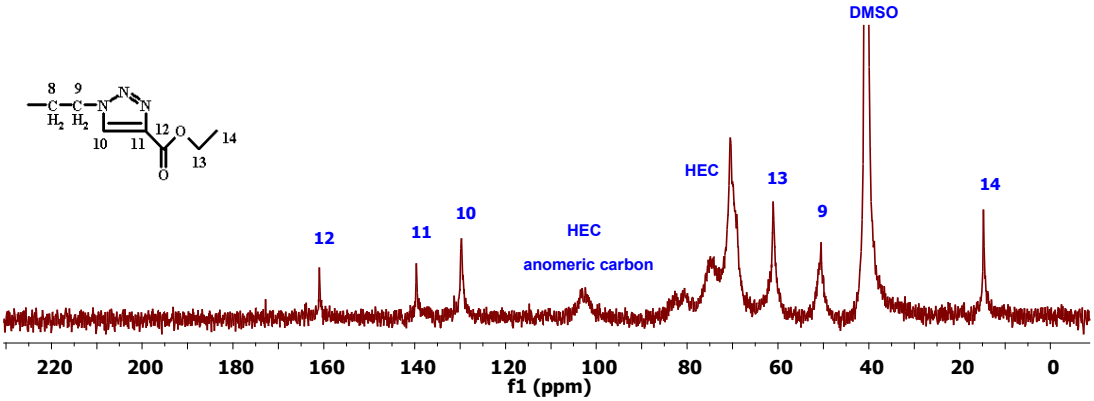


**Figure 5.20.** $^{13}$C-NMR spectrum of HEC with ester functionality **5.2** in DMSO-$d_6$ at 80 $^{o}$C

The IR spectra of **5.2** (Fig. 5.21.B) compared to that of **5.1** (Fig. 5.21.A) showed the complete disappearance of the azide peak at 2090 $cm^{-1}$, confirming the complete conversion to the clicked product. It also showed appearance of a new peak at 1718 $cm^{-1}$, assigned to the carbonyl group of ethyl ester functionality on HEC.

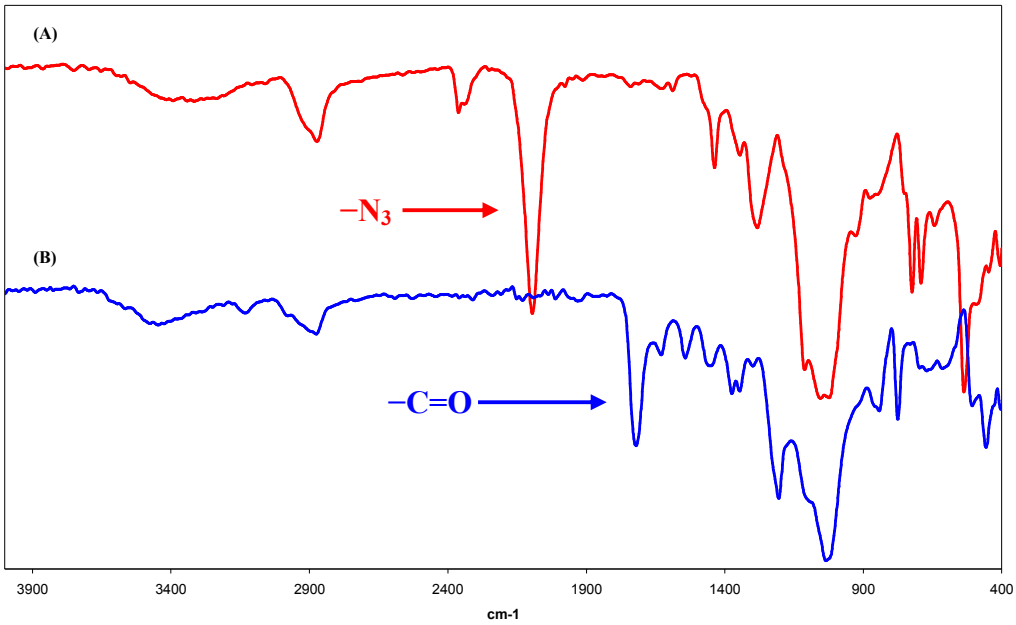


**Figure 5.21.** FT-IR spectra of (A) fully azide functionalised HEC **5.1** and (B) HEC with ester functionality **5.2**

### 5.3.3.1.2. Synthesis of HEC with Siloxyl Functionality

Click reaction between fully azide functionalised HEC **5.1** and 3-trimethylsiloxy-1-propyne was successfully carried out in DMSO containing $CuSO_4.5H_2O$ and sodium ascorbate at 70 $^oC$ for 24 hr to afford the product **5.3** (Scheme 5.4).

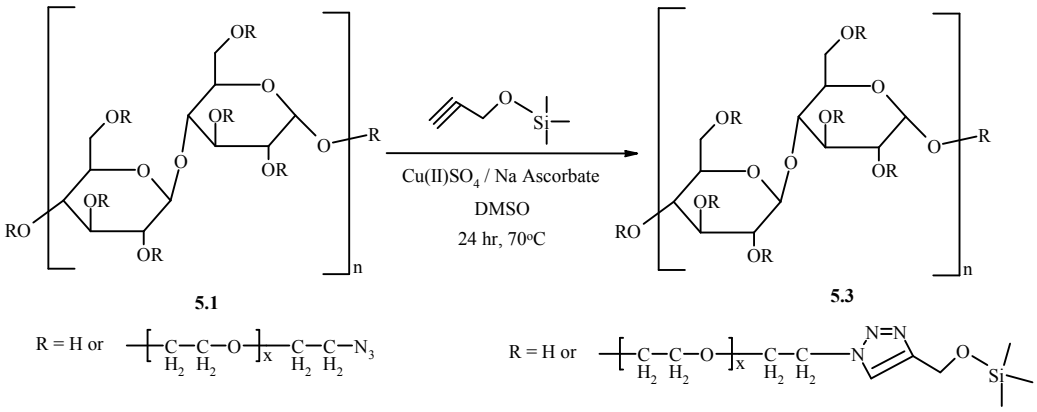


**Scheme 5.4.** Synthesis of HEC with siloxyl functionality

$^{13}C$-NMR spectrum of **5.3** showed appearance of two new peaks at 148.90 and 123.78 ppm, assigned to the triazole carbons ($C_{11}$ and $C_{10}$), respectively. It also showed a peak due to the carbon of the siloxyl functional group ($C_{12}$), Fig. 5.22. Moreover, the peaks due to the HEC backbone carbons were observed in the same regions and no

other unassignable peaks were seen in the spectrum. It was also noticed that there were no peaks for the methyl groups attached to Si atom. This is believed to be due to the hydrolysis of siloxyl groups producing alkyl alcohol and silyl alcohol. Silicon – oxygen bond in silyl ethers are known to hydrolyse under mild conditions, rendering them useful protecting groups for alcohols in organic synthesis.[31, 32]

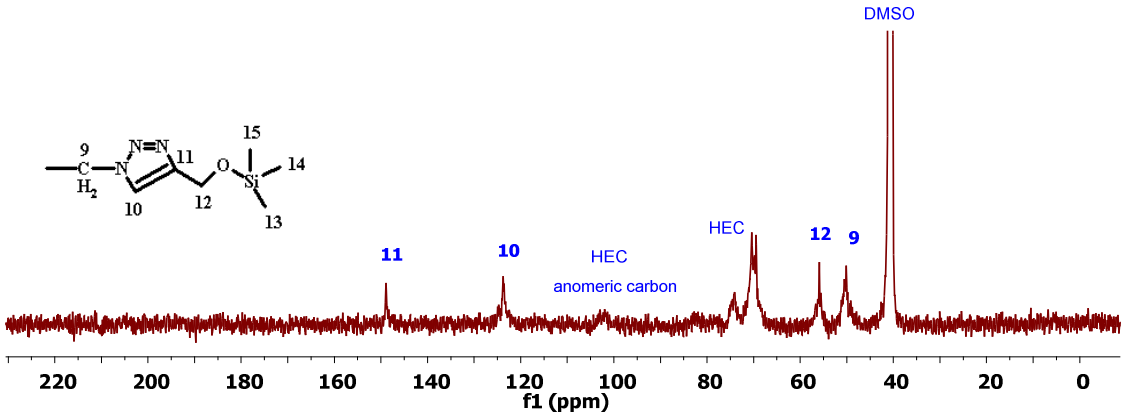


**Figure 5.22.** $^{13}$C-NMR spectrum of HEC with siloxyl functionality **5.3** in DMSO-$d_6$ at 80 $^{o}$C

### 5.3.3.1.3. Synthesis of HEC with Acrylate Functionality

Click reaction between fully azide functionalised HEC **5.1** and propargyl acrylate was successfully carried out in DMSO containing $CuSO_4.5H_2O$ and sodium ascorbate at 70 $^{o}$C for 24 hr to afford the product **5.4**, Scheme 5.5.

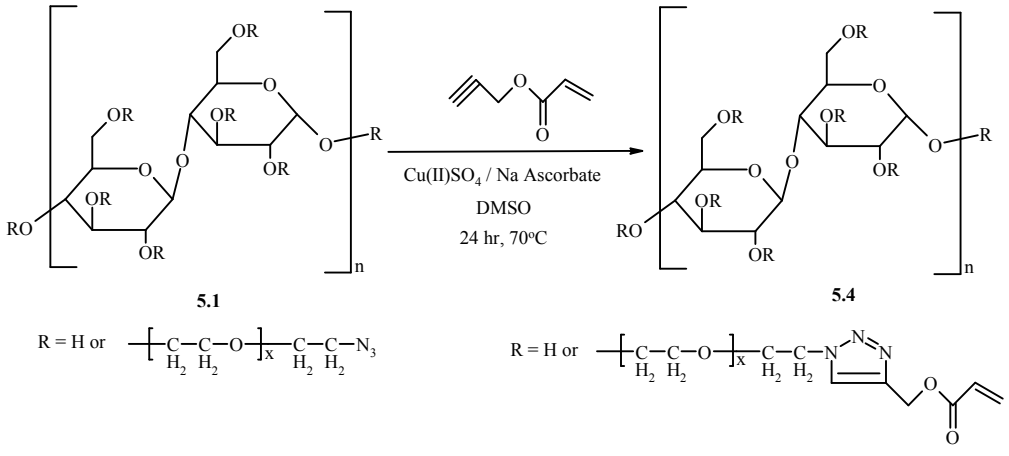


**Scheme 5.5.** Synthesis of HEC with acrylate functionality

The isolated product **5.4** was insoluble in all solvents and therefore it was not possible to run solution NMR. Solid-state $^{13}$C-NMR and FT-IR spectroscopies were used to characterise the product.

The solid-state $^{13}$C-NMR spectrum of **5.4** showed appearance of two new peaks at 142.57 and 128.29 ppm, assigned to the triazole carbons ($C_{11}$ and $C_{10}$), respectively. It also showed two other new peaks at 165.99 and 58.77 ppm due to the carbons of the acrylate functional group ($C_{13}$ and $C_{12}$), respectively (Fig. 5.23). Moreover, the peaks due to the HEC backbone carbons were observed in the same regions and no other unassignable peaks were seen in the spectrum. There were no peaks observed for the acrylate double bond (typically appear at ~127 – 131 ppm). This was believed to be due to one or a combination of the following two reasons: (1) the peaks due to the acrylate double bond were hidden under those of the triazole double bond, and/or (2) the relative high temperature (70 $^{o}$C) and long reaction time (24 hr) for the Click reaction promoted the cross-linking of the acrylate functionalities on HEC chains, which, presumably, explained the poor solubility of the product.

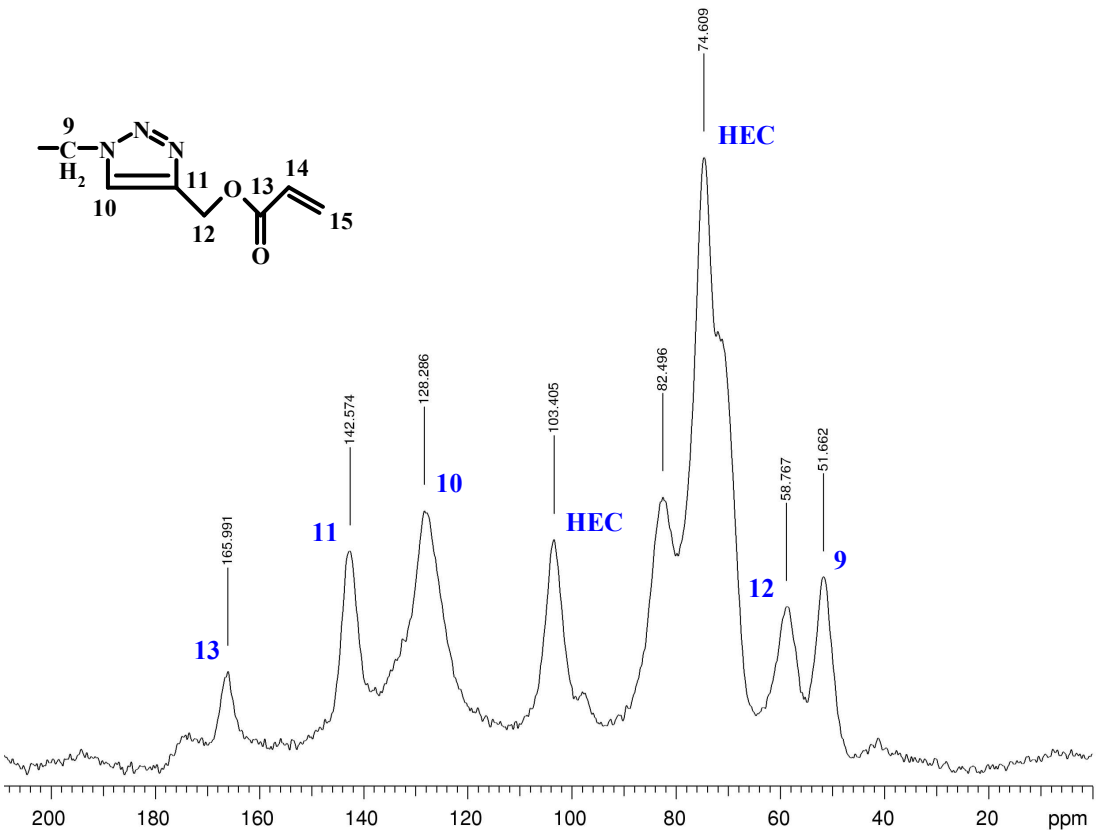


**Figure 5.23.** Solid-state $^{13}$C-NMR (CP exp.) spectrum of HEC with acrylate functionality **5.4**

The IR spectra of **5.4** (Fig. 5.24.B) compared to that of **5.1** (Fig. 5.24.A) showed the complete disappearance of the azide peak at 2090 $cm^{-1}$, confirming the complete conversion to the clicked product. It also showed the appearance of a new peak at 1714 $cm^{-1}$, assigned to the carbonyl group of the acrylate functionality on HEC.

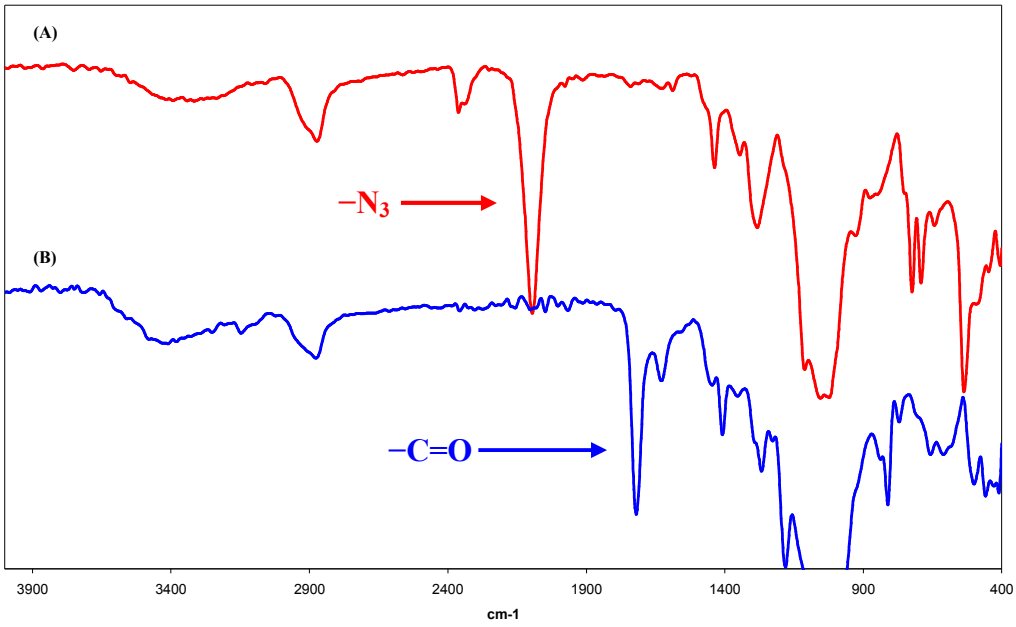


**Figure 5.24.** FT-IR spectra of (A) fully azide functionalised HEC **5.1** and (B) HEC with acrylate functionality **5.4**

#### 5.3.3.1.4. Synthesis of HEC with Epoxy Functionality

Click reaction between fully azide functionalised HEC **5.1** and glycidyl propargyl ether (GPE) was attempted in DMSO containing $CuSO_4.5H_2O$ and sodium ascorbate at 70 $^oC$ for 24 hrs, Scheme 5.6. The anticipated product was not isolated due to the good solubility behaviour of the product. The product did not precipitate from the reaction mixture and it was practically difficult to remove the large amount of the used solvent (DMSO). Therefore, it was assumed that under the used reaction conditions, the epoxide rings opened to produce the alcohol derivatives, which seemingly enhanced the solubility of the product. Although it is believed that HEC with epoxy functionality has a great potential interest, it was chosen to not carry out further investigations at that stage due to the time limit of the project.

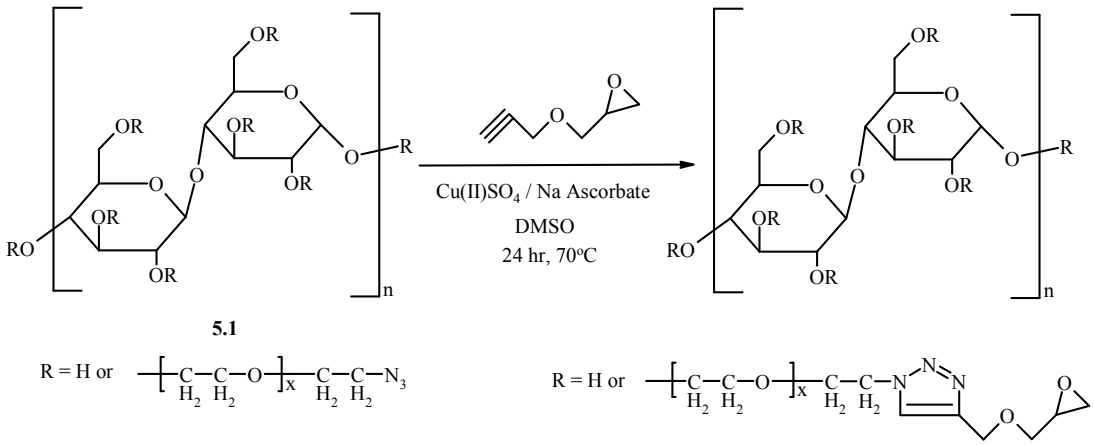


**Scheme 5.6.** Attempted synthesis of HEC with epoxy functionality

### 5.3.3.2. Synthesis of HEC with Ionic Compositions

Different ionic compositions of HEC were prepared by introducing electrolytic groups on the HEC backbone. These groups will dissociate in aqueous solutions (water), making the HEC chains charged. The resultant materials are classified as polyelectrolytes which are divided into anionic and cationic types depending on the produced charges on the polymer. Moreover, the ones which bear both cationic and anionic groups, are called zwitter-ionic polyelectrolytes or polyampholytes.[33]

#### 5.3.3.2.1. Anionic Composition

HEC with carboxylic acid functionality was successfully synthesised *via* Click reaction between fully azide functionalised HEC **5.1** and 5-hexynoic acid in DMSO containing $CuSO_4.5H_2O$ and sodium ascorbate at 70 $^oC$ for 24 hr to afford the product **5.5**, Scheme 5.7.

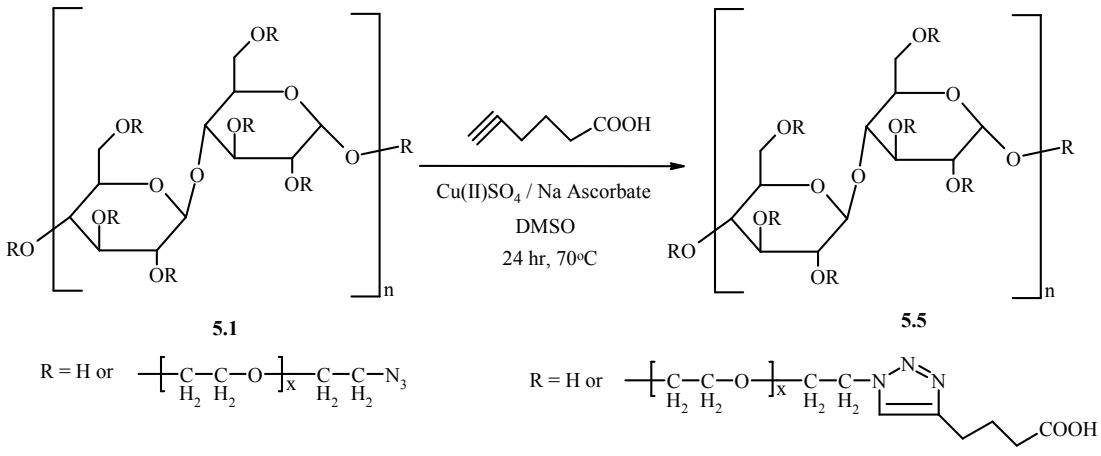


**Scheme 5.7.** Synthesis of HEC with carboxylic acid functionality

Because various interactions between the modified polymer chains may exist, the low solubility behaviour of the modified HEC limited the use of solution NMR under the standard conditions. However, it has been reported that treatment with 2% aqueous solution of acetic acid, enhances the solubility of amylose derivative, as an example of polysaccharides. This allowed the use of 2% of $CD_3COOD$ in $D_2O$ as an alternative NMR solvent.[28] Although the same enhancement in the solubility behaviour of the modified HEC products was observed when treated with 2% aqueous solution of acetic acid, but it was chosen to use, along with the FT-IR, solid-state $^{13}$C-NMR spectroscopy for easier accessibility and consistency of the characterisation tool.

Solid-state $^{13}$C-NMR spectrum of **5.5** showed the appearance of two new peaks at 147.39 and 125.31 ppm, assigned to the triazole carbons ($C_{11}$ and $C_{10}$), respectively. It also showed peaks due to the carbons of the carboxylic acid functionality ($C_{12}$, $C_{13}$, $C_{14}$ and $C_{15}$), Fig. 5.25. Moreover, the peaks due to the HEC backbone carbons were observed in the same regions and no other unassignable peaks were seen in the spectrum.

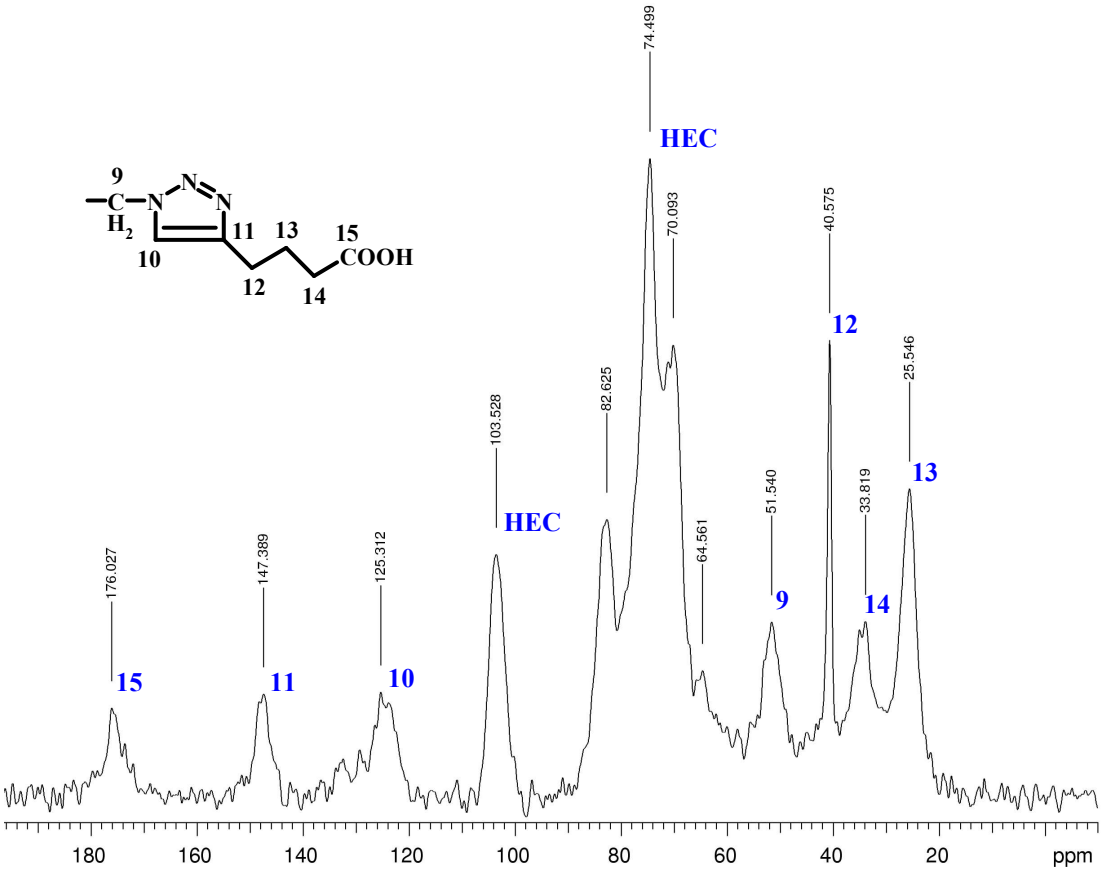


**Figure 5.25.** Solid-state $^{13}$C-NMR (CP exp.) spectrum of HEC with carboxylic acid functionality **5.5**

The IR spectra of **5.5** (Fig. 5.26.B) compared to that of **5.1** (Fig. 5.26.A) showed the complete disappearance of the azide peak at 2090 $cm^{-1}$, confirming the quantitative conversion to the clicked product. It also showed appearance of a new peak at 1707 $cm^{-1}$, assigned to the carbonyl group of the carboxylic acid functionality on HEC.

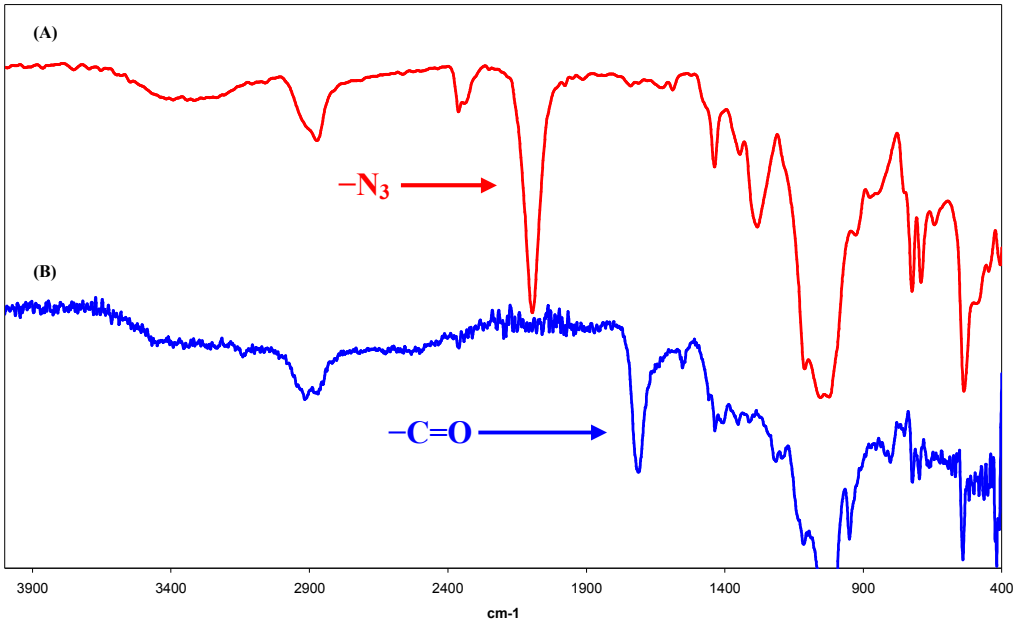


**Figure 5.26.** FT-IR spectra of (A) fully azide functionalised HEC **5.1** and (B) HEC with carboxylic acid functionality **5.5**

### 5.3.3.2.2. Cationic Composition

HEC with primary amine functionality was successfully synthesised *via* Click reaction between fully azide functionalised HEC **5.1** and propargyl amine in DMSO containing $CuSO_4.5H_2O$ and sodium ascorbate at 70 $^oC$ for 24 hr to afford the product **5.6**, Scheme 5.8.

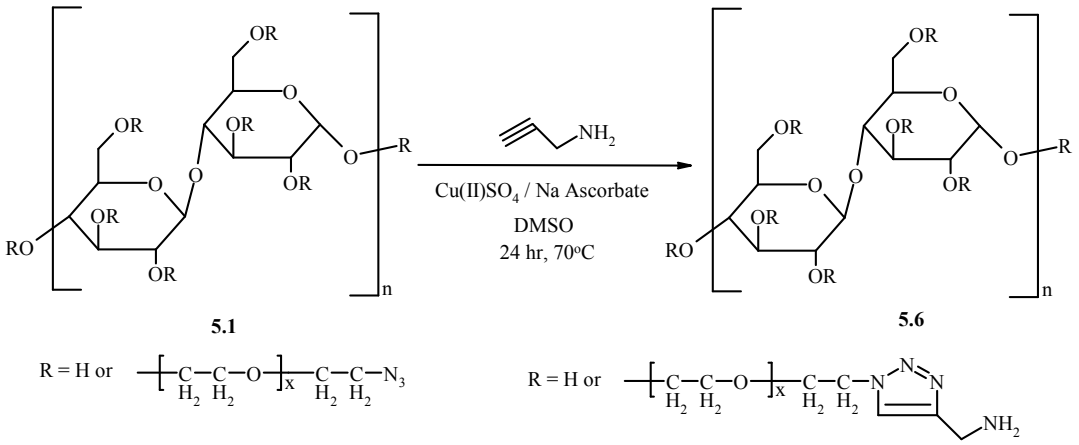


**Scheme 5.8.** Synthesis of HEC with primary amine functionality

Solid-state $^{13}$C-NMR spectrum of **5.6** showed appearance of two new peaks at 144.26 and 125.46 ppm, assigned to the triazole carbons ($C_{11}$ and $C_{10}$), respectively. It also showed a peak due to the carbon of the primary amine functionality ($C_{12}$), Fig. 5.27. Moreover, the peaks due to the HEC backbone carbons were observed in the same regions.

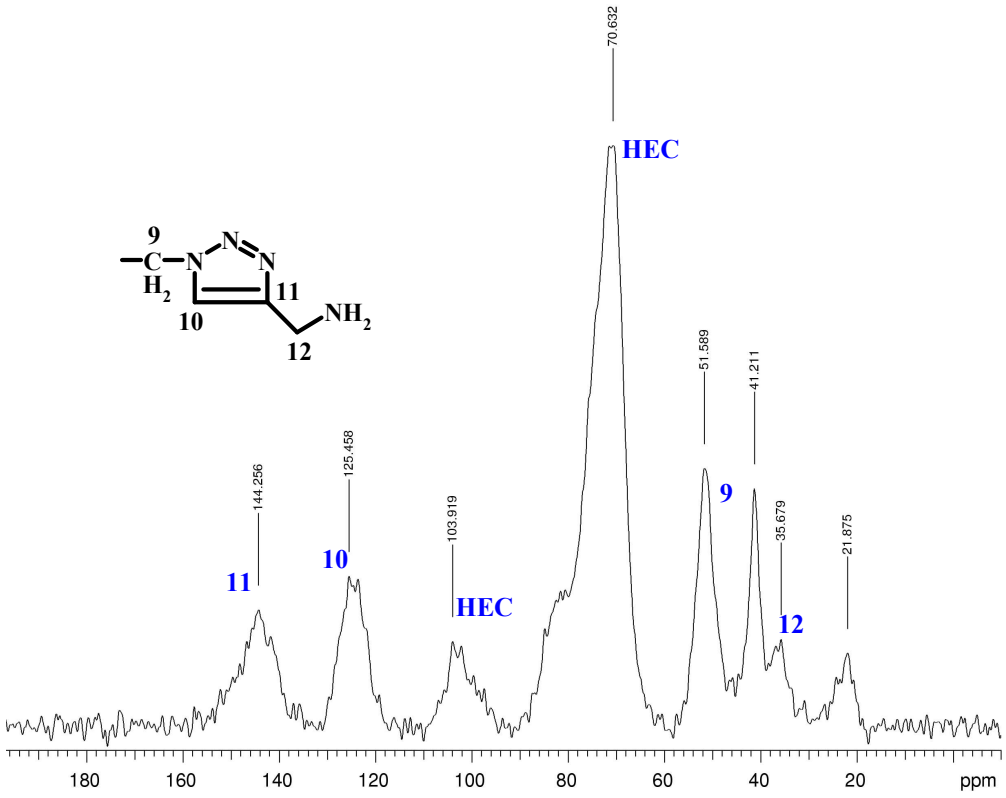


**Figure 5.27.** Solid-state $^{13}$C-NMR (CP exp.) spectrum of HEC with primary amine functionality **5.6**

The IR spectra of **5.6** (Fig. 5.28.B) compared to that of **5.1** (Fig. 5.28.A) showed the complete disappearance of the azide peak at 2090 $cm^{-1}$, confirming the complete conversion to the clicked product. Moreover, it showed a new peak at 1635 $cm^{-1}$, assigned to the primary amine functionality on HEC.

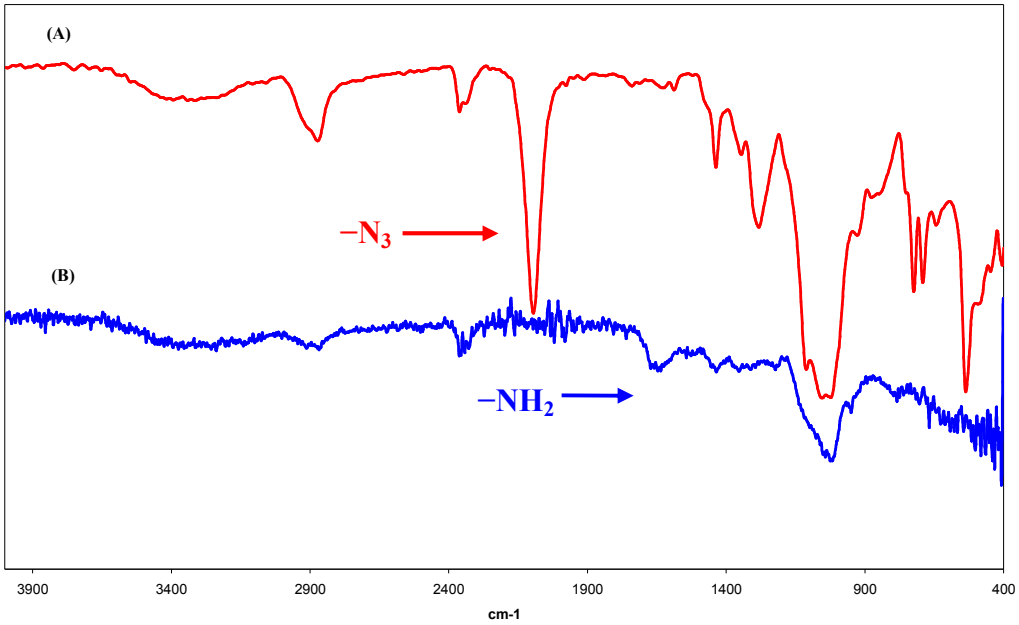


**Figure 5.28.** FT-IR spectra of (A) fully azide functionalised HEC **5.1** and (B) HEC with primary amine functionality **5.6**

### 5.3.3.2.3. Zwitter-ionic Composition

HEC with both carboxylic acid and primary amine functionalities was successfully synthesised *via* Click reaction between fully azide functionalised HEC **5.1** and a mixture of 5-hexynoic acid and propargyl amine (1:1 mol %) in DMSO containing $CuSO_4.5H_2O$ and sodium ascorbate at 70 $^oC$ for 24 hr to afford the product **5.7**, Scheme 5.9.

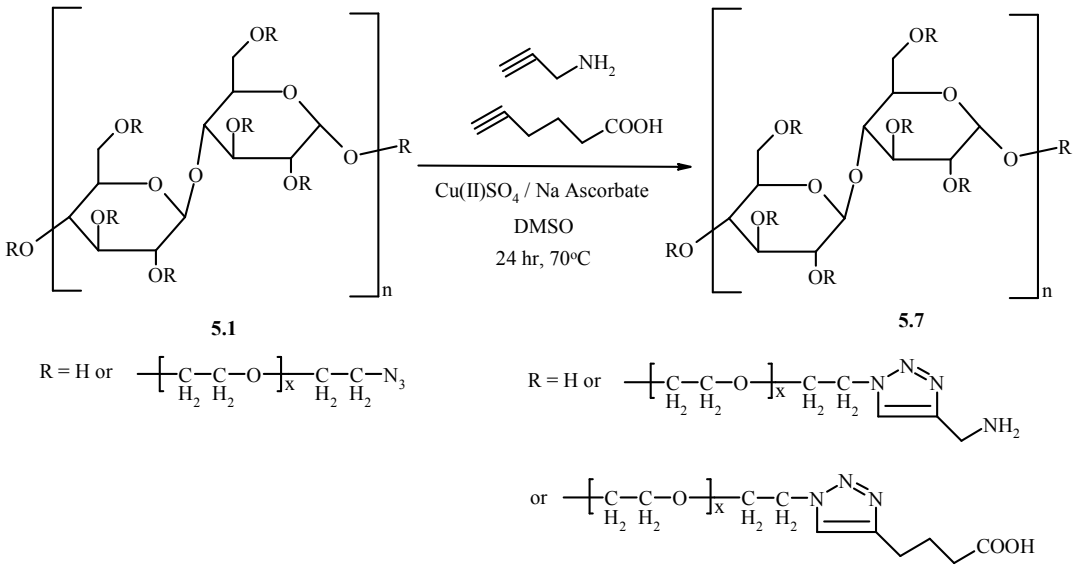


**Scheme 5.9.** Synthesis of HEC with both carboxylic acid and primary amine functionalities

Solid-state $^{13}$C-NMR spectrum of **5.7** showed appearance of two new peaks at 147.59 and 123.11 ppm, assigned to the triazole carbons ($C_{11}$ and $C_{10}$), respectively. It also showed a peak due to the carbons of the carboxylic acid and propargyl amine functionalities, Fig. 5.29. Moreover, the peaks due to the HEC backbone carbons were observed in the same regions.

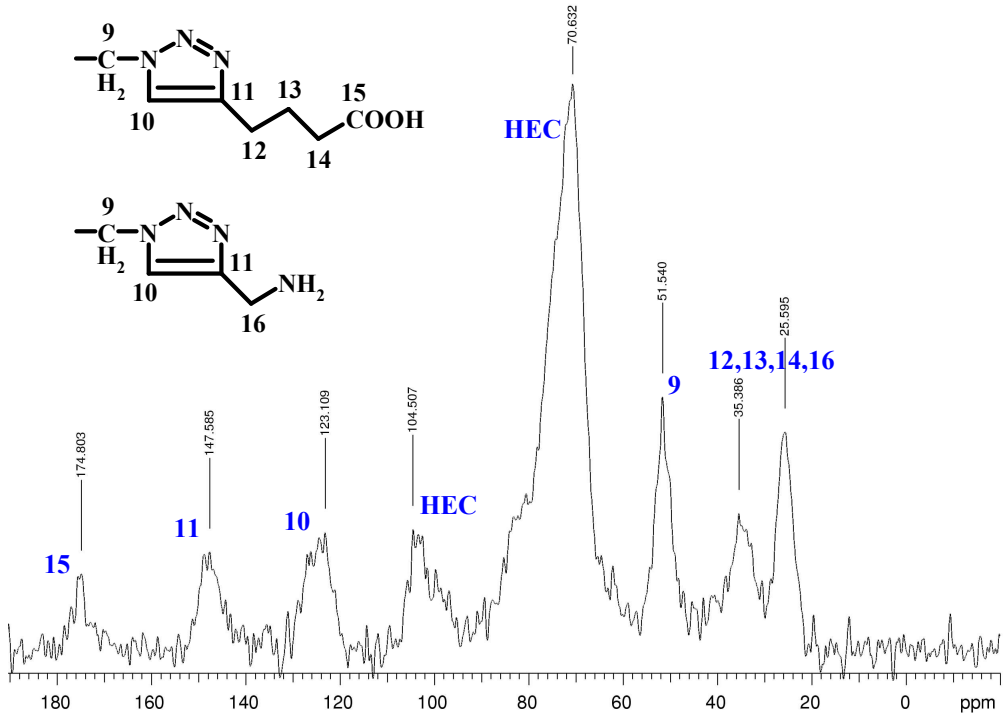


**Figure 4.29.** Solid-state $^{13}$C-NMR (CP exp.) spectrum of HEC with both carboxylic acid and primary amine functionalities **5.7**

The IR spectra of **5.7** (Fig. 5.30.B) compared to that of **5.1** (Fig. 5.30.A) showed the complete disappearance of the azide peak at 2090 $cm^{-1}$, confirming the quantitative conversion to the clicked product. Moreover, it shows the overlap of the two close peaks at 1704 and 1635 $cm^{-1}$, corresponding to the carbonyl and primary amine groups, respectively.

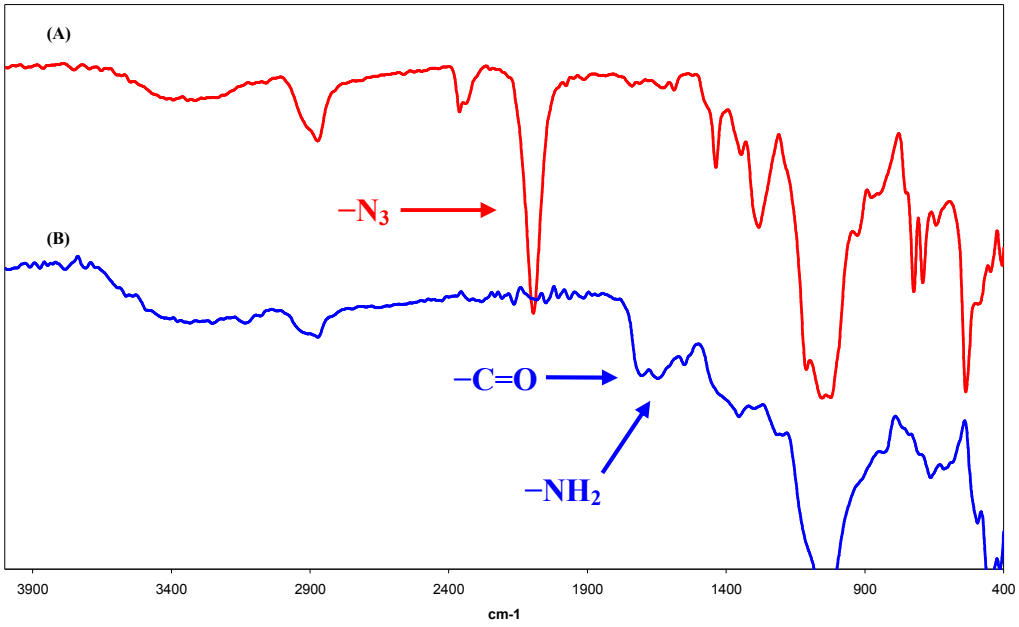


**Figure 5.30.** FT-IR spectra of (A) fully azide functionalised HEC **5.1** and (B) HEC with both carboxylic acid and primary amine functionalities **5.7**

### 5.3.3.3. Synthesis of HEC Containing PDMS Grafts with Different Compositions

In the previous sections, the preparation of HEC with neutral and ionic compositions was disclosed. One of the potential applications of these compositions is for the personal care products. However, in some products, other components may need to be added to these compositions to enhance the delivery of certain properties of the final products. Traditionally, formulations containing physically bound additives have been used in the production of many commercial personal care products. Undoubtedly, the formulations containing chemically bound compounds would offer better products and provide a diverse choice.

This part of the work deals with the synthesis of HEC with chemically bound compositions for possible personal care and cosmetics applications. The compositions discussed here are designed to have the combination of the unique properties of both HEC and PDMS. Over the years, it has been a challenge for the industrial sectors to bind PDMS chemically to HEC, due to the immiscibility of hydrophobic PDMS with

hydrophilic HEC. Sequential Click reactions on HEC was thought to be an efficient method to incorporate the PDMS grafts on the HEC backbone bearing other functionalities.

### 5.3.3.3.1. Synthesis of Alkyne Terminated PDMS

For the first modification attempt, a commercially available mono-hydroxy terminated PDMS (PDMS-OH) ($M_n$ ~1000 $gmol^{-1}$) was used. All the peaks were assigned for the $^1$H-NMR spectrum of PDMS-OH, Fig. 5.31. Deuterium exchange experiment using $D_2O$ was performed to confirm the right assignment for the OH proton. The integration ratios of the OH proton ($H_{16}$) against the terminal $CH_3$ protons ($H_1$) and the methyl protons attached to silicon atoms ($H_{5\text{-}10}$) suggested that the degree of polymerisation of ~11, i.e. molecular weight of ~1058 $gmol^{-1}$ which is comparable to the average molecular weight provided by the manufacturer (~1000 $gmol^{-1}$, i.e. n = 10).

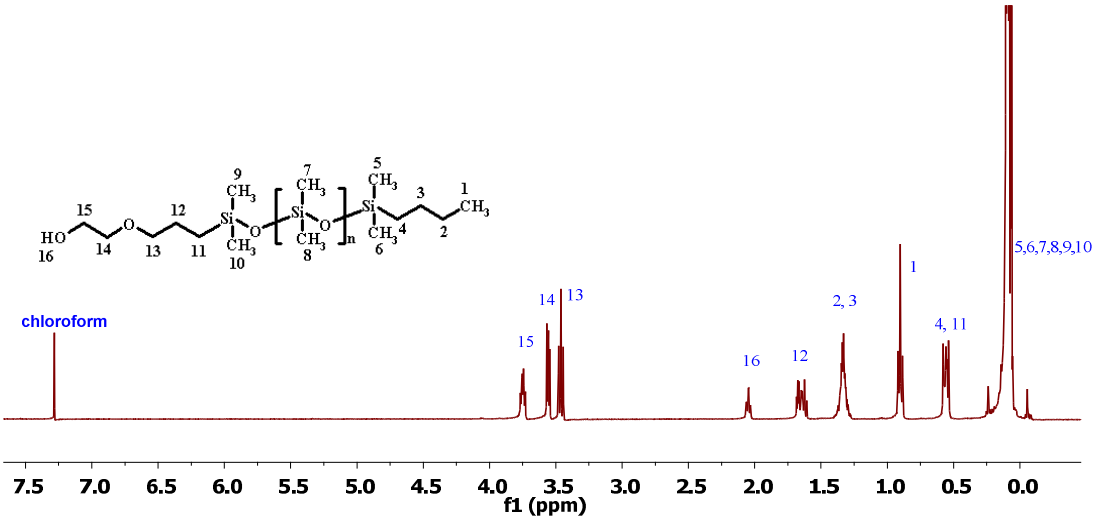


**Figure 5.31.** $^1$H-NMR spectrum of PDMS-OH in $CDCl_3$ (without internal reference)

An etherification reaction between PDMS-OH and propargyl bromide using dry THF containing NaH was attempted. The mixture was stirred at ambient temperature for 24 hr and the product was recovered, Scheme 5.10.

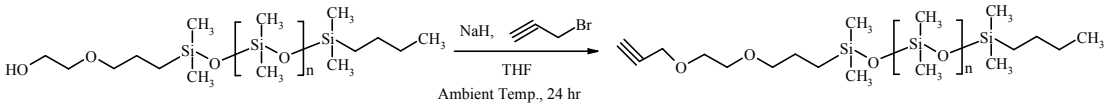


**Scheme 5.10.** Attempted synthesis of mono-alkyne terminated PDMS

The $^{1}$H-NMR spectrum of the recovered product is shown in Figure 5.32. The spectrum indicated the existence of both peaks due to the OH ($H_{16}$) and the alkyne ($H_a$ and $H_b$) groups. Based on the integration ratios, the quantity of the end groups (either OH or alkyne) compared to the methyl groups attached to silicon atoms are much lower than if they were all in the same molecule. The reaction was repeated several times and similar results were obtained.

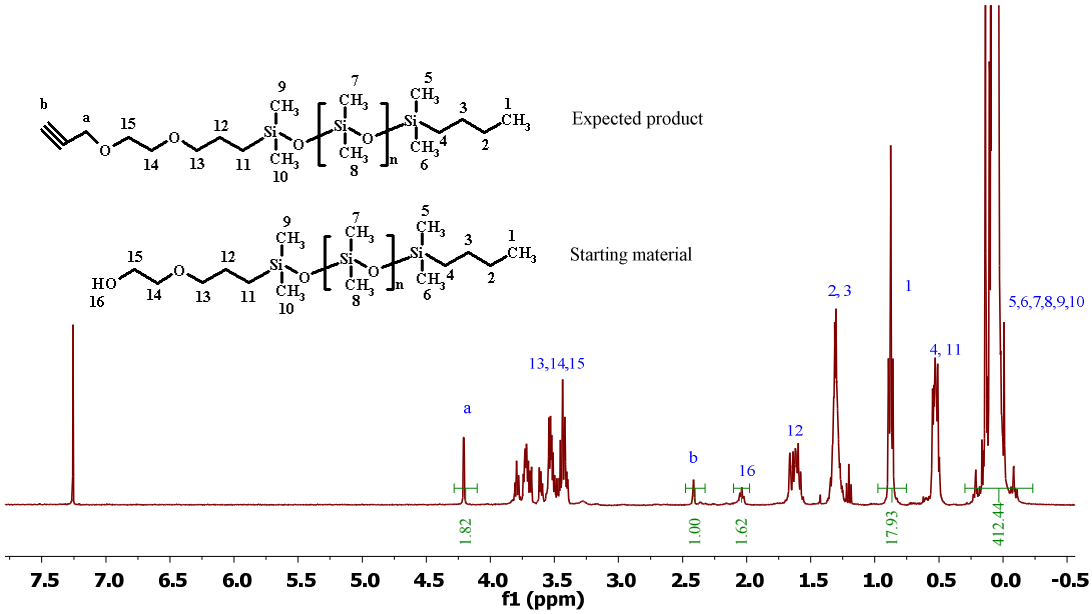


**Figure 5.32.** $^{1}$H-NMR spectrum of the product, recovered from the reaction described in Scheme 5.10, in $CDCl_3$

It is believed that in presence of base catalyst (sodium hydride), silanoate anion formed that reacts with the polymer backbone (i.e. backbiting) to produce a mixture of cyclic siloxane and short chains terminated with either hydroxyl or alkynyl groups.

The existence of the cyclic PDMS was reported.[34-37] The formation of the macrocycles was attributed to the ring-chain equilibration of siloxane oligomers in the presence of silanolate.[38-41] The formation of cycles is favoured at the expense of chain formation with increasing dilution.[42]

Therefore, an efficient alternative method was developed for synthesis of alkyne terminated PDMS with linear topology. The method was based on ring opening of epoxide group with primary amine group. Mono-epoxide terminated PDMS (PDMS-EPO) with an average molecular weight of ~1000 gmol$^{-1}$ was used for this purpose. The PDMS-EPO was fully characterised by NMR and GPC. Figure 5.33.A shows the assigned $^{1}$H-NMR spectrum of PDMS-EPO. The integration ratios between the epoxide protons ($H_{15}$ and $H_{16}$) and the terminal $CH_3$ protons ($H_1$) and the methyl protons

attached to silicon atoms ($H_{5\text{-}10}$) suggested the degree of polymerisation (DP) of ~11. This gives the number average molecular weight of ~1118 $gmol^{-1}$ which is comparable to $M_n$ provided by the supplier.

The reaction between PDMS-EPO and propargyl amine was successfully performed to produce the alkyne terminated PDMS (PDMS-Alk) **5.8**, Scheme 5.11. The PDMS-EPO was neatly mixed with excess propargyl amine and stirred at 80 $^oC$ for 18 hr.

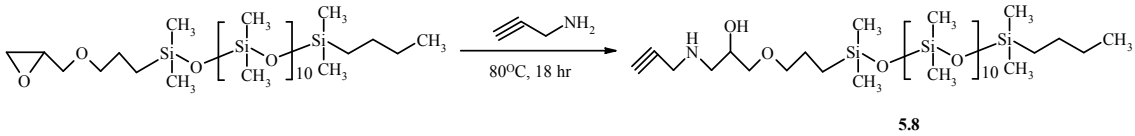


5.8

**Scheme 5.11.** Synthesis of mono alkyne terminated PDMS (PDMS-Alk)

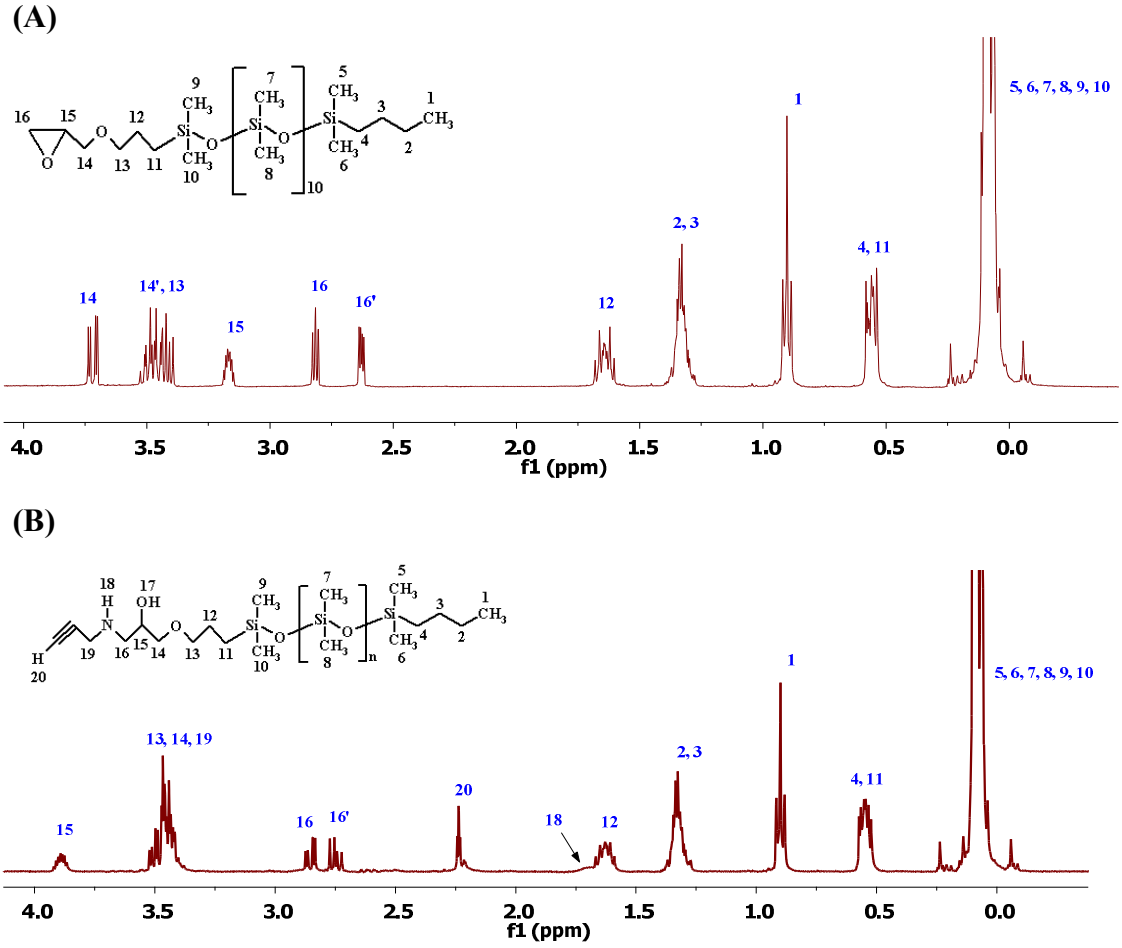


**Figure 5.33.** $^1$H-NMR spectra of (A) mono epoxide terminated PDMS (PDMS-EPO) and (B) mono alkyne terminated PDMS (PDMS-Alk) **5.8** in $CDCl_3$

PDMS-Alk **5.8** was fully characterised by $^1$H-NMR. The $^1$H-NMR spectrum of **5.8** (Fig. 5.33.B) compared to that of PDMS-EPO (Fig. 5.33.A) showed a shift of the peak, assigned $H_{15}$ from 3.17 to 3.89 ppm, indicating complete opening of the epoxide

rings. The integration ratio of the peaks due to alkyne ($H_{20}$) and the terminal methyl group ($H_1$) confirmed complete conversion of PDMS-EPO to PDMS-Alk product.

### 5.3.3.3.2. Neutral Composition

The grafting of PDMS onto HEC bearing ester functionality was successfully achieved *via* sequential Click reactions to produce a neutral (non-ionic) composition. The fully azide functionalised HEC **5.1** was clicked with PDMS-Alk **5.8** and ethyl propiolate (Scheme 5.12). The synthetic procedure targeted to graft ~25 wt % of HEC with PDMS. Hence, only 5 mol % (0.05 molar equivalents) of PDMS-Alk per azide groups on HEC was used. Subsequently, the rest of the free azide groups were clicked with ethyl propiolate. It was important to allow the Click reaction between PDMS-Alk and **5.1** to proceed to completion before the addition of ethyl propiolate. This was achieved by following the reaction with $^{13}$C-NMR.

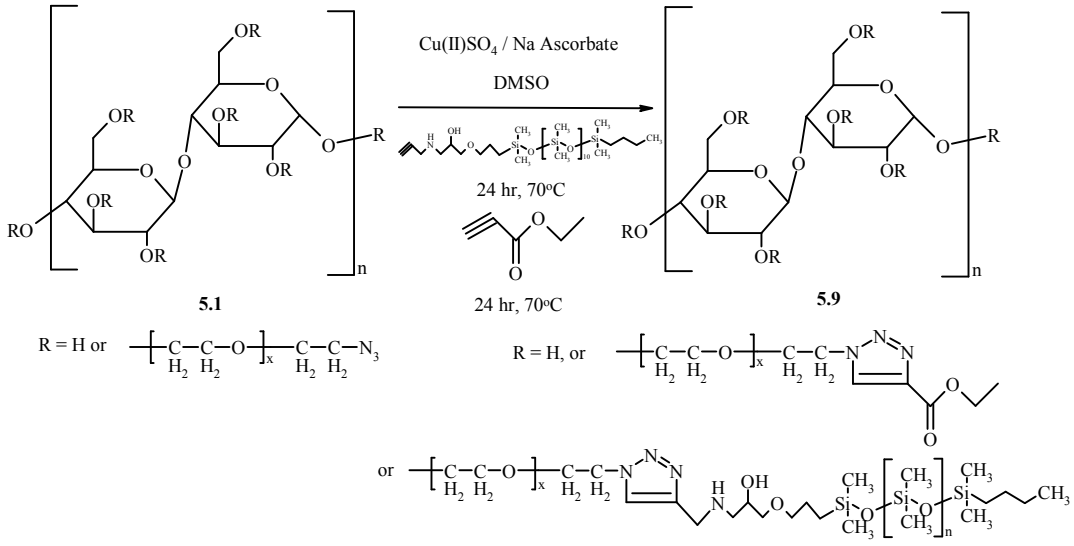


**Scheme 5.12.** Synthesis of PDMS grafted onto HEC bearing ester functionality

Due to insolubility of the product, solid-state $^{13}$C-NMR spectroscopy was used to prove the successful Click reactions of both PDMS and ethyl propiolate on HEC. Two NMR experiments were run to study the compositional structure of the material; (1) the cross polarisation (CP) experiment which detects predominantly the rigid parts of the polymeric material (HEC backbone) and (2) the direct polarisation (DP) experiment which detects predominantly the flexible parts (grafted chains).

The CP solid-state $^{13}$C-NMR spectrum of **5.9** showed two new peaks at 139.78 and 130.53 ppm, assigned to the triazole ring, $C_{11}$ and $C_{10}$, respectively. It also showed

peaks due to the ethyl ester functionality, methyl groups of PDMS and HEC backbone, Fig. 5.34.A. However, the DP solid-state $^{13}$C-NMR spectrum of **5.9** showed the peaks due to the HEC backbone with very low intensity and the peak for the methyl groups of PDMS with high intensity, Fig. 5.34.B.

The IR spectrum of **5.9** (Fig. 5.35.B) compared to that of **5.1** (Fig. 5.35.A) showed no residual peak at 2090 $cm^{-1}$ for the azide group, confirming the complete conversion to the clicked product. It also showed appearance of a new peak at 1720 $cm^{-1}$, assigned to the carbonyl group of the ethyl ester functionality on HEC. Furthermore, it showed three significant peaks at 1262, 1202 and 800 $cm^{-1}$ due to the dimethyl siloxyl functionalities of PDMS chains on HEC backbone.

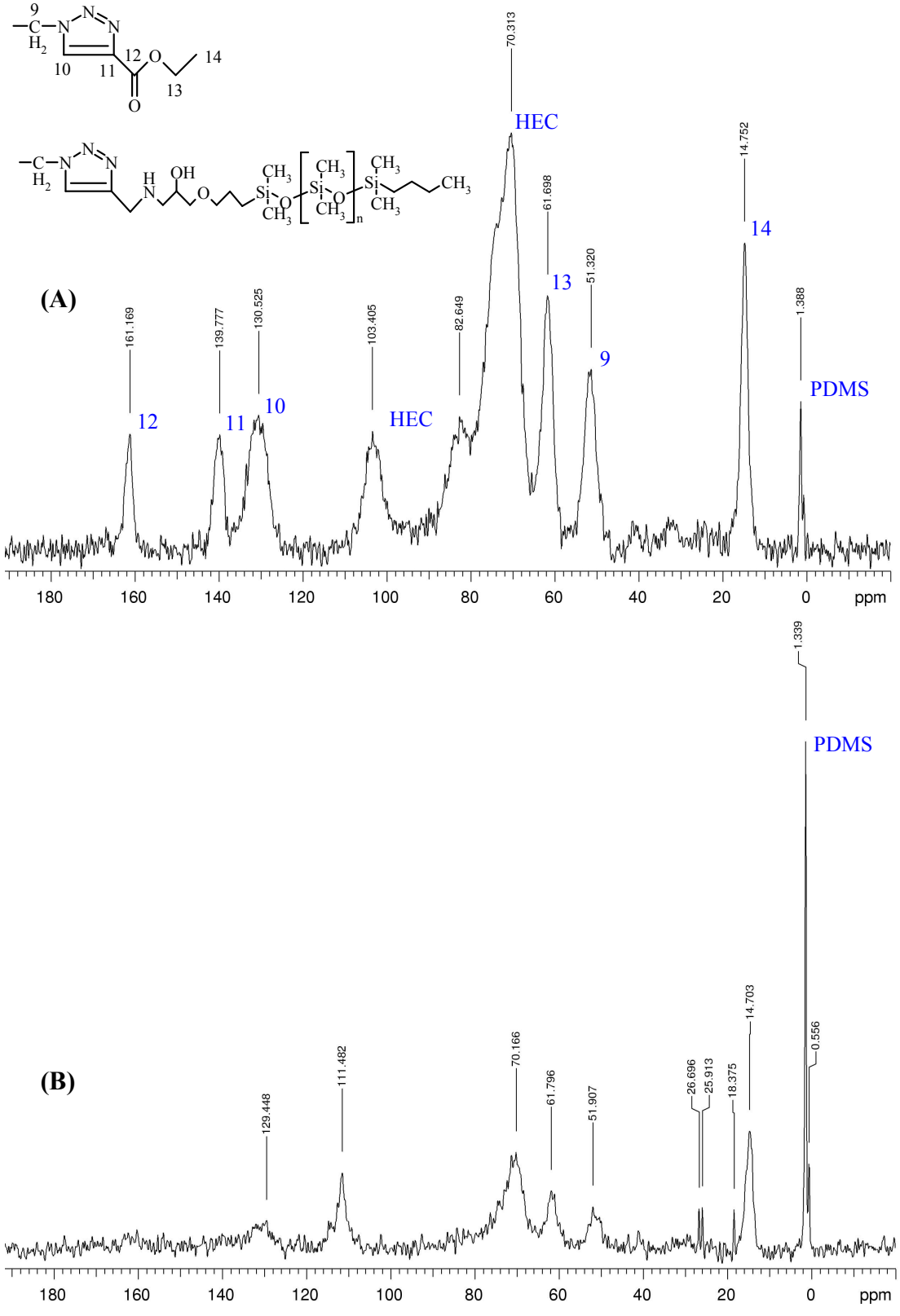


**Figure 5.34.** Solid-state $^{13}$C-NMR spectra of PDMS grafted onto HEC bearing ester functionality **5.9** (A) CP exp. and (B) DP exp.

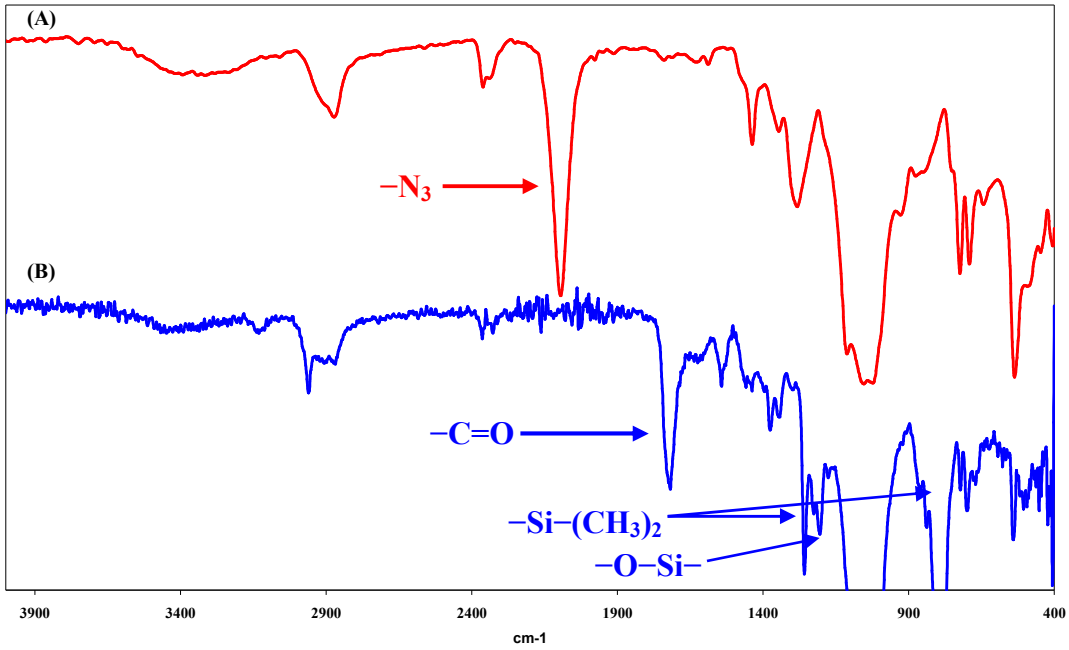


**Figure 5.35.** FT-IR spectra of (A) fully azide functionalised HEC **5.1** and (B) PDMS grafted onto HEC bearing ester functionality **5.9**

The elemental analysis results on the reprecipitated product showed that the sample contained ~8.2 % silicon. This is very close to the estimated calculation of ~7.5 %, within estimated error.

#### 5.3.3.3.3. Cationic Composition

PDMS grafted onto HEC bearing primary amine functionality was successfully prepared. This composition was achieved by performing Click reaction between the fully azide functionalised HEC **5.1** and the PDMS-Alk **5.8** followed by subsequent Click reaction between the remaining azide groups with propargyl amine, Scheme 5.13.

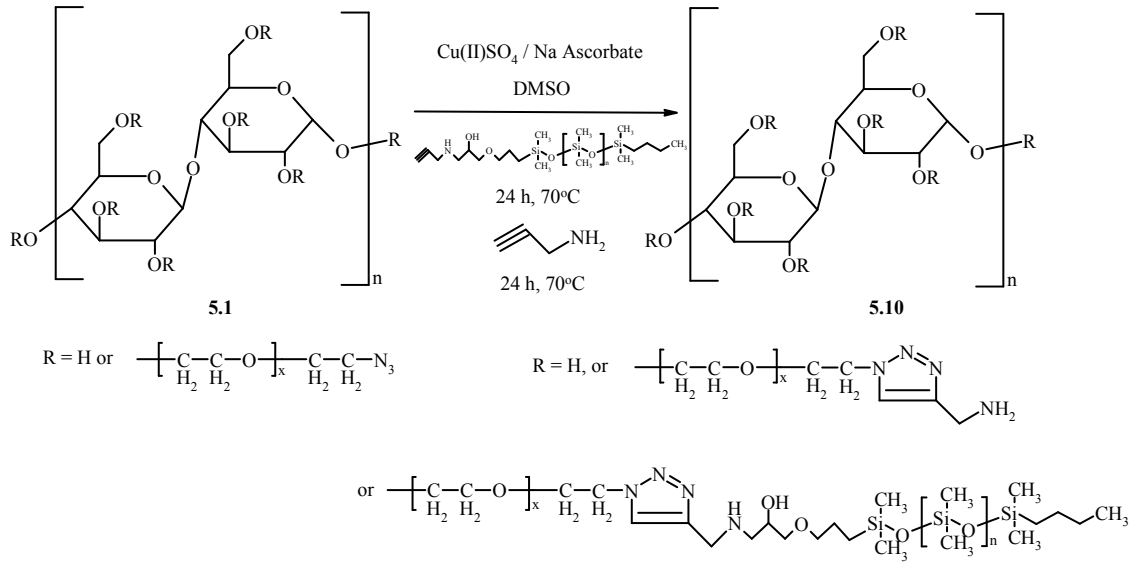


**Scheme 5.13.** Synthesis of PDMS grafted onto HEC bearing primary amine functionality

The CP solid-state $^{13}$C-NMR spectrum of **5.10** showed the successful Click reaction on HEC as demonstrated by appearance of two new peaks at 142.57 and 124.46 ppm, assigned to the triazole ring (Fig. 5.36.A). The DP spectrum of **5.10** showed the flexible grafted chains of PDMS as well as the carbons of the primary amine functionality as assigned in the spectrum (Fig. 5.36.A).

The IR spectrum of **5.10** (Fig. 5.37.B) compared to that of **5.1** (Fig. 5.37.A) showed no residual peak at 2090 cm$^{-1}$ for the azide group, confirming the complete conversion to the clicked product. It also showed appearance of a new peak at 1640 cm$^{-1}$, assigned to the primary amine functionality on HEC. Furthermore, it showed two significant peaks at 1258 and 800 cm$^{-1}$ due to the dimethyl siloxyl functionalities of PDMS chains on HEC backbone.

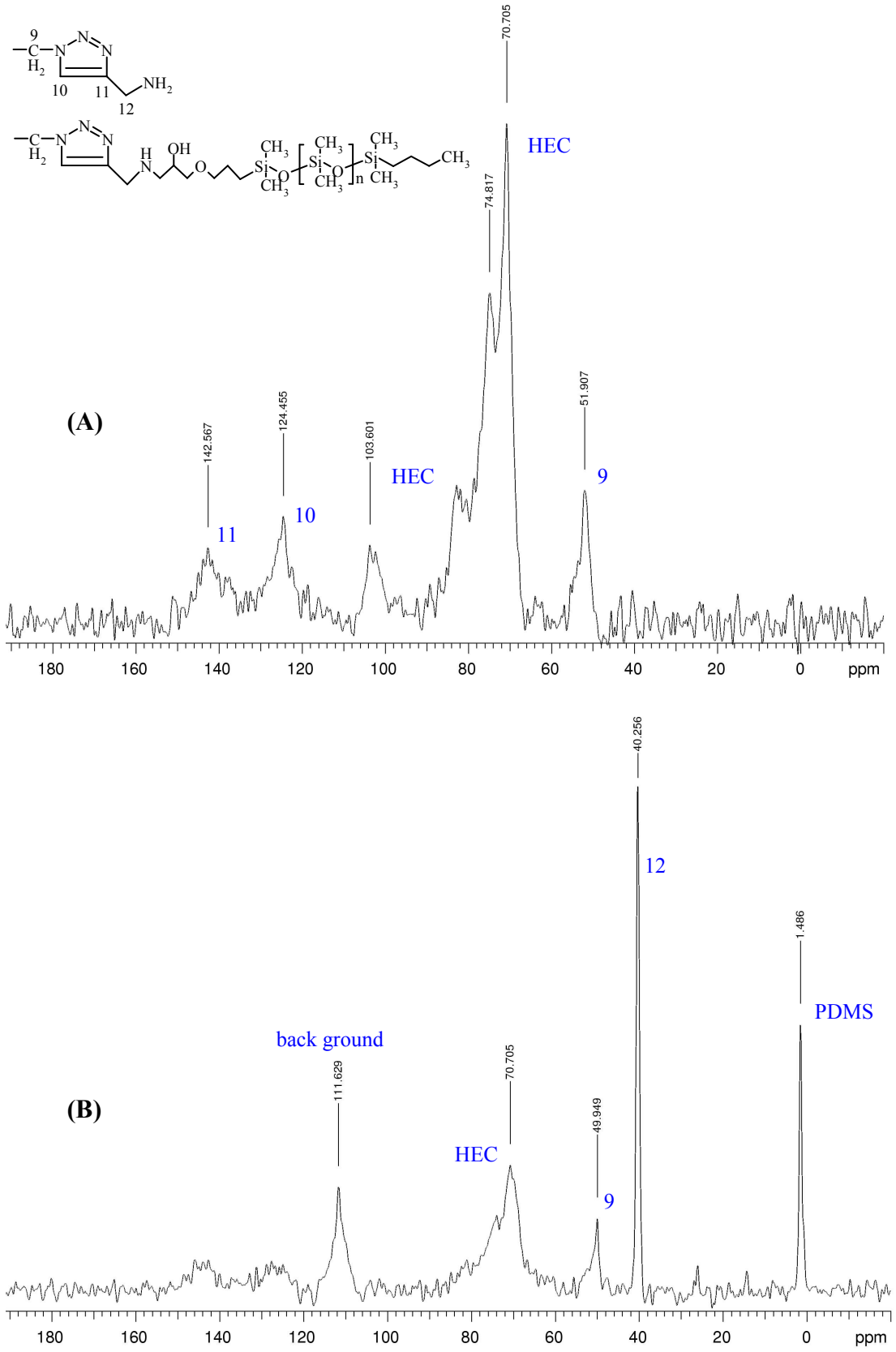


**Figure 5.36.** Solid-state $^{13}$C-NMR spectra of PDMS grafted onto HEC bearing primary amine functionality **5.10** (A) CP exp. and (B) DP exp.

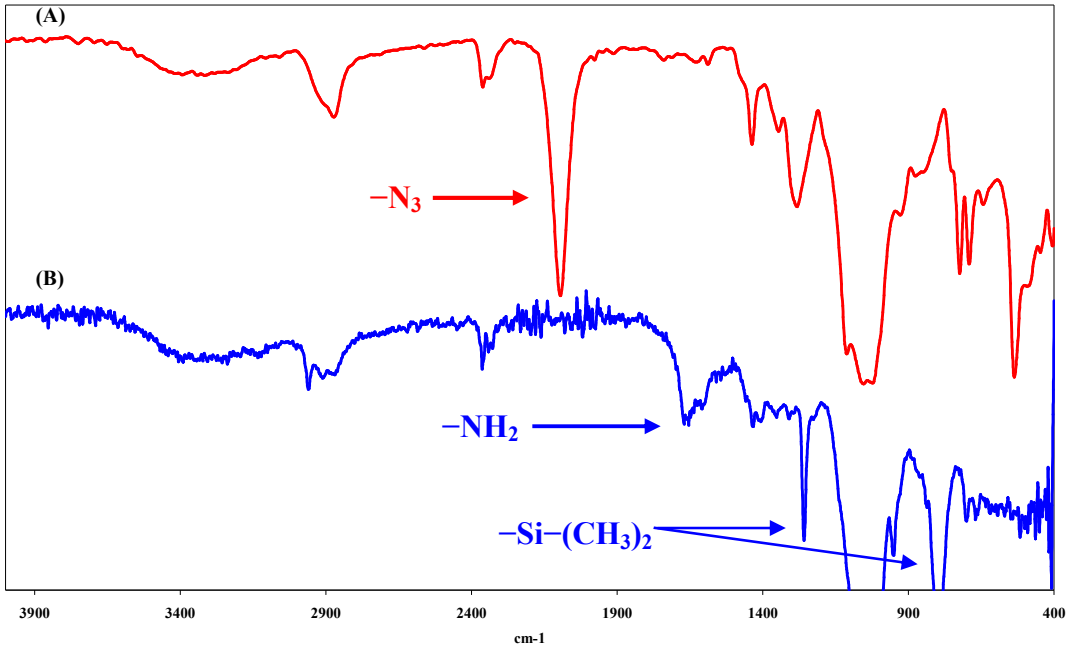


**Figure 5.37.** FT-IR spectrum of (A) fully azide functionalised HEC **5.1** and (B) PDMS grafted onto HEC bearing primary amine functionality **5.10**

The elemental analysis results showed that the sample contains ~4.2 % Si compared to the calculated value of ~7.5 %. The difference was attributed to the possible error in the estimated calculation. The theoretical calculation of the Si is not very accurate as the commercially available HEC is not very well defined.

#### 5.3.3.3.4. Anionic Composition

PDMS grafted onto HEC bearing carboxylic acid functionality was investigated. This composition was targeted by performing Click reaction between the fully azide functionalised HEC **5.1** and the PDMS-Alk **5.8** followed by a subsequent Click reaction between the remaining un-clicked azide groups on HEC with 5-hexynoic acid, Scheme 5.14.

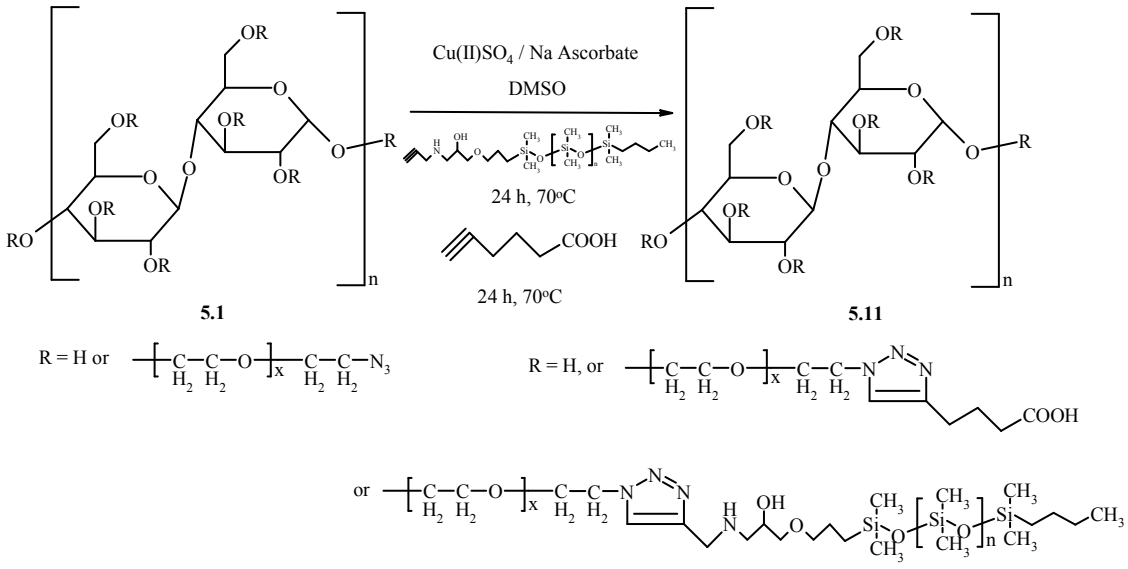


**Scheme 5.14.** Synthesis of PDMS grafted onto HEC bearing carboxylic acid functionality

The CP solid-state $^{13}$C-NMR spectrum showed very weak peaks at the region of triazole ring, Fig. 5.38.A. However, the DP spectrum showed the flexible grafted chains of PDMS as well as the carbons of the carboxylic acid functionality, Fig. 5.38.B.

The IR spectrum of **5.11** (Fig. 5.39.B) compared to that of **5.1** (Fig. 5.39.A) showed a considerable residual peak at 2090 cm$^{-1}$ for the azide group, indicating that the Click reaction has not proceeded to completion. However, it showed a small peak at 1714 cm$^{-1}$, which is probably due to the carbonyl of the carboxylic acid functionality on HEC, as well as peaks at 1254 and 800 cm$^{-1}$ due to the dimethyl siloxyl functionalities of PDMS chains on HEC backbone.

The elemental analysis results showed that the sample contains ~5.3 % silicon indicating successful Click reaction with PDMS. The reaction was repeated with excess 5-hexynoic acid and the same results were obtained. The reason for the incomplete reaction of HEC partially clicked PDMS with 5-hexynoic acid is presently not understood. One possible explanation is that the extra hydrogen bonding between the acid functionality on the HEC hinders the diffusion of the reagent and hence the reaction.

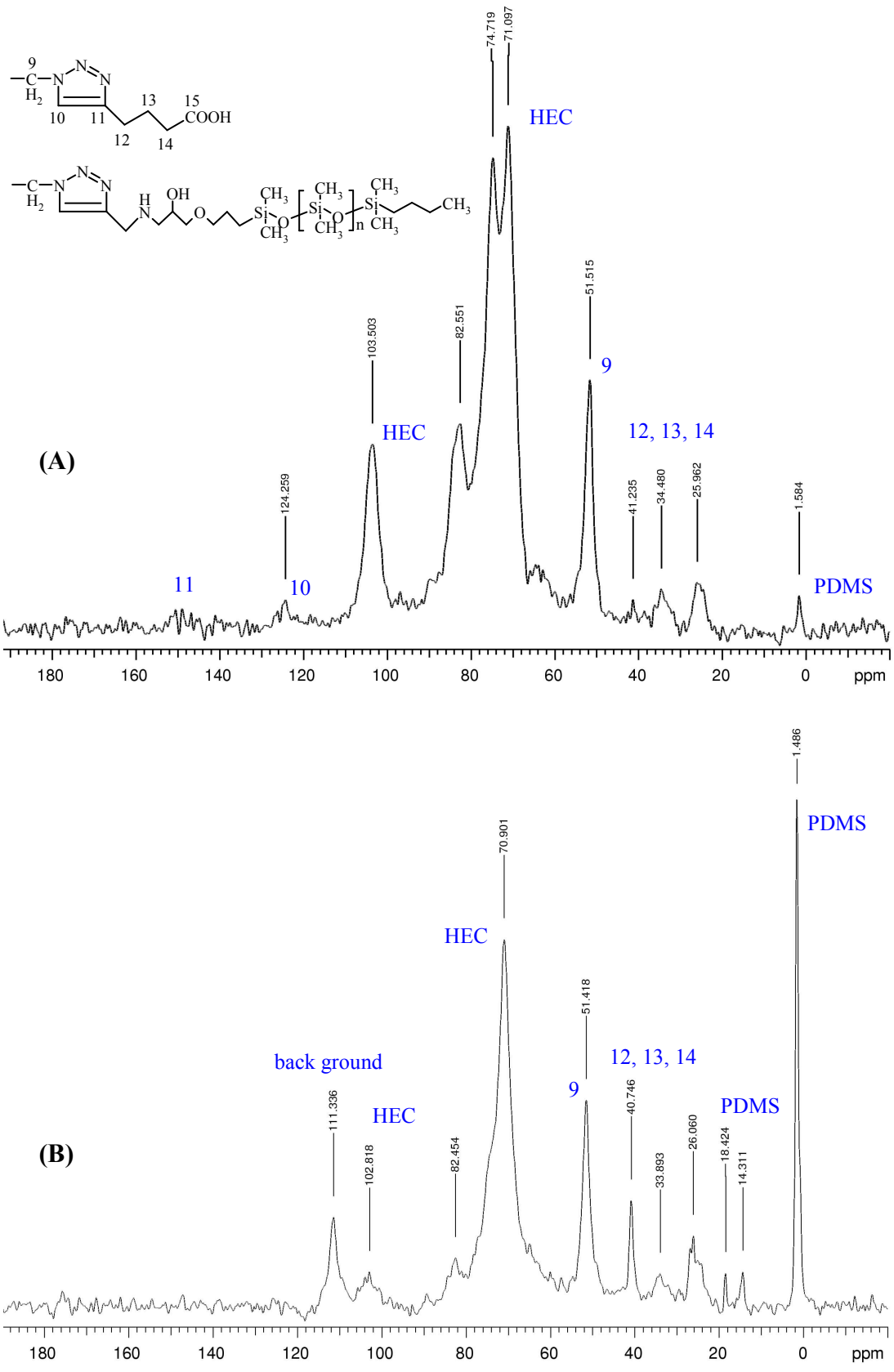


**Figure 5.38.** Solid-state $^{13}$C-NMR spectra of PDMS grafted onto HEC bearing carboxylic acid functionality **5.11** (A) CP exp. and (B) DP exp.

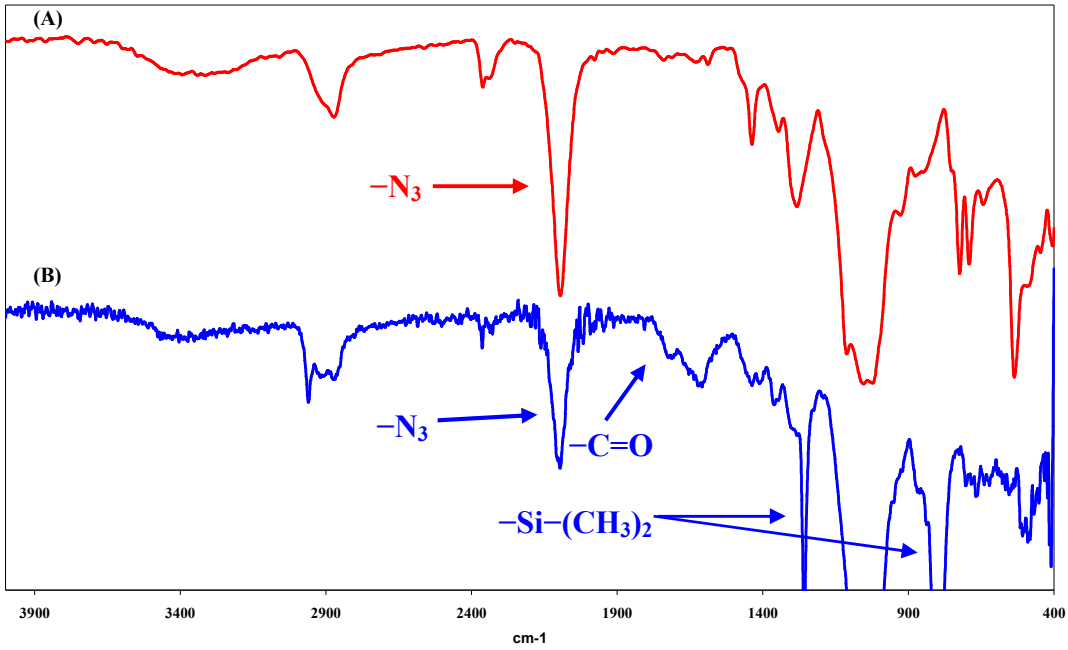


**Figure 5.39.** FT-IR spectrum of (A) fully azide functionalised HEC **5.1** and (B) PDMS grafted onto HEC bearing carboxylic acid functionality **5.11**

Another strategy for synthesis of an anionic composition of PDMS grafted HEC was investigated based on the hydrolysis of the previously prepared neutral composition of PDMS grafted HEC (see section 5.3.3.2.2). The hydrolysis was carried out under a relatively mild condition. The sample was dissolved in aqueous solution of NaOH (1N) and stirred at 40 $^{o}$C for 3 hr. The elemental analysis results showed that the sample contains ~1.6 % silicon. The silicon content was a lot lower than the initial value of ~8.2 %. This indicated that during the hydrolysis process, some of the grafted PDMS chains were degraded.

### 5.3.3.3.5. Zwitterionic Composition

PDMS grafted onto HEC bearing primary amine and carboxylic acid functionalities was prepared by performing Click reaction between the fully azide functionalised HEC **5.1** and PDMS-Alk **4.8** followed by another Click reaction between the remaining un-clicked azide groups on HEC and a mixture of propargyl amine and 5-hexynoic acid (1:1, mol %), Scheme 5.15. As previously, the synthetic procedure targeted to graft ~25 wt % of PDMS onto HEC (i.e. 5 mol % (0.05 molar equivalents) of PDMS-Alk per azide groups on HEC). The prepared product is classified as a zwitterionic composition because it contains potentially both positive and negative charges.

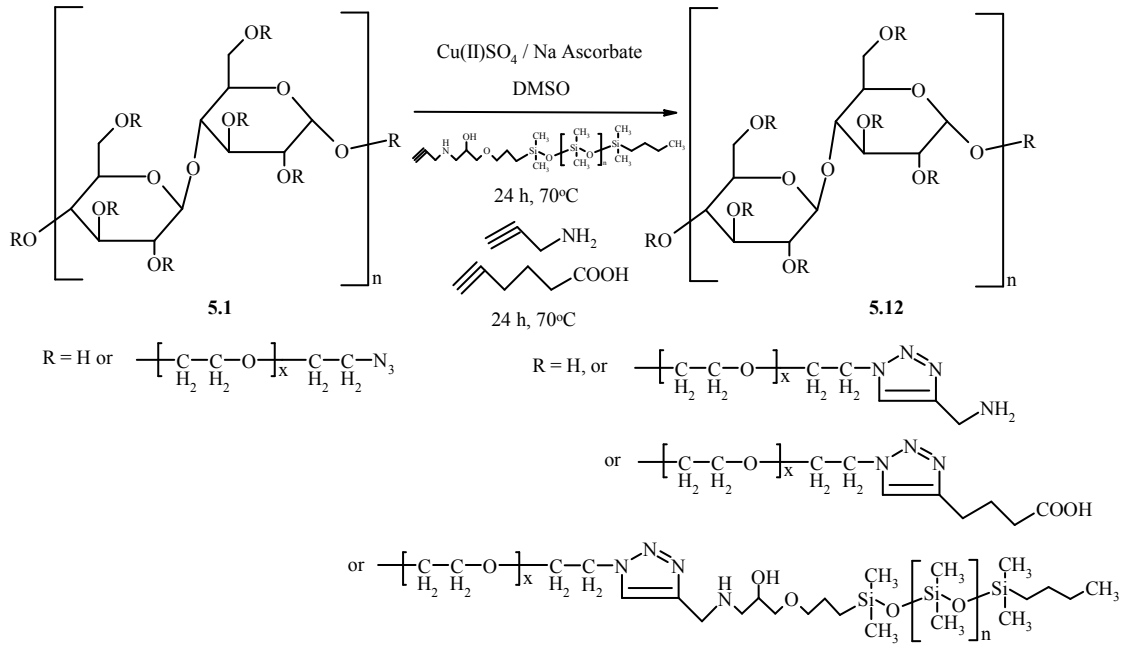


**Scheme 5.15.** Synthesis of PDMS grafted onto HEC bearing primary amine and carboxylic acid functionalities

The CP Solid-state $^{13}$C-NMR spectrum of **5.12** showed the successful Click reaction on HEC as demonstrated by appearance of two new peaks at 147.93 and 125.85 ppm, assigned to the triazole ring and all the grafted components (PDMS and primary amine and carboxylic acid functionalities) as assigned in the spectrum, Fig. 5.40.A. However, the DP spectrum of **5.12** showed mainly the flexible grafted chains of PDMS as assigned in the spectrum, Fig. 5.40.B.

The IR spectrum of **5.12** (Fig. 5.41.B) compared to that of **5.1** (Fig. 5.41.A) showed no residual peak at 2090 cm$^{-1}$ for the azide group, confirming the complete conversion to the clicked product. It also showed appearance of new peaks at 1716, 1640 cm$^{-1}$ due to the carbonyl group of the carboxylic acid functionality and the primary amine functionality on HEC, respectively. Furthermore, it showed two significant peaks at 1256 and 800 cm$^{-1}$ due to the dimethyl siloxyl functionalities of PDMS chains on HEC backbone.

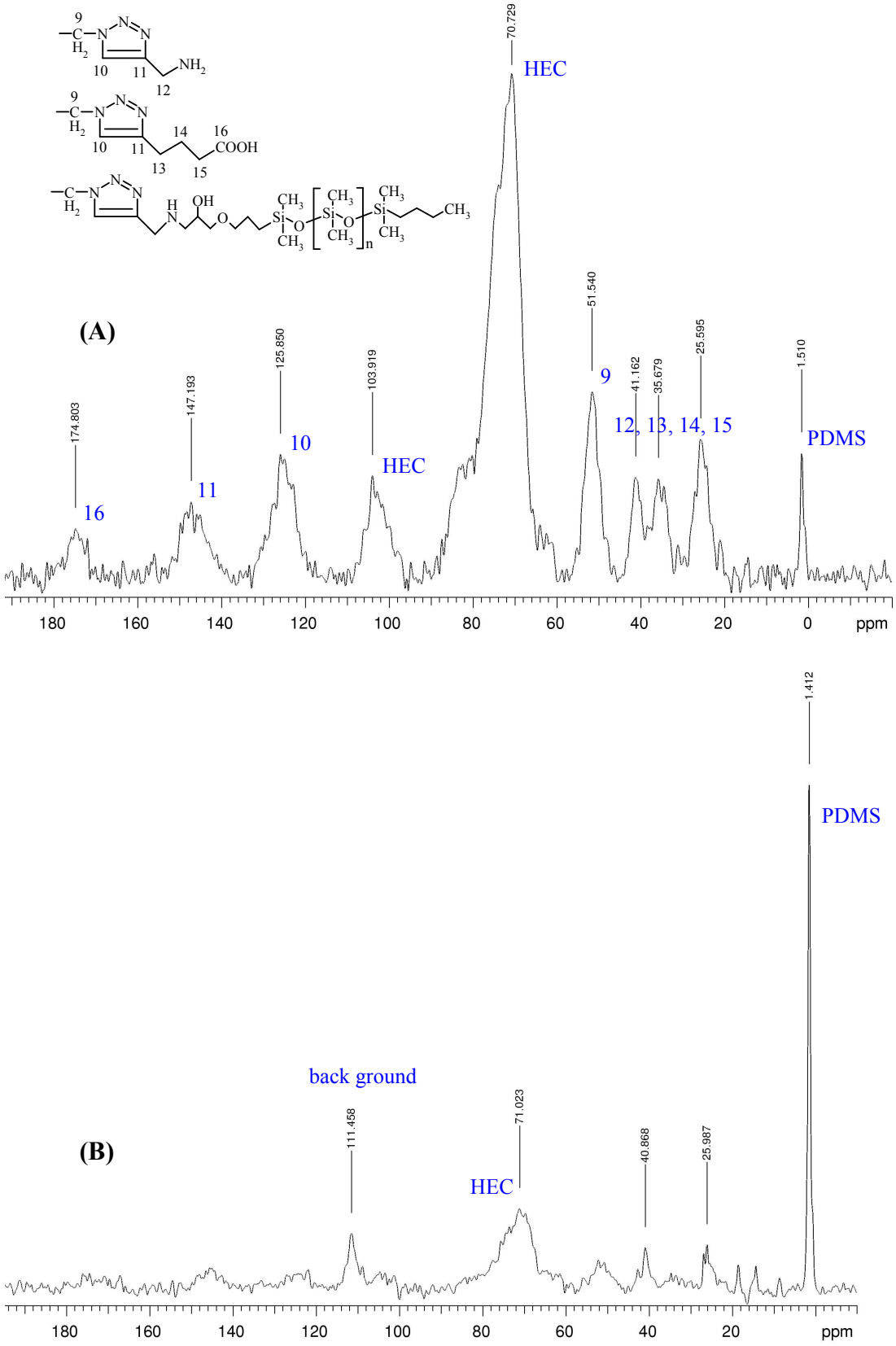


**Figure 5.40.** Solid-state $^{13}$C-NMR spectra of PDMS grafted onto HEC bearing primary amine and carboxylic acid functionalities (A) CP exp. and (B) DP exp.

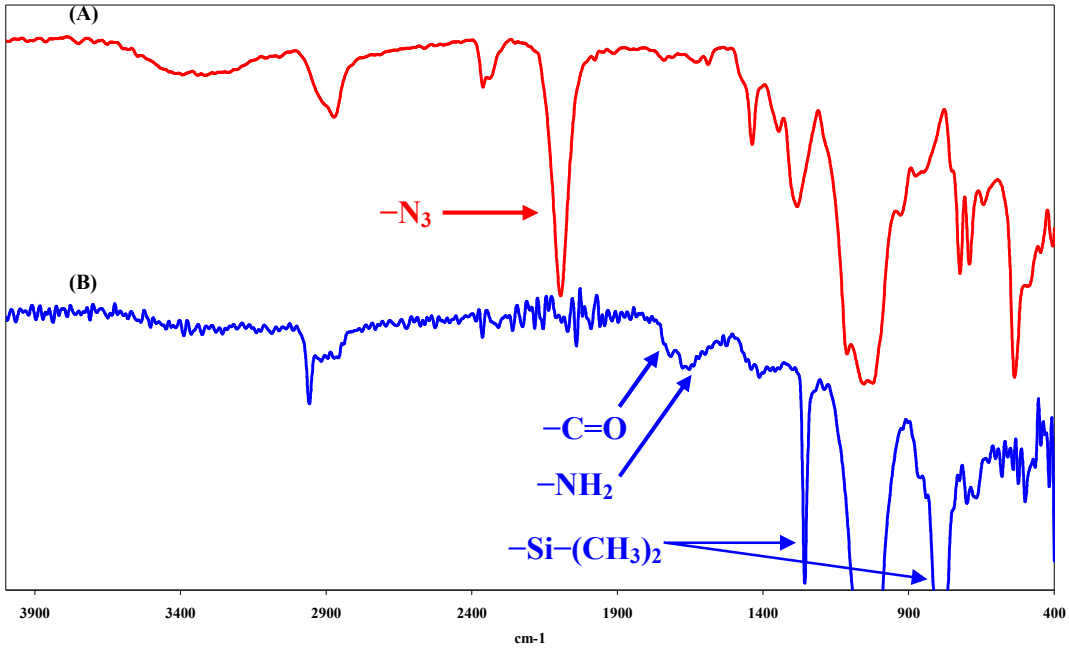


**Figure 5.41.** FT-IR spectrum of (A) fully azide functionalised HEC **5.1** and (B) PDMS grafted onto HEC bearing primary amine and carboxylic acid functionalities

#### 5.3.3.4. Hydrophobic Modification of HEC

The hydrophobic version of HEC was prepared *via* grafting with polyesters such as PLA and PCL. These polyester grafts are known to be hydrophobic and biodegradable.

##### 5.3.3.4.1. Synthesis of HEC with PLA Grafts

PLA was successfully grafted onto HEC backbone with a ratio of 1:1 wt % and the excess remaining azide functionalities on HEC were capped with ester functionality *via* sequential Click reactions. In one pot, the fully azide functionalised HEC **5.1** was clicked with mono-alkyne end capped PLA (chapter 4) followed by another Click reaction with ethyl propiolate. The synthetic procedure was designed to ensure the consumption of all the azide functionalities on HEC with hydrophobic grafts/functionalities.

The procedure involved the sequential addition of the mono-alkyne end capped PLA and ethyl propiolate to a solution of fully azide functionalised HEC **5.1** in DMSO, containing the copper catalytic system, Scheme 5.16. It was important to allow the Click reaction between mono-alkyne end capped PLA to proceed to completion before

the addition of ethyl propiolate. Otherwise, ethyl propiolate is likely to compete with mono-alkyne end capped PLA in Click reaction, affecting the grafting yield.

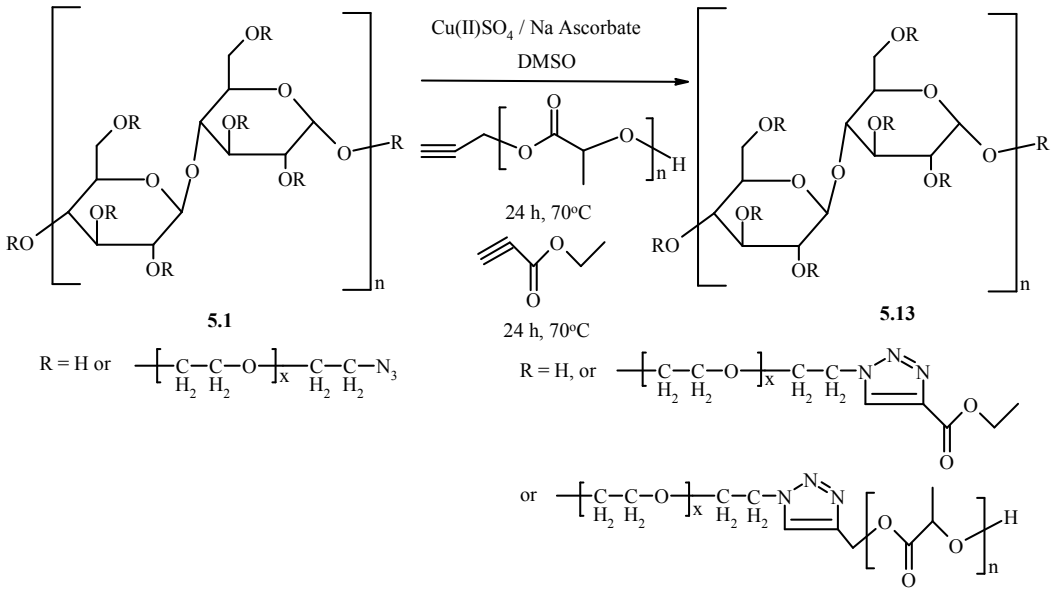


**Scheme 5.16.** Synthesis of HEC grafted with PLA

The CP solid-state $^{13}$C-NMR spectrum of **5.13** showed the successful Click reaction on HEC as demonstrated by appearance of two new peaks at 140.41 and 130.79 ppm, assigned to the triazole ring (Fig. 5.42). It also showed the peaks due to PLA grafts as well as those for ethyl propiolate functionality. Moreover, the peaks corresponding to the HEC backbone were observed in the same regions and no other unassignable peaks were seen in the spectrum.

The IR spectrum of **5.13** (Fig. 5.43.B) compared to that of **5.1** (Fig. 5.43.A) showed no residual peak at 2090 cm$^{-1}$ for the azide group, confirming the complete conversion to the clicked product. It also showed appearance of a new peak at 1742 cm$^{-1}$, assigned to the carbonyl group of the ethyl ester functionality and PLA grafts on HEC. Furthermore, it was observed that the intensity of the peak at ~3400 cm$^{-1}$, due to the OH groups (moisture and structure) was reduced, indicating the hydrophobic character of the final product.

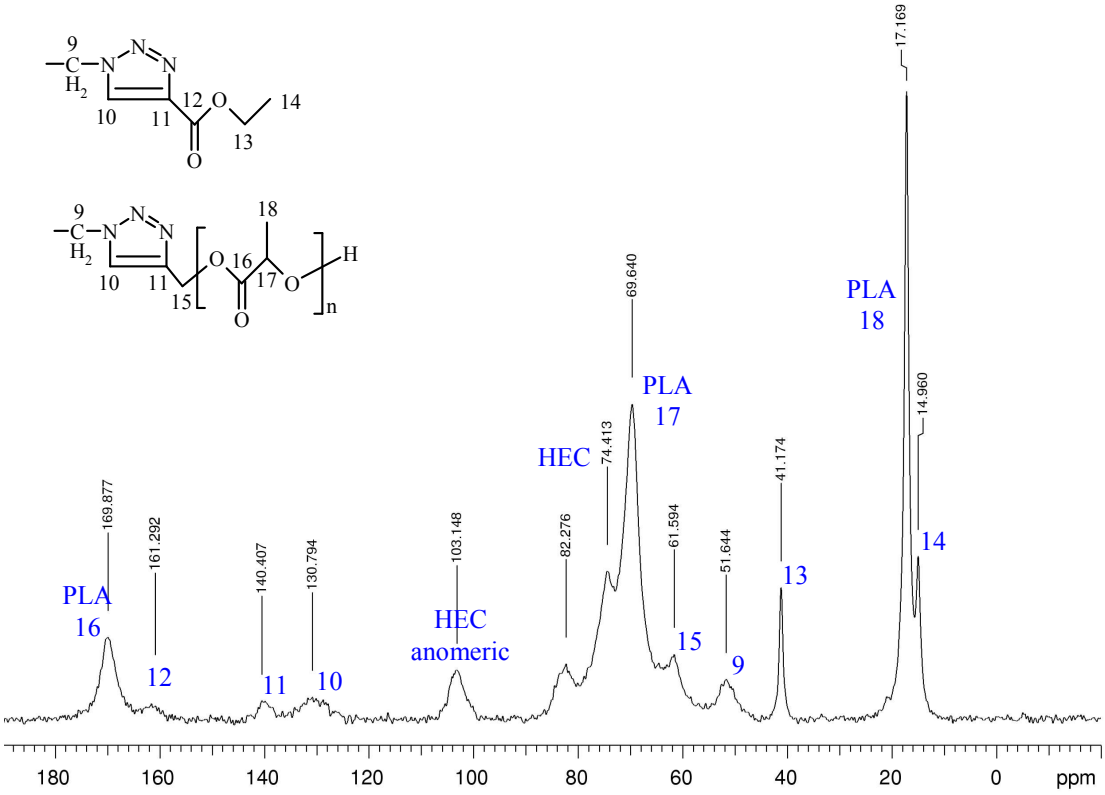


**Figure 5.42.** Solid-state $^{13}$C-NMR (CP exp.) spectrum of HEC grafted with PLA **5.13**

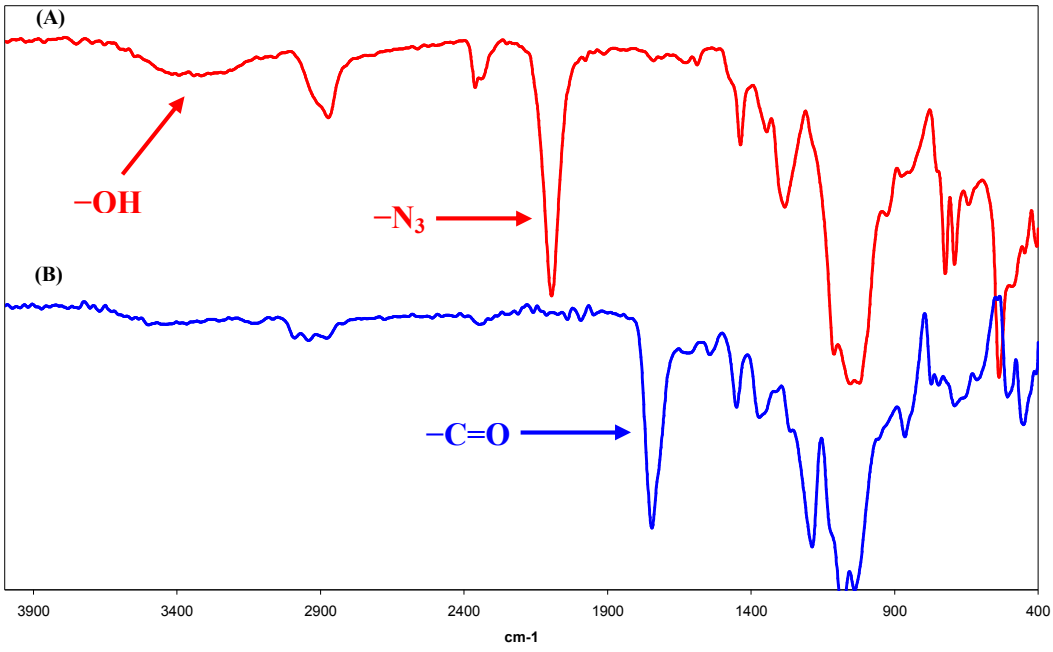


**Figure 5.43.** FT-IR spectrum of (A) fully azide functionalised HEC **5.1** and (B) HEC grafted with PLA **5.13**

The same methodology was used to prepare fully PLA grafted HEC (HEC-g-PLA) in order to increase the graft density and therefore to investigate the architecture of the resulting material.

Atomic force microscopy (AFM) was used to investigate the architecture of HEC grafted polymers. Tapping-mode micrographs were used in an attempted to visualise individual polymer chains. Spin-casting of a dilute polymer solution (~1 mg / 100 mL) was necessary to disperse individual polymer chains for imaging. HEC was spin-cast from water on the surface of a clean silicon wafer to produce a thin film with an average thickness of ~1 nm. Analysis of tapping mode AFM images indicated that HEC formed uniform oval features as shown in Fig. 5.44.A and B, with different scales. The multiple measurements of these hemi-ellipsoidal (rugby ball) features gave an average height of ~10 nm and width of ~50 nm, Fig. 5.44.C.

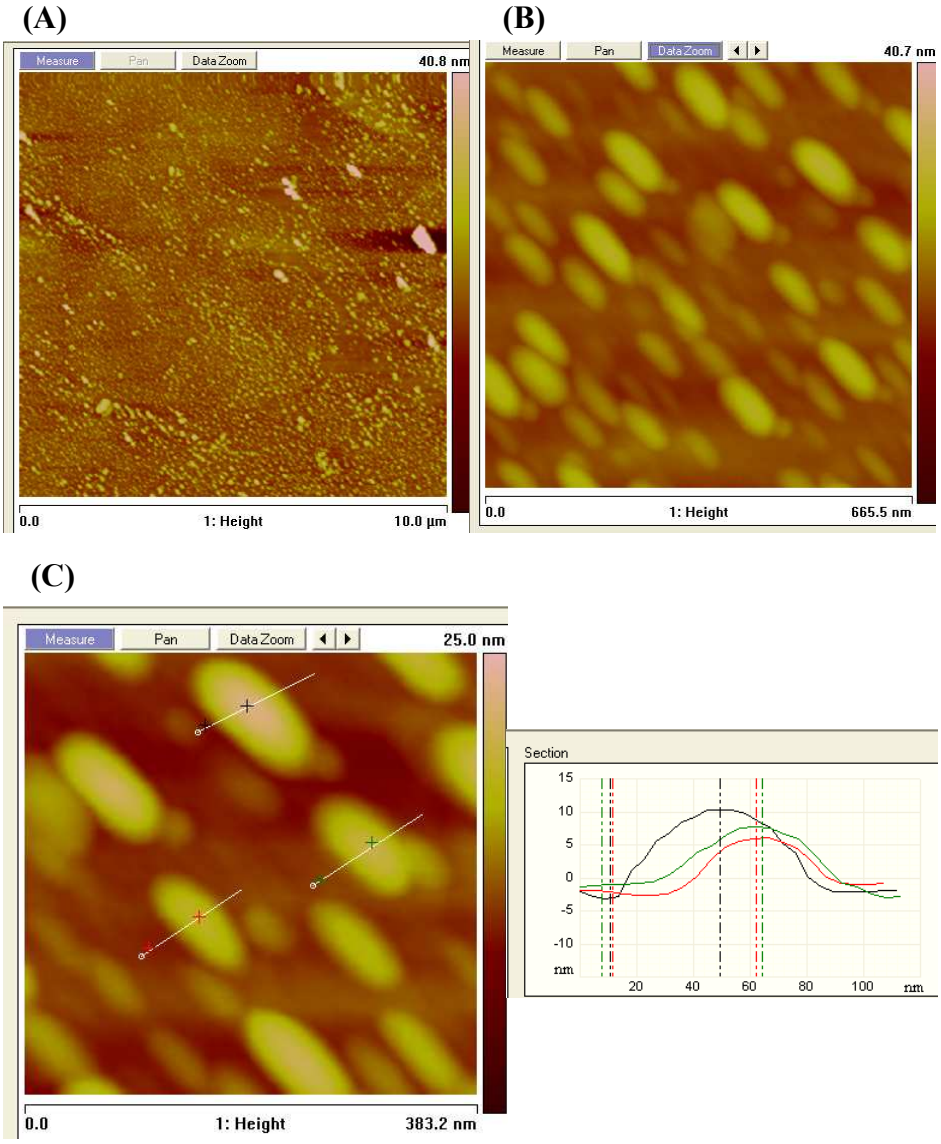


**Figure 5.44.** Tapping mode AFM images of HEC; (A) 10 µm scale, (B) 665 nm scale and (C) 383 nm scale with cross-sectional analysis.

AFM of HEC-g-PLA revealed extended wormlike structures, Fig. 5.45.A, which are characteristic for polymer brushes.[43] Measuring multiple polymer brushes gave an average contour height of ~2 nm and width of ~17 nm, as shown in Fig. 5.45.B. These wormlike structures were expected from the densely grafted nature of HEC-g-PLA. The formation of wormlike structures suggested that the HEC backbone exhibits an extended conformation with side chains stretched and flattened on the surface, presumably because of the steric repulsion between PLA side chains on repeating unit of the HEC backbone.

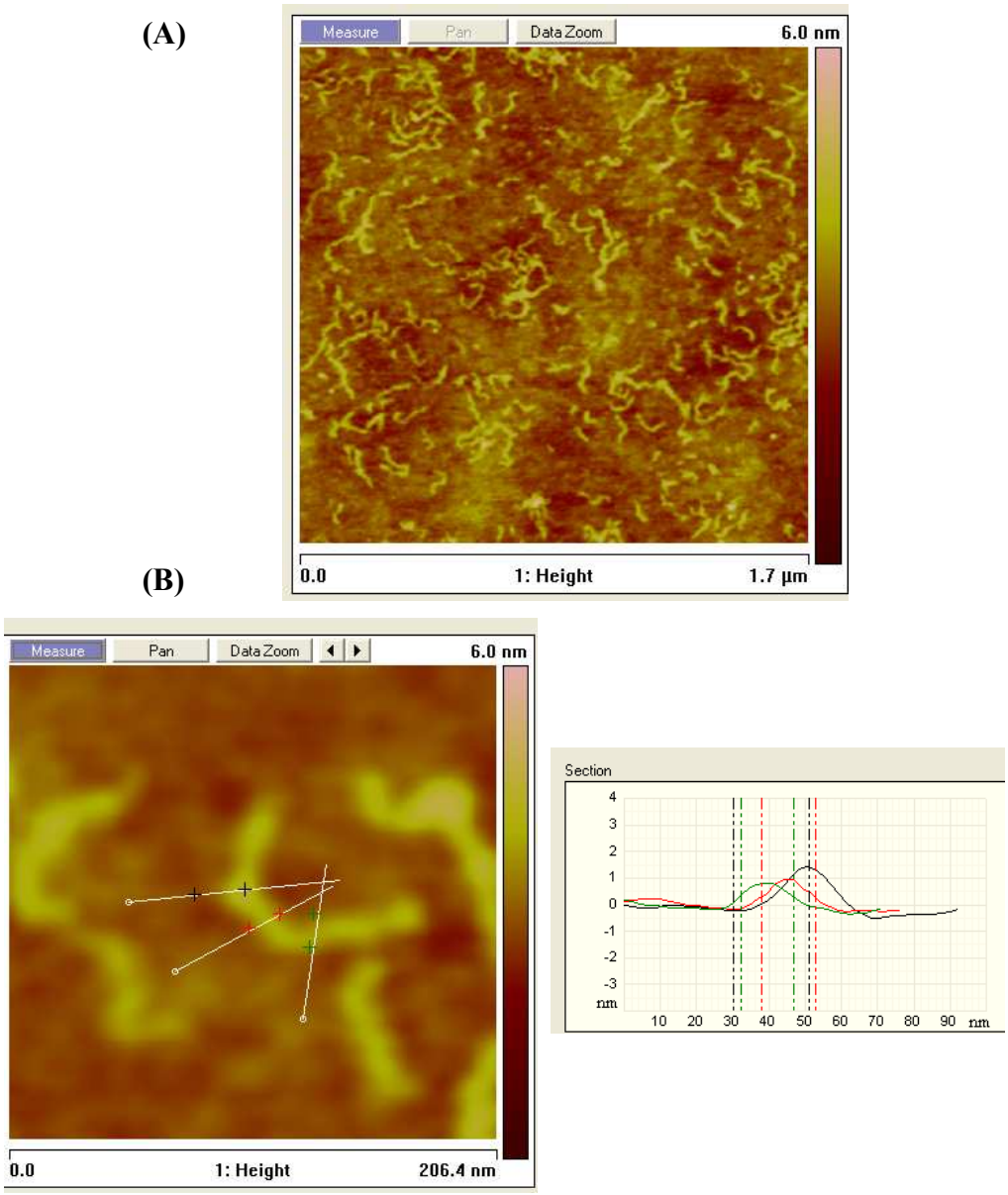


**Figure 5.45.** Tapping mode AFM images of HEC-g-PLA brush polymer; (A) 1.7 µm scale and (B) 206 nm scale with cross-sectional analysis.

### 5.3.3.4.2. Synthesis of HEC with PCL Grafts

PCL was also grafted onto HEC backbone to produce a hydrophobically modified HEC with potentially biodegradable grafts (PCL). The same synthetic strategy used in the previous section (5.3.3.3.2) was applied here. The weight ratio of the fully azide functionalised HEC **5.1** to the mono-alkyne end capped PCL (chapter 4) was 1:1 wt % and the excess remaining azide functionalities on HEC were capped with ester functionality *via* sequential Click reactions.

The procedure involved the sequential addition of the mono-alkyne end capped PLA and ethyl propiolate to a solution of fully azide functionalised HEC **5.1** in DMSO, containing the copper catalytic system, Scheme 5.17.

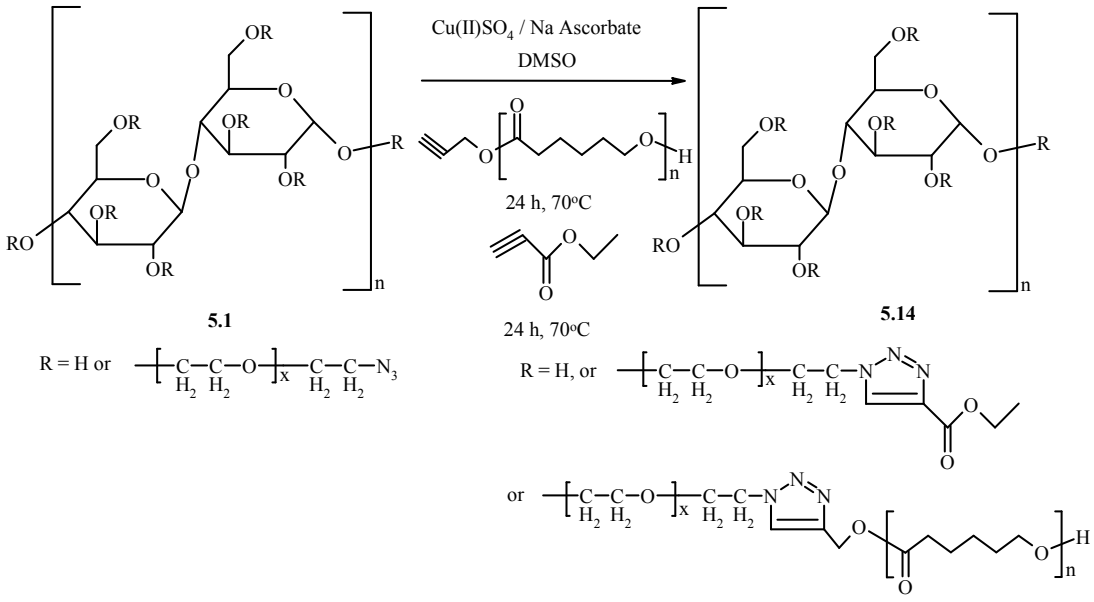


**Scheme 5.17.** Synthesis of HEC grafted with PCL

The CP Solid-state $^{13}$C-NMR spectrum of **5.14** showed the successful Click reaction on HEC as demonstrated by appearance of two new peaks at 139.75 and 131.53 ppm, assigned to the triazole ring, Fig. 5.46. It also showed the peaks due to PCL grafts as well as those for ethyl propiolate functionality. Moreover, the peaks corresponding to the HEC backbone were observed in the same regions and no other unassignable peaks were seen in the spectrum.

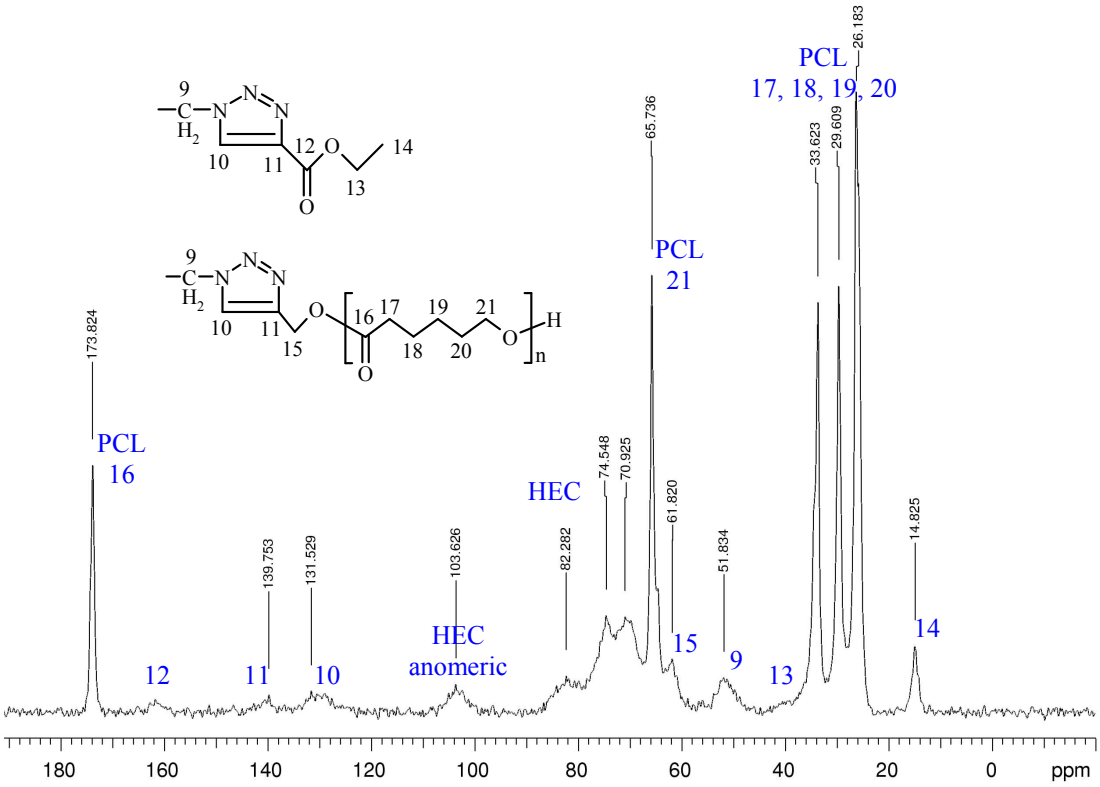


**Figure 5.46.** Solid-state $^{13}$C-NMR (CP exp.) spectrum of HEC grafted with PCL **5.14**

The IR spectrum of **5.14** (Fig. 5.47.B) compared to that of **5.1** (Fig. 5.47.A) showed no residual peak at 2090 cm$^{-1}$ for the azide group, confirming the complete conversion to the clicked product. It also showed appearance of a new peak at 1735 cm$^{-1}$, assigned to the carbonyl group of the ethyl ester functionality and PCL grafts on HEC. Furthermore, the decrease in the intensity of the peak at ~3400 cm$^{-1}$, due to the OH groups (moisture and structure) indicated the hydrophobic character of the product.

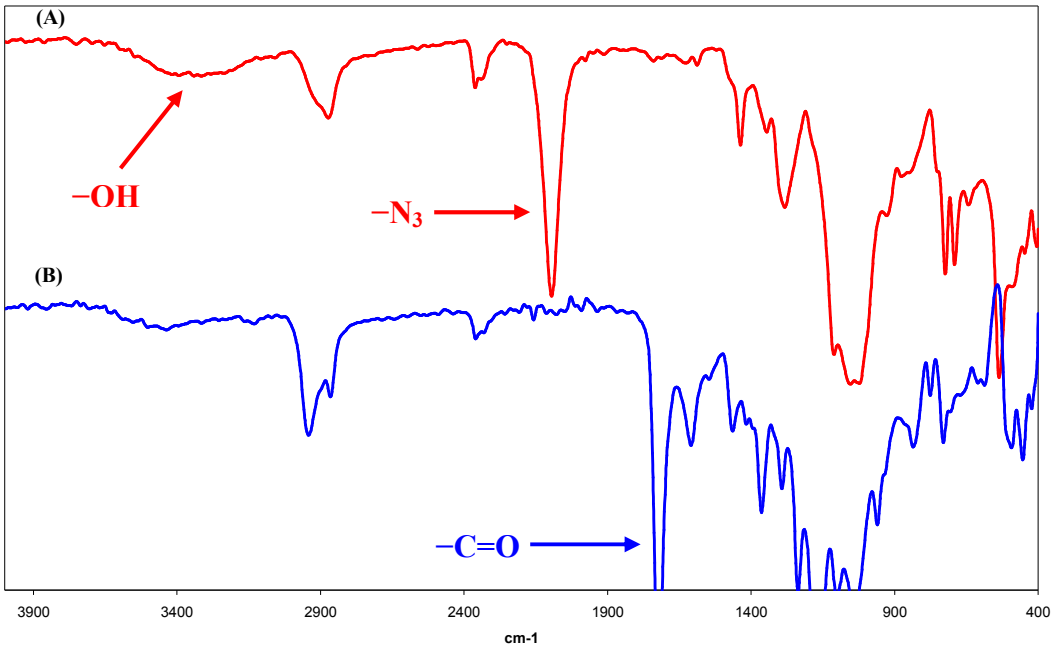


**Figure 5.47.** FT-IR spectrum of (A) fully azide functionalised HEC **5.1** and (B) HEC grafted with PCL **5.14**

### 5.3.3.5. Hydrophilic Modification of HEC

The hydrophilically modified HEC was prepared *via* grafting with PEG. The PEG grafts are known to be hydrophilic and biocompatible.

#### 5.3.3.5.1. Synthesis of Mono-alkyne Terminated PEG methyl ether

Mono-alkyne terminated PEG methyl ether **5.15** was successfully prepared by etherification reaction between commercially available mono-hydroxyl terminated PEG methyl ether ($M_n$ ~550 $gmol^{-1}$) and propargyl bromide, Scheme 5.18.

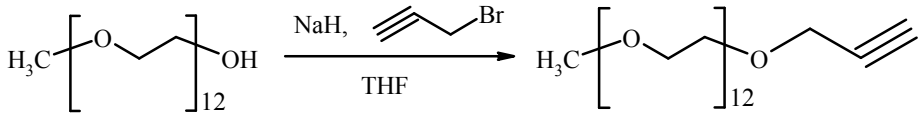


**5.15**

**Scheme 5.18.** Synthesis of mono-alkyne terminated PEG methyl ether

The hydroxyl group of the mono-hydroxyl terminated PEG methyl ether was quantitatively converted into alkyne functionality to produce **5.15**, according to $^1$H-NMR spectroscopy. This was shown by the complete disappearance of the peak due to

the hydroxyl groups in PEG at 2.92 ppm, Fig. 5.48.A. Moreover, the peaks due to the alkyne proton ($H_6$) at 2.40 and the $CH_2$ protons adjacent to the alkyne group ($H_5$) at 4.12 ppm, were observed (Fig. 5.48.B).

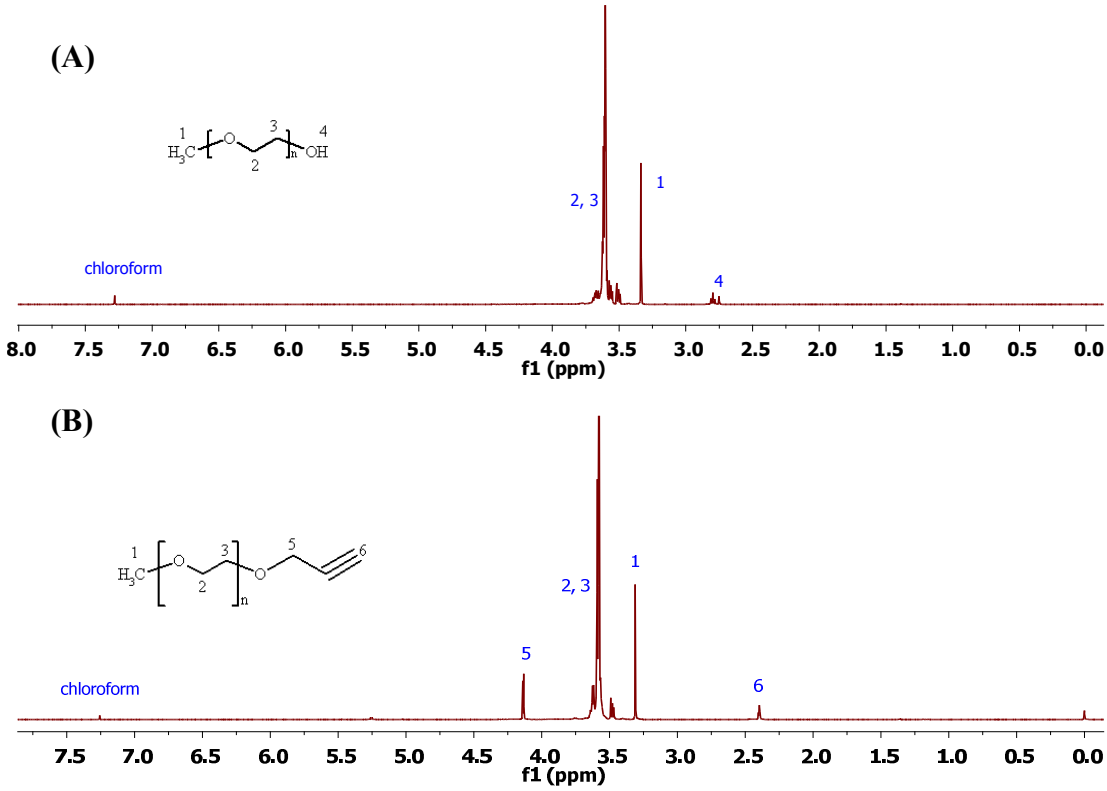


**Figure 5.48.** $^1$H-NMR spectra of (A) mono-hydroxyl terminated PEG methyl ether and (B) mono-alkyne terminated PEG methyl ether **5.15** in $CDCl_3$

### 5.3.3.5.2. Synthesis of HEC with PEG Grafts

PEG was successfully grafted onto HEC backbone *via* Click reaction between the fully azide functionalised HEC **5.1** and mono-alkyne terminated PEG methyl ether **5.15**, Scheme 5.19. The synthetic procedure aimed to produce fully PEG grafted HEC (HEC-g-PEG).

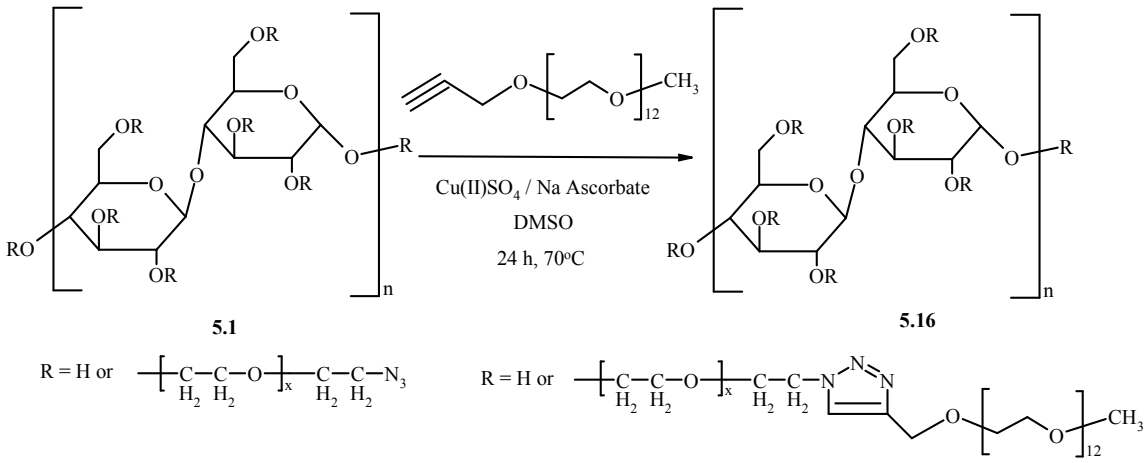


**Scheme 5.19.** Synthesis of HEC-g-PEG

Grafting with PEG improved the solubility of HEC and hence it was possible to characterise the grafted product by solution NMR in DMSO-$d_6$. The solution $^{13}$C-NMR spectrum of **5.16** showed clearly the successful Click reaction on HEC as demonstrated by appearance of two new peaks at 144.88 and 124.60 ppm, assigned to the triazole ring (Fig. 5.49). It also showed the peaks due to PEG grafts ($C_{13}$, $C_{14}$ and $C_{15}$) as well as those for HEC backbone. Moreover, there were no other unassignable peaks seen in the spectrum.

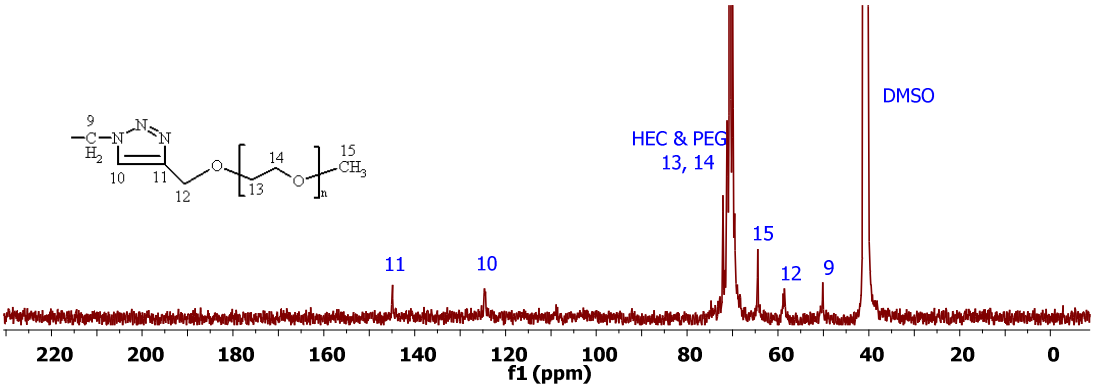


**Figure 5.49.** $^{13}$C-NMR spectrum of HEC-g-PEG **5.16** in DMSO-$d_6$ at 80 $^{o}$C

The IR spectrum of **5.16** (Fig. 5.50.B) compared to that of **5.1** (Fig. 5.50.A) showed no residual peak at 2090 $cm^{-1}$ for the azide group, confirming the complete conversion to the clicked product. It also showed the enhancement in the hydrophilic character of the HEC-g-PEG as demonstrated by the increase in the intensity and broadening of the peak due to OH groups at ~3500 $cm^{-1}$.

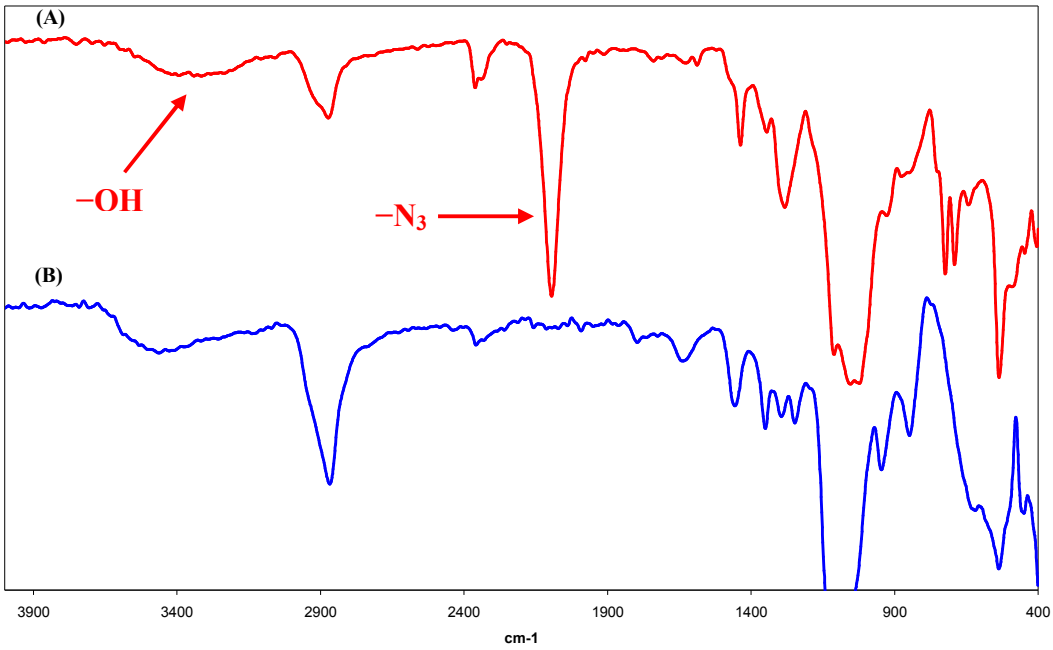


**Figure 5.50.** FT-IR spectrum of (A) fully azide functionalised HEC **5.1** and (B) HEC-g- PEG **5.16**

## 5.4. Summary

Click chemistry was utilised successfully on HEC to produce new polysaccharide based materials. For the first time, the azide functionalisation reaction of HEC was demonstrated using a one pot reaction procedure. $^{13}$C-NMR spectroscopy was shown to be an efficient method for quantitative determination of the azide functionalities on HEC. Different functionalities were introduced onto HEC *via* coupling reaction between azide functionalised HEC and alkyne terminated compounds. FT-IR was shown to be an easy method to demonstrate success of Click reactions and the complete conversion of azide functionalities to triazole rings. Solid state $^{13}$C-NMR spectroscopy was also shown to be a good alternative characterisation method for materials with poor solubility behaviour. Neutral and ionic compositions of HEC were successfully obtained. Carboxylic acid and/or 1$^{ry}$ amine functionalities on HEC will dissociate in aqueous medium to generate polyelectrolytes or polyampholytes.

Novel compositions of HEC containing PDMS chains were prepared *via* sequential Click reactions. Alkyne terminated PDMS was first prepared and then coupled with only about 5 % of the azide functionalities on HEC. The remaining azide functionalities on HEC were subsequently reacted with other alkyne terminated compounds. These compositions were designed so that HEC is chemically bonded to PDMS and bears charged functionalities along the polymer backbone, which is expected to receive a great interest by Akzo Nobel in personal care and cosmetics applications.

PLA, PCL and PEG were grafted onto HEC backbone using Click reaction to obtain hydrophobically and hydrophilically modified HEC materials. In these processes, alkyne terminated PLA, PCL or PEG were reacted with azide functionalised HEC using different molar ratios. AFM images of the fully HEC-g-PLA revealed that the material is a brush polymer.

## 5.5. References


1. Z. J. Witczak, K. A. Nieforth, *Carbohydrates in drug design*. Marcel Dekker: New York, **1997**.
2. K. L. Goa, P. Benfield, *Drugs* **1994**, *47*, 536-566.
3. T. E. McAlindon, M. P. LaValley, D. T. Felson, *Jama-Journal of the American Medical Association* **2000**, *284*, 1242-1242.
4. Shao, B.-M.; Xu, W.; Dai, H.; Tu, P.; Li, Z.; Gao, X.-M. *Biochemical and Biophysical Research Communications* **2004**, *320*, 1103–1111.
5. Zhang, W.; Yang, J.; Chen, J.; Hou, Y.; Han, X. *Biotechnology and Applied Biochemistry* **2005**, *42*, 9–15.
6. M. Rinaudo, *Biomacromolecules* **2004**, *5*, 1155-1165.
7. G. L. Brode, R. L. Kreeger, E. M. Partain, J. L. Pavlichko, *Journal of the Society of Cosmetic Chemists* **1988**, *39*, 78-78.
8. H. J. Buschmann, E. Schollmeyer, *Journal of Cosmetic Science* **2002**, *53*, 185-191.
9. E. D. Goddard, J. V. Gruber, *Principles of Polymer Science and Technology Cosmetics and Personal Care*. Dekker: New York, **1999**.
10. R. A. A. Muzzarelli, C. Muzzarelli, *Polysaccharides I: Structure, Characterization and Use*: *Advances in Polymer Science* **2005**, *186*, 151-209.
11. T. Akimoto, K. Kawahara, Y. Nagase, T. Aoyagy, *Macromol. Chem. Phys.* **2000**, *201*, 2729.
12. R. Wagner, L. Richter, R. Wersig, G. Schmaucks, B. Weiland, J. Weissmüller, J. Reiners, *Applied Organometallic Chemistry* **1996**, *10*, 421.
13. R. Wagner, L. Richter, Y. Wu, B. Weiland, J. Weissmüller, J. Reiners, E. Hengg, A. Kleewein, *Applied Organometallic Chemistry* **1998**, *12*, 47.
14. D. Henkensmeier, B. C. Abele, A. Candussio, J. Thiem, *Macromolecular Chemistry and Physics* **2004**, *205*, 1851.
15. C. Racles, T. Hamaide, *Macromolecular Chemistry and Physics* **2005**, *206*, 1757.
16. C. Racles, T. Hamaide, A. Ioanid, *Applied Organometallic Chemistry* **2006**, *20*, 235.
17. WO2006127883 (**2006**), Dow Corning Corp and Genencor Int., invs.: E. J. Joffre, B. K. Johnson, B. J. Swanton, M. S. Starch.

18. WO2006127882 (**2006**), Dow Corning Corp and Genencor Int., invs.: F. V. Carrillo, M. Costello, S. F. A. Creutz, L. Deklippel, B. Henault, E. J. Joffre, J. C. McAuliffe, V. K. O'Neil, C. Simon.
19. K. J. Quinn, J. M. Courtney, *British Polymer Journal* **1988**, *20*, 25-32.
20. M. Rutnakornpituk, P. Ngamdee, P. Phinyocheep, *Polymer* **2005**, *46*, 9742-9752.
21. J. Schulze Nahrup, Z. M. Gao, J. E. Mark, A. Sakr, *International Journal of Pharmaceutics* **2004**, *270*, 199–208.
22. S. Kobayashi, H. Uyama, S. Kimura, *Chemical Reviews* 2001, *101*, 3793.
23. M. Jahn, D. Stoll, R. A. J. Warren, L. Szabo, P. Singh, H. J. Gilbert, V. M.-A. Ducros, G. J. Davis, S. G. Withers, *Chemical Communications* **2003**, *33*, 1327.
24. S. Halila, M. Manguian, S. Fort, S. Cottaz, T. Hamaide, E. Fleury, H. Driguez, *Macromolecular Chemistry and Physics* **2008**, *209*, 1282–1290.
25. M. Krouit, J. Bras, M. N. Belgacem, *European Polymer Journal* **2008**, *44*, 4074–4081.
26. A. L. Cimecioglu, D. H. Ball, S. H. Huang, D. L. Kaplan, *Macromolecules* **1997**, *30*, 155-156.
27. J. Shey, K. M. Holtman, R. Y. Wong, K. S. Gregorski, A. P. Klamczynski, W. J. Orts, G. M. Glenn, S. H. Imam, *Carbohydrate Polymers* **2006**, *65*, 529-534.
28. A. L. Cimecioglu, D. H. Ball, D. L. Kaplan, S. H. Huang, *Macromolecules* **1994**, *27*, 2917-2922.
29. R. Appel, *Angewandte Chemie-International Edition in English* **1975**, *14*, 801-811.
30. J. R. Demember, L. D. Taylor, S. Trummer, L. E. Rubin, C. K. Chiklis, *Journal of Applied Polymer Science* **1977**, *21*, 621-627.
31. T. D. Nelson, R. D. Crouch, *Synthesis-Stuttgart* **1996**, 1031.
32. Z. P. Tan, L. Wang, J. B. Wang, *Chinese Chemical Letters* **2000**, *11*, 753-756.
33. A. V. Dobrynin, R. H. Colby, M. Rubinstein, *Journal of Polymer Science Part B-Polymer Physics* **2004**, *42*, 3513-3538.
34. W. Patnode, D. F. Wilcock, *Journal of the American Chemical Society* **1946**, *68*, 358-363.
35. D. W. Scott, *Journal of the American Chemical Society* **1946**, *68*, 2294-2298.
36. D. F. Wilcock, *Journal of the American Chemical Society* **1946**, *68*, 691-696.
37. S. J. Clarson, J. A. Semlyen, *Polymer* **1986**, *27*, 91-95.
38. J. F. Brown, Slusarcz.Gm, *Journal of the American Chemical Society* **1965**, *87*, 931.
39. K. Dodgson, J. A. Semlyen, *Polymer* **1977**, *18*, 1265-1268.

40. J. A. Semlyen, *Cyclic polymers. Second edition* **2000**, Kluwer Academic Publishers, ISBN 0-306-47117-5, i-xx, 1-790.
41. B. M. White, W. P. Watson, E. E. Barthelme, H. W. Beckham, *Macromolecules* **2002**, *35*, 5345-5348.
42. H. R. Kricheldorf, G. Schwarz, *Macromolecular Rapid Communications* **2003**, *24*, 359-381.
43. Y. Xia, J. A. Kornfield, R. H. Grubbs, *Macromolecules* **2009**, *42*, 3761-3766.

# Chapter 6

# Combination of Click Chemistry and ROMP

## 6.1. Introduction

Synthesis of macromolecules with complex but well-defined molecular structures has been a challenge for synthetic polymer chemists. The properties of the macromolecules depend on not only the chemical composition and molecular weight of the chains but also their topology. Graft copolymers, which contain extensive regular branching along a linear polymer backbone, are particularly useful as they accommodate a large number of functional groups on much less volume than linear polymers of the same molecular weight. When the side chains are distributed densely enough so that they are stretched away from the backbone, these highly compact macromolecules adopt cylindrical or wormlike structures.[1,2] These macromolecules are a special class of graft copolymers and known as cylindrical (bottle) brush polymers.[3-5]

Three general methods have been applied to synthesise graft copolymers; "grafting from", "grafting onto", and "grafting through".[4,5] The "grafting from" method involves the growth of side chains from polymeric backbones with pendant initiation sites. The only downside for this strategy is the possible limited initiation efficiency from the pendant initiation sites due to their high density.[6] The "grafting onto" method has the advantage of allowing for individual preparation of backbone polymers and side chains. The down side is that the grafting becomes progressively more difficult as the conversion increases, leading to limited grafting density, even when a large molar excess of side chains is used.[7,8] The only method guarantees complete grafting (e.g., one side chain per repeating unit) is "grafting through", known as the macromonomer approach. Additionally, this approach can afford the most precise and easiest control of side chain and main chain lengths, provided that the polymerisation is efficient and controlled. However, synthesis of polymacromonomers with a high DP and low PDI remains synthetically challenging, largely due to the inherently low concentration of polymerisable groups and the severe steric hindrance of side chains.

The applications for the properly tailored graft copolymers are usually affected by the properties of the backbone and the branches (side chains). Polynorbornenes are selected as the backbones for graft copolymers because the ROMP of substituted norbornenes is a well-established methodology for the synthesis of structurally precise polymers. Moreover, ruthenium Grubbs catalysts have been used in the ROMP of macromonomers because of their excellent functional group tolerance.[9-11] and their ability to polymerise sterically demanding monomers.[12-14]

PEG is a very attractive side chain for graft copolymers because of its water solubility and biocompatibility. Development of PEG functionalised materials has been widely reported in the literature,[15-17] with increasing interest in biomedical applications.[18-21] The synthesis of PEG macromonomers which undergo ROMP has been reported by Gnanou et al.[22-25] by the combination of anionic polymerisation and ROMP. Recently, different research groups reported the synthesis of amphiphilic comb-like polymers by ROMP of PEG macromonomers.[26-29] The post polymerisation technique has also been used to design polynorbornene-based block copolymers containing PEG as a hydrophilic block and a hydrocarbon chain as a hydrophobic block. The copolymers were self-assembled to form nanoparticles.[30] More recently, ROMP-based synthesis followed by PEGylation *via* Click chemistry has been reported to generate amphiphilic copolymers, which are able to self-assemble and accumulate at tumor sites. This was also claimed to be potentially useful for cancer *in-vivo* diagnosis.[31]

Aliphatic polyesters such as PLA and PCL are another interesting potential candidate as side chains for graft copolymers. Indeed, the unique properties of these polymers, such as biodegradability, biocompatibility and good mechanical properties, justified their importance in the field of biomaterials. Moreover, the versatility of ROP of lactides and lactones has opened the way to the molecular engineering of these biodegradable polymers.[32] They have been widely used in biomedical applications such as sutures, drug delivery carriers, scaffolds in tissue engineering and implants to ensure a temporary mechanical or therapeutic function.[33-36] Recently, Khosravi et al.[37] described the synthesis of well-characterised oxanorbornene-based macromonomers with either one (*exo*-) or two (*exo,exo*- or *endo,exo*-) PLA chains of variable length. They also investigated the subsequent ROMP reactions of these macromonomers catalysed by well-defined Grubbs ruthenium initiators. Furthermore, the hydrolytic degradation behaviour of the graft copolymers was studied in detail and the results indicated that, by changing the length of the polyoxanorbornene backbone chain and the PLA grafts, it is possible to tailor the properties of the polymers under degradation to enhance their potential utility in biomedical applications. Xie et al.[38] reported the preparation of a novel well-defined amphiphilic brush copolymer based on polynorbornene with two different grafts, one hydrophobic PCL graft and one hydrophilic poly(2-(dimethylamino)ethyl methacrylate), on the same unit along the backbone. The synthetic method for this complex architecture involved combination of ROP, ROMP and ATRP. Grubbs et al.[39] reported the synthesis of a series of random

and block copolymers from a pair of macromonomers containing PLA and poly(*iso*- or *n*-butylacrylate) (P*i*BA/P*n*BA) side chains at similar molecular weights. The norbornenyl macromonomer containing P*i*BA/P*n*BA was prepared by coupling azido-terminated polymers P*i*BA/P*n*BA made by ATRP with alkyne-functionalised norbornene. The norbornenyl macromonomer containing PLA was prepared by ROP of lactide using hydroxy functionalised norbornene as initiator. The self-assembly studies of these macromolecules suggested that the brush block copolymer backbone adopted an extended conformation.

Despite the importance of PEG and PCL as side chains for graft copolymers, little work, compared to the bulk of the literature, has really been reported on PEG / PCL functionalised polynorbornenes. This chapter reports the facile synthesis of various graft copolymers prepared efficiently by a combination of Click chemistry and well-defined ROMP. The combination of the two techniques allows the synthesis of polymeric materials with novel microstructures. The graft copolymers are prepared *via* two different methods; "grafting through" (the macromonomer approach) and "grafting onto". The side chains in the graft copolymers are PEG and PCL as they are known to be biocompatible / biodegradable.

## 6.2. Experimental

### 6.2.1. Materials

Grubbs 1st generation (**G-I**) ($RuCl_2(PCy_3)_2(=CHPh)$) and 2nd generation (**G-II**) ($RuCl_2(PCy_3)(IMes)_2(=CHPh)$) initiators were purchased from Sigma – Aldrich.

All other chemicals and reagents used in the synthesis were also purchased from Sigma – Aldrich and used without further purification. All dry solvents were obtained from the Solvent Purification System (SPS), Chemistry Department, Durham University.

### 6.2.2. Instrumentation and Measurements

$^1$H-NMR spectra were recorded using deuteriated solvent lock on a Varian Mercury 400 or a Varian Inova 500 spectrometer at 400 MHz and 500 MHz, respectively. Chemical shifts are quoted in ppm, relative to tetramethylsilane (TMS), as the internal reference. $^{13}$C-NMR spectra were recorded at 101 MHz or 126 MHz (2000 scans) using continuous broad band proton decoupling and a 3 S recycle dely, and therefore not quantitative; chemical shifts are quoted in ppm, relative to $CDCl_3$ (77.550 ppm). The following abbreviations are used in listing NMR spectra: s = singlet, d = doublet, t = triplet, q = quartet, m = multiplet, b = broad.

Electron Impact (EI) and Electrospray ($ES^+$) mass spectra were recorded on a Thermo Finnigan LTQ FT spectrometer operating at 70 eV with the ionisation mode as indicated.

FT-IR spectra were recorded on a Perkin Elmer 1600 series FT-IR spectrometer fitted with a golden gate. The samples were used as solids or liquids.

Molecular weight analysis was carried out by gel permission chromatography (GPC) on a Viscotek TDA 302 with refractive index detector. Two 300 mm PLgel 5 μm mixed C columns (with a linear range of molecular weight from 200 to 2 000 000 $gmol^{-1}$) were used. THF was used as the eluent with a flow rate of 1.0 $mLmin^{-1}$ at 30 $^oC$.

A Digital Instruments Nanoscope IV AFM was used to record tapping mode micrographs of the irradiated polymers. 256 x 256 line images were recorded at a scanning speed of 1 Hz, and an integrated hot stage was used to carry out annealing steps between scans. Annealing was carried out for 1800 s at 110, 121.5, and 132.2 $^oC$. Surface height versus cross-section was measured for each AFM image with the Nanoscope V6 online software.

### 6.2.3. Synthesis of Azide Terminated PEG mono-methyl ether 6.1

ρ-Toluenesulfonyl chloride (6.9 g, 36 mmol) was added slowly to a solution of PEG mono-methyl ether ($M_n$ ~550) (2 g, 3.6 mmol) in pyridine (36 ml) in a two-necked round-bottom flask, equipped with magnetic stirrer and solid addition funnel. The reaction mixture was stirred for 24 hr at ambient temperature. The reaction mixture was poured into ice cold water (50 mL) and was then extracted three times with DCM. The organic layer was washed twice with cold hydrochloric acid (6M) and three times with cold distilled water. The organic layer was dried over anhydrous $MgSO_4$ and the solvent was removed under reduced pressure to give a viscous liquid; tosyl terminated PEG mono-methyl ether intermediate; confirmed by NMR. Sodium azide (13 g, 0.2 mol) was added to the viscous liquid product and the mixture was stirred in DMF (36 ml) at 120 °C for 24 hr. The solvent was removed under reduced pressure. DCM (30 mL) was then added and was washed three times with cold distilled water. The organic layer was dried over anhydrous $MgSO_4$ and the solvent was removed under reduced pressure to give a viscous liquid **6.1**, yield 68 % (1.4 g, 2.5 mmol).

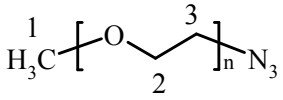


**6.1**

**Figure 6.1.** Structure of azide terminated PEG mono-methyl ether with numerical assignment for NMR

$^1$H-NMR (500 MHz, $CDCl_3$): δ 3.60 – 3.49 (m, 48H, $H_{2,3}$), 3.33 (s, 3H, $H_1$).
$^{13}$C-NMR (126 MHz, $CDCl_3$): δ 72.11 – 70.22 ($C_{2,3}$), 59.22 ($C_1$), 50.85 ($C_4$).
FT-IR ($cm^{-1}$): ~2100 (-$N_3$).

### 6.2.4. Synthesis of *exo*-2,3-Dicarboxylic Acid Anhydride-7-Oxanorbornene 6.2

The product **6.2** was prepared according to the following literature procedure.[40,41]
Maleic anhydride (9.8 g, 0.1 mol) was dissolved in $Et_2O$ (50 mL) in a three-necked 100 mL round-bottom flask, equipped with magnetic stirrer, thermometer, reflux condenser and rubber seal septum, under $N_2$ atmosphere. Furan (8.0 mL, 7.5 g, 0.11 mol – 10 % excess) was injected to the solution. The mixture was stirred at ambient temperature for 48 hr. Well-defined needles appeared in the flask. The crystals were filtered, washed

with $Et_2O$ and dried under reduced pressure at ambient temperature for 24 hr to give the product **6.2**, mp 120 – 122 $^oC$, yield 80 % (13.3 g, 0.08 mol).

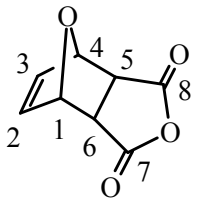


**6.2**

**Figure 6.2.** Structure of *exo*-2,3-dicarboxylic acid anhydride-7-oxanorbornene monomer with numerical assignment for NMR

$^1$H-NMR (400 MHz , DMSO-$d_6$): δ 6.58 (t, $J$ = 0.9 Hz, 2H, $H_{2,3}$), 5.35 (t, 2H, $H_{1,4}$), 3.33 (m, 2H, $H_{5,6}$).
$^{13}$C-NMR (101 MHz, DMSO-$d_6$): δ 171.5 ($C_{7,8}$), 136.8 ($C_{2,3}$), 81.6 ($C_{1,4}$), 49.1 ($C_{5,6}$).

### 6.2.5. Synthesis of *exo,exo*-2,3-Bis(Hydroxymethyl)-7-Oxanorbornene 6.3

The product **6.3** was prepared according to the following literature procedure.[40,41]
A solution of exo-2,3-dicarboxylic acid anhydride-7-oxanorbornene **6.2** (4.15 g, 25 mmol) in THF (80 mL) was added dropwise to a slurry of $LiAlH_4$ (1.99 g, 52.5 mmol – 5 % excess) in THF (40 mL) in a three-necked 250 mL round-bottom flask, equipped with magnetic stirrer, thermometer, reflux condenser and kept under $N_2$ atmosphere. The mixture was stirred at ambient temperature for 12 hr, followed by gentle reflux at 70 $^oC$ for 5 hr. Aqueous solution of NaOH in water (5 %, 2 mL) was added to the cooled mixture to destroy excess reagent. The solid was removed by filtration. The filtrate was dried over anhydrous $MgSO_4$ and was then flashed through an alumina column. The solvent was removed under reduced pressure to give a viscous liquid product **6.3**, yield 59 % (2.3 g, 14.8 mmol).

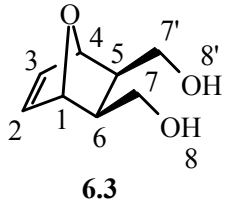


**6.3**

**Figure 6.3.** Structure of *exo,exo*-2,3-bis(hydroxymethyl)-7-oxanorbornene monomer with numerical assignment for NMR

$^{1}$H-NMR (400 MHz, $CDCl_3$): δ 6.40 (t, *J* = 0.9 Hz, 2H, $H_{2,3}$), 4.69 (t, *J* = 0.9 Hz, 2H, $H_{1,4}$), 4.09 (bs, 2H, $H_{8,8'}$), 3.80 (m, 4H, $H_{7,7'}$), 1.95 (m, 2H, $H_{5,6}$).
$^{13}$C-NMR (101 MHz, $CDCl_3$): δ 135.8 ($C_{2,3}$), 81.2 ($C_{1,4}$), 62.7 ($C_{7,7'}$), 42.4 ($C_{5,6}$).
ESI-MS: $[179.2 + Na]^+$.

### 6.2.6. Synthesis of *exo*,*exo*-2,3-Bis(Propargoxymethyl)-7-Oxanorbornene 6.4

A solution of *exo*,*exo*-2,3-bis(hydroxymethyl)-7-oxanorbornene **6.3** (2.35 g, 0.0151 mol) in THF (20 mL) was added dropwise at 0 $^{o}$C to a slurry of NaH (0.744 g, 0.031 mol – 5 % excess) in THF (15 mL) in a three-necked 250 mL round-bottom flask, equipped with magnetic stirrer, thermometer, reflux condenser and kept under $N_2$ atmosphere. After 30 min, propargyl bromide (80 % in toluene) (3.5 mL, 4.61 g, 0.031 mol – 5 % access) was syringed. The mixture was kept another 30 min at 0 $^{o}$C and then stirred at ambient temperature for 15 hr. The solvent was removed under reduced pressure. $Et_2O$ (100 mL) was added to the residue. The organic layer was washed with water (2x20 mL) and dried over anhydrous $MgSO_4$. The product was purified by flash column chromatography (alumina column). The solvent was removed under reduced pressure to give the orange viscous product **6.4**, yield 66 % (2.31 g, 0.01 mol).

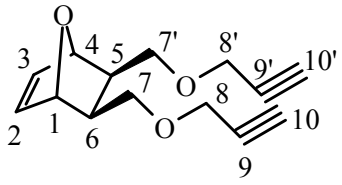


**6.4**

**Figure 6.4.** Structure of *exo,exo*-2,3-bis(propargoxymethyl)-7-oxanorbornene monomer with numerical assignment for NMR

$^{1}$H-NMR (400 MHz, $CDCl_3$): δ 6.32 (t, *J* = 0.9 Hz, 2H, $H_{2,3}$), 4.79 (t, *J* = 0.9 Hz, 2H, $H_{1,4}$), 4.10 (m, 4H, $H_{8,8'}$), 3.50 (m, 4H, $H_{7,7'}$), 2.45 (t, *J* = 2.4 Hz, 2H, $H_{10,10'}$), 1.91 (m, 2H, $H_{5,6}$).
$^{13}$C-NMR (101 MHz, $CDCl_3$): δ 135.44 ($C_{2,3}$), 80.49 ($C_{1,4}$), 79.67 ($C_{9,9'}$), 74.57 ($C_{10,10'}$), 69.46 ($C_{7,7'}$), 58.23 ($C_{8,8'}$), 39.81 ($C_{5,6}$).
ESI-MS: $[255.2 + Na]^+$.

### 6.2.7. Synthesis of Oxanorbornenyl Di-PEG Macromonomer 6.5

In a vial, azide terminated PEG mono-methyl ether **6.1** (500 mg, 0.86 mmol), alkyne functionalised oxanorbornene monomer **6.4** (100 mg, 0.43 mmol), copper (II) sulfate pentahydrate (22 mg, 0.086 mmol), sodium ascorbate (34 mg, 0.172 mmol), and t-butanol / water (3:1, 8 mL) were stirred. The mixture was heated up to 55 $^{o}$C in an oil bath for 24 hr. The product was extracted with DCM. The organic layer was washed three times by distilled water and dried over anhydrous $MgSO_4$. The solvent was removed under reduced pressure to give the oily product **6.5**, yield 95 % (570 mg, 0.41 mmol).

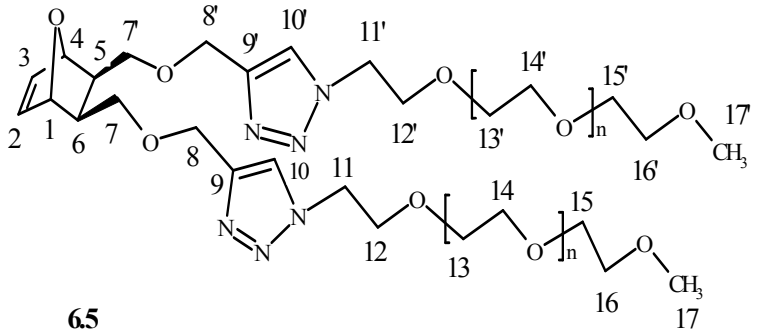


**Figure 6.5.** Structure of oxanorbornenyl di-PEG macromonomer with numerical assignment for NMR

$^{1}$H-NMR (500 MHz, $CDCl_3$): δ 7.70 (s, 2H, $H_{10,10'}$), 6.25 (s, 2H, $H_{2,3}$), 4.75 (s, 2H, $H_{1,4}$), 4.55 (s, 4H, $H_{8,8'}$), 4.49 (m, 4H, $H_{11,11'}$), 3.81 (m, 4H, $H_{12,12'}$), 3.59 – 3.49 (m, 80H, $H_{13,13',14,14',15,15',16,16',7,7'}$), 3.31 (s, 6H, $H_{17,17'}$), 1.85 (m, 2H, $H_{5,6}$).

$^{13}$C-NMR (126 MHz, $CDCl_3$): δ 144.99 ($C_{9,9'}$), 135.72 ($C_{2,3}$), 124.05 ($C_{10,10'}$), 80.78 ($C_{1,4}$), 72.15 ($C_{16,16'}$), 70.82 – 70.70 ($C_{13,13',14,14',15,15'}$), 70.04 ($C_{7,7'}$), 69.70 ($C_{12,12'}$), 64.69 ($C_{8,8'}$), 59.27 ($C_{17,17'}$), 50.46 ($C_{11,11'}$), 40.10 ($C_{5,6}$).

GPC: $M_n$ = 1,490 gmol$^{-1}$, $M_w$ = 1,680 gmol$^{-1}$, PDI =1.1.

### 6.2.8. Synthesis of Polyoxanorbornene-g-PEG 6.6

In a vial, a solution of the PEG macromonomer **6.5** (166 mg, 0.12 mmol) in $CDCl_3$ (0.6 mL) was added to a solution of Grubbs ruthenium 2$^{nd}$ generation initiator (10 mg, 0.012 mmol) in $CDCl_3$ (0.4 mL). The mixture was stirred for 10 – 15 min at ambient temperature. A sample of the mixture was transferred into an NMR tube equipped with

Young's tap to monitor the reaction progress by $^{1}$H-NMR. The polymer was precipitated in hexane and reprecipitated from DCM into hexane.

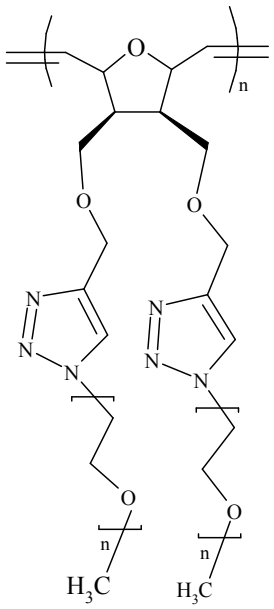

**6.6**

**Figure 6.6.** Structure of polyoxanorbornene-g-PEG

### 6.2.9. Synthesis of *exo*-5-{[(6-Bromohexyl) Oxy] Methyl}-2-Norbornene Monomer 6.7

The product **6.7** was prepared by the following literature procedure.[42]

A mixture of an n-hexane solution (150 mL) of *exo*-5-norbornene-2-methanol (8.46 mL, 0.07 mol), 1,6-dibromohexane (51.24 g, 0.21 mol), tetrabutylammonium hydrogen sulphate (1.19g, 3.5 mmol) and 50 % NaOH aqueous solution was allowed to react with stirring at ambient temperature for 12 hr. The mixture was boiled for a short time (about 1 hr). The resulting solution was extracted two times with diethyl ether (70 mL, each). Then it was washed two times with hydrochloric acid aqueous solution (20 %, 100 mL, each). The product was separated by evaporating the solvent after drying the solvent with anhydrous magnesium sulphate. The crude product was purified by vacuum distillation (b.p. 120 $^{o}$C under 1mmHg, yield 65%).

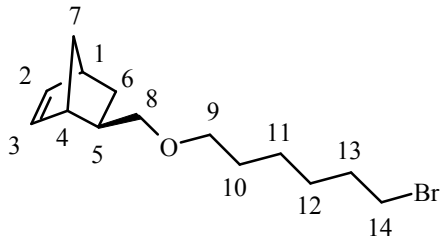


**6.7**

**Figure 6.7.** Structure of *exo*-5-{[(6-bromohexyl) oxy] methyl}-2-norbornene monomer with numerical assignment for NMR

$^1$H NMR (700 MHz, $CDCl_3$) δ 6.05 (ddd, $J$ = 3.0 Hz, 5.6 Hz, 37.7 Hz, 2H, $H_{2,3}$), 3.46 – 3.34 (m, 5H, $H_{8,9,14}$), 3.28 (t, $J$ = 9.2 Hz, 1H, $H_8$), 2.77 (s, 1H, $H_4$), 2.71 (s, 1H, $H_1$), 1.91 – 1.80 (m, 2H, $H_{10}$), 1.70 – 1.62 (m, 1H, $H_5$), 1.57 (m, 2H, $H_{13}$), 1.48 – 1.41 (m, 2H, $H_{11}$), 1.36 (ddd, $J$ = 5.4 Hz, 10.3 Hz, 11.0 Hz, 2H, $H_{12}$), 1.32 – 1.25 (m, 2H, $H_7$), 1.21 (ddd, $J$ = 2.0 Hz, 8.5 Hz, 10.8 Hz, 1H, $H_6$), 1.07 (dt, $J$ = 3.9 Hz, 11.6 Hz, 1H, $H_6$).
$^{13}$C NMR (176 MHz, $CDCl_3$) δ 136.58 (s, $C_2$), 136.55 (s, $C_3$), 75.52 (s, $C_8$), 70.79 (s, $C_9$), 44.97 (s, $C_7$), 43.67 (s, $C_1$), 41.50 (s, $C_4$), 38.84 (s, $C_5$), 33.81 (s, $C_{14}$), 32.73 (s, $C_{10}$), 29.71 (s, $C_6$), 29.50 (s, $C_{13}$), 27.97 (s, $C_{11}$), 25.39 (s, $C_{12}$).

### 6.2.10. Synthesis of Bromide Functionalised Polynorbornene 6.8

Using [M]/[I] = 10; DP = 10:

In a vial, a solution of the bromide functionalised norbornene monomer **6.7** (500 mg, 1.74 mmol) in $CDCl_3$ (1 mL) was added to a solution of Grubbs ruthenium 1$^{st}$ generation initiator (143 mg, 0.174 mmol) in $CDCl_3$ (0.5 mL). The mixture was stirred for 10 – 15 min at ambient temperature. A sample of the mixture was transferred into an NMR tube equipped with a young's tap to monitor the reaction progress by $^1$H-NMR. The polymer was precipitated into methanol. Ethyl vinyl ether (0.1 mL) was added to the polymer solution in a minimum amount of THF. The solution was stirred for 3 hr at ambient temperature. The polymer was reprecipitated into methanol and filtered. The polymer was dried under reduced pressure to give polymer **6.8**, yield 90 % (450 mg).

Using [M]/[I] = 200; DP = 200:

In a similar procedure, a solution of bromide functionalised norbornene monomer **6.7** (500 mg, 1.74 mmol) in $CDCl_3$ (1 mL) and a solution of Grubbs ruthenium 1$^{st}$ generation initiator (7.2 mg, 0.0087 mmol) in $CDCl_3$ (0.2 mL) were used. The polymer was dried under reduced pressure to give polymer **6.8**, yield 95 % (475 mg).

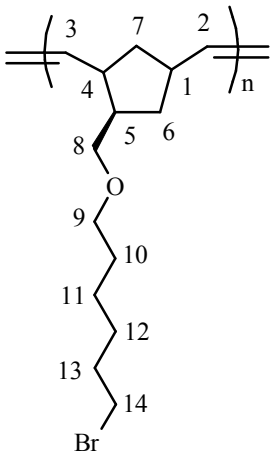


**6.8**

**Figure 6.8.** Structure of bromide functionalised polynorbornene with numerical assignment for NMR

$^{1}$H NMR (400 MHz, $CDCl_3$) δ 5.22 (m, 2H, $H_{2,3}$), 3.37 (m, 5H, $H_{8,9,14}$), 3.13 (t, $J$ = 8.5 Hz, 1H, $H_8$), 2.43 (s, 1H, $H_4$), 2.05 (s, 1H, $H_1$), 1.84 (m, 4H, $H_{10,13}$), 1.66 (s, 1H, $H_5$), 1.61 – 1.02 (m, 8H, $H_{11,12,7,6}$).

$^{13}$C NMR (101 MHz, $CDCl_3$) δ 131.91 (m, $C_{2,3}$), 74.12 (s, $C_8$), 70.84 (s, $C_9$), 46.52 (m, $C_7$), 45.15 (m, $C_1$), 41.70 (m, $C_4$), 36.59 (m, $C_5$), 33.90 (s, $C_{14}$), 32.76 (s, $C_{10}$), 29.17 (m, $C_{6,13}$), 28.01 (s, $C_{11}$), 25.42 (s, $C_{12}$).

### 6.2.11. Synthesis of Azide Functionalised Polynorbornene 6.9

Using polymer **6.8** of DP = 10:

In a vial, sodium azide (1.131 g, 0.0174 mol) was added to a solution of bromide functionalised polynorbornene **6.8** (400 mg) in DMF / THF (1:1, 5 mL). The mixture was stirred in an oil bath at 60°C for 24 hr. The product was precipitated by adding water. The polymer was filtered and washed three times by water. The polymer was reprecipitated from DMF / THF into water. After filtration, the polymer was dried under reduced pressure to give polymer **6.9**, yield 89 % (355 mg).

Using polymer **6.8** of DP = 200:

In a similar procedure, sodium azide (1.131 g, 0.0174 mol) and a solution of bromide functionalised polynorbornene **6.8** (360 mg) in DMF / THF (1:1, 5 mL) were used. The polymer was dried under reduced pressure to give polymer **6.9**, yield 92 % (330 mg).

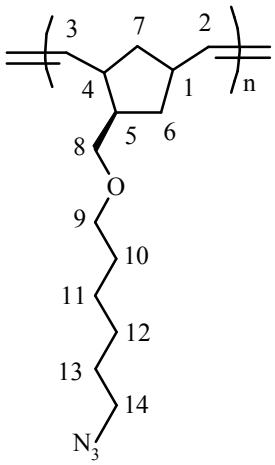


**6.9**

**Figure 6.9.** Structure of azide functionalised polynorbornene with numerical assignment for NMR

$^{1}$H NMR (400 MHz, $CDCl_3$) δ 5.23 (m, 2H, $H_{2,3}$), 3.36 (m, 3H, $H_{8,9}$), 3.24 (t, $J$ = 6.9 Hz, 2H, $H_{14}$), 3.14 (m, 1H, $H_8$), 2.43 (s, 1H, $H_4$), 2.04 (s, 1H, $H_1$), 1.84 (s, 2H, $H_{10}$), 1.64 (s, 1H, $H_5$), 1.57 − 1.11 (m, 10H, $H_{11,12,13,7,6}$).

$^{13}$C NMR (101 MHz, $CDCl_3$) δ 132.21 (m, $C_{2,3}$), 73.16 (s, $C_8$), 69.86 (s, $C_9$), 50.42 (s, $C_{14}$), 45.05 (m, $C_7$), 43.97 (m, $C_1$), 40.84 (m, $C_4$), 35.38 (m, $C_5$), 30.32 (s, $C_{10}$), 29.56 (s, $C_6$), 28.82 (s, $C_{13}$), 26.60 (s, $C_{11}$), 25.80 (s, $C_{12}$).

### 6.2.12. Synthesis of Polynorbornene-g-PCL 6.10

Using polymer **6.9** of DP = 10:

In a vial, azide functionalised polynorbornene **6.9** (50 mg, 0.02 mmol, 0.2 mmol of azide groups), alkyne end capped PCL (chapter 4) (2.291 g, 0.2 mmol), $CuSO_4.5H_2O$ (5 mg, 0.02 mmol), sodium ascorbate (8 mg, 0.04 mmol) and DMF / THF / water (1:1:0.1, 5.5 mL) were stirred. The mixture was kept in an oil bath at 60 $^{o}$C for 24 hr. The polymer was preciptated by adding water. The polymer was isolated by filtration. The polymer was reprecipitated from DMF / THF into water. After filtration, the polymer was dried under reduced pressure to give the clicked copolymer **6.10**, yield 90 % (2.11 g).

Using polymer **6.9** of DP = 200:

In a similar procedure, azide functionalised polynorbornene **6.9** (50 mg, 0.001 mmol, 0.2 mmol of azide groups), alkyne end capped PCL (chapter 4) (2.291 g, 0.2 mmol), $CuSO_4.5H_2O$ (5 mg, 0.02 mmol), sodium ascorbate (8 mg, 0.04 mmol) and DMF / THF

/ water (1:1:0.1, 5.5 mL) were used. The polymer was dried under reduced pressure to give the clicked copolymer **6.10**, yield 93 % (2.175 g).

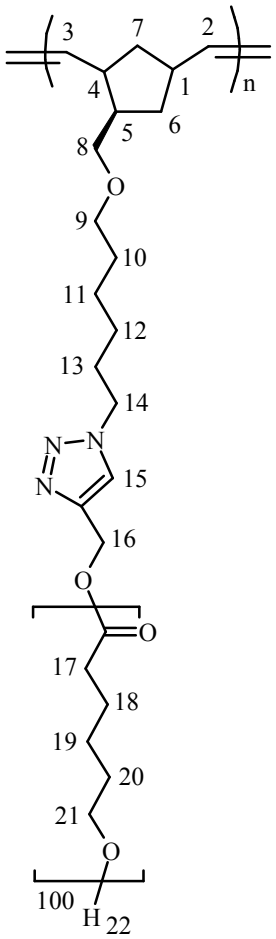

**6.10**

**Figure 6.10.** Structure of polynorbornene-g-PCL with numerical assignment for NMR

$^1$H NMR (400 MHz, $CDCl_3$) δ 7.56 (s, 1H, $H_{15}$), 5.34 (m, 2H, $H_{2,3}$), 4.67 (d, $J$ = 2.1, 2H, $H_{16}$), 4.06 (t, $J$ = 6.58, 198H, $H_{21}$), 3.63 (t, $J$ = 6.5, 2H, $H_{21}$), 3.40 – 3.23 (m, 6H, $H_{8,9,14}$), 2.50 – 2.00 (m, 202H, $H_{4,1,17}$),1.90 (s, 2H, $H_{10}$), 1.80 (s, 1H, $H_{22}$), 1.72 – 1.52 (m, 401H, $H_{5,18,20}$), 1.46 − 1.29 (m, 210H, $H_{11,12,13,7,6,19}$).

### 6.2.13. Synthesis of Polynorbornene-g-PEG 6.11

In a vial, azide functionalised polynorbornene **6.9** of DP = 200 (200 mg, 0.004 mmol, 0.8 mmol of azide groups), alkyne terminated PEG mono-methyl ether (chapter 5) (470 mg, 0.8 mmol), $CuSO_4.5H_2O$ (20 mg, 0.08 mmol), sodium ascorbate (32 mg, 0.16 mmol) and THF / water (10:1, 11 mL) were stirred. The mixture was heated to 60 $^o$C in

an oil bath for 24 hr. The polymer was precipitated by adding water. The polymer was isolated by filtration. The polymer was reprecipitated from THF into water. After filtration, the polymer was dried under reduced pressure to produce the clicked polymer **6.11**, yield 94 % (630 mg).

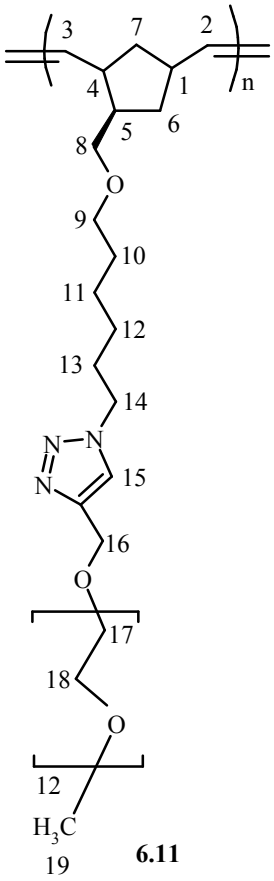


**6.11**

**Figure 6.11.** Structure of polynorbornene-g-PEG with numerical assignment for NMR

$^1$H NMR (400 MHz, THF-$d_6$) δ 7.70 (s, 1H, $H_{15}$), 5.25 (m, 2H, $H_{2,3}$), 4.23 (s, 2H, $H_{16}$), 3.47 – 3.18 (m, 57H, $H_{8,9,14,17,18,19}$), 2.71 (s, 1H, $H_4$), 2.06 (s, 1H, $H_1$), 1.62 – 1.06 (m, 13H, $H_{5,10,11,12,13,7,6}$).

### 6.2.14. Synthesis of Random Copolymer 6.12 Containing PEG Grafts and Bromide Functionalities

In a vial, a solution of the bromide functionalised norbornene monomer **6.7** (200 mg, 0.7 mmol) and PEG mono-methyl ether clicked oxanorbornene monomer **6.5** (200 mg, 0.15 mmol) in $CDCl_3$ (0.8 mL) was added to a solution of Grubbs ruthenium 2$^{nd}$ generation initiator (72 mg, 0.085 mmol) in $CDCl_3$ (0.4 mL). The mixture was stirred for 24 hr at ambient temperature. The polymer was precipitated into hexane. Ethyl vinyl ether (0.1 mL) was added to the polymer solution in a minimum amount of THF. The

solution was stirred at ambient temperature for 3 hr. The copolymer was reprecipitated into hexane and filtered. The copolymer was dried under reduced pressure to give the copolymer **6.12**, yield 79 % (315 mg).

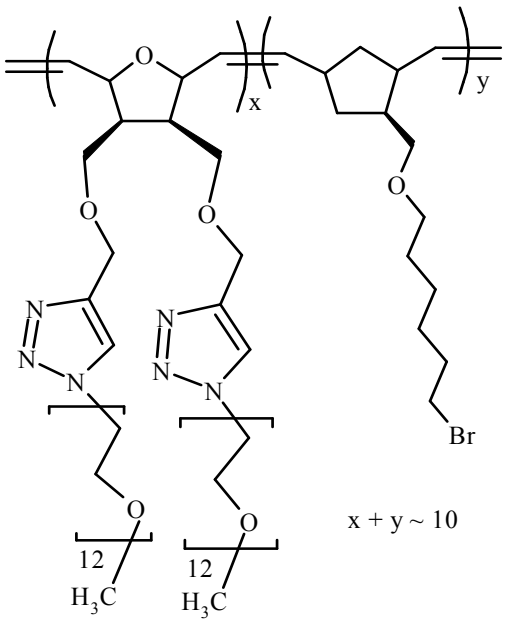


**6.12**

**Figure 6.12.** Structure of random copolymer containing PEG and bromide functionalities

### 6.2.15. Synthesis of Random Copolymer 6.13 Containing PEG Grafts and Azide Functionalities

In a vial, sodium azide (228 mg, 3.5 mmol) was added to a solution of the copolymer **6.12** (200 mg) in DMF / THF (1:1, 2 mL). The mixture was stirred in an oil bath at 60°C for 24 hr. The product was extracted into DCM and washed three times by water. The organic layer was dried under magnesium sulphate then filtered. The solvent was removed and the product was dried under reduced pressure to give the copolymer **6.13**, yield 76 % (152 mg).

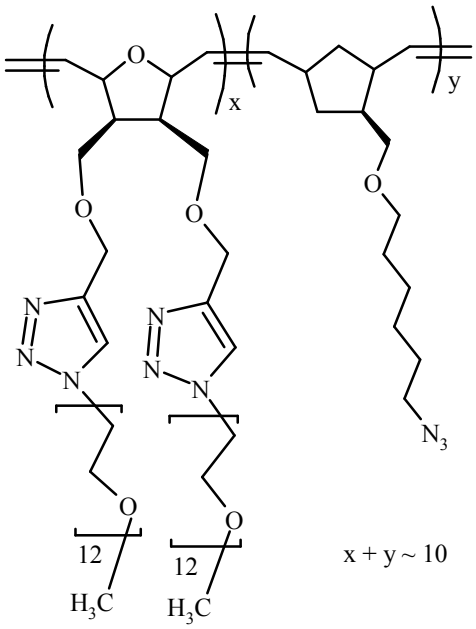


**6.13**

**Figure 6.13.** Structure of random copolymer containing PEG and azide functionalities

### 6.2.16. Synthesis of Random Copolymer 6.14 Containing PEG and PCL Grafts

In a vial, the azide functionalised copolymer **6.13** (50 mg, 0.11 mmol of azide groups), alkyne end capped PCL (chapter 4) (1.214 g, 0.11 mmol), $CuSO_4.5H_2O$ (3 mg, 0.011 mmol), Na Ascorbate (5 mg, 0.022 mmol) and DMF / THF / water (1:1:0.1, 5.5 mL) were stirred. The mixture was heated up to 60 $^oC$ in an oil bath for 24 hr. The copolymer was precipitated by adding water. The copolymer was isolated by filtration. The polymer was reprecipitated from DMF / THF into water. After filtration, the copolymer was dried under reduced pressure to produce the clicked copolymer **6.14**, yield 88%.

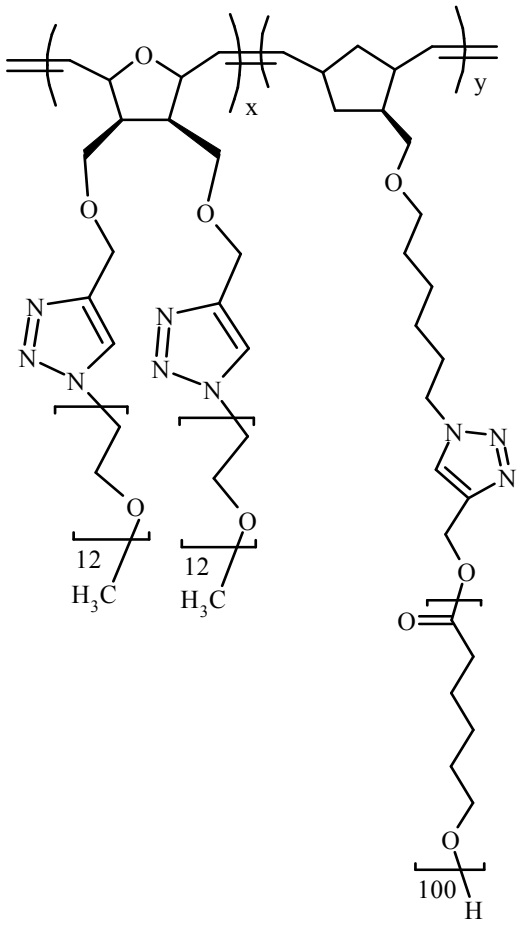


**6.14**

**Figure 6.14.** Structure of random copolymer containing PEG and PCL grafts

## 6.3. Results and Discussion

### 6.3.1. Synthesis and Characterisation of Polyoxanorbornene-g-PEG

The "grafting through" method (the macromonomer approach) was used to produce polyoxanorbornene grafted with PEG side chains. The method involved combination of Click chemistry and ROMP. The macromonomer was prepared *via* Click reaction which was then subjected to ROMP to obtain graft copolymer.

The oxanorbornene based group was chosen for two reasons. First, norbornene based monomers are to have high ring strains. The ROMP of substituted norbornenes is a well-established methodology for the synthesis of polymers with precise structures.[37] *exo*-Norbornene isomers were used in this study because they exhibit significantly higher reactivity than their *endo*- analogues due to reduced steric hindrance at the olefin.[43-45] Ruthenium Grubbs catalysts are the most widely used initiators for ROMP because of their excellent functional group tolerance.[46,47,10] Second, the presence of the oxygen in the 7-position is expected to make the backbone more hydrophilic[48] and hence increase the probability of biocompatibility of the backbone.

#### 6.3.1.1. Synthesis of Azide Terminated PEG mono-methyl ether

The azide terminated PEG mono-methyl ether **6.1** was successfully prepared by tosylation of the hydroxyl functionality of a commercially available hydroxy terminated PEG mono-methyl ether ($M_n$ ~550 $gmol^{-1}$; DP (n) = 12) and subsequent substitution with sodium azide, Scheme 6.1.

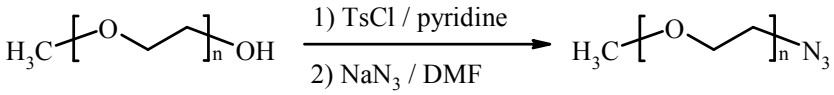


**6.1**

**Scheme 6.1.** Synthesis of azide terminated PEG mono-methyl ether

The hydroxyl group of the PEG mono-methyl ether was quantitatively converted into azide functionality through the formation of a tosyl terminated PEG mono-methyl ether intermediate. The structure of the intermediate was checked by $^1$H-NMR. The $^1$H-NMR spectrum of tosyl terminated PEG mono-methyl ether intermediate (Fig. 6.15.B) compared to that of hydroxy terminated PEG mono-methyl ether (Fig. 6.15.A) showed

complete disappearance of the OH peak at 2.80 ppm ($H_4$) and appearance of new peaks corresponding to the tosyl functionality ($H_{5,5'}$, $H_{6,6'}$ and $H_7$). The reaction was continued without isolating the tosylated PEG intermediate to produce the final azide terminated PEG product **6.1** which was fully characterised by $^1$H- & $^{13}$C-NMR. The $^1$H-NMR spectrum of **6.1** (Fig. 6.15.C) compared to that of tosyl terminated PEG mono-methyl ether (Fig. 6.15.B) showed complete disappearance of the peaks corresponding to tosyl functionality ($H_{5,5'}$, $H_{6,6'}$ and $H_7$) and appearance of a new peak at 3.50 ppm assigned to $CH_2$ adjacent to azide functionality ($H_{3(terminal)}$).

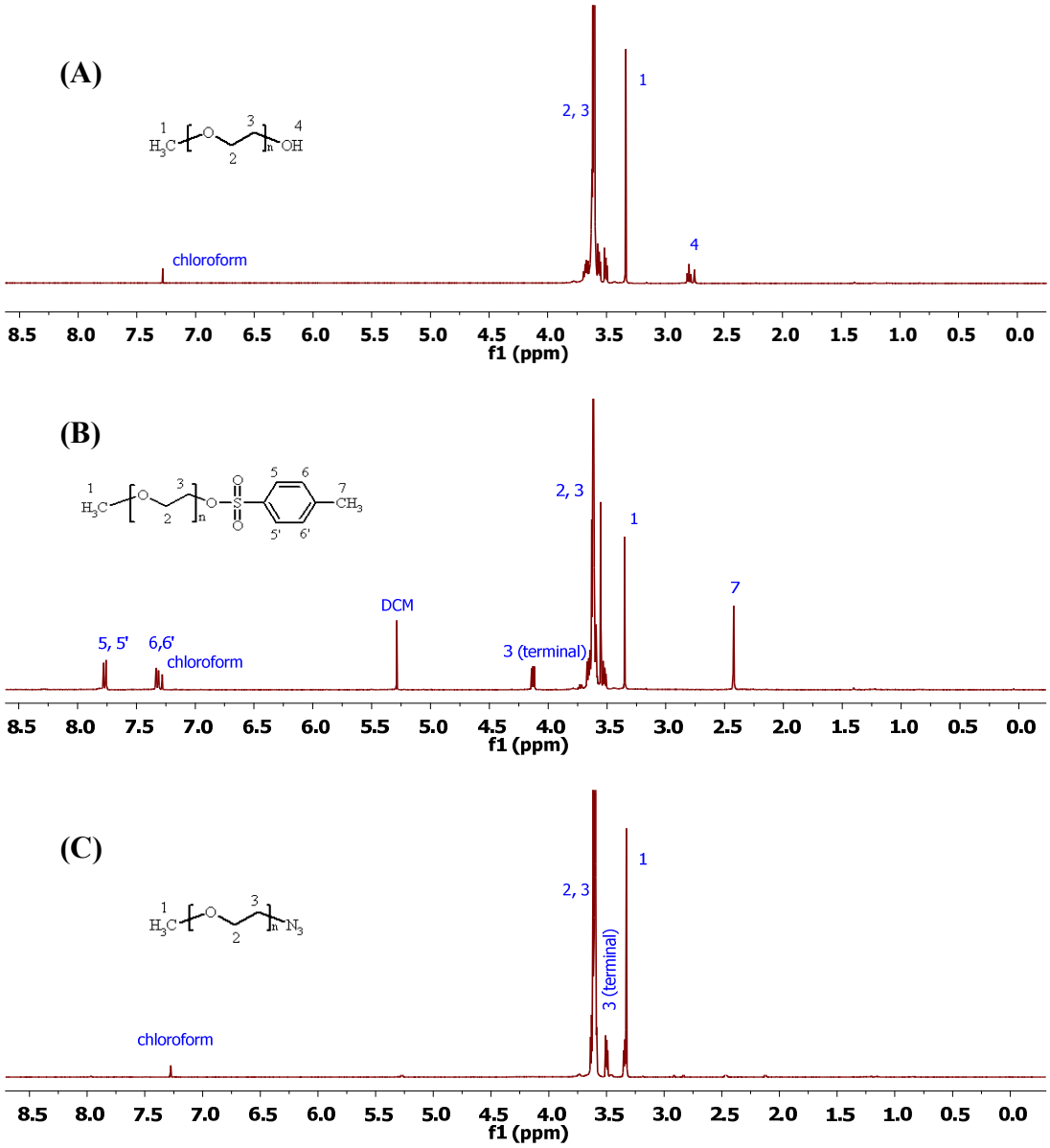


**Figure 6.15.** $^1$H-NMR spectra of (A) hydroxy terminated PEG mono-methyl ether, (B) tosyl terminated PEG mono-methyl ether, and (C) azide terminated PEG mono-methyl ether **6.1** in $CDCl_3$

The $^{13}$C-NMR spectrum of **6.1** (Fig. 6.16.B) compared to that of hydroxy terminated PEG mono-methyl ether (Fig. 6.16.A) showed shift of $H_{3(terminal)}$ peak from 61.64 ppm to 50.88 ppm, indicating the successful attachment with azide group.

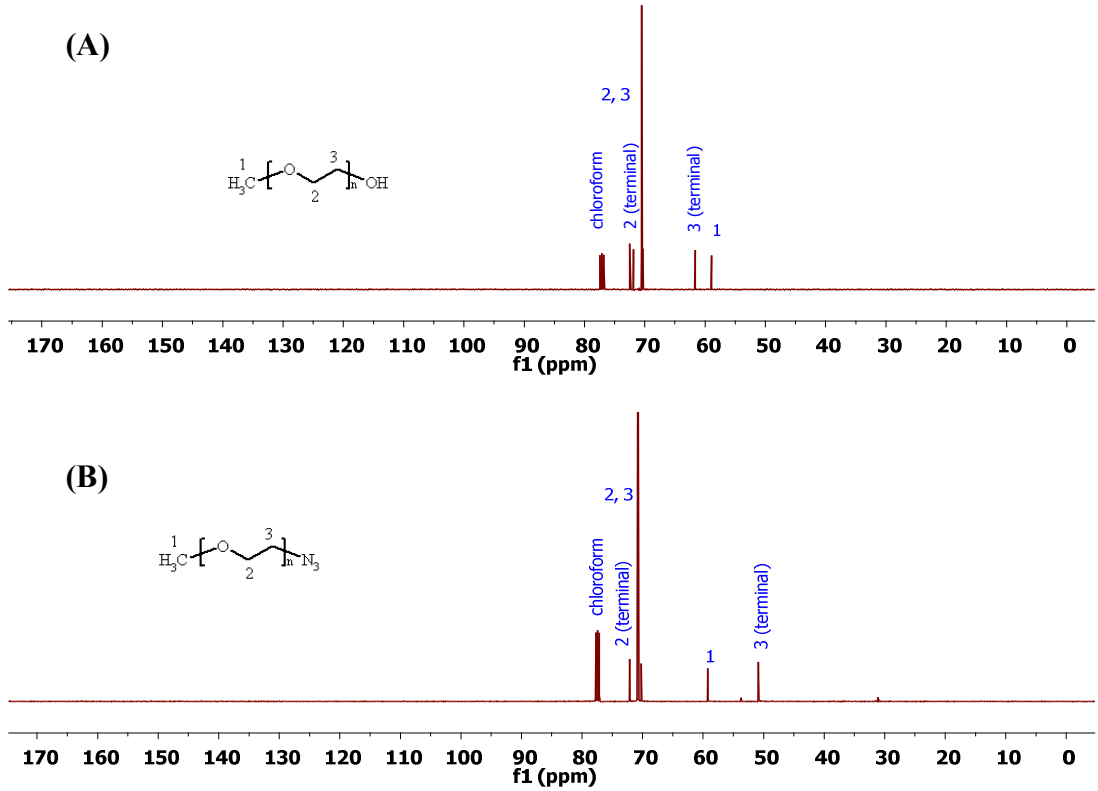


**Figure 6.16.** $^{13}$C-NMR spectra of (A) hydroxy terminated PEG mono-methyl ether and (B) azide terminated PEG mono-methyl ether **6.1** in $CDCl_3$

The FT-IR spectrum of **6.1** showed the appearance of a strong peak due to the azide group at ~2100 $cm^{-1}$, Fig. 6.17.

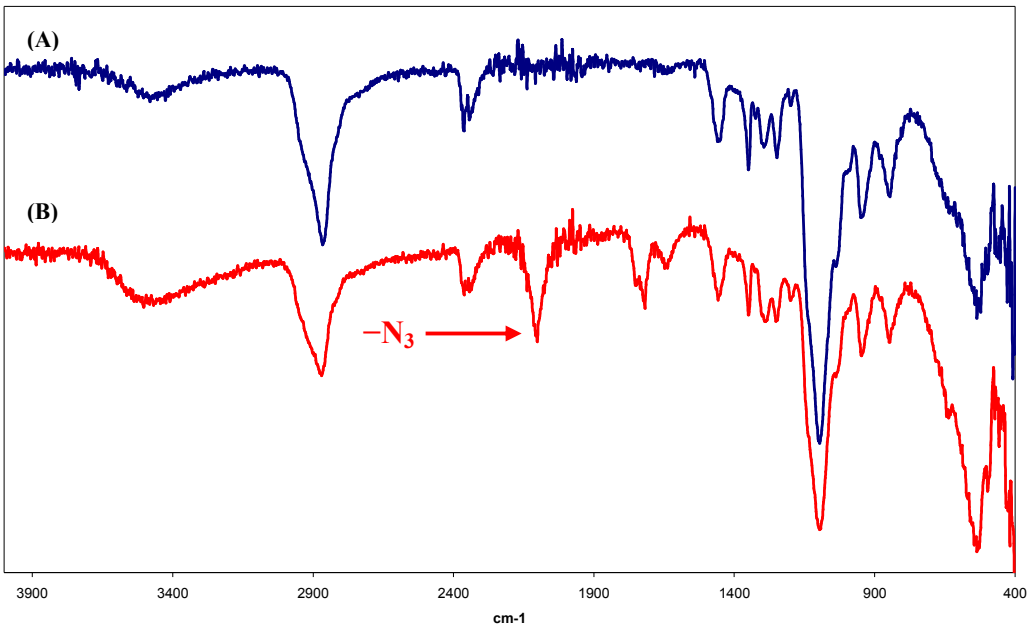


**Figure 6.17.** FT-IR spectra of (A) hydroxy terminated PEG mono-methyl ether and (B) azide terminated PEG mono-methyl ether **6.1**

### 6.3.1.2. Synthesis of Di-alkyne Functionalised Oxanorbornene

*exo,exo*-Oxanorbornene monomer **6.4** bearing two terminal alkyne functionalities (*exo,exo*-2,3-bis(propargoxymethyl)-7-oxanorbornene) was synthesised *via* three steps (Scheme 6.2). It was reported that the classical Diels-Alder reaction of furan and maleic anhydride results in a mixture of crystalline *exo* contaminated with *endo* in amounts determined by reaction time.[49] The synthesis of *exo*-2,3-dicarboxylic acid anhydride-7-oxanorbornene **6.2** was performed by allowing the reaction to run at ambient temperature for 48 hr. Crude **6.2** was reduced with lithium aluminium hydride to afford the diol **6.3**. Double Williamson ether synthesis using purified **6.3** and excess NaH in the presence of excess propargyl bromide produced the di-alkyne **6.4** in 66 % yields after purification, Scheme 6.2.

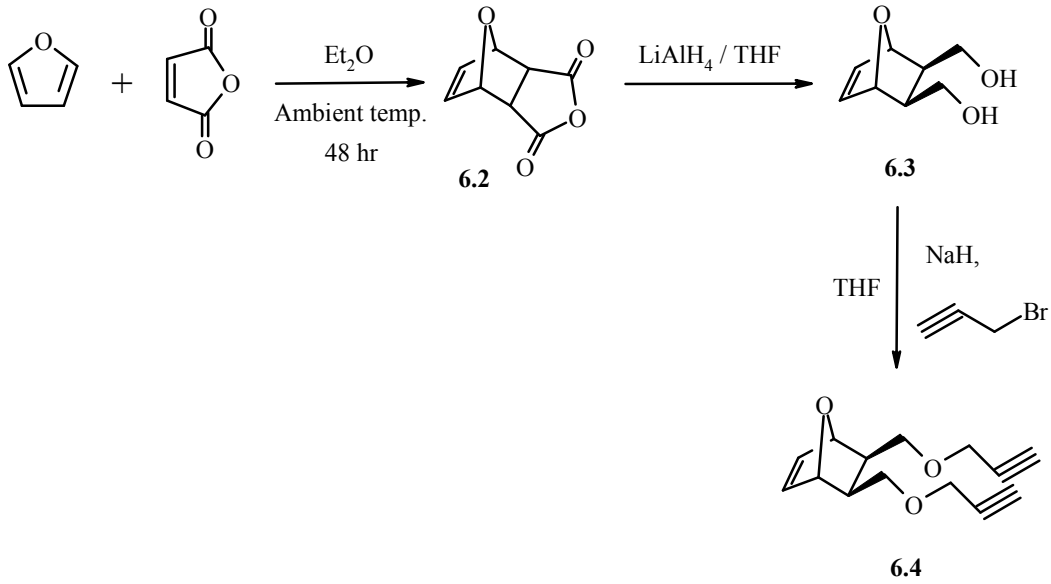


**Scheme 6.2.** The synthetic stages involved in the synthesis of di-alkyne functionalised oxanorbornene

The final product **6.4** as well as the intermediates were characterised by NMR. The $^{1}$H-NMR spectrum of **6.3** (Fig. 6.18.B) compared to that of **6.2** (Fig. 6.18.A) showed appearance of two new peaks due to the newly formed di-alkanol substituents on oxanorbornene ($H_{8,8'}$) and ($H_{7,7'}$) at 4.02 and 3.73 ppm, respectively. It also showed shift for all the peaks, ($H_{2,3}$), ($H_{1,4}$), and ($H_{5,6}$), to lower chemical shift values as indicated in the spectra (Fig. 6.18.A and Fig. 6.18.B). This confirmed the successful formation of **6.3**. The $^{1}$H-NMR spectrum of **6.4** (Fig. 6.18.C) compared to that of **6.3** (Fig. 6.18.B) showed complete disappearance of the peak corresponding to hydroxyl groups at 4.02 ppm ($H_{8,8'}$) and appearance of a new peak at 2.47 ppm, assigned to the protons of the alkyne functionalities ($H_{10,10'}$). Integrations of oxanorbornenyl olefin peak ($H_{2,3}$) and the terminal alkyne proton ($H_{10,10'}$) peak gave a 1:1 ratio, indicating the introduction of two alkyne functionalities. Moreover, ESI-MS result of **6.4** showed a base peak at 255.2, which is in a good agreement with the theoretical calculation for $[M + Na]^{+}$.

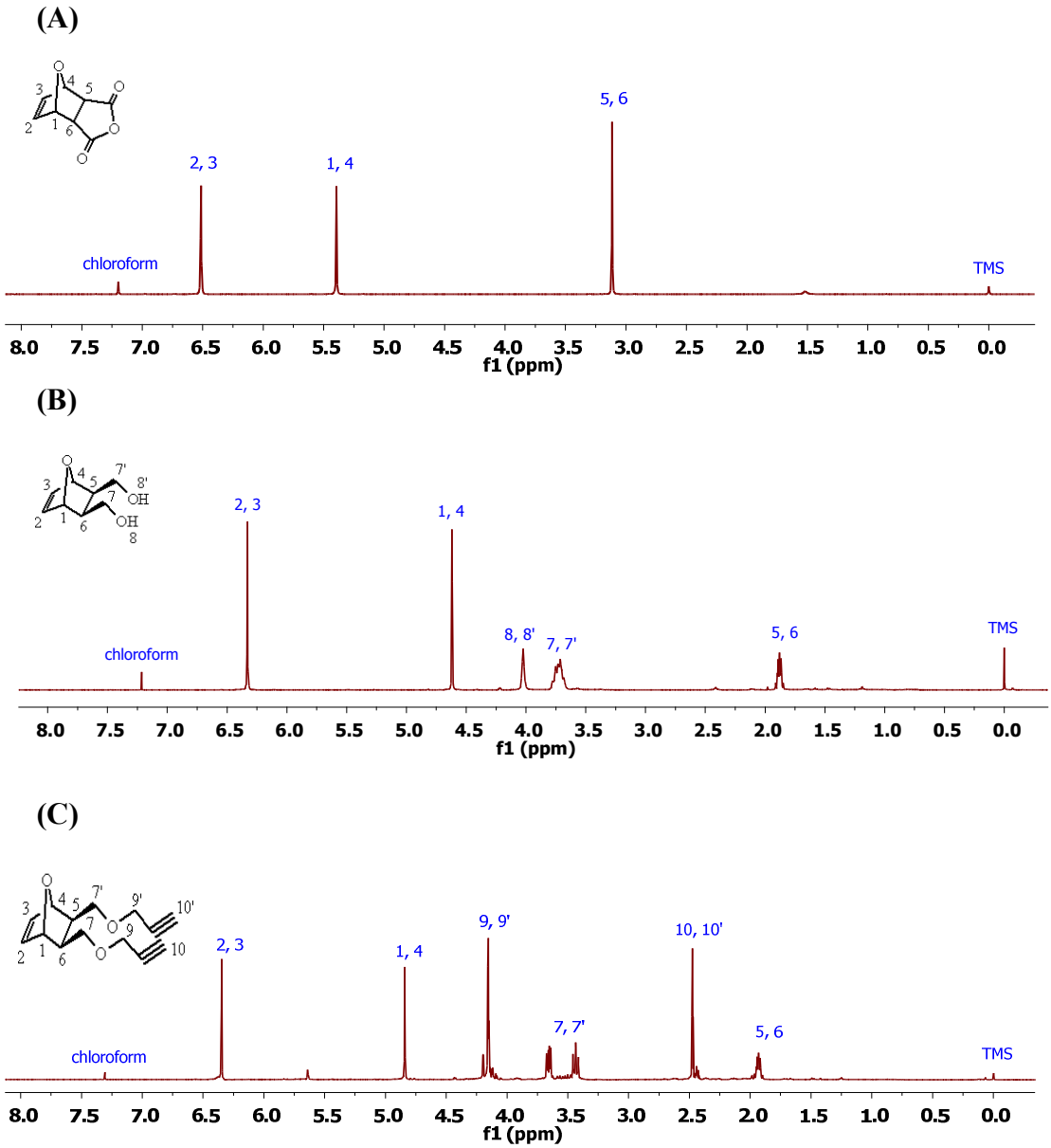


**Figure 6.18.** $^{1}$H-NMR spectra of (A) dicarboxylic acid anhydride functionalised oxanorbornene **6.2**, (B) diol functionalised oxanorbornene **6.3**, and (C) di-alkyne functionalised oxanorbornene **6.4** in $CDCl_3$

### 6.3.1.3. Synthesis of Oxanorbornenyl Di-PEG Macromonomer

Oxanorbornenyl macromonomer **6.5** containing two PEG chains were synthesised by Click reaction between azide terminated PEG mono-methyl ether **6.1** and di-alkyne functionalised oxanorbornene **6.4**, Scheme 6.3.

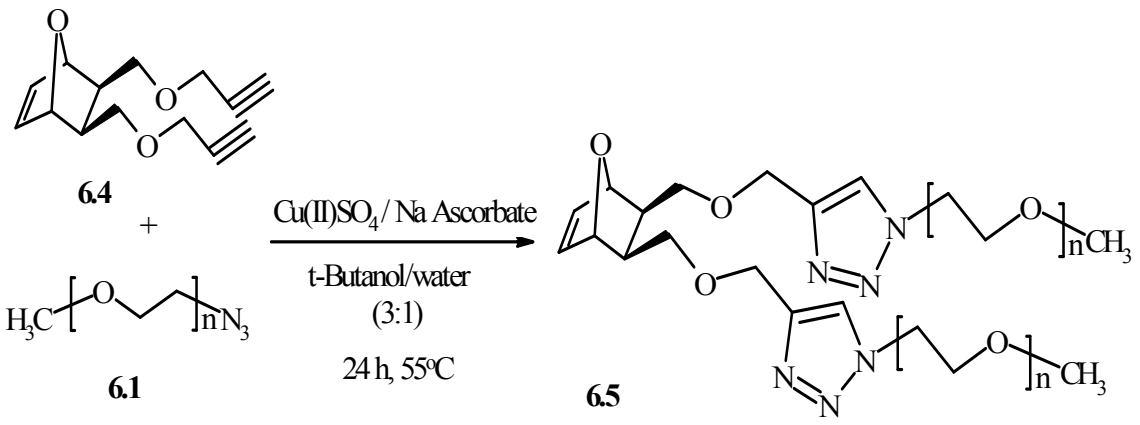


**Scheme 6.3.** Synthesis of oxanorbornenyl di-PEG macromonomer

The macromonomer **6.5** was characterised by $^{1}$H- and $^{13}$C-NMR. The oxanorbornenyl group was readily observed by both $^{1}$H- and $^{13}$C-NMR spectra, shown in Fig. 6.19 and 6.20, respectively. The main evidence for the attachment of two PEG chains with oxanorbornenyl functionality is the resonance at 7.70 ppm assigned to the newly formed triazole proton ($H_{10,10'}$) in the $^{1}$H-NMR spectrum (Fig. 6.19). Integrations of the olefin peak in oxanorbornenyl moiety ($H_{2,3}$) and the triazole proton ($H_{10,10'}$) showed a 1:1 ratio, indicating the presence of two triazole rings per one oxanorbornenyl group. Moreover, $^{13}$C-NMR spectrum of the macromonomer **6.5** (Fig. 6.20) showed appearance of two peaks at 144.99 and 124.05 ppm, corresponding to the triazole carbons ($C_{9,9'}$ and $C_{10,10'}$).

The GPC trace of the macromonomer **6.5** showed that the average molecular weight ($M_n$) is 1,490 gmol$^{-1}$ with PDI of 1.1. This result also clearly confirmed the attachment of oxanorbornenyl group with two chains of PEG.

FT-IR spectrum of the macromonomer **6.5** (Fig. 6.21.B) compared to that of azide terminated PEG mono-methyl ether **6.1** (Fig. 6.21.A) showed the complete disappearance of the azide peak, indicating the full conversion of the azide functionality to triazole.

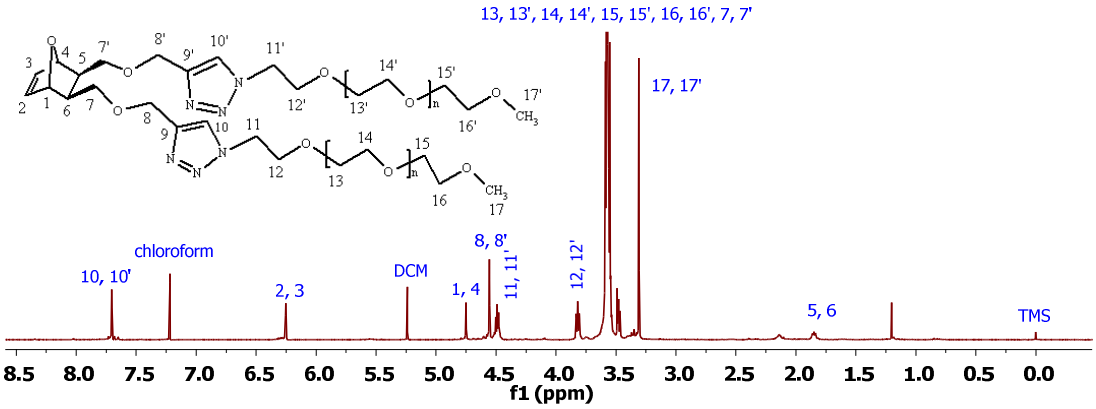


**Figure 6.19.** $^{1}$H-NMR spectrum of oxanorbornenyl PEG macromonomer **6.5** in $CDCl_3$

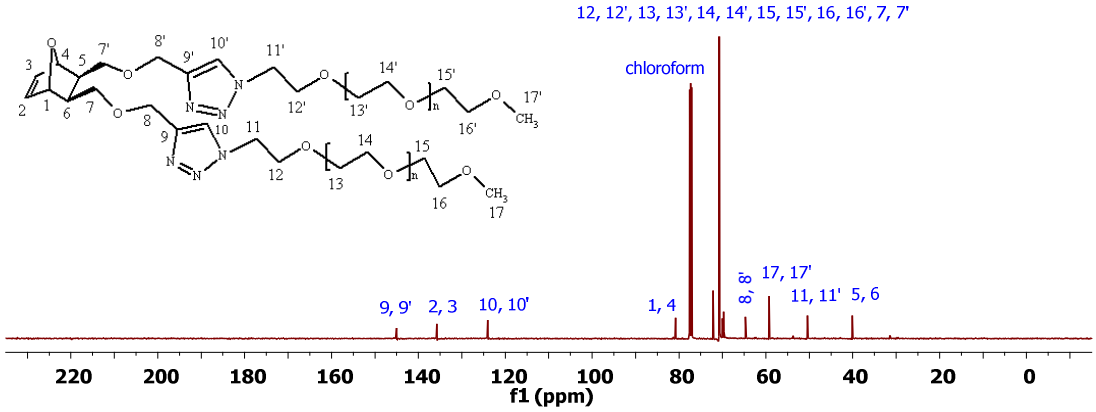


**Figure 6.20.** $^{13}$C-NMR spectrum of oxanorbornenyl PEG macromonomer **6.5** in $CDCl_3$

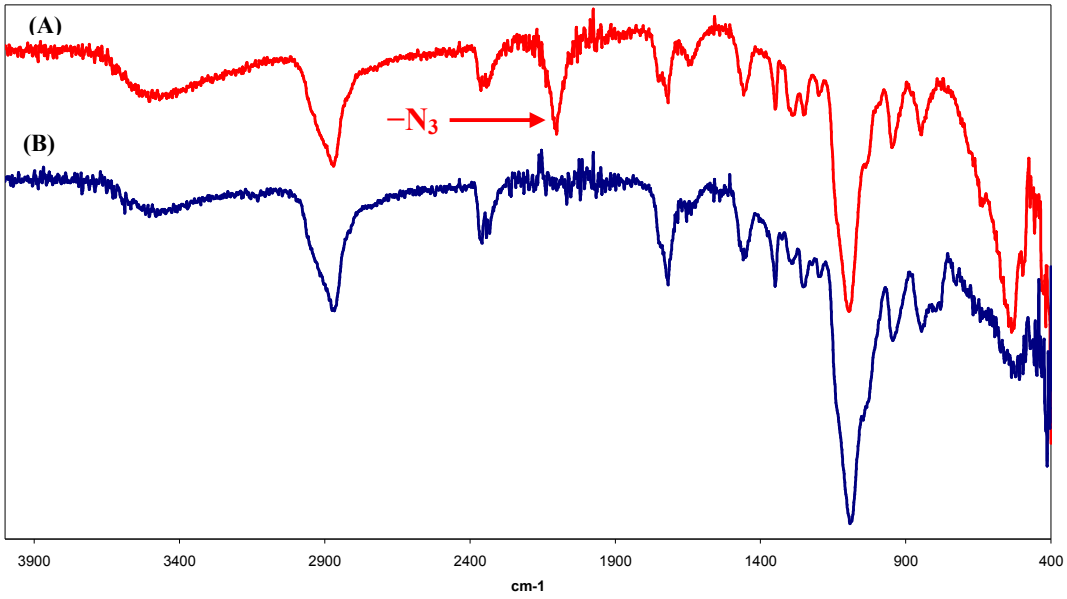


**Figure 6.21.** FT-IR spectra of (A) azide terminated PEG mono-methyl ether **6.1** and (B) oxanorbornenyl PEG macromonomer **6.5**

### 6.3.1.4. ROMP of Oxanorbornenyl Di-PEG Macromonomer

ROMP of the well-characterised oxanorbornenyl PEG macromonomer **6.5** was attempted using first generation Grubbs ruthenium initiator (**G-I**), and no polymerisation was observed as indicated by the $^1$H-NMR. The alkylidene proton of **G-I** was not observed in $^1$H-NMR spectrum, taken after 20 min of the reaction. When the second generation of Grubbs ruthenium initiators (**G-II**) was used, ROMP of the macromonomer **6.5** was successful (Scheme 6.4). The ROMP reaction was monitored by $^1$H-NMR, using macromonomer to initiator molar ratio [M]/[I] of 10 in $CDCl_3$.

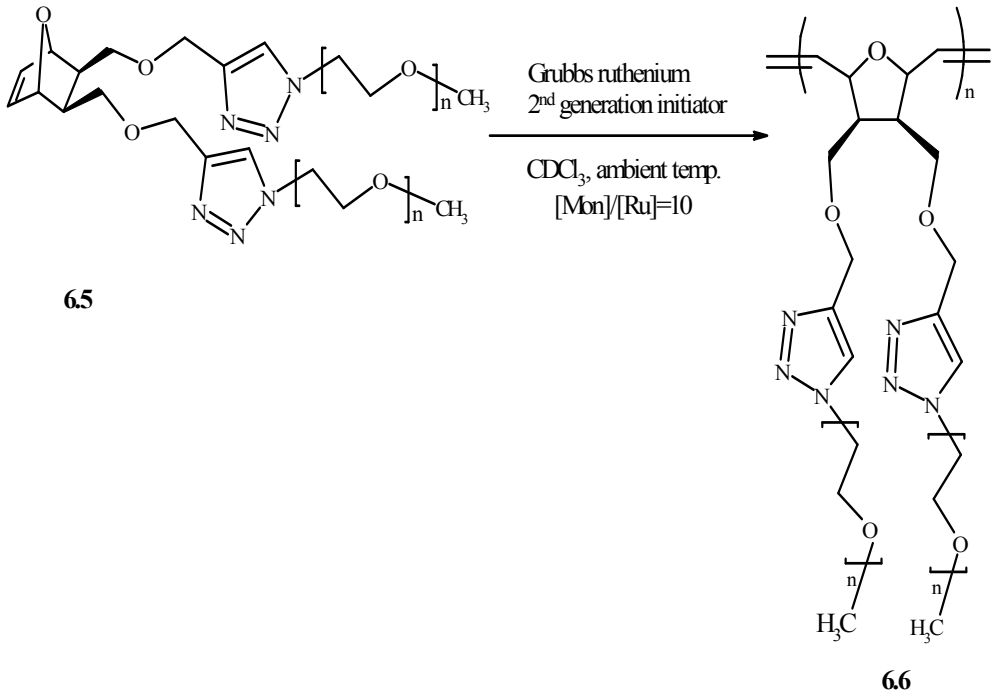


**6.5** **6.6**

**Scheme 6.4.** Synthesis of polyoxanorbornene-g-PEG

The $^1$H-NMR of the reaction mixture, taken after 30 min, showed the presence of residual alkylidene proton of **G-II** initiator at 19.07 ppm but no peaks due to propagating alkylidene. It also showed peaks corresponding to polyoxanorbornene backbone chain at 5.54 and 5.26 ppm, corresponding to *cis*- and *trans*- double bonds. The integration of the peak due to vinylic proton of the polymer and unreacted monomer at 6.25 ppm showed conversion of monomer to polymer of 3 % (Fig. 6.22.A). However, after 24 hr, the spectrum showed conversion of monomer to polymer of 76 % and complete disappearance of the alkylidene proton signal at 19.07 ppm (Fig. 6.22.B). There was no increase in the conversion when the reaction was run for 48 hr.

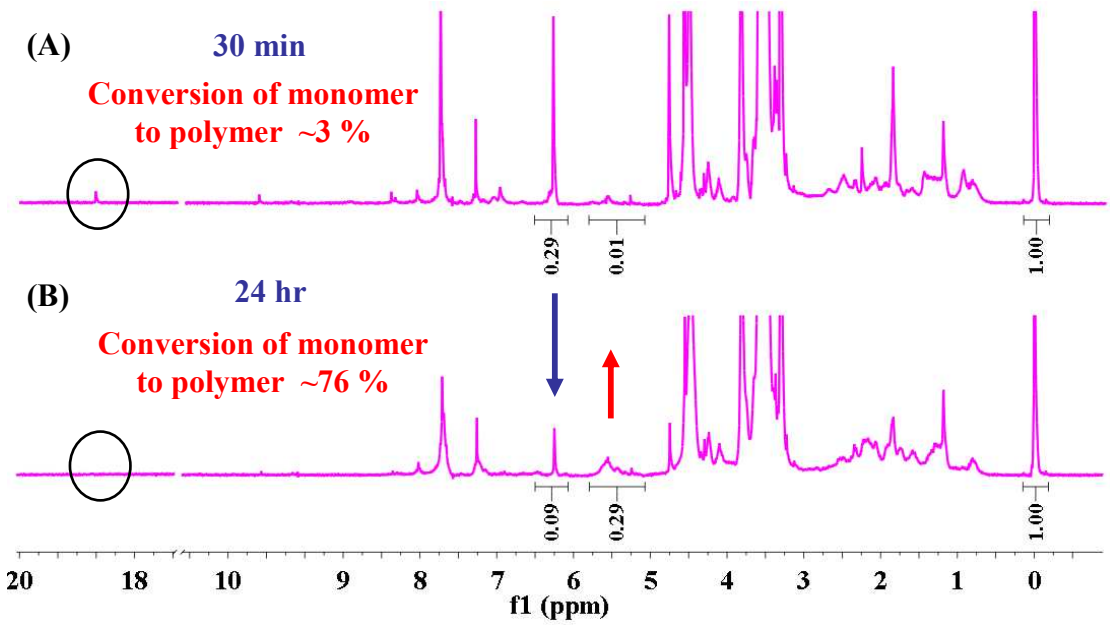


**Figure 6.22.** $^{1}$H-NMR monitoring of the course of ROMP of oxanorbornenyl di-PEG macromonomer **6.5**; (A) after 30 min and (B) after 24 hr

### 6.3.2. Synthesis and Characterisation of Norbornene Graft Copolymers

The "grafting onto" method was used to produce norbornene graft copolymers with different side chains. The method involved combination of Click chemistry and ROMP. Functionalised polynorbornene was prepared *via* ROMP using ruthenium Grubbs catalyst and then Click chemistry was applied to graft either hydrophobic (PCL) or hydrophilic (PEG) side chains.

#### 6.3.2.1. ROMP of Bromide Functionalised Norbornene Monomer

Well-characterised bromide functionalised norbornene monomer **6.7** was subjected to ROMP using Grubbs ruthenium initiator **G-I** and the polymerisation reaction was terminated using ethyl vinyl ether to give the final product **6.8**, Scheme 6.5. The molecular weight of the graft copolymer was controlled by varying the macromonomer : initiator molar ratio [M]/[I]. Two different DP of 10 and 200 were obtained.

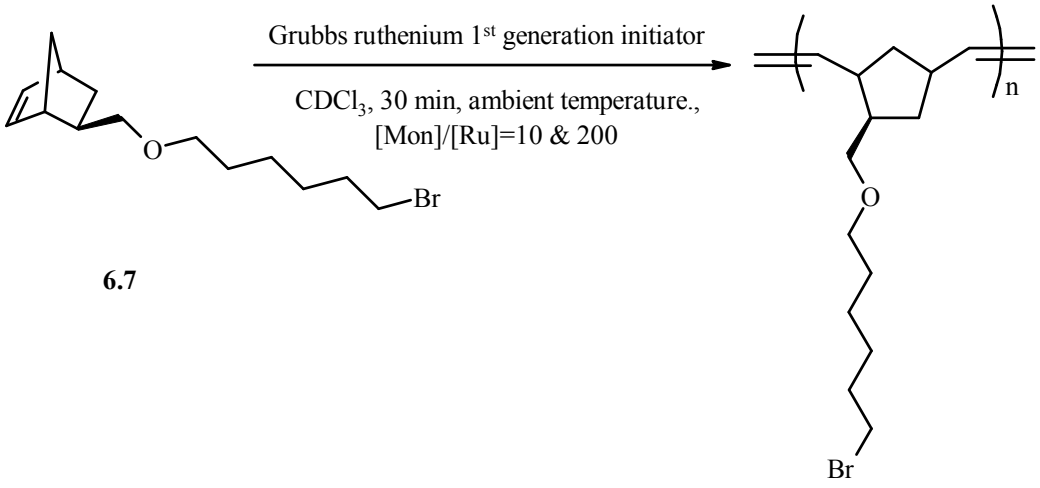


**6.7**

**6.8**

**Scheme 6.5.** Synthesis of bromide functionalised polynorbornene

Examination of the $^{1}$H-NMR spectrum of polymer **6.8** (Fig. 6.23.B) compared to that of monomer **6.7** (Fig. 6.23.A) showed complete disappearance of the peak due to the norbornenyl double bond at 6.05 ppm and appearance of two peaks at 5.30 and 5.17 ppm, corresponding to *cis*- and *trans*- double bonds of the polymer. The successful ROMP was also demonstrated by $^{13}$C-NMR. The $^{13}$C-NMR spectrum of polymer **6.8** (Fig. 6.24.B) compared to that of monomer **6.7** (Fig. 6.24.A) showed complete disappearance of the peak due to the norbornenyl double bond at 136.57 ppm and appearance of a peak at 131.91 ppm, corresponding to the double bonds of the polymer.

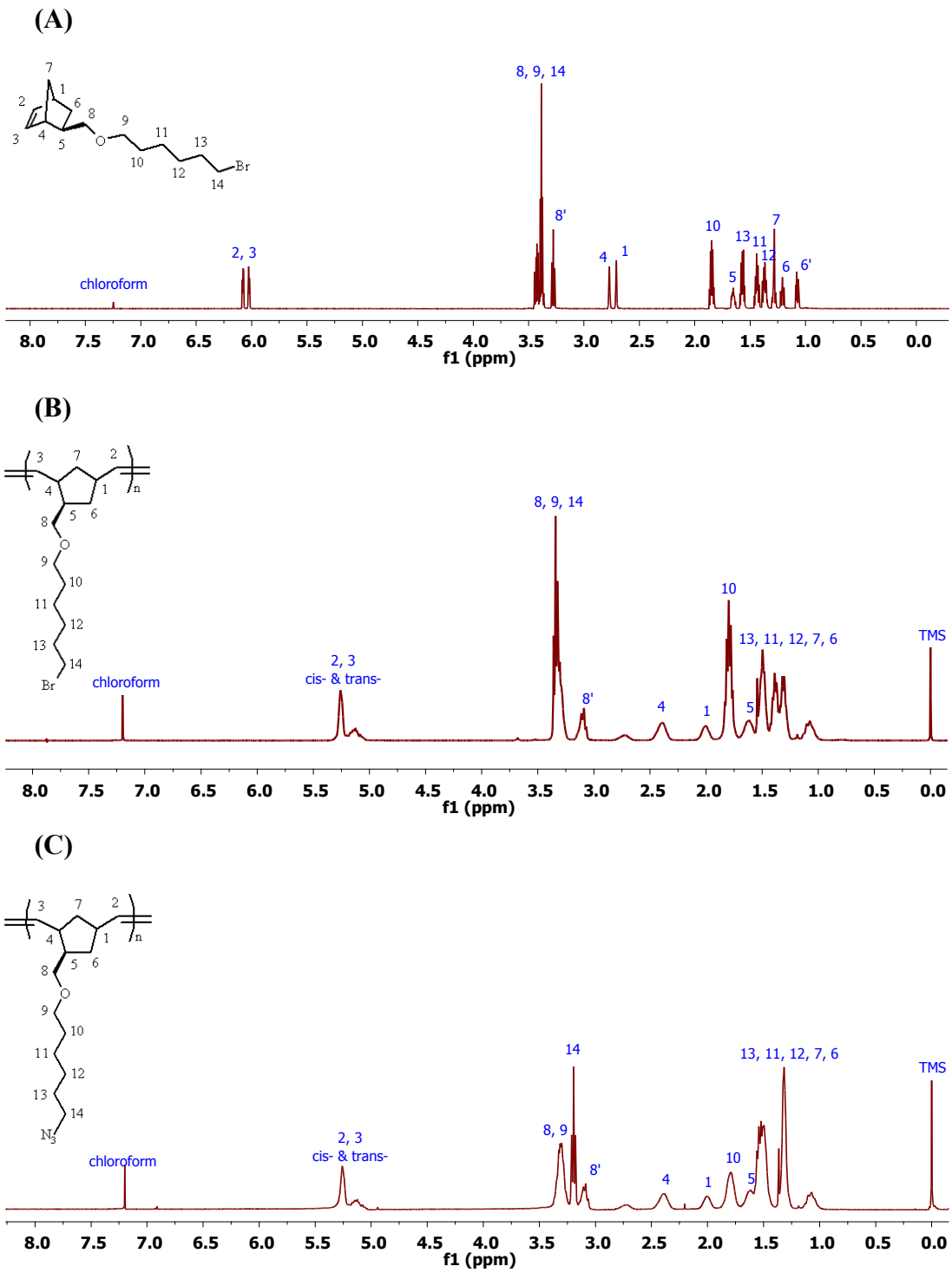


**Figure 6.23.** $^{1}$H-NMR spectrum of (A) bromide functionalised norbornene **6.7**, (B) bromide functionalised polynorbornene **6.8** and (C) azide functionalised polynorbornene **6.9** in $CDCl_3$

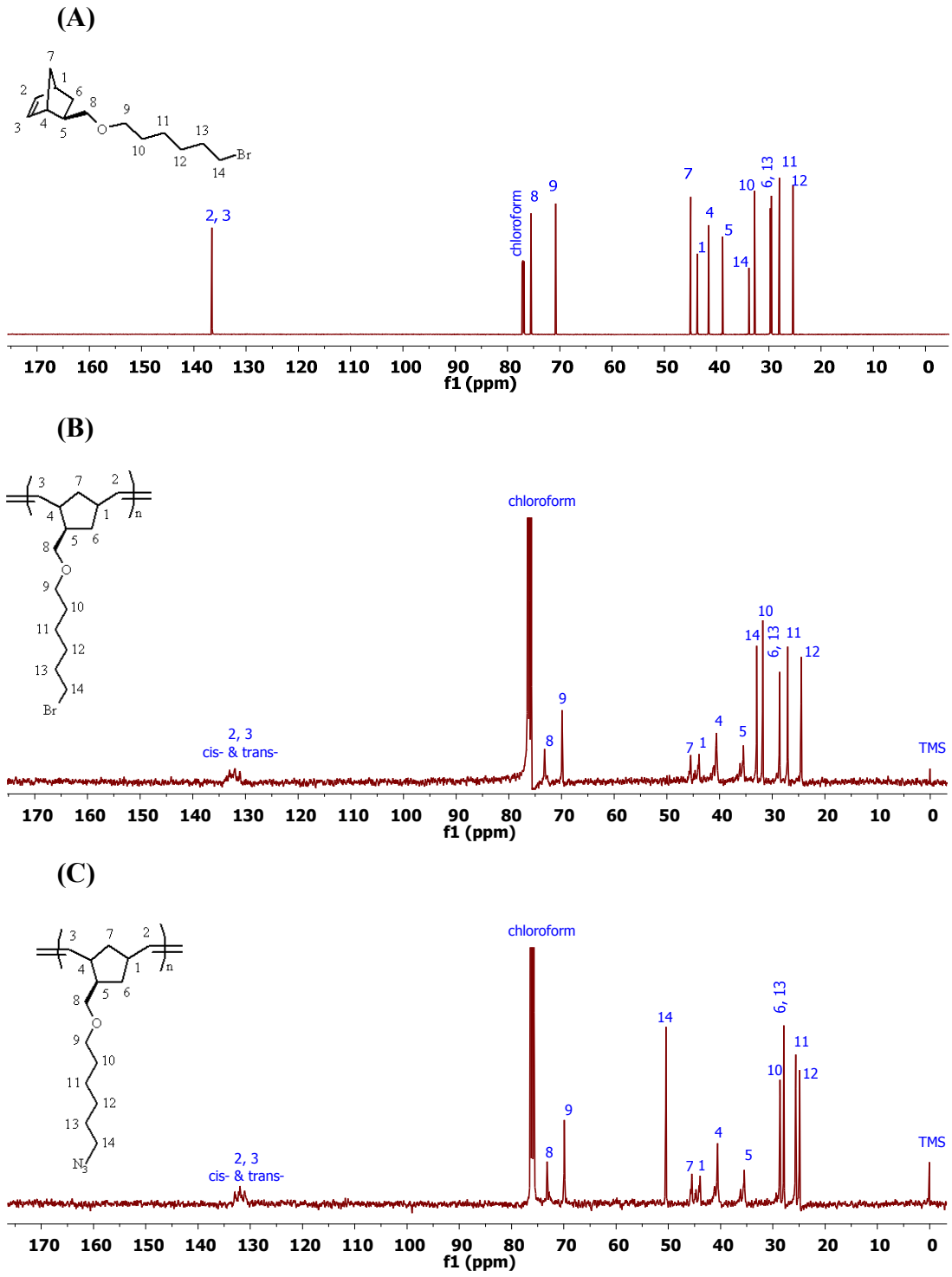


**Figure 6.24.** $^{13}$C-NMR spectrum of (A) bromide functionalised norbornene **6.7**, (B) bromide functionalised polynorbornene **6.8** and (C) azide functionalised polynorbornene **6.9** in $CDCl_3$

### 6.3.2.2. Synthesis of Azide Functionalised Polynorbornene

The azide functionalisation of polymer **6.8** was performed by reaction with $NaN_3$ to produce polymer **6.9** in high yield, Scheme 6.6.

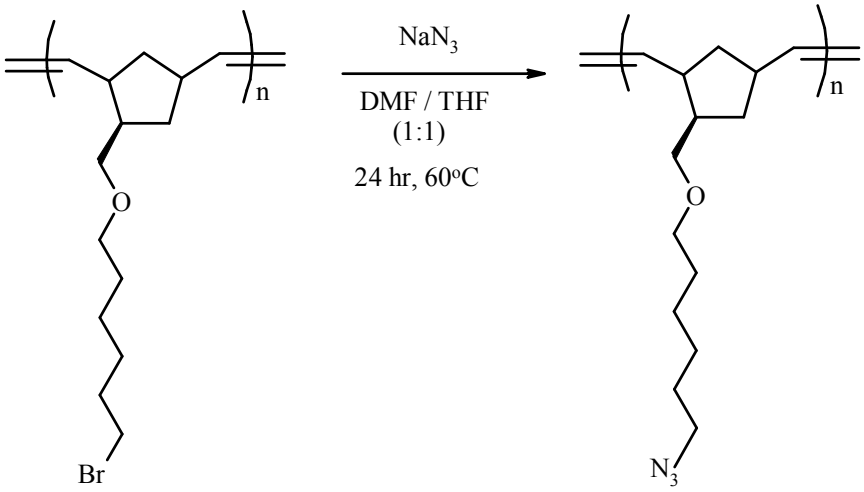


**6.8** **6.9**

**Scheme 6.6.** Synthesis of azide functionalised polynorbornene

The $^{1}$H-NMR spectrum of **6.9** (Fig. 6.23.C) compared to that of **6.8** (Fig. 6.23.B) showed a shift for the peak due to the terminal $CH_2$ ($C_{14}$) from 3.34 ppm to 3.19 ppm. Also, the $^{13}$C-NMR spectrum of **6.9** (Fig. 6.24.C) compared to that of **6.8** (Fig. 6.24.B) showed a shift for the peak due to the terminal $CH_2$ ($C_{14}$) from 32.96 ppm to 50.47 ppm. These indicated the successful complete transformation from $–CH_2$-Br to $–CH_2$-$N_3$.

The FT-IR provided further evidence for the successful azide functionalisation reaction. The spectrum of **6.9** (Fig. 6.25.B) compared to that of **6.8** (Fig. 6.25.A) showed appearance of a new peak at 2094 cm$^{-1}$, corresponding to the azide group.

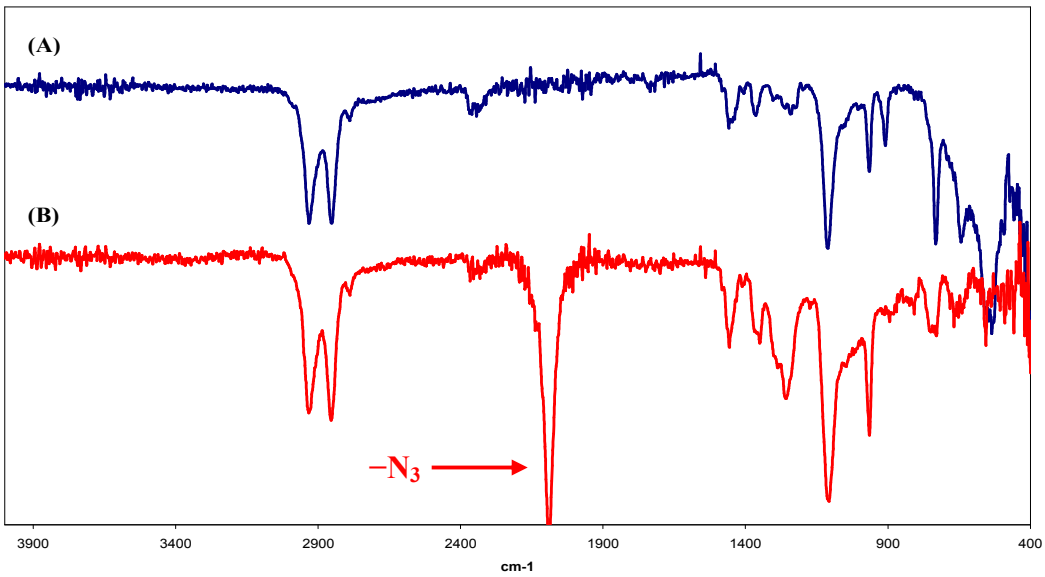


**Figure 6.25.** FT-IR spectra of (A) bromide functionalised polynorbornene **6.8** and (B) azide functionalised polynorbornene **6.9**

### 6.3.2.3. Synthesis of Polynorbornene-g-PCL

The azide functionalised polynorbornene **6.9** was coupled with a stoichiometric amount of alkyne end capped PCL **4.2** to produce polynorbornene-g-PCL **6.10**, Scheme 6.7.

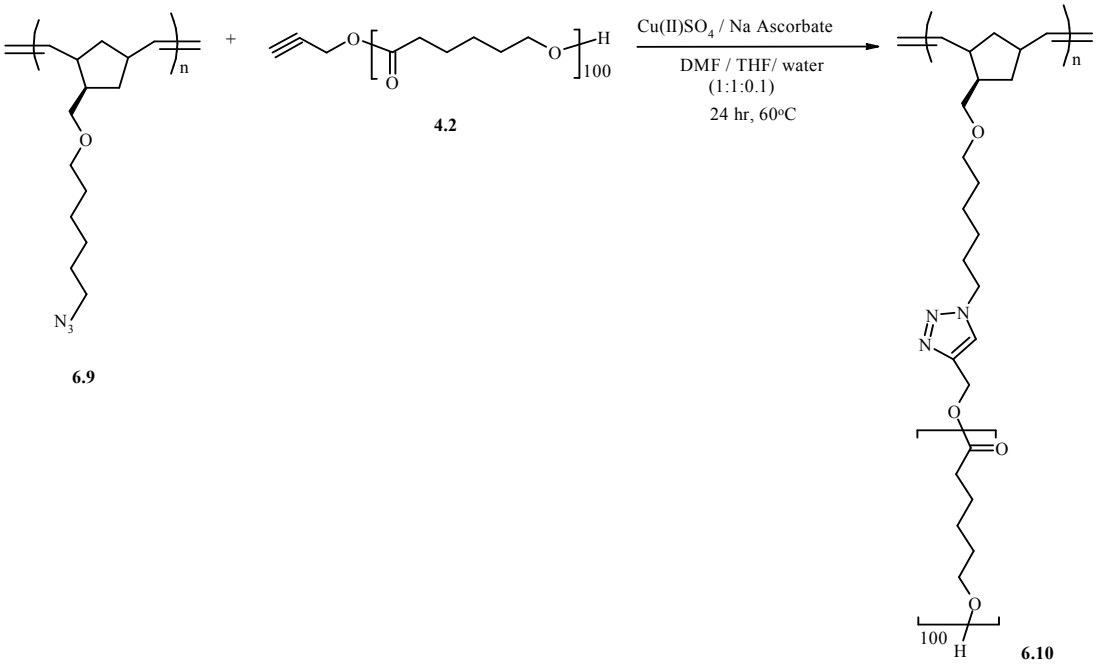


**Scheme 6.7.** Synthesis of polynorbornene-g-PCL

The successful Click reaction between **6.9** and **4.2** was clearly demonstrated by $^1$H-NMR and FT-IR. $^1$H-NMR spectrum of **6.10** showed appearance of a new peak at 7.56 ppm due to triazole proton as well as all the peaks due to polynorbornene and PCL grafts as assigned in Fig. 2.26. Moreover, the FT-IR spectrum of **6.10** (Fig. 6.27.B) compared to that of **6.9** (Fig. 6.27.A) showed complete disappearance of the azide peak at 2094 cm$^{-1}$ and appearance of a new peak at 1722 cm$^{-1}$ due to the carbonyl group of PCL.

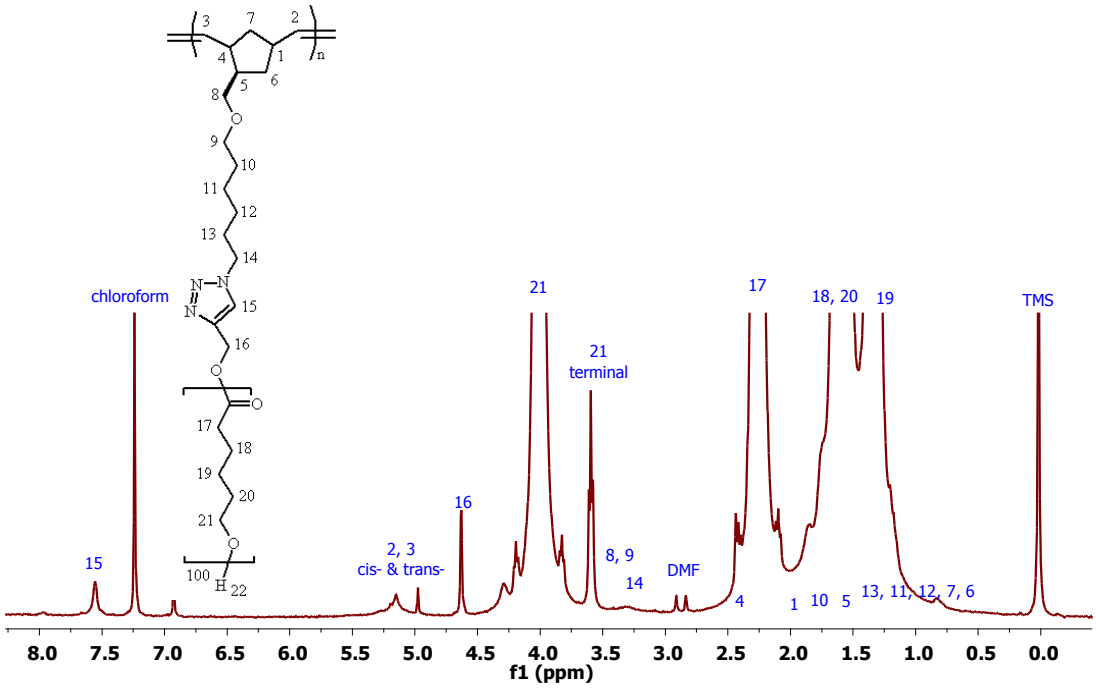


**Figure 6.26.** $^{1}$H-NMR spectrum of polynorbornene-g-PCL **6.10** in $CDCl_3$

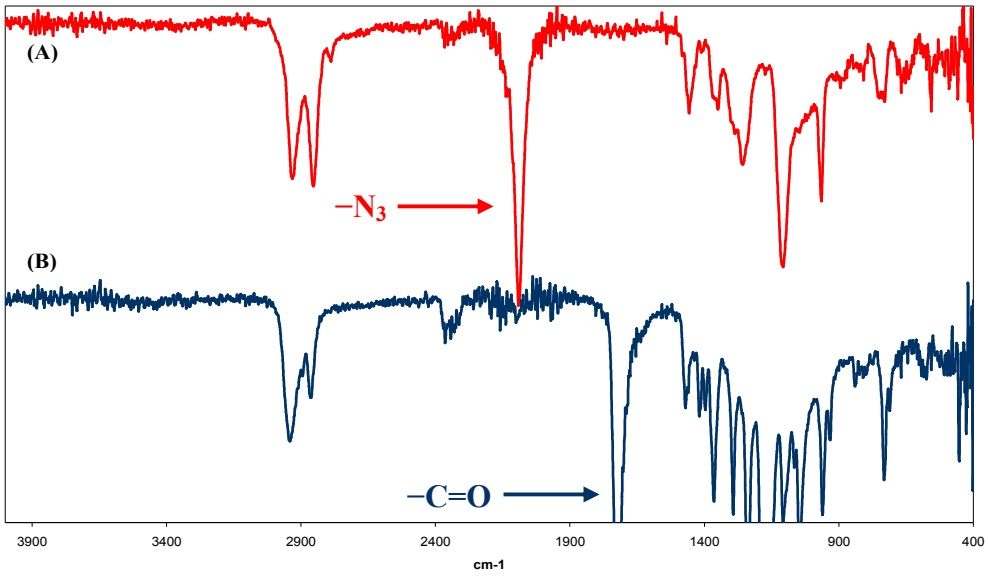


**Figure 6.27.** FT-IR spectra of (A) azide functionalised polynorbornene **6.9** and (B) polynorbornene-g-PCL **6.10**

### 6.3.2.4. Synthesis of Polynorbornene-g-PEG

The azide functionalised polynorbornene **6.9** was coupled with a stoichiometric amount of alkyne terminated PEG mono-methyl ether **5.15** to produce polynorbornene-g-PEG **6.11**, Scheme 6.8.

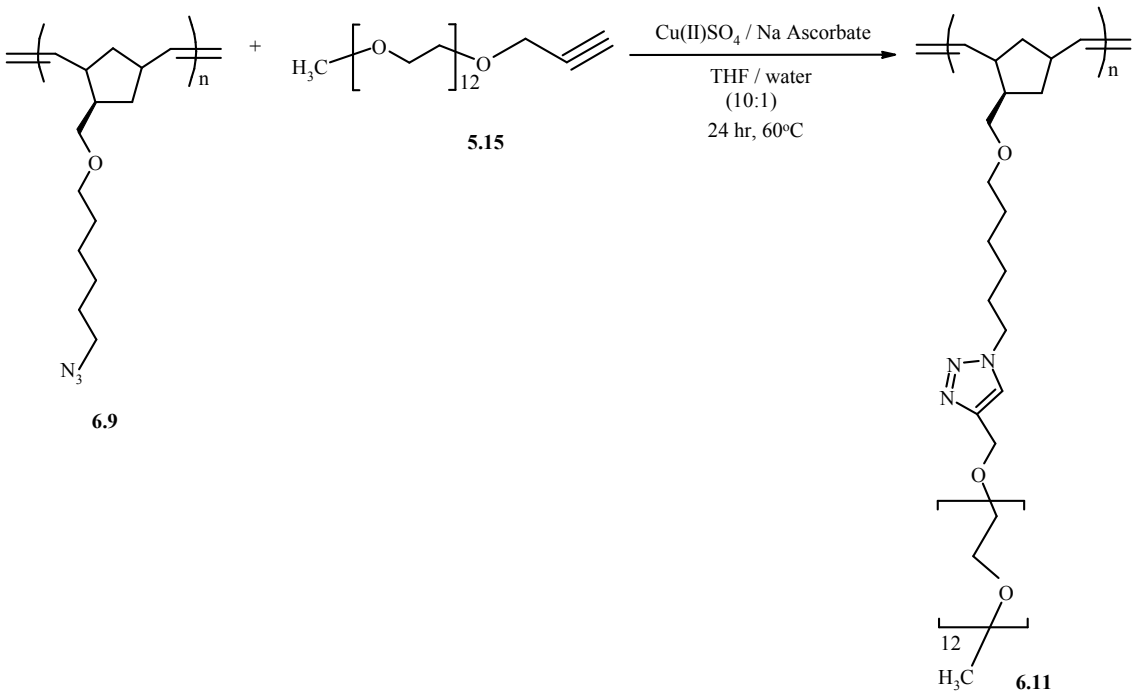


**Scheme 6.8.** Synthesis of polynorbornene-g-PEG

The successful Click reaction between **6.9** and **5.15** was clearly demonstrated by $^{1}$H-NMR and FT-IR. The $^{1}$H-NMR spectrum of **6.11** showed appearance of a new peak at 7.70 ppm due to triazole proton as well as all the peaks due to polynorbornene and PEG grafts as assigned in Fig. 2.28. Moreover, the FT-IR spectrum of **6.11** (Fig. 6.29.B) compared to that of **6.9** (Fig. 6.29.A) showed complete disappearance of the azide peak at 2094 cm$^{-1}$. The appearance of a new peak at ~3400 cm$^{-1}$ due to hydroxyl groups indicated the increase in the moisture content of the material as a result of PEG grafts.

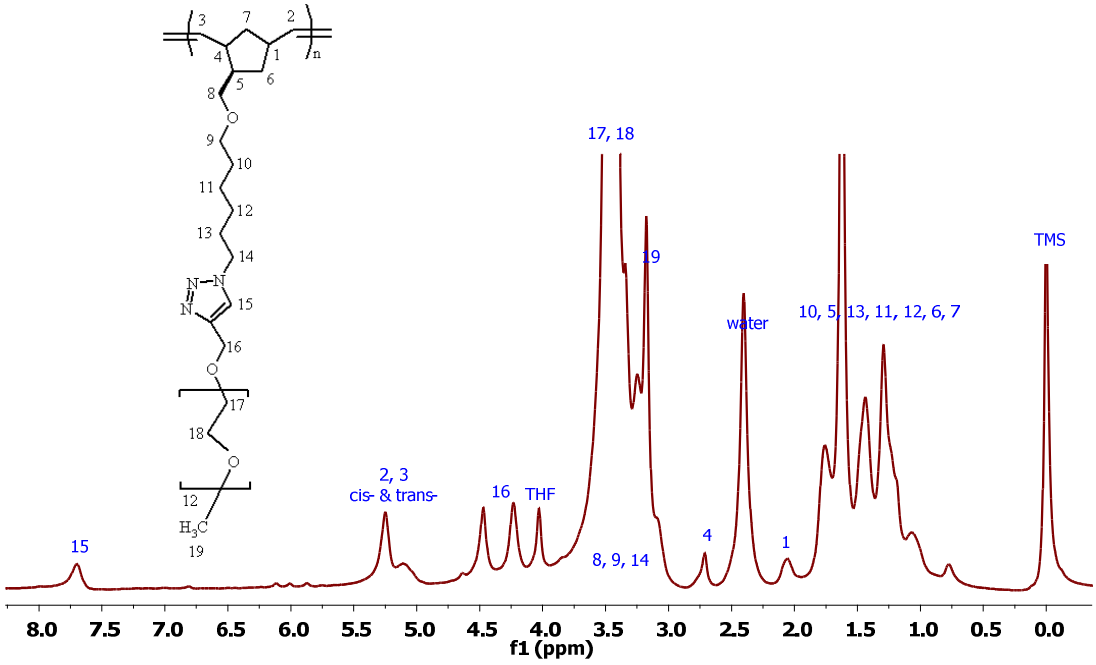


**Figure 6.28.** $^{1}$H-NMR spectrum of polynorbornene-g-PEG **6.11** in $CDCl_3$

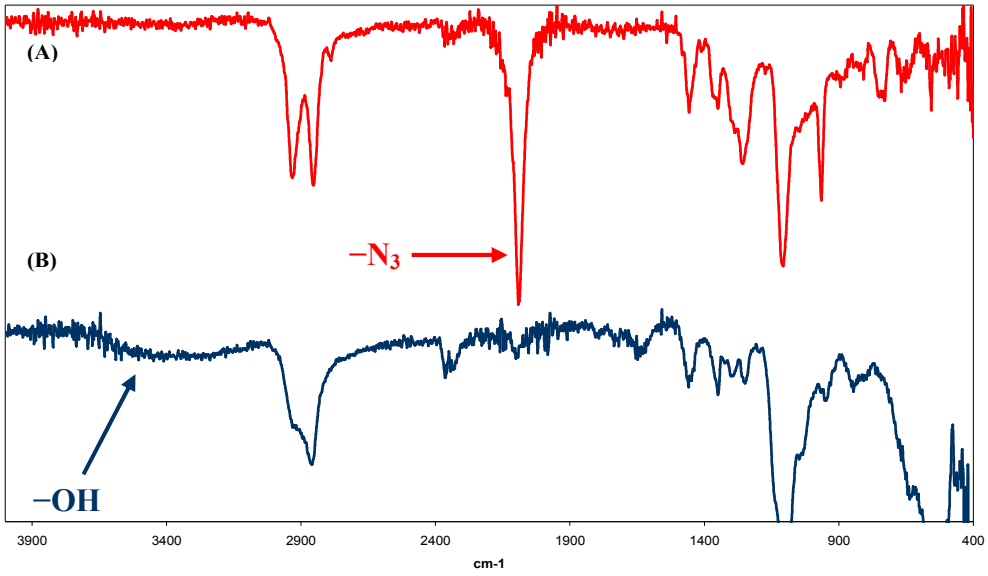


**Figure 6.29.** FT-IR spectra of (A) azide functionalised polynorbornene **6.9** and (B) polynorbornene-g-PEG **6.11**

### 6.3.2.5. AFM Analysis of Polynorbornene Graft Copolymers on Silicon Surface

AFM analysis, using the same method used in chapter 5, section 5.3.3.3.1, was used to investigate the structures of the polymer chains of polynorbornene-g-PCL **6.10** and polynorbornene-g-PEG **6.11** with theoretical backbone DP of ~200. Thin films with an average thickness of ~1 nm were produced on the surface of a clean silicon wafer by spin-casting of a dilute polymer solution (~1 mg / 100 mL) from chloroform. AFM images of polynorbornene-g-PCL showed that the chains exhibit uniform isotropic features, Fig. 6.30.A and B. The multiple measurements of these features gave an average height of ~4.4 nm and radius of ~16.1 nm, Fig. 6.30.C. The same features were also observed in the case of polynorbornene-g-PEG, Fig. 6.31.A and B. However, the measurements showed a consistency in the radius of the features of ~18 nm and a considerable decrease in the height features to be of ~2.6 nm, Fig. 6.31.C. This is presumably due to the length of the PEG side chains in polynorbornene-g-PEG is much shorter than the length of PCL in polynorbornene-g-PCL.

The AFM images of polynorbornene-g-PCL and polynorbornene-g-PEG did not show the formation of wormlike structures expected for brush polymers. This is probably due to the lack of steric repulsion between the PCL or PEG side chains. The "grafting onto" strategy used in the synthesis of these copolymers is known to produce graft copolymers with ill-defined architectures, due to unavailability of all active sites. Therefore, one explanation might be due to limited number of grafts along the backbone

chain, which reduces the repulsion interaction. However, the IR analysis of both polynorbornene-g-PCL and polynorbornene-g-PEG showed that all azides have been reacted, indicating that approximately each cyclopentane ring in polynorbornene backbone has a PCL or PEG attached chain. The graft copolymers have *cis/trans* double bonds along the backbone chains as well as the head/tail orientations (connectivity), since cyclopentane is mono substituted. This would probably be expected to reduce the steric repulsion between the grafted chains.

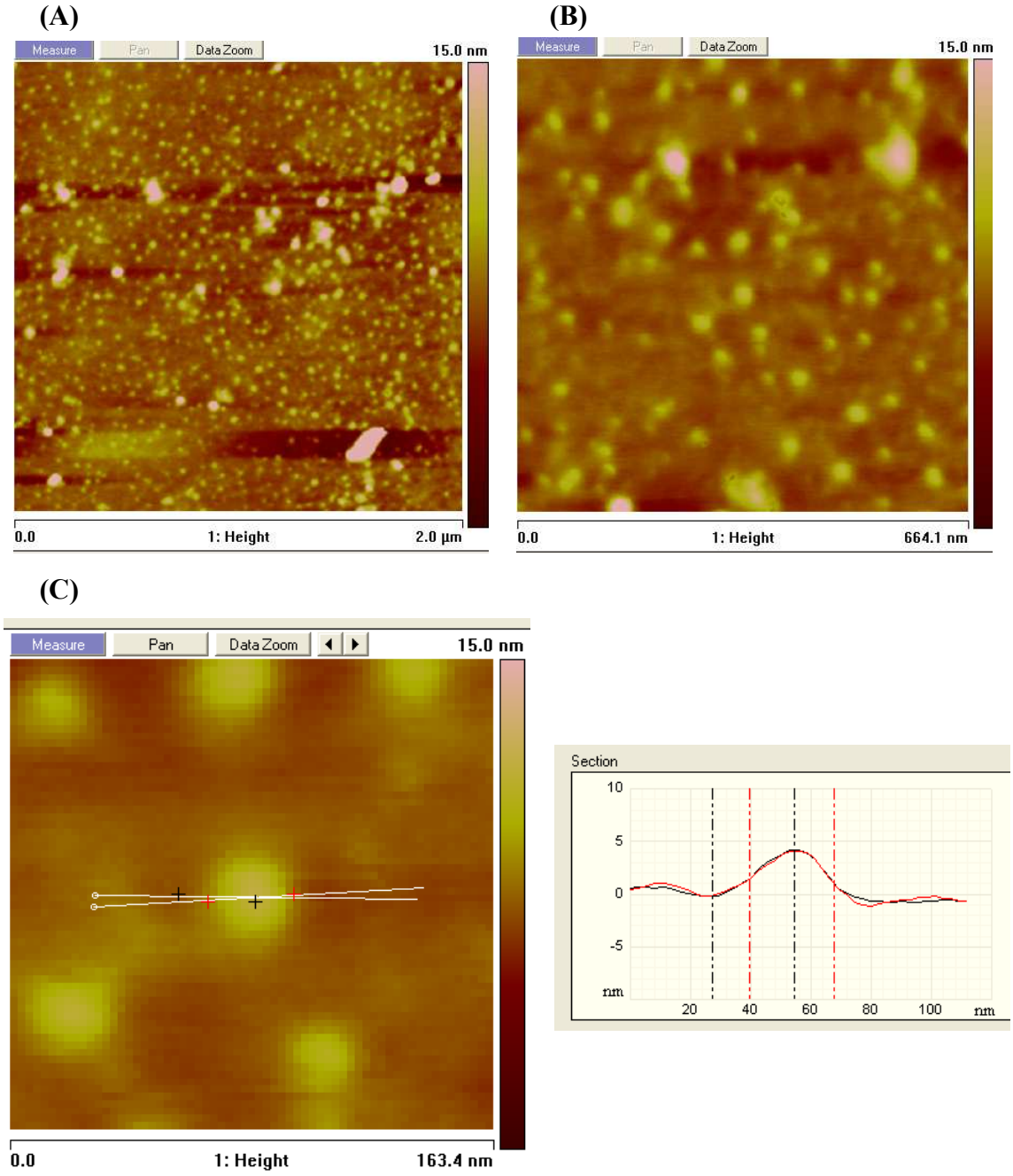


**Figure 6.30.** Tapping mode AFM images of polynorbornene-g-PCL; (A) 2 µm scale, (B) 664 nm scale and (C) 163 nm scale with cross-sectional analysis.

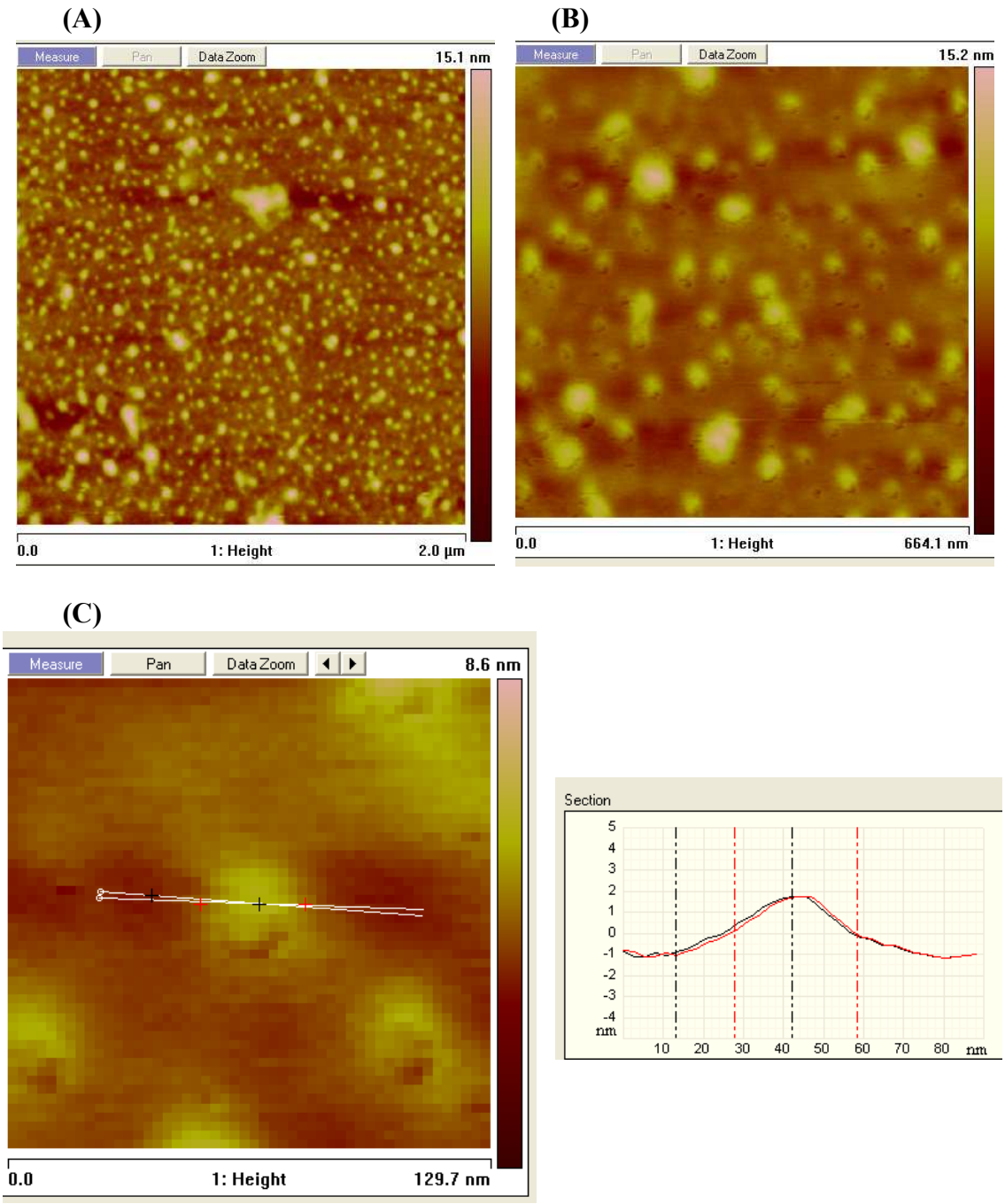


**Figure 6.31.** Tapping mode AFM images of polynorbornene-g-PEG; (A) 2 µm scale, (B) 664 nm scale and (C) 129 nm scale with cross-sectional analysis.

### 6.3.3. Synthesis and Characterisation of Random Copolymer Containing PEG and PCL grafts

In this section, the preparation of random copolymer composed of two different units, (1) polyoxanorbornene-g-PEG and (2) polynorbornene-g-PCL, is demonstrated. The design involved side chains containing hydrophilic/biocompatible (PEG) and hydrophobic/biodegradable (PCL). The synthetic strategy involved three steps to obtain the final copolymer.

The first step was ROMP of a mixture of oxanorbornenyl PEG macromonomer **6.5** and bromide functionalised norbornene monomer **6.7** with ratio of 1:1 wt% (**6.7**: **6.5**; 82:18 mol%). The polymerisation was performed using ruthenium initiator **G-II** and mixed monomers to initiator molar ratio [M]:[I] of 10:1 in $CDCl_3$. The resulting copolymer **6.12** contains PEG grafts as well as bromide functionalities, Scheme 6.9.

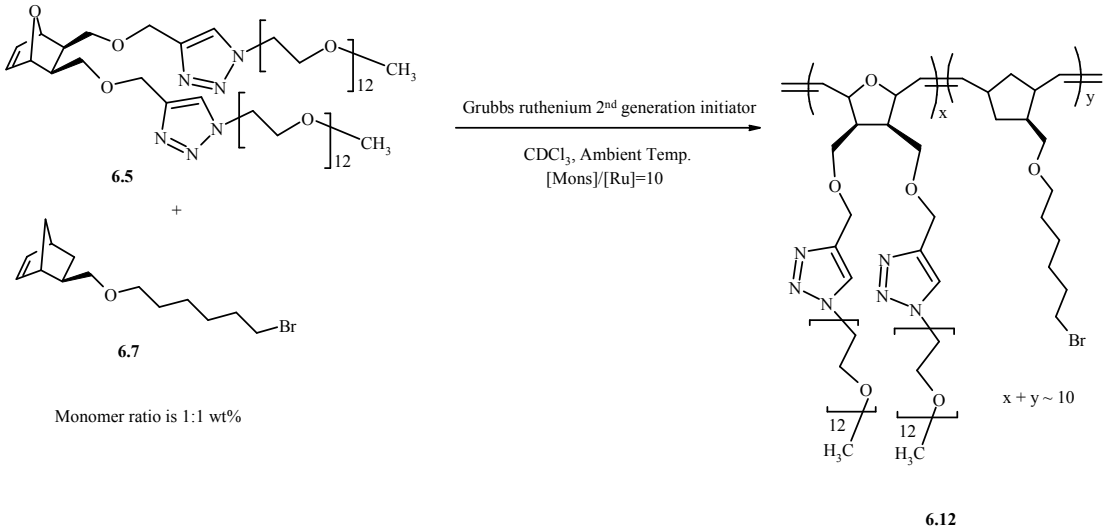


**Scheme 6.9.** Synthesis of random copolymer containing PEG grafts and bromide functionalities

The reaction was continued to the next step, which involved conversion of bromide functionalities in **6.12** to azide functionalities to produce copolymer **6.13** *via* reaction with sodium azide, Scheme 6.10.

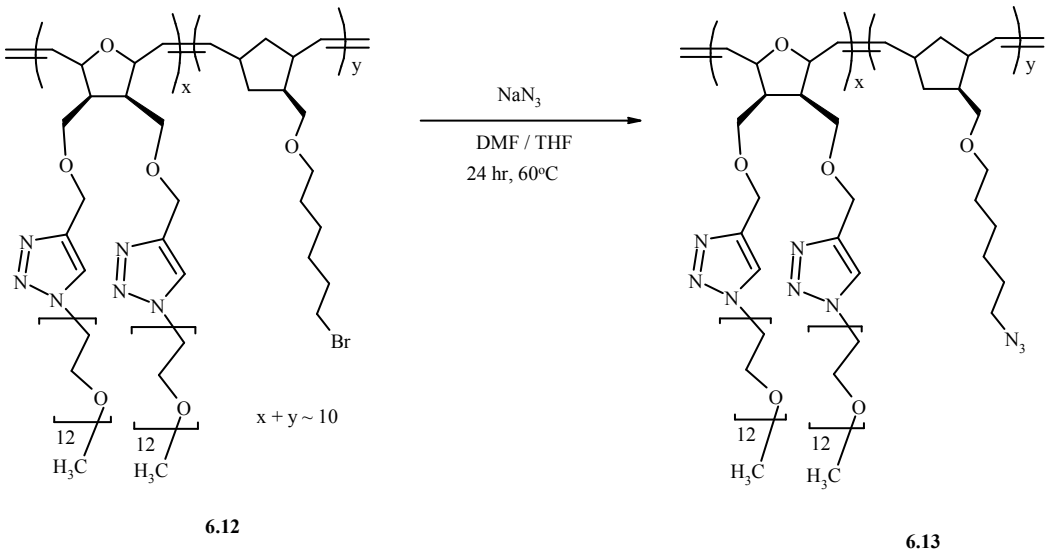


**Scheme 6.10.** Synthesis of random copolymer containing PEG grafts and azide functionalities

The $^{1}$H-NMR of **6.13** showed peaks corresponding to the copolymer backbone chain at 5.10 − 5.25 ppm, due to *cis*- and *trans*- double bonds. It also showed a peak due to the triazole proton at 7.65 ppm. This indicated the successful ROMP step as well as the incorporation of polyoxanorbornene-g-PEG in the copolymer composition. However, the incorporation of polynorbornene in the copolymer was indicated by the appearance of a peak due to the azide group at ~2100 cm$^{-1}$ in the IR spectra, Fig. 6.32.

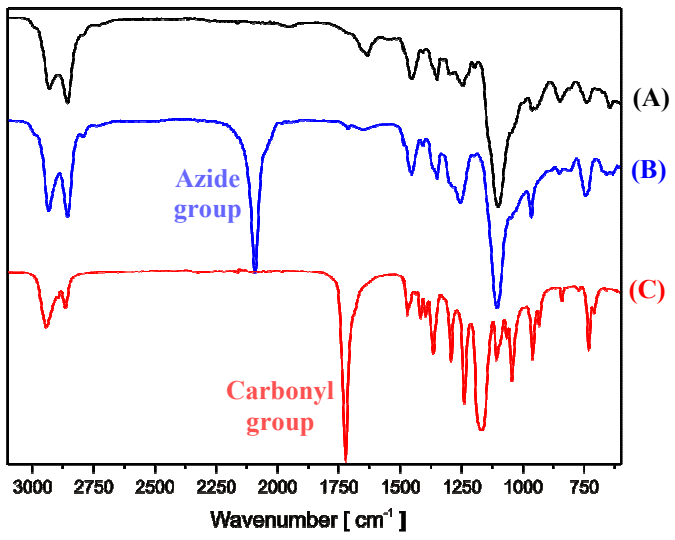


**Figure 6.32.** FT-IR spectra of (A) random copolymer **6.12** containing PEG grafts and bromide functionalities**,** (B) random copolymer **6.13** containing PEG grafts and azide functionalities, and (C) random copolymer **6.14** containing PEG and PCL grafts

The final step involved Click reaction between random copolymer **6.13** and alkyne end capped PCL **4.2** to produce the final random copolymer **6.14** containing PEG and PCL grafts, Scheme 6.11.

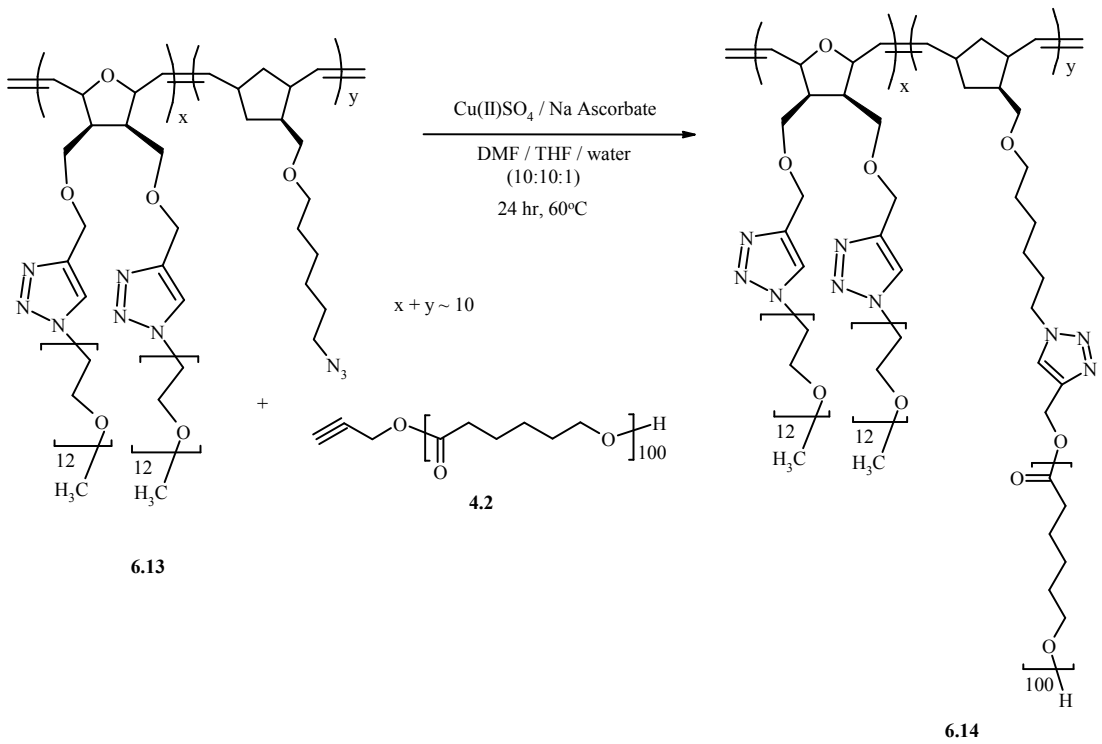


**Scheme 6.11.** Synthesis of random copolymer containing PEG and PCL grafts

The successful synthesis of **6.14** was demonstrated by the disappearance of the azide peak at ~2100 $cm^{-1}$ as well as the appearance of a peak due to the carbonyl group of PCL at ~1740 $cm^{-1}$ in IR spectra, Fig. 6.32.C.

## 6.4. Summary

Different polynorbornene/polyoxanorbornene graft copolymers were efficiently synthesised by combination of Click chemistry and ROMP. The final materials as well as the intermediates were fully characterised by NMR and IR spectroscopy. Two different grafting routes were employed to synthesise these graft copolymers.

"Grafting through" route involved the synthesis of oxanorbornenyl di-PEG macromonomer followed by ROMP. Click coupling of azide terminated PEG with di-alkyne functionalised oxanorbornene was used to synthesise the oxanorbornenyl PEG macromonomer, which contained two PEG chains per each oxanorbornene moiety. The ROMP of the oxanorbornenyl di-PEG macromonomer using Grubbs ruthenium 2$^{nd}$ generation initiator (**G-II**) produced graft polymer with good conversion (76 %, based on NMR).

The ROMP of bromide functionalised norbornene was carried out using Grubbs ruthenium 1$^{st}$ generation initiator (**G-I**), followed by reaction with sodium azide. The Click reaction with alkyne terminated PCL and PEG prepolymers was found to be a general and highly facile "grafting onto" route for the synthesis of a variety of graft copolymers; polynorbornene-g-PCL and polynorbornene-g-PEG. AFM tapping mode images of these graft polymers with DP of ~200 showed isotropic globular features instead of wormlike structures.

Random graft copolymer containing PEG and PCL side chains was successfully prepared *via* ROMP of a mixture of oxanorbornenyl di-PEG and bromide functionalised norbornene, using **G-II**, followed by reaction with sodium azide and then Click reaction with alkyne end capped PCL.

## 6.5. References


1. M. Wintermantel, M. Gerle, K. Fischer, M. Schmidt, I. Wataoka, H. Urakawa, K. Kajiwara, Y. Tsukahara, *Macromolecules* **1996**, *29*, 978 – 983.
2. S. S. Sheiko, M. Müller, *Chemical Reviews* **2001**, *101*, 4099 – 4124.
3. V. Percec, C. H. Ahn, G. Ungar, D. J. P. Yeardley, M. Müller, S. S. Sheiko, *Nature (London)* **1998**, *391*, 161 – 164.
4. N. Hadjichristidis, S. Pispas, H. Iatrou, *Chemical Reviews* **2001**, *101*, 3747.
5. M. Zhang, A. H. E. Müller, *Journal of Polymer Science Part A: Polymer Chemistry* **2005**, *43*, 3461 – 3481.
6. B. S. Sumerlin, D. Neugebauer, K. Matyjaszewski, *Macromolecules* **2005**, *38*, 702 – 708.
7. H. Gao, K. Matyjaszewski, *Journal of the American Chemical Society* **2007**, *129*, 6633 – 6639.
8. M. Schappacher, A. Deffieux, *Science* **2008**, *319*, 1512 – 1515.
9. P. Schwab, R. H. Grubbs, J. W. Ziller, *Journal of the American Chemical Society* **1996**, *118*, 100 – 110.
10. J. A. Love, J. P. Morgan, T. M. Trnka, R. H. Grubbs, *Angewandte Chemie International Edition* **2002**, *41*, 4035 – 4037.
11. J. Huang, H. J. Schanz, E. D. Stevens, S. P. Nolan, *Organometallics* **1999**, *18*, 5375 – 5380.
12. S. Jha, S. Dutta, N. B. Bowden, *Macromolecules* **2004**, *37*, 4365 – 4374.
13. H. D. Maynard, S. Y. Okada, R. H. Grubbs, *Macromolecules* **2000**, 33, 6239 – 6248.
14. S. Rajaram, T. L. Choi, M. Rolandi, J. M. J. Fréchet, *Journal of the American Chemical Society* **2007**, *129*, 9619 – 9621.
15. A. M. Nathan-Ravi, P. Hamilton, F. Horkay, *Journal of Polymer Science Part B: Polymer Physics* **2002**, *40*, 2677.
16. H. Q. Xie, D. Xie, *Progress in Polymer Science* **1999**, *24*, 275.
17. R. Venkatesh, L. Yajjou, C. E. Koning, B. Klumperman, *Macromolecular Chemistry and Physics* **2004**, *205*, 2161.
18. P.A. Bertin, K. J. Watson, S. T. Nguyen, *Macromolecules* **2004**, *37*, 8364.
19. J. Zimberlin, N. Sanabria-Delong, G. N. Tew, A. J. Crosby, *Soft Matter* **2007**, *3*, 763.
20. J. M. Zhu, *Biomaterials* **2010**, *31*, 4639 – 4656.

21. J. F. Lutz, H. G. Borner, K. Weichenhan, *Macromolecules* **2006**, *39*, 6376 – 6383.
22. V. Héroguez, Y. Gnanou, M. Fontanille, *Macromolecules* **1997**, *30*, 4791.
23. A. Chemtob, V. Héroguez, Y. Gnanou, *Macromolecules* **2002**, *35*, 9262.
24. A. Chemtob, V. Héroguez, Y. Gnanou, *Macromolecules* **2004**, *42*, 2705.
25. D. Quémener, A. Bousquet, V. Héroguez, Y. Gnanou, *Macromolecules* **2006**, *39*, 5589.
26. M. B. Runge, S. Dutta, N. B. Bowden, *Macromolecules* **2006**, *39*, 498.
27. K. Breitenkamp, T. Emrick, *Journal of Polymer Science Part A: Polymer Chemistry* **2005**, *43*, 5715.
28. S. C. G. Biagini, A. L. Parry, *Journal of Polymer Science Part A: Polymer Chemistry* **2007**, *45*, 3178.
29. S. f. Alfred, Z. M. Al-badri, A. E. Madkour, K. Lienkamp, G. N. Tew, *Journal of Polymer Science part A: Polymer Chemistry* **2008**, *46 (8)*, 2640-2648.
30. A. Carillo, M. J. Yanjarappa, K. V. Gujraty, R. S. Kane, *Journal of Polymer Science part A: Polymer Chemistry* **2006**, *44*, 928.
31. K. Miki, K. Oride, S. Inoue, Y. Kuramochi, R. R. Nayak, H. Matsuoka, H. Harada, M. Hiraoka, K. Ohe, *Biomaterials* **2010**, *31*, 934 – 942.
32. A. C. Albertsson, I. K.Varma, *Biomacromolecules* **2003,** *4*, 1466-1486.
33. K. A. Athanasiou, G. G. Niederauer, C. M. Agrawal, *Biomaterials* **1996**, *17*, 93 – 102.
34. J. C. Middleton, A. J. Tripton, *Biomaterials* **2000**, *21*, 2335 – 2346.
35. E. S. Place, J. H. George, C. K. Williams, M. M. Stevens, *Chemical Society Reviews* **2009**, *38*, 1139 – 1151.
36. R. J. Pounder, A. P. Dove, *Polymer Chemistry* **2010**, *1*, 260 – 271.
37. I. Czelusniak, E. Khosravi, A. M. Kenwright, C. W. G. Ansell, *Macromolecules* **2007**, *40*, 1444 – 1452.
38. M. Xie, J. Dang, H. Han, W. Wang, J. Liu, X. He, Y. Zhang, *Macromolecules* **2008**, *41*, 9004 – 9010.
39. Y. Xia, B. D. Olsen, J. A. Kornfield, R. H. Grubbs, *Journal of the American Chemical Society* **2009**, *131*, 18525–18532.
40. S. Y. Lu, J. M. Amass, N. Majid, D. Glennon, A. Byerley, F. Heatley, P. Quayle, C. Booth, S. G. Yeates, J. C. Padget, *Macromolecular Chemistry and Physics* **1994**, *195 (4)*, 1273 – 1288.

41. J. T. Manka, A. G. Douglass, P. Kaszynski, A. C. Friedli, *Journal of Organic Chemistry* **2000**, *65*, 5202 – 5206.
42. J. H. Lee, J. W. Park, J. M. Ko, Y. H. Chang, S. K. Choi, *Polymer Bulletin* **1993**, *31*, 339-346.
43. J. Asrar, *Macromolecules* **1992**, *25*, 5150-5156.
44. J. M. Pollino, L. P. Stubbs, M. Weck, *Macromolecules* **2003**, *36*, 2230-2234.
45. J. D. Rule, J. S. Moore, *Macromolecules* **2002**, *35*, 7878-7882.
46. J. K. Huang, H. J. Schanz, E. D. Stevens, S. P. Nolan, *Organometallics* **1999**, *18*, 5375-5380.
47. P. Schwab, R. H. Grubbs, J. W. Ziller, *Journal of the American Chemical Society* **1996**, *118*, 100-110.
48. J. G. Hamilton, J. Kay, J. J. Rooney, *Journal of Molecular Catalysis A-Chemical* **1998**, *133*, 83-91.
49. F. A. L. Anet, *Tetrahedron Letters* **1962**, 1219-1222.

# Chapter 7
# General Conclusions and Future Work

## 7.1. General Conclusions

The exploitation of copper catalysed Huisgen 1,3-dipolar azide – alkyne cycloaddition, as an efficient Click reaction, was demonstrated for the synthesis of novel biopolymers with potential medical/industrial applications.

The application of Click chemistry on model compounds was initiated in order to get familiar with the chemistry of Click reactions and the systematic characterisation. The chemical modifications on model compounds were carried out successfully and NMR spectroscopy was found to be a good choice for characterisation of the resulting products. The systematic synthesis and characterisation provided extremely useful knowledge and understanding.

The Click chemistry was then applied on trehalose to demonstrate the applicability of Click chemistry on a saccharide model compound, which is closely related to 2-hydroxyethyl cellulose (HEC). The di-azide functionalised trehalose was synthesised by tosylation followed by acetylation and subsequent reaction with sodium azide. Different functionalities such as ester, acrylate and epoxide groups were successfully introduced *via* Click chemistry. NMR and FT-IR spectroscopies were found to be efficient characterisation tools to follow up the Click modification reactions. The di-acrylate functionalised trehalose showed the potential as a cross-linking agent in the free radical polymerisation of HEMA to generate three-dimensional networks. Indeed, the successful application of Click chemistry on trehalose, an interesting symmetrical disaccharide compound, would open up the opportunities to synthesise wide range of trehalose-based biomaterials.

The interest was extended to prepare trehalose-based glycopolymers to produce novel materials. Glycopolymers containing PCL or PLA were synthesised *via* combination of ROP and Click chemistry. The ROP of lactide and ε-caprolactone, using stannous octoate and propargyl alcohol, was carried out to synthesise alkyne end capped PLA and PCL which were then coupled with di-azide functionalised trehalose by Click reaction. NMR and IR were used to prove the structure of the materials. The combination of ROP with Click chemistry was shown to be an original method to use trehalose as a disaccharide spacer between two PCL or PLA chains. The insertion of trehalose onto aliphatic polyesters would produce functional materials, which is expected to facilitate the attachment of drugs, improvement of biocompatibility, control in the biodegradation rate, increase of bio-adhesion, and induction of hydrophilicity.

A new class of temperature responsive glycopolymers was synthesised *via* copper wire catalysed Click-polymerisation of di-azide functionalised trehalose with di-alkyne terminated PEG. The cloud point of the aqueous solution of glycopolymer was evaluated and showed an LCST at ~39 $^{o}$C, known as fever temperature. In addition, the phase transition was shown to be reversible. The protection of the secondary hydroxyl groups in trehalose was found to be essential to promote the hydrophobic character of the glycopolymer and hence the hydrophobic/hydrophilic interactions. The results also indicated that the ideal molecular weight of PEG to produce glycopolymer exhibiting phase transition at the fever temperature was ~600 gmol$^{-1}$, which is very close to that of trehalose moiety (~644 gmol$^{-1}$). The temperature responsive glycopolymer is anticipated to be biocompatible and biodegradable due to the presence of PEG and trehalose, respectively. To the best of our knowledge, this is the first example reported in the literature describing the preparation of temperature responsive glycopolymer based on trehalose and PEG using Click-polymerisation technique. Moreover, up to date the use of copper wire as an alternative catalyst for Click chemistry is still uncommon in the literature, despite its great potential in producing Cu-free products or with very low copper contaminants. However, the mechanism and the exact amount of copper contamination need to be investigated if the materials are going to be used in biomedical applications.

The Click reaction was utilised to introduce different compositions on HEC in order to produce personal care products for Akzo Nobel. The modification of HEC *via* Click chemistry was achieved by functionalisation and grafting of HEC with small molecules and/or macromolecules. For the first time, the azide functionalisation reaction of HEC was carried out using a one pot reaction procedure. The neutral composition contained ester, acrylate, siloxyl and epoxide groups. The ionic compositions containing carboxylic acid and/or primary amine are expected to give polyelectrolyte based HEC in basic or acidic media. Moreover, the composition containing both carboxylic acid and primary amine would be expected to form polyampholytes. The HEC containing PDMS with neutral (ester) and/or ionic (carboxylic acid and amine) functionalities were prepared by sequential Click reactions. These compositions are expected to generate interest in personal care and cosmetics applications. It is believed that the chemical attachment of PDMS on HEC with different charges along the backbone would make these compositions capable of replacing the current Akzo Nobel personal care product, which is based on HEC quaternary ammonium salt with physically bonded PDMS. Click reaction was also used to graft different polymers such as PLA, PCL or PEG onto

HEC backbone. Some of these modified HEC materials were shown to possess brush-like architecture as revealed by AFM images. Click chemistry was shown to be a very powerful chemical methodology for the modification of polysaccharides. The methodology would yield compounds, which are not accessible *via* the commonly applied modification reactions such as etherification and esterification. Therefore, the Click modification strategy should significantly broaden the structural diversity of polysaccharide-based materials.

The research was then moved towards combining Click reaction with well-defined ROMP to produce a series of novel graft copolymers. This was accomplished by "grafting through" (the macromonomer approach) and "grafting onto" techniques. The "grafting through" method involved the synthesis of oxanorbornenyl di-PEG macromonomer by Click coupling of azide terminated PEG with di-alkyne functionalised oxanorbornene. The macromonomer was then subjected to ROMP to produce polyoxanorbornene-g-PEG. On the other hand, polynorbornene-g-PCL and polynorbornene-g-PEG were prepared by the "grafting onto" method. This was achieved by ROMP of bromide functionalised norbornene monomer followed by reaction with sodium azide and then Click reaction with alkyne terminated PCL and PEG, respectively. AFM analysis of these graft polymers indicated that they do not exhibit brush-like architectures. Random graft copolymer containing PEG and PCL side chains was also prepared by ROMP of a mixture of oxanorbornenyl di-PEG and bromide functionalised norbornene followed by reaction with sodium azide and then Click reaction with alkyne end capped PCL. The combination of Click chemistry and ROMP was shown to be a facile and efficient method to design tailored macromolecular architectures. The well-characterised complex graft copolymers are expected to possess novel solution properties.

## 7.2. Future Work

The di-acrylate functionalised trehalose has been used as a cross-linker in the free radical polymerisation of HEMA to produce three-dimensional networks. It would be interesting to use this new cross-linker in the polymerisation of acrylamide and acrylic acid to produce glycopolymers, which are expected to be pH responsive hydrogels.

It has been shown that the polymerisation of trehalose with PEG produces a temperature responsive material with phase transition at the fever temperature under neutral condition. In order to use this material in biomedical applications, the phase transition needs to be studied at different pH media. Moreover, Gelest produces silanol terminated PDMS with different molecular weight which can similarly be alkyne functionalised. Di-azide functionalised trehalose can then be polymerised with the di-alkyne terminated PDMS to produce a biomaterial, which combines the properties of silicones and saccharides.

The graft copolymers prepared by the combination of ROMP and Click did not show brush-like structures, due to the lack of steric repulsion between the grafts probably because of *cis/trans* double bonds and head/tail complexities among the backbone chains. It will be interesting to hydrogenate the double bonds in the backbone chains or use di-functionalised norbornene monomers to eliminate these complexities and investigate AFM of the resulting graft copolymers. It would also be very interesting to investigate the temperature responsiveness of the graft polymers containing PEG segments. In particular, polynorbornene-g-PEG is expected to exhibit phase transition, if the hydrophilic/hydrophobic ratio were adjusted and optimised.